1972

Watershed evapotranspiration by the combination method

Keith Earnest Saxton
Iowa State University

Watershed evapotranspiration by the combination method

by

Keith Earnest Saxton

A Dissertation Submitted to the
Graduate Faculty in Partial Fulfillment of
The Requirements for the Degree of
DOCTOR OF PHILOSOPHY

Major: Agricultural Engineering

Approved:

Signature was redacted for privacy.

In Charge of Major Work

Signature was redacted for privacy.

For the Major Department

Signature was redacted for privacy.

For the Graduate College

Iowa State University
Ames, Iowa
1972

TABLE OF CONTENTS

	Page
INTRODUCTION	1
OBJECTIVES	7
LITERATURE REVIEW	8
Introduction	8
Historical Interest in Evapotranspiration	9
Evapotranspiration as a Hydrologic Component	12
Selecting an Approach	14
The Combination Equation	24
ET Rates Less Than Potential	28
PROCEDURES	33
Potential ET	33
Potential to Actual ET	43
Evaluation	54
INSTRUMENTATION	56
Experiment Location	56
Micrometeorological Instruments	62
Other Measurements and Observations	71
DATA COLLECTION	73
Collection Methods	73
Instrument Calibrations	75
Reduction	81
METEOROLOGICAL DATA CHARACTERISTICS	88
Net Radiation	88
Other Variables	100

TABLE OF CONTENTS
(Continued)

	Page
POTENTIAL ET CALCULATIONS	106
Initial Calculations	106
Estimating Wind Parameters	108
Potential ET Values	111
Error Analyses	134
ACTUAL ET CALCULATIONS	147
Rational ET Model Description	148
Results and Evaluation	167
SUMMARY AND CONCLUSIONS	193
LITERATURE CITED	197
ACKNOWLEDGEMENTS	205
APPENDIX A DERIVATION OF THE COMBINATION EQUATION	206
Step I: Vertical Energy Balance	207
Step II: Applying Dalton Transport Function	209
Step III: Penman's Psychrometric Assumption	210
Step IV: Turbulent Transport Theory	213
APPENDIX B REVIEW OF WIND PROFILE PARAMETERS	229

LIST OF TABLES

		Page
Table 1.	Polynomial equations representing the annual trend of the ratio daily net radiation over daily solar radiation	94
Table 2.	Equations defining relative error of the combination model and wind parameter	138
Table 3.	Distribution of water extraction by transpiration, percent	158
Table 4.	Monthly summary of calculated ET, components, and related variables for 1969	179
Table 5.	Monthly summary of calculated ET, components, and related variables for 1970	181
Table 6.	Summary of soil moisture movement, for grass during 1969	192
Table B-1.	Summary of wind profile parameter values from various references	238
Table B-2.	Summary of prediction equations for roughness parameter, Z_o	241
Table B-3.	Example values of calculated wind profile parameters Z_o and d	242

LIST OF FIGURES

		Page
Figure 1.	Schematic of the soil-plant-air system to be modeled	45
Figure 2.	Flow chart of the potential to actual ET conversions	48
Figure 3.	Location of the experimental watersheds which contained the ET instrumentation sites	57
Figure 4.	Topography and instrumentation of the experimental watersheds near Treynor, Iowa	58
Figure 5.	Topography of the ET instrumentation sites	60
Figure 6.	Cross section profile A-A of the instrumentation sites shown in figure 5	61
Figure 7.	Instrument sensors over grass	65
Figure 8.	Details of grass site sensors	65
Figure 9.	Vacuum pump used for air circulation	66
Figure 10.	Details of mounting Fritschen-type net radiometer	66
Figure 11.	Instrument sensors over corn	67
Figure 12.	Details of corn site sensors	67
Figure 13.	Recorder shelter located midway of corn and grass sites	68
Figure 14.	Net radiometer recorders, wind accumulator, and millivolt reference	68
Figure 15.	Multipoint recorder, motor-ventilated wet-dry bulb psychrometer, and electric cattle fencer	70
Figure 16.	Net radiometers mounted parallel for calibration	70

		Page
Figure 17.	Calibration curves of the Minneapolis-Honeywell Dew Probes	77
Figure 18.	Calibration curve for neutron soil moisture probe	80
Figure 19.	Typical diurnal patterns of vapor pressure deficits	85
Figure 20.	Annual distribution of daily net radiation over grass during 1970	89
Figure 21.	Daily net radiation over grass compared with daily solar radiation at Omaha, Nebraska, March 13 to December 1, 1970	91
Figure 22.	Annual trend of the ratio of net over total radiation during 1970 with corn cover	92
Figure 23.	Daily net radiation over grass compared with that over corn, March 13 to December 1, 1970	95
Figure 24.	Annual distribution of the ratio of grass over corn daily net radiation during 1970	96
Figure 25.	Net radiation over grass compared to Class A pan evaporation, March 15 to October 30, 1970	98
Figure 26.	Annual distribution of the ratio of pan evaporation over net radiation over grass during 1970	99
Figure 27.	Annual distribution of the ratio delta/gamma during 1970	101
Figure 28.	Annual distribution of average daytime vapor pressure deficits during 1970	102
Figure 29.	Comparison of average daytime vapor pressure deficits over grass and corn, March 12 to September 22, 1970	103
Figure 30.	Annual distribution of measured daytime wind travel 0.6 to 0.8 meter above grass surface during 1970	105

		Page
Figure 31.	Annual distribution of crop and wind profile parameters for grass during 1969	113
Figure 32.	Annual distribution of crop and wind profile parameters for grass during 1970	114
Figure 33.	Annual distribution of crop and wind profile parameters for corn during 1969	115
Figure 34.	Annual distribution of crop and wind profile parameters for corn during 1970	116
Figure 35.	Annual distribution of calculated daily potential ET for grass during 1969	118
Figure 36.	Annual distribution of calculated daily potential ET for grass during 1970	119
Figure 37.	Comparison of computed daily potential ET for grass and corn, March 9 to December 1, 1969	120
Figure 38.	Annual distribution of potential ET of grass over potential ET of corn during 1969	121
Figure 39.	Annual distribution of net radiation over computed potential ET for grass during 1969	123
Figure 40.	Annual distribution of net radiation over computed potential ET for corn during 1969	124
Figure 41.	Comparison of computed daily potential ET for grass with net radiation over grass, March 12 to December 1, 1970	125
Figure 42.	Comparison of computed daily potential ET for grass with pan evaporation, March 15 to October 30, 1970	126

		Page
Figure 43.	Annual distribution of pan evaporation over computed potential ET for grass during 1969	128
Figure 44.	Annual distribution of radiation term over aerodynamic term for grass during 1969	129
Figure 45.	Annual distribution of radiation term over aerodynamic term for grass during 1970	130
Figure 46.	Annual accumulative values of net radiation, calculated potential ET, and pan evaporation for grass and corn during 1969	131
Figure 47.	Annual accumulative values of net radiation, calculated potential ET, and pan evaporation for grass and corn during 1970	132
Figure 48.	Relative error values for the combination equation for grass during 1969	140
Figure 49.	Relative error values for the combination equation for corn during 1969	141
Figure 50.	Relative error values for the wind parameters for grass during 1969	143
Figure 51.	Relative error values for the wind parameters for corn during 1969	144
Figure 52.	Schematic of the rational model for computing actual evapotranspiration and soil moisture status	149
Figure 53.	Estimated relationship for converting potential to actual soil evaporation	152
Figure 54.	Estimated relationship for soil-to-plant transfer	154

		Page
Figure 55.	Relationships representing plant transpirability during the year depending upon the phenological plant status	155
Figure 56.	Tension-moisture content relationship for Monona silt loam - 60 in. depth (Melvin 1970, p. 130)	163
Figure 57.	Conductivity estimates for Monona silt loam - 60 in. depth (Melvin 1970, p. 169)	165
Figure 58.	Accumulative volumes related to potential and actual ET and soil moisture in the top 6 feet, for grass during 1969	170
Figure 59.	Accumulative volumes related to potential and actual ET and soil moisture in the top 6 feet, for grass during 1970	171
Figure 60.	Accumulative volumes related to potential and actual ET and soil moisture in the top 6 feet, for corn during 1969	172
Figure 61.	Accumulative volumes related to potential and actual ET and soil moisture in the top 6 feet, for corn during 1970	173
Figure 62.	Accumulative actual ET and its components of transpiration, soil evaporation, and interception evaporation for grass during 1969	174
Figure 63.	Accumulative actual ET and its components of transpiration, soil evaporation, and interception evaporation for grass during 1970	175
Figure 64.	Accumulative actual ET and its components of transpiration, soil evaporation, and interception evaporation for corn during 1969	176

		Page
Figure 65.	Accumulative actual ET and its components of transpiration, soil evaporation, and interception evaporation for corn during 1970	177
Figure 66.	Soil moisture volumes calculated by the rational ET model compared to observed values for grass during 1969	183
Figure 67.	Soil moisture volumes calculated by the rational ET model compared to observed values for grass during 1969	184
Figure 68.	Soil moisture volumes calculated by the rational ET model compared to observed values for grass during 1970	185
Figure 69.	Soil moisture volumes calculated by the rational ET model compared to observed values for grass during 1970	186
Figure 70.	Soil moisture volumes calculated by the rational ET model compared to observed values for corn during 1969	187
Figure 71.	Soil moisture volumes calculated by the rational ET model compared to observed values for corn during 1969	188
Figure 72.	Soil moisture volumes calculated by the rational ET model compared to observed values for corn during 1970	189
Figure 73.	Soil moisture volumes calculated by the rational ET model compared to observed values for corn during 1970	190
Figure A-1.	Major vertical energy components during daylight conditions for an agricultural field	227
Figure A-2.	Schematic of psychrometric chart for demonstrating Penman's assumptions	227

		Page
Figure A-3.	Schematic of instantaneous vertical wind velocities	228
Figure A-4.	Definition sketch of mixing length concept.	228
Figure B-1.	Wind effects on d for corn and grass	244
Figure B-2.	Wind effects on Z_o	244

INTRODUCTION

On this small planet for which mankind must depend as its ship on a continuous journey through space, the life sustaining substance of water is plentiful. But man is strongly dependent on the distribution and quality of this water as it occurs on our sphere. Beyond his body needs, man uses water for nearly every major activity in his pursuit of life and happiness. It is therefore imperative that we understand the occurrence of water as it traverses the many devious paths of the earth's atmosphere and geologic structure. This endless system is commonly referred to as the hydrologic cycle.

Within the hydrologic cycle of a watershed, the process of evapotranspiration (ET) is second only to precipitation in the movement of water. Hydrologic budgets of watersheds in humid regions, such as eastern United States, show that 26 to 28 in. of the more than 40 in. of rainfall is returned to the atmosphere by ET. In subhumid regions with precipitation of 25 to 30 in., such as the eastern great plains regions, ET accounts for 22 to 26 in. from vegetated land. Of course, in more arid climates nearly all of the precipitation is utilized by ET.

The processes within the hydrologic system are highly interdependent, particularly in the soil-plant-atmospheric system which encompasses ET. The rate and amount of infiltration are strongly dependent on antecedent soil moisture conditions, plant canopy, and soil characteristics. The distribution and amount of surface runoff are largely dependent on rainfall intensity and infiltration rates. Thus, ET not only moves large quantities of water, but it also has strong ties to many other factors within the hydrologic cycle.

Evapotranspiration is also the necessary process of water expenditure for crop production. Irrigation projects in arid regions exemplify this view when lands bearing little useful produce are turned into fruitful acreages by the purchase and expenditure, through ET, of irrigation water. In more humid regions, where natural rainfall circumvents this water purchase, the term "expenditure" seems less appropriate; however the process of ET for production is just as important.

The need for understanding the ET process is most pronounced in two disciplines, hydrology and irrigation. Although ET is the same for both, research and application take on a different significance. For irrigation, water

is applied when needed in significant amounts, and the availability of water seldom limits the amount of ET. Under natural rainfall regimes of the hydrologic cycle, water input is sporadic, and water availability often limits ET.

Hydrologic studies, historically, have centered on measurements and estimation schemes addressed principally to those features directly related to design needs. For example, stream flow quantities were estimated by statistics of long-term measurements in conjunction with empirical adjustments based on major influencing factors such as precipitation or land management. These techniques avoided cause-and-effect relationships, which are often undefined or complicated. Recent knowledge has resulted in a trend to be more inclusive; thus, intermediate processes such as ET and infiltration have gained considerable importance in hydrologic studies. Computer modeling of deterministic relationships has greatly enhanced statistical design approaches. Because of the large magnitude of ET and the many interrelations of ET with other hydrologic processes, it is apparent that ET has major importance in hydrologic models.

In hydrologic research and modeling of agricultural watersheds, the occurrence and movement of water is monitored where it is most abundant or is significant to

man's applications. Thus, we continuously measure the amount and rate of precipitation and stream flow, and occasionally monitor soil and ground water. Evapotranspiration often is not measured, but is estimated by soil moisture depletion or as a residual in the watershed hydrologic budget.

The reason for utilizing ET estimates in lieu of more precise measurements is found in the nature of the ET process. Evapotranspiration involves the phase change of liquid water to vapor, and the transport of this vapor from the soil or plant surface upward through the turbulent boundary layer of the earths atmosphere. Neither the phase change nor the turbulent transport are easy to directly measure by currently available techniques.

The required accuracy of daily ET estimates is not readily definable; however, for continuity to persist through weeks and months of model operation, the accumulative ET estimates must conform closely to actual amounts. An operational hydrologic model requires values of daily ET quantities of an accuracy that allows adequate characterization of the interrelated variables such as soil moisture, infiltration, and percolation. Using average daily values for periods of weeks or months has been attempted with some success, but the daily variation is enough to cause significant deviation in some situations.

One set of accuracy criteria could be based on weekly soil moisture measurements which have adequate, but yet limited, accuracy for hydrologic model definition and verification. With a neutron probe, the soil water in a 6-ft soil profile is definable within about 5%, for example 21.0 ± 1.0 in. in a moderatly wet profile. Daily ET values of 0.30 in. would give a weekly accumulative volume of 2.10 ± 0.21 in. (if the accuracy was ± 10%), which would provide much better volume estimates than soil moisture measurements. Accumulative seasonal ET amounts of about 24.0 ± 1.20 in. (if the accuracy was ± 5%) would compare favorably with good soil moisture measurements. Thus, comparable accuracy could be obtained if daily ET estimates were accurate to 15%, weekly volumes accurate to 10%, and seasonal volumes accurate to 2 to 5%.

In summary, it has become obvious in recent years that man's quality of life, and perhaps his extended existence, is dependent on our understanding and management of our water resources. Of particular concern is water used in crop production; this use occurs under two similar but separable water regimes -- irrigation and rainfall. The considerations for this study centered around understanding the ET of agricultural watersheds under rainfall regimes.

The purpose was to better define ET quantities and interrelationships so more precise hydrologic models could be developed; and they, in turn, become tools for future research and design. Only by understanding these naturally occurring phenomena will we be able to manage water for the betterment of mankind.

OBJECTIVES

The general objective of this study was to implement a procedure for estimating daily actual evapotranspiration (ET) from agricultural watersheds which have corn and grass crops, loessial soils, and a subhumid climate.

Specific objectives were:

1. To study procedures for estimating daily actual ET, and to select a method that has good physical basis and that feasibly can be implemented on research watersheds.

2. To obtain data for necessary calculations and verifications of daily actual ET.

3. To develop procedures and mathematical models for processes related to ET for routine use in hydrologic models.

4. To verify the procedures and models by comparing computed results with field observations.

LITERATURE REVIEW

Introduction

To meet the stated objectives, it is necessary to: (1) review the techniques of others for estimating evapotranspiration (ET) and its relationship to general hydrology or hydrologic research, (2) select a method that appears best suited to our problem requirements, and (3) define the details and assumptions of this method. In addition, it is interesting, and worthwhile for added perspective, to briefly review the historic development of ET knowledge.

It is important to keep in view the bounds of our problem. Our general objective was to estimate daily actual ET in a subhumid climate (western Iowa) from small grass and corn covered watersheds which have deep permeable loessial soils. The techniques must be practical within the limits of instrumentation and calculations, and adaptable to continuous operation from very early spring to late fall.

Numerous applications are made of ET among the several disciplines it encompasses. So it behooves us to review only those articles and books which have a rather direct interest. We are fortunate in that several good

symposia proceedings and comprehensive literature reviews have been published in the past 5 to 10 years. These provide excellent reviews of principal articles published in recent years. Some good examples are Rosenberg, Hart, and Brown (1968), Robinson and Johnson (1961), National Research Council of Canada (1961), American Society of Agricultural Engineers (1962, 1966), and Great Plains Agricultural Council (1970). Also, several books written in recent years very adequately summarize the "state of the art" of ET research and applications, such as Chow (1964), Rose (1966), Eagleson (1970), and Kozlowski (1968).

Historical Interest In Evapotranspiration

Evaporation and evapotranspiration have intrigued man for as long as he has wondered about the comings-and-goings of the rains and rivers. Throughout recorded history, scholars wondered why water mysteriously turned to vapor and seemingly disappeared into the air. By 346 BC, when Aristotle wrote the first treatise on meteorology, evaporation was already generally associated with the sun's heat (Biswas 1970, p. 65). Biswas (1970, p. 65) reported that Aristotle "...believed that the heat responsible for evaporation came from the sun and also from the 'other heat from above', but he did not explain his second source." Leonardo da Vinci is quoted as having

written in the late 1400's: "Where there is life there is heat, and where vital heat is, there is movement of vapor." (Biswas 1970, p. 141). It is apparent that little real knowledge about ET had been gained to this time. Edmond Halley, a co-founder of experimental hydrology in the late 1600's reported on experiments in evaporation where he explained: "The process of evaporation was that if an 'atom of water' was heated so that it expanded to become a bubble ten times its original diameter, it would become lighter than air and consequently rise upwards." (Biswas 1970, p. 223). By the late 1700's, pan evaporation was being measured much as we now do; and in 1795 Dalton constructed a lysimeter (10-in. diameter, 3-ft deep) complete with runoff and drainage measurements (Biswas 1970, p. 275). In 1802, Dalton put forth a generalized theory of vapor pressure for estimating the rate of evaporation which is still used and which we will consider later in this chapter and in the derivation shown in Appendix A (Dalton 1802). Several equations have been based on Dalton's Law. Some of these dating from 1886 to 1958 are listed by Veihmeyer (1964).

The 1800's through the first few decades of the 1900's were periods of increased observational activity. For example, during these years the United States established a widespread stream flow and rainfall gaging system.

Increased irrigation in the west stimulated interest in estimating the ET from irrigated areas in various climatic regions and the evaporation from supply reservoirs. Thornthwaite and Holzman (1942, p. 63) quote an article by Marsh (1864, p. 24) in which he states:

> "There is one branch of research which is of the utmost importance ... but which, from the great difficulty of direct observation upon it, has been less successfully studied than almost any other problem of physical science. I refer to the proportions between precipitation, superficial drainage, absorbtion, and evaporation. Precise actual measurement of these quantities upon even a single acre of ground is impossible ... ".

Thornthwaite and Holzman (1942, p. 63) then follow this assessment with one of their own by saying:

> "In the intervening years (1864-1942, authors note) much progress has been made in the measurement of precipitation and run-off, and recently much attention has been given to the problems involved in the measurement of infiltration into different soils and under different forms of soil management. But the measurement of evaporation has continued to be impossible, despite the fact that it has become increasingly necessary as measurements of rainfall, run-off, and infiltration have been improved."

Because of measurement complexities, until the late 1940's nearly all efforts for predicting ET were centered around correlations of observed evaporation or ET with observations of related variables such as pan evaporation, air temperature and air humidity (Blaney and Criddle 1950). During the 1950's Dalton's law (equation) was still

considered to be true, and turbulence theory had become better understood from research conducted during the early aviation history of the 1930's (Thornthwaite and Holzman 1942). The vertical radiant energy budget was generally known and considered quite influential. Yet, progress toward generalized applications has been slow. Dale (1966) states "...despite the voluminous work on the ET problem, its use has still not reached common operating levels." He continues by asking "...is the trouble with the invention, the innovation, or the diffusion?" Much of this same stigma exists today but instrumentation and computers have allowed further advances.

Evapotranspiration as a Hydrologic Component

The process of evapotranspiration (ET) can be approached from many viewpoints. For example, an irrigation engineer views ET as the consumptive use of water, a plant physiologist as that process necessary for plant growth, and a meteorologist as a source of water vapor. To a hydrologist, ET is just one of the processes that results in water movement--although an important process.

Hydrologists have tried to measure, understand, and modify ET for many years. Much effort has been expended in attempting to define the principle variables and relationships of ET, and how other hydrologic parameters vary if ET is altered. McGuinness and Harrold (1962) found that small-area streamflow at Coschocton, Ohio was regulated primarily by seasonal ET. Knisel and Baird (1969) found they could accurately predict runoff from a 3-acre watershed near Riesel, Texas by using a procedure which predicted soil moisture from ET-related variables. Dreibelbis and Amerman (1964) related elements of the water budget to soil types and agronomic practices by their effect on the magnitude of ET. Much of watershed management for altering water yields is based upon altering the ET from the watersheds. Numerous experiments have been conducted, particularly on forested areas, to verify these effects (Goodell 1966).

Hydrologic research is rapidly changing. We are moving from a period of observation into the infancy of understanding. And one of the most recent factors giving new impetus to this direction has been the development of computers which have the ability to store and operate complicated digital models and to assimilate vast amounts of observed data. Hershfield (1966) aptly related

hydrologic models and hydrologic research when he stated:

> "With the increasing importance of water conservation, more detailed knowledge of the entire watershed is required if it is to be managed for optimum development of water resources. The need is especially great for increased understanding of the fundamental processes that operate in a watershed. This understanding can hardly be gained without the help of computers,...."
>
> "A model, however, is only a beginning. Solutions on paper are meaningless if they cannot be tested against observed data...."
>
> "...The watershed must become a prime observational facility."

Certainly ET has been observed as an important component of hydrology. If we are to understand and model the hydrologic cycle with an aim of manipulating the variables for our benefit, then we must learn to implement adequate and feasible measurement and prediction techniques.

Selecting an Approach

The first, and perhaps most important, step in implementing a method for measuring ET is to select the most appropriate method. A cursory review of the literature or texts will reveal that numerous methods have been developed, tested, and applied. There have been several excellent summaries prepared which categorize the more prominent methods, for example Veihmeyer (1964), Rosenberg et al. (1968), and Tanner (1967).

Before discussing the various available methods, it will first be useful to briefly review the physics of the ET process and the criteria of our situation. Almost all basic meterology texts describe the process of ET; for example Byers (1959, p. 328) discusses evaporation as do Sutton (1953, p. 302), and Rose (1966, p. 78). Evaporation and ET are determined by much the same physics and are often treated as a whole with modifications inserted when necessary.

In summary, ET is the process of changing water located in plants or soil from liquid to vapor, and transporting this vapor upward into the atmosphere. Thus, for ET to proceed, water must be present in conjunction with energy for its phase change, and a transporting mechanism must function. Water and energy have the soil and plant surfaces as their main point of confluence, and the water vapor is moved upward by the turbulent transport processes of the atmospheric boundary layer. Tanner (1957) gives a good account of this process. This visualization will be useful for categorizing the various methods of ET measurement.

Another point to review before discussing ET methods is the criteria for our application. For hydrologic research or hydrologic model verification, we must be able to measure or estimate the actual daily ET that has occurred. This is to be contrasted with estimating seasonal ET amounts

as is done when designing an irrigation project. The point to be made is that the method must describe day-to-day variation rather than time averaged values. This requirement stems from the need to know the soil moisture profile status at the begining of each hydrologic event; thus, day-to-day soil moisture extraction must be known.

Several references have been mentioned which categorize the approaches for estimating or measuring ET. Rather than repeat the details, let us simply list the more common approaches along with a brief explanation and discussion of their value for meeting our objectives.

Tanner (1967) gives one of the more complete accounts of ET measurement. He lists three classes: (1) water balance, (2) micrometeorological, and (3) empirical. Let us follow his categorization further with comments added about their potential application.

I. Water balance methods:

A. Catchments--Research watersheds qualify, but do not give daily values.

B. Soil water depletion--daily readings would be required with their inaccuracies and large labor requirement. Tanner (1967, p. 536) states that values are useable if for sample periods of 1 week or longer, but error due to drainage may result.

C. Lysimetry--This is a good time-proven approach. Recent developments for building large weighing lysimeters with

controlled soil moisture tensions have added to their success. ET rates for time periods as short as one hour are readily obtainable. They have two major problems. First, good quality weighing lysimeters are expensive, and, second, a high level of management is required to maintain them as representative of a natural site throughout a growing season. Maintaining comparable soil moisture profiles is particularly difficult.

II. Micrometeorological Measurements:

A. Profile methods--These require gradient measurements of wind, humidity, and air temperature directly above the surface in question, plus good definition of the wind boundary-layer profile. Tanner (1967, p. 551) notes that wind profile measurements are some of the most difficult to make and evaluate. In addition, defining the humidity and temperature gradients requires precise instrumentation and skill.

B. Energy balance--These methods follow directly from our description of the ET process which showed that large quantities of energy are necessary for ET. Tanner (1957) notes that 240 million BTU are required for each acre-inch of ET. This heat comes primarily from solar radiation but advected sensible heat may also be a significant source under certain conditions. As shown by Tanner (1960) the complete energy balance is quite complicated, but usually only the vertical energy balance is used and small terms are assumed negligible over periods of a day or longer. Instrumentation for this approach has advanced rapidly in recent years, probably the most significant being the development of an economical and reliable radiometer such as that described by Fritschen (1963a, 1965a). This approach has been shown to be reliable on an hourly and a daily basis (Tanner, 1960), but the assumptions must be understood (Tanner 1967, p. 546).

C. Combination methods--Several methods have combined the energy balance and aerodynamic (profile) methods, primarily to simplify required measurements. These combined methods possess the strengths of the vertical heat budget and the turbulent transfer methods. But two sets of assumptions and conditions are also imposed. In recent years, the Penman method (Penman 1948, 1956) has been modified to include measured values of net radiation, wind travel, and vapor pressure deficit, all at one height; plus wind profile parameters (Tanner and Pelton 1960). This method has received considerable attention and recent verification over sensitive lysimeters showed it to be quite accurate for time periods as short as one hour under advective conditions (van Bavel 1966).

D. Eddy Correlation Methods--These measure water vapor in transit in the turbulent air above the evaporating surface and, as such, are the most direct measurement approach. However, instrumentation has not been developed to fulfill the necessary requirements of speed and accuracy; thus this appro ch remains mostly in theory.

III. Empirical Methods:

To follow a lead from Tanner (1957, p. 555) in which he states "Since this...is concerned with measurement rather than semiquantitative guessing, empirical methods are not reviewed completely." I neither will review empirical methods in detail. During the past 50 years of ET research, most effort has been directed toward developing empirical methods; several have stood the test of use quite well. A note of caution though--most have been used for predictions of weeks, months, or seasons rather than days.

At a conference in 1966 (Amer. Soc. of Civil Eng. 1966) many of the more current empirical methods used for predicting ET were reviewed. As expected, none are readily applicable to daily estimates, particularly when used outside the region where they were developed. Tanner (1967, p. 555) groups empirical methods into four classes according to their dependance on: (1) radiation (2) temperature, (3) humidity, or (4) evaporimeters. Methods based on radiation have received considerable attention of late, and Tanner (1967, p. 559) groups them into two classes: (1) those based on a rational energy budget but which rely on empirical approximations to utilize existing weather data, and (2) those that are completely empirical, such as regression equations. Tanner also comments: "Because radiation methods are tied more closely to energy supply, they show greatest promise for short-term as well as long-term estimates." The energy balance methods have a physical basis and can be considered in the micrometeorological class; however, several of their variables often must be estimated, thus their applications become empirically based. The method of Penman (1948, 1956) was recently well verified by measuring all variables (Tanner and Pelton 1960, van Bavel 1966).

Direct correlation of net radiation with ET has also been prominent in recent years, particularly since better net radiometers have become available. Often additional variables have been considered, such as air temperature. Some recent examples are the work of Jensen and Haise (1963) and Linacre (1967). Mustonen and McGuinness (1968) correlated measured ET from sensitive lysimeters with daily air and dew point temperatures, wind movement, and solar radiation. For more details of empirical methods, the reader is referred to more complete summaries such as that of Veihmeyer (1964, p. 11-26).

Tanner (1967) concludes his review of empirical methods with the following evaluation:

> "Methods such as those of Penman, McIlroy, Ferguson, and Budyko, which are based on the energy balance, appear most valuable, and have the widest applicability of all methods, particularly when sensible heat transfer from the surrounds is large. Shallow and sunken pans and methods utilizing radiation (with temperature corrections) are the next best choice. Radiation methods may be especially useful for short-period estimates in humid regions where climate is variable. Properly installed pans and radiation methods, when calibrated, are much preferred over calibrated and uncalibrated mean temperature methods."

At this point, the question of whether these methods are predicting actual or potential ET needs to be discussed. This differentiation becomes important for watershed applications because actual ET is often considerably different from potential ET. Water balance methods generally account for actual ET because they measure actual water in place. Under the micrometeorological class, the profile and eddy correlation methods mostly relate to actual ET; but the energy balance and combination methods assume adequate water present at the surface to utilize the bulk of the measured energy. Most empirical methods predict potential ET because they were usually developed for irrigated situations. However, most of these methods account for crop growth; thus, they recognize less than potential ET situations until adequate canopy develops, and again as the crop matures. Good examples are Jensen and Haise (1963, p. 23) and USDA-SCS (1967, pp. 66-88). Some methods have also accounted for the lack of soil moisture, as often is the case under natural rainfall distribution, in which both crop growth and soil moisture effects are involved (Shaw 1963, 1964).

We now have reviewed the major methods available for measuring ET, and raised some salient points about their application to watershed hydrologic research. Of those considered, there are two that stand out as most applicable

for day-to-day ET measurement and are worthy of further discussion: (1) the water balance method of lysimetry, and (2) the micrometeorological combination method. Both methods were recently reviewed; data presented showed that they provide reliable daily ET values throughout the year (Harrold 1966, van Bavel 1966).

Lysimeters have the advantage of providing actual ET measurements, but the representativeness of the values is questionable. It is difficult to reassemble a soil profile in a lysimeter and to maintain the soil moisture profile and crop growth similar to field conditions. These are expensive installations and require considerable maintenance of themselves and the immediately surrounding area. Infiltration and runoff are often not similar to the surrounding field. Lysimeters operate with few assumptions to be satisfied and thus can give quite reliable results if properly constructed and maintained.

The combination energy budget-aerodynamic approach only provides an estimate of the potential for ET. If water availability becomes limiting, additional techniques must be used. Tanner and Fuchs (1968) in recent work have attempted to add surface temperature to make the combination equation applicable to unsaturated surfaces, but this is a difficult measurement and little is gained

for general application. Instrumentation is generally not a severe limitation although it can be expensive. For the Penman method as given by van Bavel (1966), four variables need to be measured at a single height above the crop -- net radiation, wind travel, air temperature, and air humidity. With current electronic sensors and recorders, these measurements can be made continuously with minimal maintenance. There are several assumptions in this approach that impose some operating and accuracy limits; such as assuming soil heat and photosynthesis negligible, wind profile form and stability, and turbulent diffusion coefficients. Most of these are not severely limiting for daily measurements.

Of these two methods, the combination energy balance-aerodynamic method was chosen as the most applicable for hydrologic research. Its greatest disadvantage was the need to account for the difference between potential and actual ET; but ease of instrumentation was an equally strong advantage. In addition, this approach offered the best opportunity for use of routine meteorologic data for predictions of future watershed ET and reconstruction of past ET. This tie to available data becomes very important in hydrologic models.

The Combination Equation

Several forms for combining the vertical energy budget with aerodynamic considerations have been proposed (see Tanner 1967, p. 569). Most have been quite similar. One of the first and the one which has probably received the most attention is an equation proposed by Penman (1948). Penman (1948, p. 120) summarized his method as:

> "Two theoretical approaches to evaporation from saturated surfaces are outlined, the first being an aerodynamic basis in which evaporation is regarded as due to turbulent transport of vapor by a process of eddy diffusion, and the second being on an energy basis in which evaporation is regarded as one of the ways of degrading incoming radiation. Neither approach is new, but a combination is suggested that eliminates the parameter measured with most difficulty--surface temperature--and provides for the first time an opportunity to make theoretical estimates of evaporation rates from standard meteorological data, estimates that can be retrospective."

Penman's concluding equation was of the form

$$E = (H\Delta + E_a \gamma) / (\Delta + \gamma) \qquad (1)$$

where:

E = evaporation
H = net radiation
Δ = slope of saturated psychrometric curve
γ = psychrometric constant
E_a = $f(u)\ (e_s - e_d)$

where:

$f(u)$ = a function of the horizontal wind
e_s = saturation vapor pressure
e_d = existing vapor pressure

In early uses of this equation, estimates of net radiation were made from theoretical solar radiation, percent sunshine, reflection coefficient, and estimated upward longwave radiation. Values of E_a were also empirically estimated. The equation was later extended to include plant factors, but Tanner and Pelton (1960) reviewed this approach in some detail and concluded that it had little basis for general application. One of the most significant advances toward more direct application came when instrumentation was developed for the direct measurement of net radiation (Fritschen 1963a, 1965a). A second, and perhaps equally important improvement, was the definition of $f(u)$ in the E_a term by using turbulent transport theory (Businger 1956).

The full development of the combination equation is somewhat involved and is not readily found in literature. However, when making an application of any equation, it is important to know its derivation and the associated assumptions. The derivation of the combination equation is given in some detail in Appendix A. Even there, the reader will need some background in micrometeorology and

turbulent diffusion to fully appreciate the theories applied and their limitations. No attempt was made to include the several modifications or additions that have been made to the basic equation, such as the plant resistance terms or wind profile stability factors (Tanner 1960, Businger 1959). More detail is given concerning the turbulent transport theory because it is less clearly presented in the literature than the energy budget.

The final equations of Appendix A, numbers 41 and 42, represent the expanded version of Penman's combination equation and provide the basic model applied in this study for computing a potential ET. The equations are repeated and discussed in the section on Procedures.

The combination equation, as expressed by Penman and later modified to include measured variable inputs, has received several good reviews, discussions, and reports of verification. Tanner and Pelton (1960) wrote a particularly good review which included comments on expected relations of evaporation with evapotranspiration and a discussion of stomatal and day-length factors. They compared 48 days of data from lysimeters with values calculated by the combination method for alfalfa-brome grass cover, and concluded that:

> "...a suitable estimate of the energy balance with the Penman approximation is a valuable potential evapotranspiration reference, provided that an appropriate wind function and daytime-nighttime weighting are employed".

van Bavel (1966) reported on a similar comparsion, again using sensitive lysimeters to verify computed values arrived at by using measured variable inputs. He showed representative data from 11 days for alfalfa cover, one day for open water, and one day for wet soil. Hourly evaporation rates were both measured and calculated. These hourly values and 24-hour totals were compared. van Bavel concluded that his results:

> "...gave excellent agreement for 24-hour totals and acceptable agreement on an hourly basis."

His experiments were conducted under irrigated conditions near Phoenix, Arizona where considerable advection occurred. The model adequately represented this oasis situation. He also verified that use of daily average values for air temperature, vapor pressure, and windspeed gave results nearly identical to those derived from hourly values.

Several other recent studies have shown verifications similar to those of Tanner and Pelton (1960) and van Bavel (1966). Cooley (1969, p. 86) showed that the combination method was the best of several methods for determining evaporation from an open water surface. Hellickson (1969, p. 49) concluded that, for irrigated plots, pan evaporation

was somewhat less reliable for predicting actual ET than net radiation or the Penman potential ET method.

Most research and verification of the combination equation has been conducted under conditions suitable for near-potential evaporation or evapotranspiration rates. Some recent studies, however, have used a modified form of the equation which explicitly included a surface temperature measurement (Tanner and Fuchs 1968, Fuchs et al. 1969). Radiometric thermometers have made these surface temperature measurements more possible, but applications are yet limited. Of particular interest is the fact that good results have been obtained with the combination model, even with the somewhat more demanding conditions.

ET Rates Less Than Potential

The combination equation in its original form and many other equations for estimating ET are valid only under conditions favorable for obtaining a potential ET rate. By our earlier definition, this setting for potential ET occurs when water is readily available and the limiting ET conditions are the meteorologic sources of energy. Conditions often exist that meet or closely approximate those for potential ET such as after irrigation or soon after heavy rains. Ponds, very

wet soil, and well-watered green vegetation will supply adequate water to meet or approximate the potential ET rate.

In the case of hydrologic investigations under natural rainfall regimes, water is often not available in sufficient quantities to meet the atmospheric demand. This creates a situation where all available energy is not used for evaporation but is supplied to other processes in the microclimate, such as heating the air, soil, and plant canopy.

Ekern et al. (1967, p. 522) gave a good review of soil and cultural factors that affect ET. They note that vegetation and soil control ET by the same processes, and they classify these factors according to:

1. limiting the water supply to the site of evaporation,
2. reducing the absorption of energy, and
3. restricting vapor or heat transmission.

There are many ways of creating one or more of these three effects; thus, we will review only a few of the major considerations.

Evaporation from a bare soil is described by Gardner and Hillel (1962) as a two stage process: "In the first stage, the drying rate is constant and depends upon the evaporative conditions. During the second stage, the

drying rate continuously decreases with time and with decreasing water content of the soil." They conducted experiments of wetted soil columns and concluded that soil drying rates were closely predictable by the isothermal flow equation for water in soil. Ekern et al. (1967, p. 523) summarized the second stage of drying by noting that the rate at which bare soil supplies water to the evaporative site (soil surface) is controlled by the water content and hydraulic conductivity of the soil. Many soil properties control the soil's ability to hold and transmit water. The reader is referred to texts on the subject such as Rose (1966), Hillel (1971) and Klute (1969).

In addition to physical soil characteristics, there are also cultural or management factors that often play a significant role in limiting or modifying the soil evaporation rate. Bond and Willis (1970) describe the effects of varying amounts of straw mulch on soil water evaporation and evaporation potential. Bresler and Kemper (1970) tested soil crusting effects. Both effects are closely related to the farming practices.

Gates and Hanks (1967) provide an excellent review of plant factors that affect ET. They note that water loss from a plant leaf is related to the concentration gradient of water vapor between the saturated cell walls

of the mesophyll and the free air beyond the plant. If the water supply to the plant is inadequate, the water vapor density at the mesophyll will drop below a saturation value, and the resulting transpiration rate will be less than potential. This view of a single leaf can be extended to a full plant canopy.

Denmead and Shaw (1962) conducted one of the more extensive studies to relate plant transpiration, soil water, and plant environment. Corn was grown in 136 20-gallon containers under controlled watering. Relationships developed from these data showed that actual transpiration decreased with decreasing soil moisture content and increasing potential transpiration. These relations will be considered in the section on actual ET.

Gardner and Ehlig (1963) also considered the relation between soil moisture and plant transpiration. They derived a theoretical relationship between transpiration and soil moisture suction, and conducted laboratory experiments for verification which involved three soils and four plant species. The relationships of transpiration and soil water were similar to those derived by Denmead and Shaw (1962). Many general relationships for describing conditions which limit potential ET have been developed. Most of these have taken the form of relating

the ratio actual ET / potential ET to available soil moisture by using data from laboratory experiments, such as described by Holmes and Robertson (1963). Saxton and Lenz (1967) reviewed several of these relationships and found there were large differences among them because they were derived from many soil types, plant species, or just bare soil. This is apparently a valid approach only where calibrations for the specific conditions have been made. Many of these empirical relations also consider plant development and maturity, such as those given by Jensen and Haise (1963).

Plants can alter ET rates in ways other than limiting water supply to the evaporating surface. Some examples are variation among plant species, influence on reflected light, plant population, plant height, rooting depth, and stage of growth (Gates and Hanks 1967). The number of factors seems overwhelming; however once they are sorted according to relative magnitude and actual physical processes involved, some degree of order emerges.

PROCEDURES

In this chapter, we will discuss the procedural framework which was required prior to instrumention. The general procedures were to first instrument grass and corn sites on experimental watersheds in western Iowa to provide data for the determination of daily potential ET values by the combination method. The daily potential values were then reduced to an actual ET value by considering plant and soil moisture effects. These values were then verified by comparing them with measured soil moisture amounts in conjunction with measured watershed precipitation and surface runoff.

Potential ET

The first step was to develop a "working" form of the combination equation developed in Appendix A. Values were selected for those terms which were to be treated as constants, and measurement methods or estimating schemes determined for the other terms. As mentioned in Appendix A, it is important to maintain consistent units; thus appropriate conversion constants to match the units of the recorded values were required.

To begin, the combination equation as developed in Appendix A, is repeated and the requirements of each term considered.

$$E = \frac{(\Delta/\gamma) R_n + \dfrac{K L d_a u_a}{\left[\ln \left(\dfrac{Z_a - d}{Z_o} \right) \right]^2}}{(1 + (\Delta/\gamma)) L} \qquad (2)$$

where:

$$K = \frac{- \rho k^2 \xi}{P}$$

The symbols, definitions, and representative units are:

E	=	potential evapotranspiration rate	cm day^{-1}
Δ	=	slope of psychrometric saturation line	mb $^{o}C^{-1}$
γ	=	psychrometric constant	mb $^{o}C^{-1}$
R_n	=	net radiation flux	cal $cm^{-2} day^{-1}$
L	=	latent heat of vaporization	cal g^{-1}
d_a	=	saturation vapor pressure deficit of air	mb
u_a	=	windspeed at elevation Z_a	m day^{-1}
Z_a	=	anemometer height above soil	cm
d	=	wind profile displacement height	cm
Z_o	=	wind profile roughness height	cm
ρ	=	air density	g cm^{-3}
P	=	ambient air pressure	mb

k = von Karman coefficient (0.41) -

ξ = water/air molecular ratio (0.622) -

It is obvious that E represents the potential ET to be calculated. A number of the terms on the right can be considered constants. These terms and their values are:

γ	=	psychometric constant = 0.66	mb $^{o}C^{-1}$
L	=	latent heat of vaporization = 583	cal g^{-1}
ρ	=	air density = 1.168×10^{-3} ($25^{o}C$, 1000 mb)	g cm^{-3}
k	=	von Karman constant = 0.41	-
ξ	=	water/air molecular ratio = 0.622	-
P	=	ambient air pressure = 1,000	mb

Of course some of these, such as L, ρ, and P, are not strictly constant, however their variation is slight when compared with the other variables; therefore, they can be treated as constants in our application without significant error.

The term Δ is a function of air temperature, and values are derived from the differential of the psychrometric saturation relation. For application, values of Δ/γ versus temperature have been tabulated (van Bavel 1966). For this study, a polynomial equation was fitted

to these values with good success. The predicting equation was

$$\Delta/\gamma = 0.672 + 4.28 \times 10^{-2}\ T + 1.13 \times 10^{-3}\ T^2 + 1.66 \times 10^{-5}\ T^3 + 1.70 \times 10^{-7}\ T^4$$

Here T, ^{o}C, is the weighted average daylight air temperature. The averaging technique will be discussed in the data reduction chapter.

Remaining to be considered are the measured variables R_n, d_a and u_a, and the wind profile terms Z_a, d, and Z_o. First let us consider the measurable terms, then discuss the wind profile characteristics.

Net radiation, R_n, can be measured directly with calibrated net radiometers. These are generally shielded heat-sensing plates, one facing up and the other down, which respond only to radiant energy. Most have a hemispheric view and respond nearly equally to all wave lengths. For more details on net radiometers, their construction, and application, the reader is referred to Fritschen (1963a, 1963b, 1965a), Idso (1970), and Reifsnyder and Lull (1965).

For daily ET, the amount of daily net radiation is required. The 24-hour totals include the amount of net positive (downward) radiation amounts during hours of sunlight, and the amount of net negative (outward)

amounts at night. The nighttime values represent the release of heat stored in the soil and plant canopy during the day; thus, if these values are to be neglected in the daily heat budget (Appendix A), the nighttime radiation must be measured. This removes the diurnal error and leaves only the net 24-hour soil and plant heat storage as an error, which is usually an insignificant quantity. Thus, the flux rates sensed by net radiometers can be integrated for a 24-hour period to give a good measurement of the required daily net radiation.

Vapor pressure deficit, d_a, is defined as $e_s - e_a$; that is, the saturated vapor pressure of the air at ambient temperature minus the actual vapor pressure at ambient temperature (Appendix A). This term is easier to define than measure. First the air temperature is required, because e_s is a function of air temperature only (assuming standard atmospheric conditions) and is defined by the saturation line of the psychrometric relation. Next, the existing water vapor must be sensed because e_a is a partial pressure determined by the quantity of vapor present. Dew point temperature or relative humidity are usually sensed to determine moisture vapor present. For the combination equation, a suitable time average of

the daily d_a values is required. We will defer this discussion to the chapter on data reduction where we will examine some typical diurnal patterns and select an averaging technique.

Horizontal wind travel, u_a, is a standard meteorologic measurement. However, it has a special significance in our application. We showed by the derivation in Appendix A that vertical vapor transport was related to horizontal wind travel; thus, we are employing a measure of the horizontal wind movement as an expression representative of the turbulent mixing and transport. It is imperative to correctly define the wind profile being measured and the measurement height.

The bracketed terms Z_a, d, and Z_o define the wind profile and the height of measurement. These are standard meteorological terms derived by using turbulent flow theory over a flat, rough surface. Their measurement is quite difficult. Usually they are defined by wind profile measurements at a minimum of about 5 heights over a short (5-15 min.) interval of time; then an iterative least squares technique is applied to get a best fit equation to the profile model (Robinson 1962). This measurement is difficult and subject to several serious restrictions. Assumptions include an adiabatic temperature profile,

adequate fetch with no disturbing features, and constant roughness features of the surface. Considerable deviation from these idealistic conditions occurs on natural watersheds. Generally, the surface is undulating with some pronounced obstructions such as terraces; the crops are sometimes tall and widely spaced or have tasseling and blooming heads protruding above the general canopy level; adiabatic conditions exist for only brief periods during any day.

Obviously, methods for measuring or estimating the wind profile terms are not clearly definable. The theory and definition of the wind profile in the aerodynamic portion of the combination equation derivation was reviewed in Appendix A. To gain insight into recent measurements and attempts to define the wind profile parameters, several of the more recent references are reviewed in Appendix B. Both Tanner (1967) and van Bavel (1966) commented about the difficulties of wind profile measurements, even over reasonably smooth surfaces; and the problems would be increased over our undulating watersheds with medium-to-tall crops. Thus, it was not practical to attempt wind profile measurements.

Several have published d and Z_o values and equations for estimating Z_o values (Szeicz et al. 1969, Lemon 1963). Van Bavel (1966) suggests that calculated potential ET

amounts are not highly sensitive to these terms, therefore their accuracy would not be critical to the solution. Others (Skidmore et al. 1969, Rosenberg et al. 1968) have shown these wind terms can be quite important, and results of this study will also show this to be true. Therefore, it was concluded that d and Z_o values should be estimated from reported values.

An equation for estimating d values was developed such that it would provide values comparable to those in literature. The equation was:

$$d = (0.80) \quad (\% \text{ canopy}) \; (d/d_2) \; H$$

where:

d	= profile displacement height	cm
canopy	= estimated % of ground shading	-
(d/d_2)	= relative d values compared to those at a wind speed of 2 m sec^{-1} (see figure B-1)	-
H	= observed crop height	cm

This equation contains the variables that most influenced d as discussed in Appendix B.

The equations selected for estimating Z_o values were those summarized by Szeicz et al. (1969) and shown in table B-2, Appendix B. These were:

$$\log_{10} Z_o = -0.98 + \log_{10} H \qquad \text{(all crops except maize and sugar cane)}$$

$$\log_{10} Z_o = -1.6 + 1.1 \log_{10} H \qquad \text{(maize and sugar cane)}$$

where:

Z_o = wind profile roughness height cm

H = crop height cm

In addition, a correction to account for the streamlining effects as windspeeds increased was suggested. A correction relation of (Z_o/Z_o at 2 m sec^{-1}) versus wind speed was sketched from data by Lemon (1963) and is shown as figure B-2 in Appendix B. Although these were apparently the best estimating methods available, the analyses which follow show that values predicted by these methods could not be applied to the situation being studied, and another method was employed which estimated values for the complete wind function $[\ln (Z_a - d)/Z_o]^2$.

The length of time over which to use the average wind speed was not obvious. The first inclination was to use daily total wind travel because daily potential ET values were to be calculated. However, this approach was incorrect. The combination equation has been shown by van Bavel (1966) and others to give good results for time increments as short as 1 hour. In essence, the variables are 1-hour totals of R_n and u_a, and 1-hour averages of d_a and Δ/γ.

Note that u_a and d_a multiply in the combination equation; thus, they must represent the same 1-hour conditions. As d_a is averaged for a daily total, u_a should be weighted accordingly. But to define wind travel for several short time intervals was impractical. Thus, the wind travel was accumulated over the same period for which d_a was averaged. As will be shown in the data reduction discussion, d_a becomes nearly 0.0 each night at our location; thus d_a was averaged for the 12 hours 0600 to 1800 by 4-hour time increments, and the wind travel was accumulated for these 12 hours. A better method would have been to multiply corresponding 4-hour wind travel and d_a values but the data reduction would have been increased accordingly. Another alternative was to obtain 24-hour average d_a values and 24-hour accumulative wind travel, but this would have further departed from the incremental correspondence of d_a and u_a values. Both Tanner (1960, pp. 3399-3402) and van Bavel (1966, p. 463) considered this matter.

Each variable in the combination equation has now been discussed. The final step is to constitute the equation in a form which will readily give a solution with field-measured values. With proper constants and conversion factors, it becomes:

$$E = \frac{\xi' R_n + \frac{791\ d_a\ u_a}{[\ln(\frac{Z_a - d}{Z_o})]^2}}{(1 + \xi')(583)(2.54)} \qquad (3)$$

E	=	evapotranspiration	in. day^{-1}
ξ'	=	Δ/γ = slope of saturation line divided by psychrometric constant	-
R_n	=	net radiation	cal cm^{-2} day^{-1}
d_a	=	vapor pressure deficit	lbs in.$^{-2}$
u_a	=	wind travel	miles day^{-1}
Z_a	=	height of wind measurement from ground	cm
d	=	wind profile displacement height	cm
Z_o	=	wind profile roughness height	cm

The units represent those in which the available instruments were calibrated; thus, consistency is not maintained until proper conversion factors are inserted.

Potential to Actual ET

The reduction of potential ET values to actual ET is the second major procedural step to be defined. Several methods were mentioned in the review of literature. These ranged from purely empirical one-step processes such as the curves shown by Jensen and Haise (1963) and the USDA-SCS (1967) to more sophisticated approaches such as

discussed by Fuchs et al. (1969); however, these require additional measurements. Several others have reported on methods which sort out some of the processes involved but lump many of the others, for example those used by Shaw (1963, 1964) and Baier (1969).

For hydrologic research and hydrologic models, it seemed appropriate that the major influencing processes and their interactions should be separated and represented by the current best understanding. This would allow: (1) more complete use of current knowledge, (2) showing which portions of the processes were least understood and need further definition by research, and (3) defining those portions which are most influential in determining water movement to be available for actual ET. Just how definitive one can get in representing such a process is not clearly apparent. This choice is a matter of how many details we know, how many variables and relations can feasibly be handled in a computational scheme, and which details remain important and distinguishable on a 100-acre agricultural watershed when treated on a day-to-day basis.

The principal features affecting actual evapotranspiration can be seen in a schematic presentation of the closed soil-plant-air system shown in figure 1. Of course, the item of primary interest is the movement of water vapor

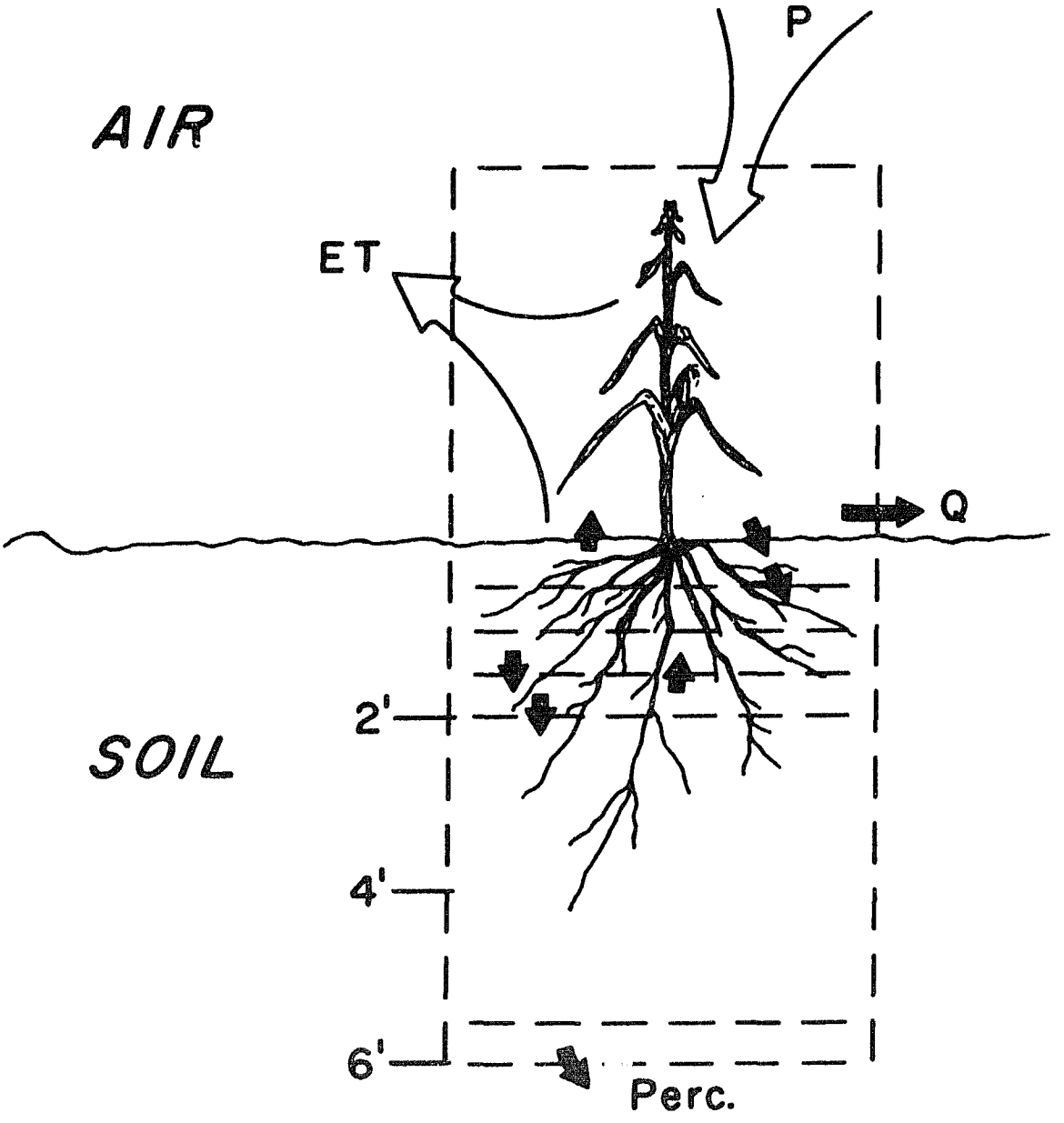

Figure 1. Schematic of the soil-plant-air system to be modeled

out of the system as ET. Tanner (1957) discussed this system and its interactions.

It is well known that the variables considered in the combination equation are those primarily responsible for furnishing the driving energy of the system in figure 1, at least for the water leaving the plant and soil surfaces and entering the air. Most of this energy will be used in ET if water is readily available on the soil and plant surfaces. However, if water is not transmitted to these surfaces at a rate sufficient to utilize the energy available, the transmission rates control the ET rate and a complete set of additional factors is inserted.

The transmission of water in soil depends on the conductivity of the soil and the tension gradients caused by the soil moisture, but conductivity is also a function of soil moisture content. For water to move upward to the soil surface for evaporation, the capillary gradients must work against gravity. For water to be available at the plant surface, it must be absorbed from the soil, transmitted through the plant, and moved to the outer leaf surfaces. This is a highly complex system and not well understood, although some aspects are obvious or have been demonstrated experimentally. For example, the plant roots must be in a soil which has sufficient moisture and the ability to transmit this moisture to the plant.

A well-watered plant will transpire enough water to utilize nearly all available energy. A plant under moisture stress will close its stomata to avoid loss of tugor, and the amount of closure depends on both the degree of moisture stress and the evaporative energy available. Plant transpiration is closely allied with its phenological state; that is, is it actively growing, setting seed, or maturing. Although plant physiologists could add a long list of items which are known about plant-water relations, these just mentioned include most of the major functions that can be represented in a model at this time.

Each of the processes limiting the obtaining of potential ET is closely associated with the amount of water present in the soil. Thus, it is imperative that the soil moisture status be known. This involves knowing the moisture initially present, that incoming as precipitation, and that out-going as surface runoff, percolation, and ET. Other horizontal fluxes should be considered in some situations.

The most obvious method of handling this system was by a mathematical model. The relations considered are sketched in figure 2. We will give a brief discussion of this model in this section with emphasis on required field measurements, then more details and specific relations

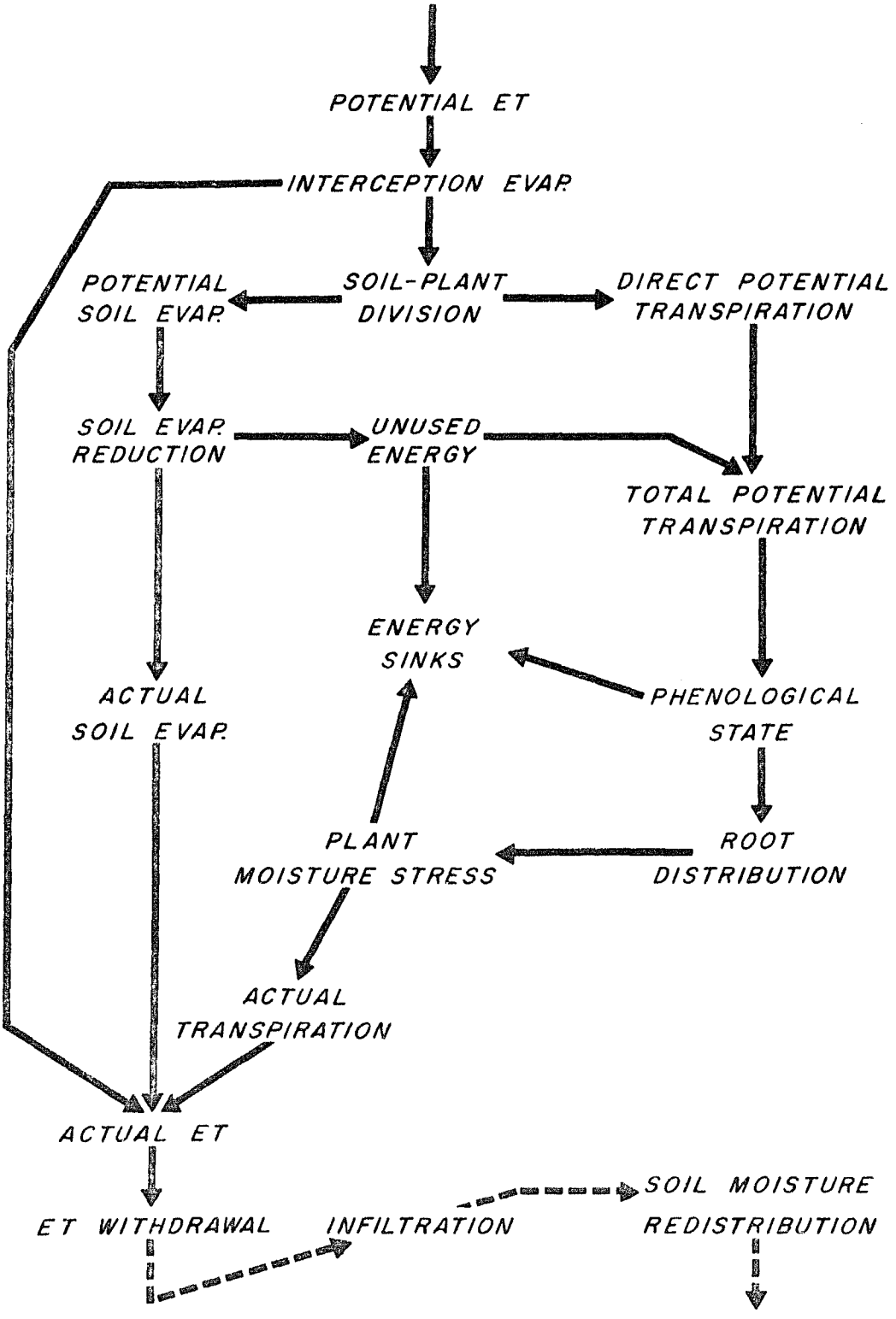

Figure 2. Flow chart of the potential to actual ET conversions

will be summarized in the sections on data reduction and calculations.

For modeling the soil-plant-air system of figure 1, three major sequences are involved: (1) calculating actual ET and substracting it from the soil profile, (2) adding infiltration to the soil profile, and (3) redistributing soil moisture. Although all three processes actually proceed simultaneously, they were treated separately on a day-to-day basis. Calculating actual ET involved separating the amount of energy expended in the major components, whereas all other steps actually involve water transfer.

Beginning at the top of figure 2, daily potential ET values calculated by the combination equation would be reduced by an interception amount if rainfall occurred, because this free water on the plants and soil would evaporate first with very little resistance. This interception evaporation would be the first component of the calculated actual ET. Maximum interception is generally assumed to be about 0.10 inch. If the potential ET was less than interception, actual ET would be equal to the potential ET, and the remaining interception would be held for evaporation the following day. This procedure could be followed regardless of whether a canopy was present. This would allow for wet soil surfaces and water in depression storage, which would evaporate with little resistance.

The potential ET reduced by the amount of interception evaporation, would next be divided between that applicable to soil evaporation or plant transpiration. An estimated canopy-shading percentage would give this division, and thus would be based essentially on radiation. Potential soil evaporation would be reduced to an actual soil evaporation by a relationship depending on the moisture status of the top 6 inches of soil. Soil evaporation could be assumed to come from only the top 6 inches of soil. A portion of the unused potential energy for soil evaporation should be transferred to the plant canopy. This portion depends on the amount of canopy present. Remaining unused soil-evaporation energy would go to other energy sinks, such as sensible heat and soil heat.

Potential transpiration, composed of the divided potential ET plus unused soil evaporation, first would be reduced by a seasonal relation associated with its phenological state which depicts the plants' ability to transpire. Next, a percentage of the daily potential transpiration would be assigned to each 6-in. soil zone depending mostly on the root distribution. Reductions due to soil moisture crop stress would then be considered for each soil zone (center of figure 2) by applying relations similar to those developed by Shaw (1963, 1964)

to each 6-in. depth increment of the 6-ft root zone. Ratio values of actual-over-potential transpiration depend on the soil moisture status and the potential ET demand by the atmosphere. Available soil moisture for each zone would be determined from the previous day's calculations, and the total daily potential ET compared and interpolated.

The actual transpiration coming from each soil zone having been calculated, actual soil evaporation from the upper zone and interception evaporation could be added to provide the amount of calculated daily actual ET. This then would be withdrawn from the soil moisture stored in the profile according to the calculated amounts for each 6-in. soil zone.

To complete the soil moisture situation in preparation for the following day's computation, infiltration and redistribution should be considered (bottom of figure 2). Daily infiltration could be evaluated as an average watershed precipitation amount minus 0.10 in. of interception minus measured watershed runoff expressed as depth from the contributing watershed. No time distribution would need to be given to the infiltration, and it could be considered stored in the upper soil zones as required without exceeding 0.9 of soil saturation.

Vertical soil moisture redistribution would then need to be computed. The best current method appears to be the standard one-dimensional Darcy equation for unsaturated flow which uses moisture-tension and moisture-conductivity relationships (Klute 1969, Melvin 1970). These relationships could be assumed to be uniformly applicable throughout the 6-ft soil profile or defined for each soil depth increment. The moisture content of successive pairs of 6-in. soil zones would determine their relative tensions and average conductivities, which would then be used to calculate the amount and direction of soil moisture movement between 6-in. zones. Constant flow rates would be used for a short time increment, then moisture contents readjusted, and new tensions and conductivities determined for the next period. The soil directly below the soil profile should be held at a constant moisture content of perhaps 0.9 times field capacity (one-third bar tension), and percolation from or to the profile allowed. These calculations would then establish the soil moisture profile conditions for the next day's calculations.

In outlining this model, several relations and parameters were required. It appears that most of the relationships can be empirically estimated based upon rationalization and results reported in literature. These

would include soil evaporation reduction, transfer of unused energy to the plant canopy, the effect of phenological state, root distribution, and plant moisture stress. Undoubtedly some of these are better defined than others, but it is not feasible to determine or verify these relationships within the scope of our current objectives.

Several soil-water parameters are required, such as saturation percentage, field-capacity, moisture-tension and moisture-conductivity relationships. Considerable research related to soil moisture has been done in recent years in the loess area of western Iowa, and most of these soil constants have been determined, although one is always concerned when applying data from another location because of the heterogeniety of soils.

The remaining observations then would be crop canopy (soil shading) and measured soil moisture contents for beginning values. Crop height is already required for the wind profile estimates; thus, a corresponding estimate of soil shading should be adequate. Soil moisture is a routine measurement of hydrologic research and poses no problem.

Evaluation

The primary study objective was to arrive at daily actual ET values; thus, these values must be checked. The most obvious, and perhaps only feasible, means would be to compare predicted and measured soil moisture extraction over periods of 1 or 2 weeks. Problems encountered here include knowing the amount of infiltration and percolation. The amount of measured watershed precipitation and runoff are available and they, as well as percolation, will be considered in the soil-plant-air model. Therefore, the best evaluation will be a comparison of measured soil moisture profiles with predicted profiles from the soil-plant-air model. This will not be a direct evaluation of actual ET and will include several other variables. Actual ET will be the largest process of water removal, and all other variables will be known or estimated with good accuracy.

Although actual ET is the variable of primary interest, it would be remiss not to verify several of the intermediary steps. As previously discussed, the only valid way of verifying the calculated potential ET values would be to maintain a situation where water was not limiting. This was not feasible. An evaporation pan approximates a potential situation except that its exposure allows more

heat to be utilized than would a large body of water or a wet field. Evaporation from a properly maintained pan does have quite a good relation to potential ET, thus, this offers a good choice to relate to the calculated potential ET. Also, potential ET is closely related to measured net radiation for days having small amounts of advection. This offers a second comparison. These two comparisons will not give an adequate quantitative check, but they will show daily sensitivity and relations which can be compared to the work of others.

INSTRUMENTATION

Data were required for each of the three study phases: (1) obtaining potential ET values, (2) converting potential to actual ET, and (3) verification. The combination energy budget-aerodynamic equation to be used for potential ET required four meteorologic variables to be sensed over both of the crops considered, corn and grass. The soil-plant-air model (figure 2) for converting potential ET to actual ET required several observations of the crop and soil status. Soil moisture data were used for verification. In this section, we will review the instrumentation used for each of these variables. Operation and calibration will be explained in the next section, data collection.

Experiment Location

Instruments were established on research watersheds 3 and 4 of the USDA Agricultural Research Service located near Treynor, Iowa. The location of these watersheds is shown in figure 3. This region is characterized by a deep loess mantle over glacial till, well developed drainage systems in the generally rolling topography, and deep permeable soils. A detailed topographic map of these watersheds is shown in figure 4. Also shown on this map are the locations of four recording rain gauges

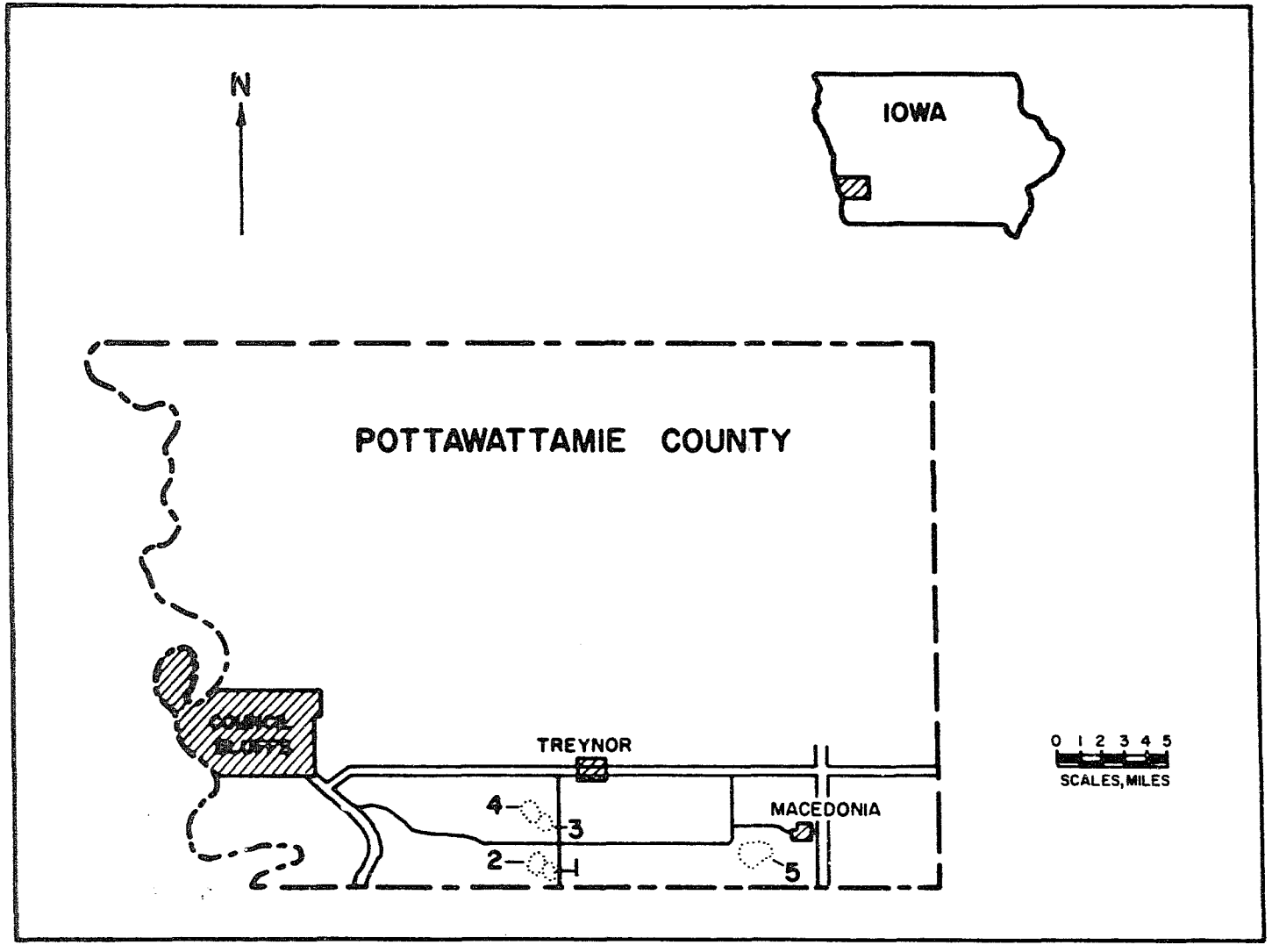

Figure 3. Location of the experimental watersheds which contained the ET instrumentation sites

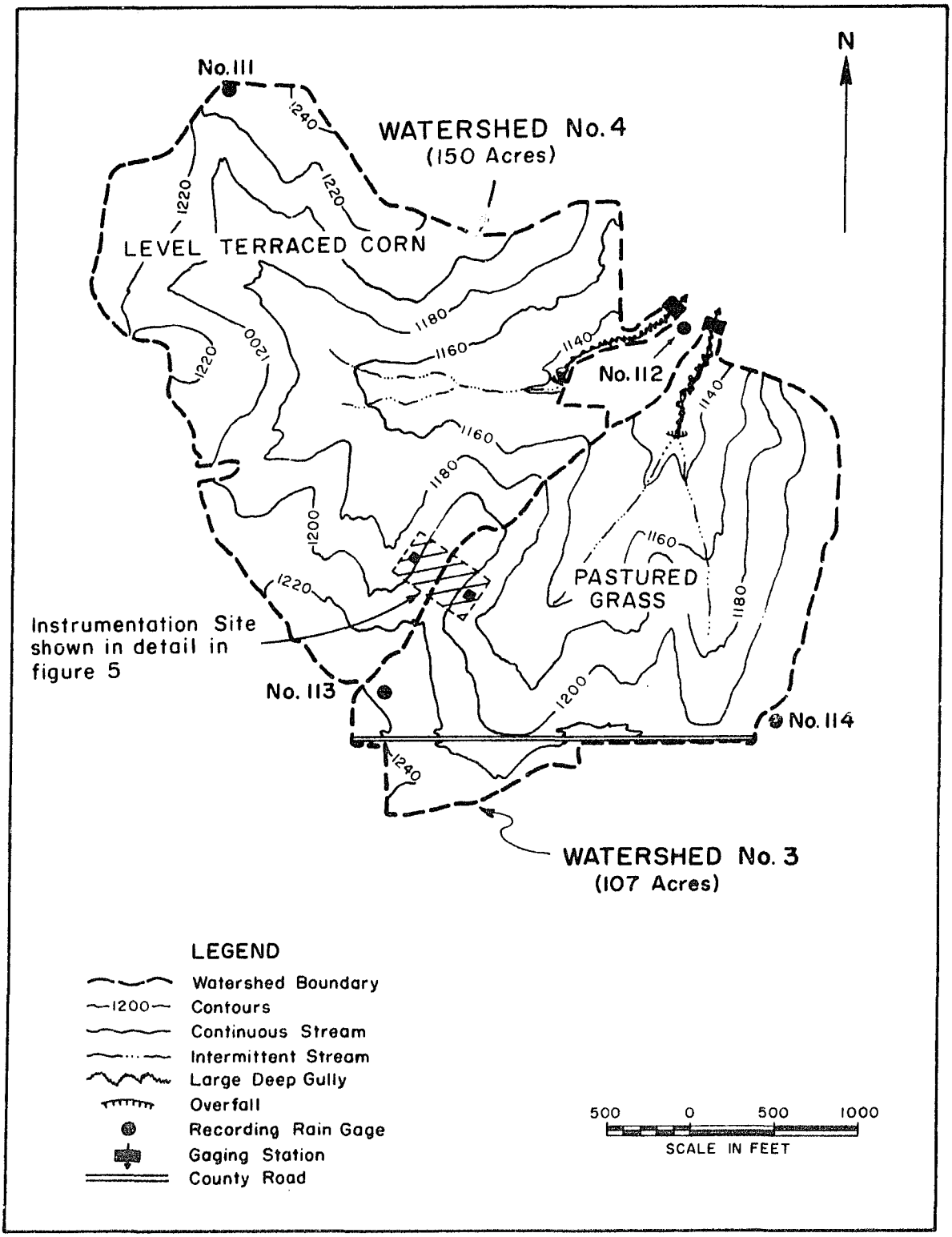

Figure 4. Topography and instrumentation of the experimental watersheds near Treynor, Iowa

and two recording stream flow stations, which were typical installations on all five of the research watersheds. Other watershed instruments not shown but which supplied data for this study are three rain gauges and the stream flow station of watershed 1, six 20-foot-deep soil moisture tubes located on watersheds 1 and 2, and three tubes located on watershed 3. Water levels from some 20 ground-water wells on the 4 watersheds were also used to estimate soil profile percolation. Additional details of these watersheds, their instrumentation, and hydrology were given by Saxton et al. (1971).

The meteorologic instruments were near the boundary of watersheds 3 and 4 within the shaded area of figure 4. A detailed topographic map of this shaded area is shown in figure 5. The watershed boundary is located on the west side of the field road. All of the area west of the field road was in corn, and all the area east was in pastured grass. The grass was mostly brome, with some orchard grass.

The cross section A-A indicated in figure 5 is shown in figure 6. Note that the vertical-to-horizontal scales are in a ratio of 1:5; thus, the vertical dimensions are quite exaggerated. From this view, all of the area left of the recorder shelter was in corn and the area to the right was in grass. It is particularly important to view

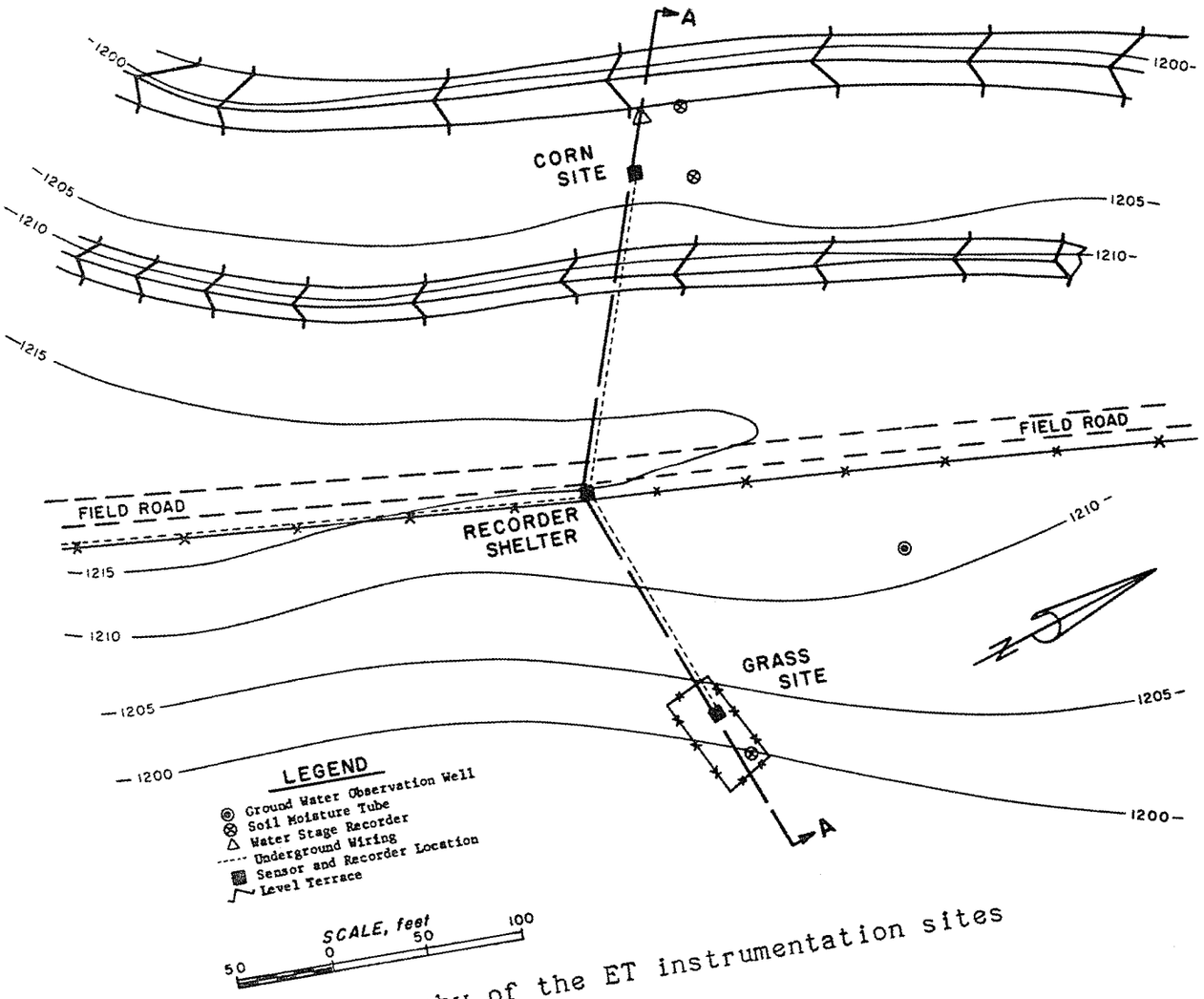

Figure 5. Topography of the ET instrumentation sites

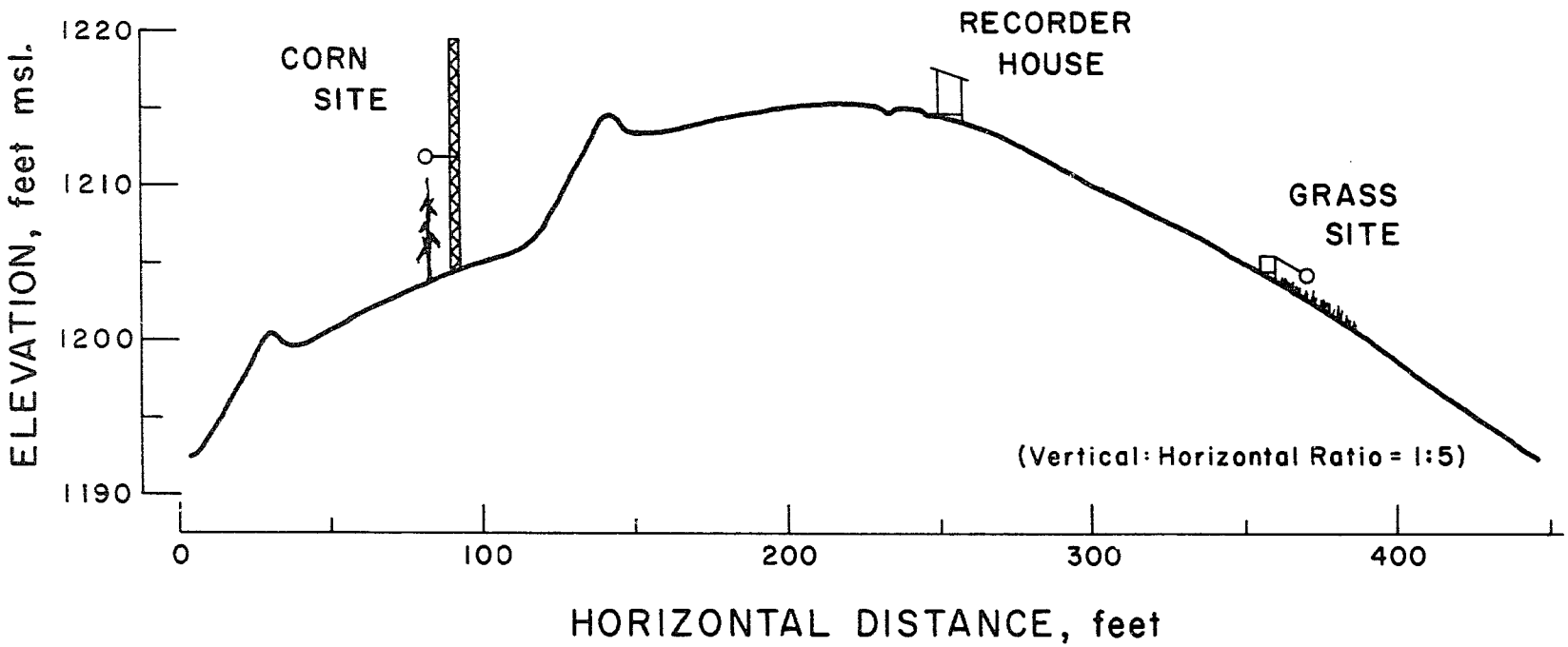

Figure 6. Cross section profile A-A of the instrumentation sites shown in figure 5

the instrumentation in its actual setting as shown in figures 5 and 6 when considering the aerodynamic measurements of vapor pressure deficit, wind travel, and wind profile parameters. Some of the more important features are slope orientation, presence of terraces, amount of site separation, and length of fetch.

Micrometeorological Instruments

Necessary measurements of the combination equation include net radiation, wind travel, and vapor pressure deficit. The first two are directly measurable. Vapor pressure deficit was calculated from measurements of ambient air temperature and dew point temperature.

Net radiation was sensed with a Fritschen-type net radiometer (Fritschen 1963a, 1965a). These radiometers have small, circular, heat-sensing surfaces facing up and down; and both surfaces are protected from convection by a 2-mil thick polystyrene hemisphere. Thermopiles located on the upper and lower surfaces are wired opposing. This arrangement provides a millivolt output corresponding to the temperature difference of the two surfaces, which can then be calibrated in terms of incident radiation. Both surfaces have a completely hemispherical view. This view angle should be considered in instrument placement

and data interpretation (Reifsnyder and Lull 1965). For this study, the radiometers were mounted about 1 meter above the crop surface and were suspended on an 8-ft pipe in a southerly direction from its mounting support.

Wind travel was measured with a standard 3-cup aluminum anemometer. Although these instruments are not the most precise, they offer a good balance between accuracy and durability. Internal contacts were wired so the measured wind travel could be electronically recorded.

An air circulation system using a paint sprayer vacuum pump was established at both sites. An insulated air intake box was located 1 meter above the crop surface, and this box contained a copper-constantan thermocouple for sensing air temperature. This air was then pulled through a 6-in. length of 2-in. diameter pipe which contained a Minneapolis-Honeywell Dew Probe for sensing dew point temperature. These dew probes respond to the equilibrium vapor pressure between the air and lithium chloride. After passing over the dew probe, the air was pulled through the pump and discharged. A valve on the discharge side of the pump was used to pressurize the plastic domes of the net radiometer. The air flow rate over the dew probe was controlled by valves to keep within the instrument's heating capabilities. The dew probe

sensor was a thermocouple which measured the equilibrum temperature established in the lithium chloride bobbin.

The meteorologic instruments and mountings are shown in figures 7 through 15. The sensors mounted over grass are shown in figure 7. The grass was maintained at a height of less than 1 foot; thus, the instruments were mounted stationary. The net radiometer is mounted on the long bracket. The air intake box was located on the back of this bracket and the anemometer to one side. A closer view in figure 8 shows the dew probe in its pipe section, and a bottle of desiccant used to dry the air which was slowly circulated through the net radiometer to prevent condensation on the inside of the plastic hemispheres. The shelter box on the left contains the vacuum pump which is shown in figure 9. Figure 10 shows a close view of the net radiometer in its mounted position.

A similar set of sensors was mounted over corn, as shown in figure 11. In this case, a tower with a sliding cradle was used to maintain the sensors a uniform distance above the crop. A more detailed view is shown in figure 12 where the cradle has been lowered for bare soil conditions.

Signals from both sets of sensors were carried through underground wires to a recorder shelter shown in figure 13, which was located on the watershed divide between the two

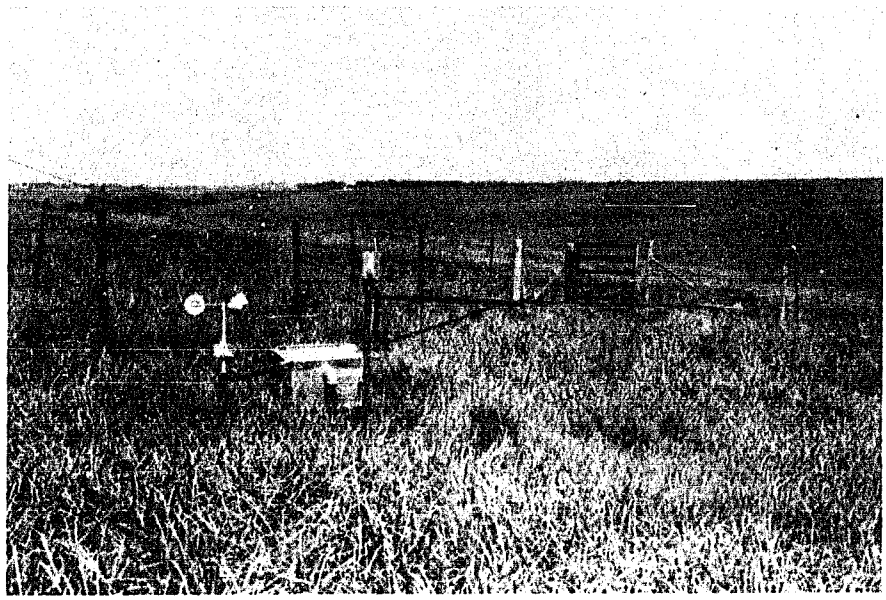

Figure 7. Instrument sensors over grass

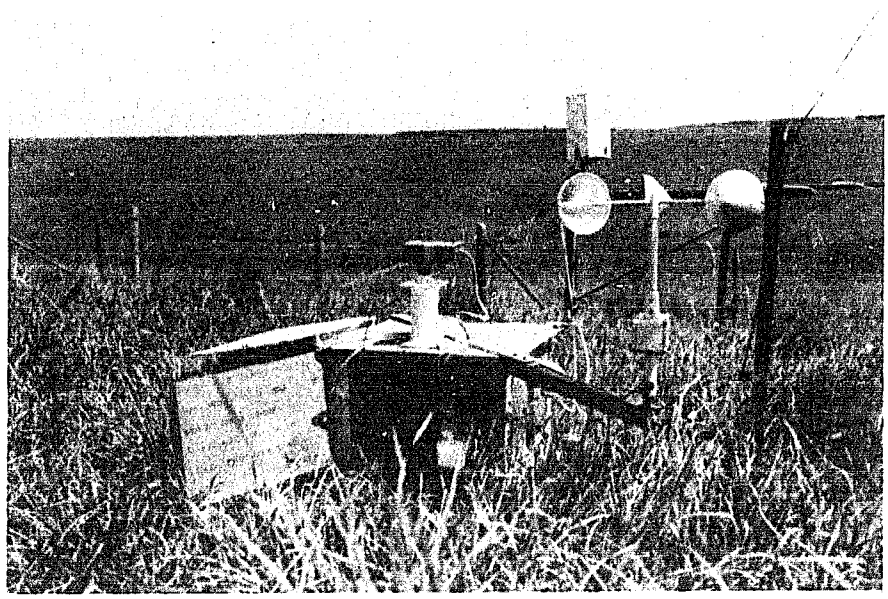

Figure 8. Details of grass site sensors

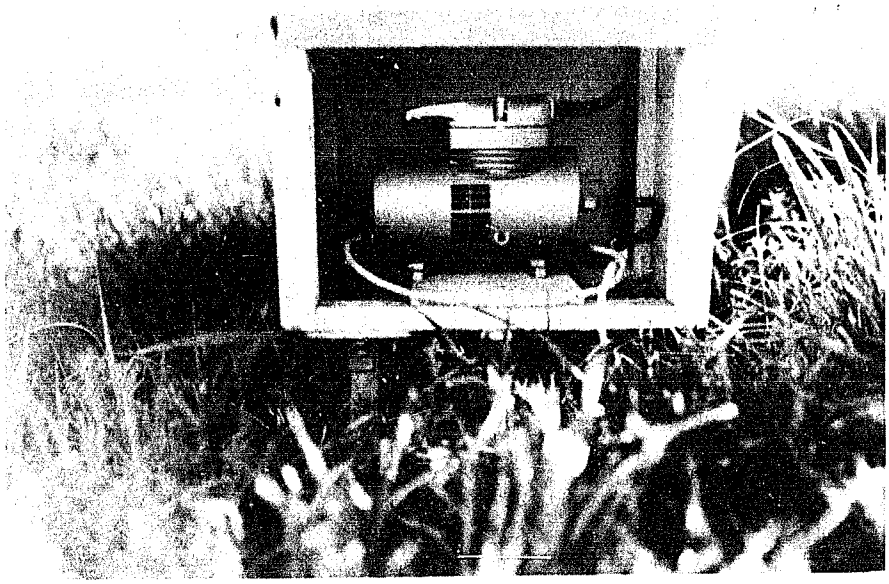

Figure 9. Vacuum pump used for air circulation

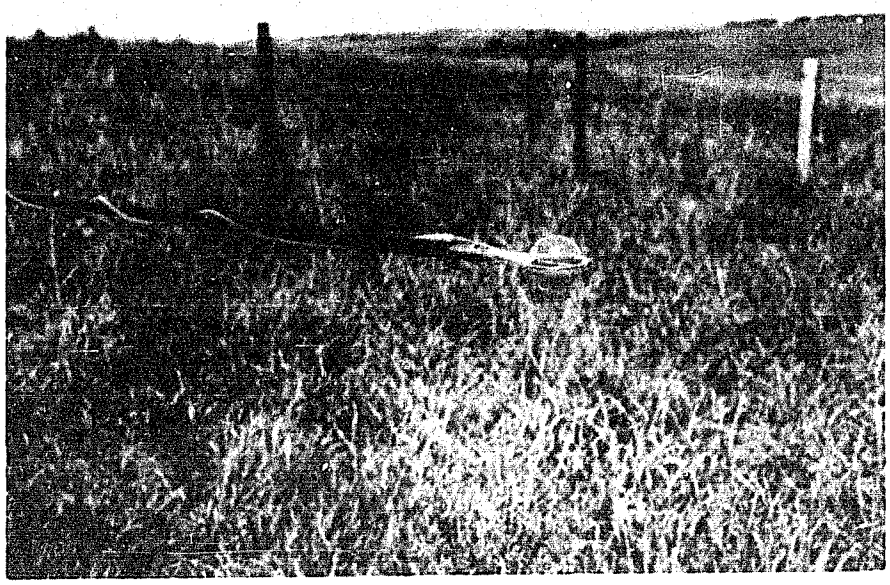

Figure 10. Details of mounting Fritschen-type net radiometer

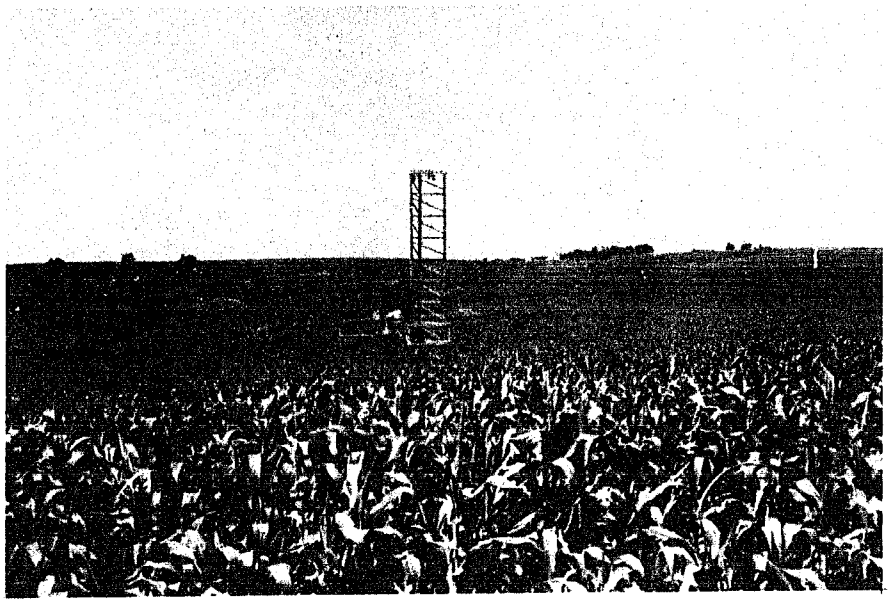

Figure 11. Instrument sensors over corn

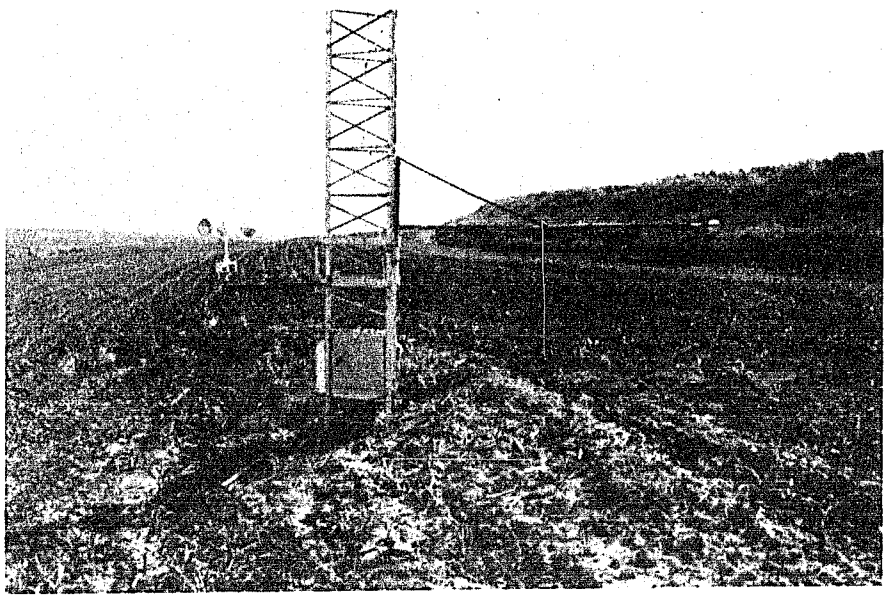

Figure 12. Details of corn site sensors

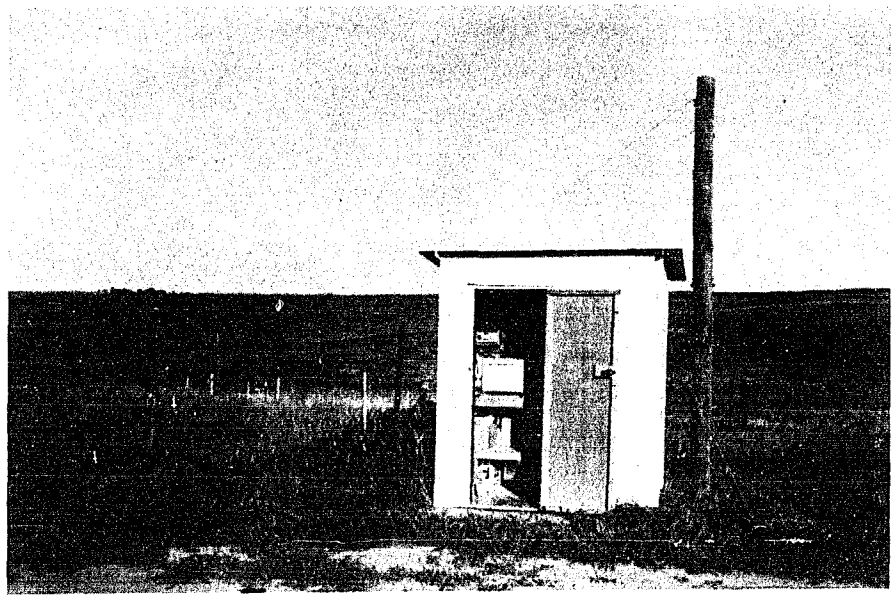

Figure 13. Recorder shelter located midway of corn and grass site

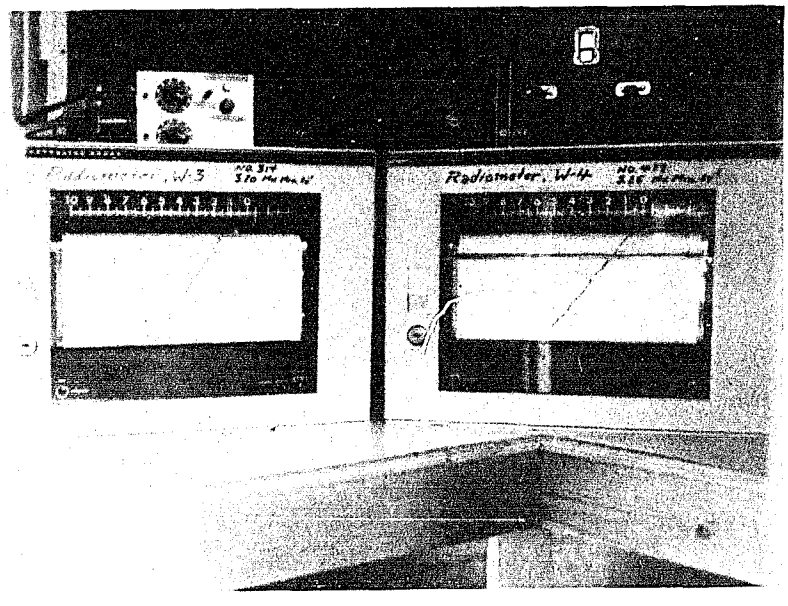

Figure 14. Net radiometer recorders, wind accumulator, and millivolt reference

sensor sites. Three strip-chart analog recorders were used which all had chart speeds of 2 inches per hour. Two were single-pen millivolt recorders with attached ball-disk integrators, shown in figure 14. Each instrument continuously recorded and integrated the signal from one net radiometer.

All other signals were recorded on a multipoint recorder, shown in figure 15, which was capable of recording either millivolts or temperature on any of 24 channels. Air temperatures and dew probe cavity temperatures were recorded directly. For recording wind travel, an "accumulator" was designed and constructed by the University of Missouri electronics shop. This unit, shown on top of the left recorder in figure 14, sensed the closure of a switch in the anemometer which occurred for each mile of wind travel measured. For each such switch closure, the accumulator produced an additional 10 percent of maximum millivolt output, and this output was recorded on the multipoint recorder. The recorded trace was a series of 10 steps from 0 to full scale and then resetting to 0, and each step represented 1 mile of wind travel. The electronic accumulator had two complete channels for recording both anemometers which allowed continuous recording of wind travel with a counting accuracy of about 1 mile for any given period.

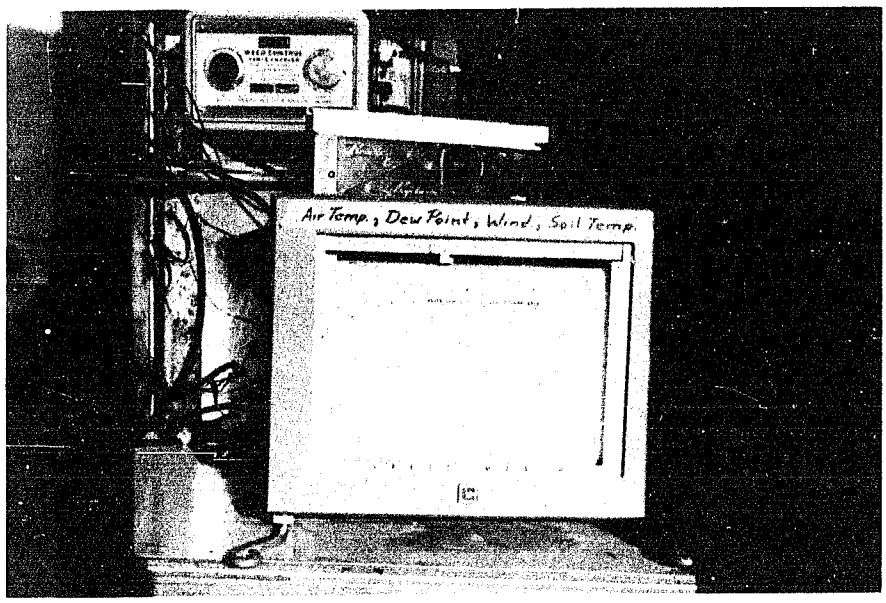

Figure 15. Multipoint recorder, motor ventilated wet-dry bulb psychrometer, and electric cattle fencer

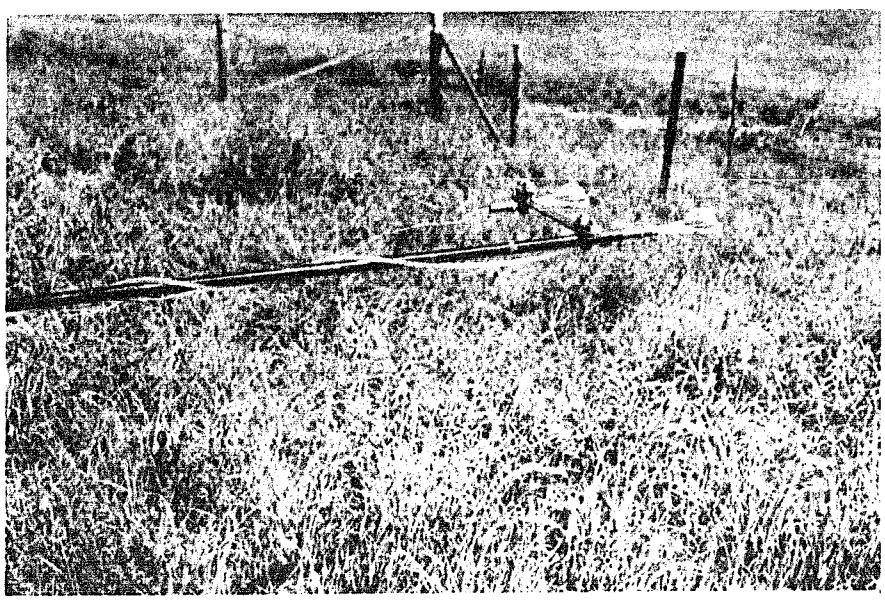

Figure 16. Net radiometers mounted parallel for calibration

Other Measurements and Observations

In addition to the instruments for meteorologic data, several items were visually observed and periodically recorded in the experimental log. Crop heights were recorded at least weekly during periods of active growth, and estimates of crop canopy were made at the same time. The canopy estimates were based on an estimate of soil shading; thus, an 80% canopy would shade 80% of the soil surface at high noon. This obviously was not a very scientific measurement, but the data proved very useful. Many other visual observations were recorded such as crop color, soil surface roughness condition and wetness, weed growth, stage of crop maturity, heading and tasseling, and unusual weather occurrences such as hail and snow.

Soil moisture was measured by the neutron and gravimetric methods under both corn and grass. Instrumentation and procedures previously established for hydrologic research of the experimental watersheds were used. Six 20-ft neutron access tubes had been installed on watersheds 1 and 2 under corn, and three tubes on watershed 3 under grass. One of the tubes for grass was at the grass ET site, and two additional tubes were installed near the corn ET site for comparison with the other measurements beneath corn (figure 5).

A standard meteorologic station previously installed on the research watersheds completed the instrumentation required for this study. Its location was about 750 ft southwest of the meteorologic instruments. Rain gauge number 113 (figure 4) was one of these instruments. Other instruments included a recording hygrothermograph in a standard screened shelter and a standard Class A Weather Bureau evaporation pan. The hygrothermograph had hair elements for the humidity sensor and a bimetallic strip for the temperature sensor. Only the temperature recorder was given special calibration attention by weekly comparison to maximum-minimum thermometers. The evaporation pan was carefully installed and operated according to standard Weather Bureau instructions (Holtan et al. 1962, p. 108). A standard 3-cup anemometer was included, but water temperature was not measured.

DATA COLLECTION

Data collection consisted of operating meteorologic sensors over both corn and grass and making frequent observations of crop and soil moisture conditions. The meteorologic instruments were installed in June 1968. After a period of "debugging", reliable data were obtained beginning in early July 1968 and continuing until December 1, 1968. Several radiometers failed during this period and some difficulty was encountered with the dew probes being heated externally above their operating temperatures by heat from the vacuum pump. Therefore data for this 5-month period were not analyzed. Data were again collected from March 9 to December 1, 1969 and March 13 to December 1, 1970. These 2 years of data formed the basis of all analyses presented.

Collection Methods

All meteorologic sensors and recorders were run continuously. For net radiation, it was necessary to make continuous measurements to obtain both daytime positive (net downward) and nighttime negative (net upward) radiation. The nighttime values of other variables were not used in the analyses; but the complete

diurnal patterns were often helpful in noting data irregularities, and better timing accuracy of the recorders was obtained by running them continuously.

Soil moisture measurements were made at about weekly intervals during the growing season, May to September. Measurements were made at 2- to 3-week intervals during March, April, October, and November. Gravimetric samples were taken at depth increments of 0-3, 3-9, 9-15 and 15-24 in. near each of the neutron access tubes. Neutron probe readings were taken at 6-in. increments from 2 ft to 4 ft, then at 1-ft increments down to and including 18 ft.

Rain gauges and stream flow recorders were operated continuously throughout the year. Ground water levels were measured manually once each week in all observation wells. The water level of the evaporation pan and wind travel recorded by the associated anemometer were read manually at about 0800 hour each day. Some weekend days were not observed, but a diligent field staff kept these instances to a minimum.

The loss of data due to instrument maintenance or failure was very minimal considering the requirement of continuous measurements during all except the very coldest part of the year. The net radiometers were somewhat

troublesome. Several of those first obtained failed because a junction in one of the thermopiles opened causing an open circuit. Vapor condensation on the inside of the plastic hemispheres of the radiometers caused some problems during the first year of operation, but a dry air circulation system solved this problem the second year. A note by Fritschen (1963b) showed that this condensation does not significantly affect the radiation measurements. Maintaining underground thermocouple wire to the grass and corn sites for temperature and dew probe records presented some problems. Moisture and rodents were the apparent problems. It was apparent after the first year's operation that the air properties were very similar over the two crops; therefore these sensors were moved to the recorder shelter for the last part of the second year's operation, and a single measurement made for application to both crops. Wind travel and net radiation measurements were continued over the respective crops.

Instrument Calibrations

Establishing and maintaining correct instrumentation calibration is an important aspect of data collection. An independent calibration was established for each of the sensors and recorders used to collect the meteorologic

data, with the exception of wind anemometers. The following paragraphs discuss each of these calibrations.

The net radiometers were new instruments which had been factory calibrated against a standard. Experience has shown that the rating of these instruments is quite stable over extended periods of use and, because of occasional wiring failures, no radiometer was used more than a few months before being replaced by a new one. This failure was abrupt and unrelated to the calibration. In addition, radiometers were compared by mounting them side-by-side as shown in figure 16 (shown with figure 15). Results of these comparisons usually agreed within 5 to 10% of the factory calibration. It was assumed that the factory calibrations were under more controlled and precise conditions; therefore, the factory-supplied ratings were applied in all cases. For assurance, the radiometers on the corn and grass sites were occasionally transposed if no replacements were installed.

The Minneapolis-Honeywell Dew Probes were calibrated in the laboratory against a precise dew point condensation hygrometer. The calibration points are shown in figure 17, and the factory calibration curve is shown as the solid line. The calibration of the dew probes tested was some-

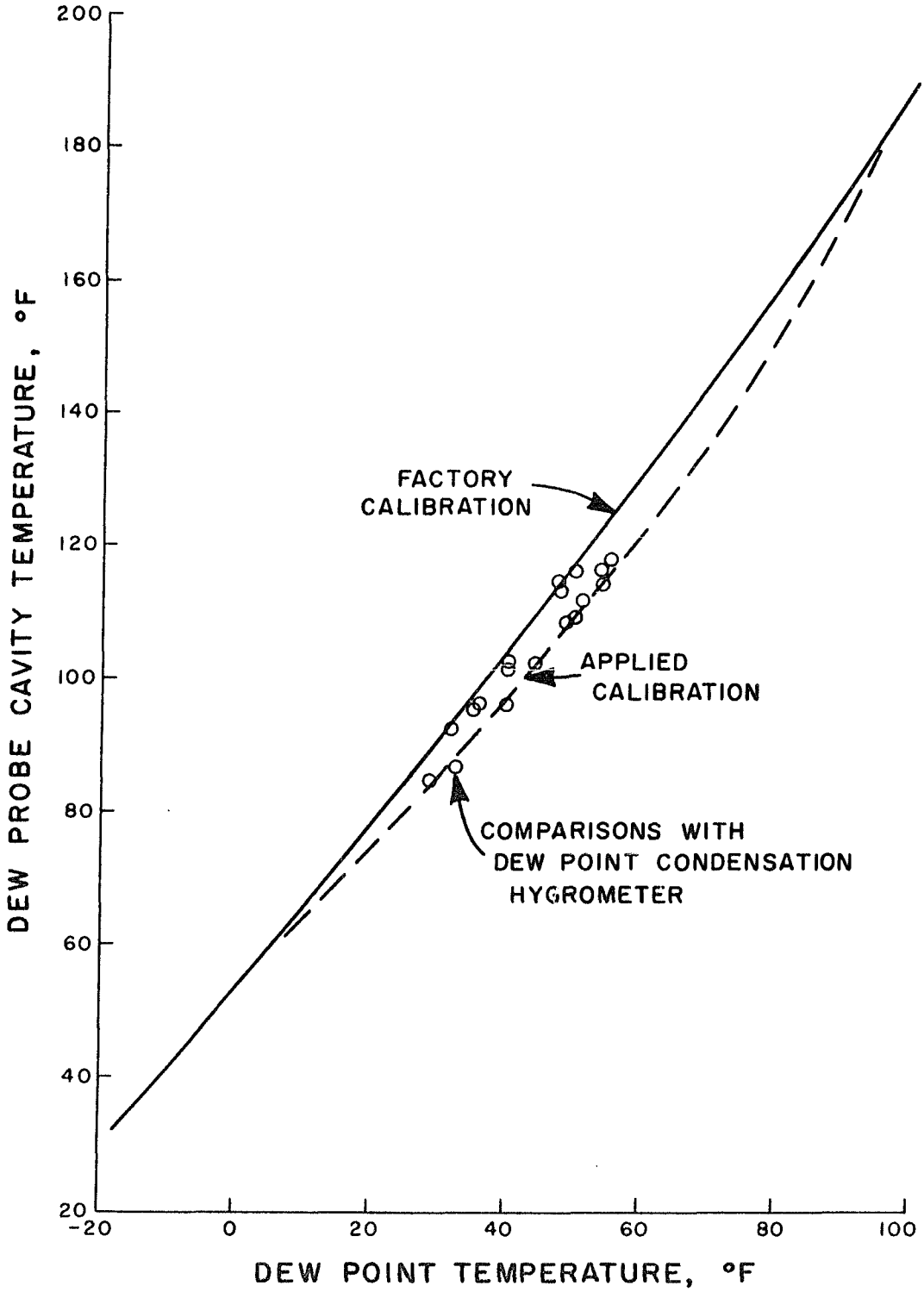

Figure 17. Calibration curves of the Minneapolis-Honeywell Dew Probes

what different from the standard factory calibration; therefore another calibration curve was sketched and is shown as the dashed curve in figure 17. A polynomial equation was developed to represent this calibration curve which facilitated its use in data reduction.

All three recorders were checked for accuracy every 1 to 2 months by using a precise millivolt source obtained for that purpose. This instrument was standardized with an attached galvanometer for each use. All recorders maintained their calibrations within a 3% error. The temperature range of the multipoint recorder was frequently verified with thermometer measurements of the ambient air temperature. Accuracy was always within 1 to 2 °F.

The integrator calibrations of the net radiometer recorders were also verified, first by a laboratory check using constant voltage inputs and then with actual, recorded net radiation amounts. In the laboratory checks, the expected integrator counts could be calculated because the area being measured was that beneath a constant line. The integrators met their stated accuracy of about 1%. Several sections of recorded net radiation traces of one-half to a full day were measured with an integrimeter. When the traces were smooth and relatively easy to follow,

the measured area always agreed with that of the recorder integrator within 2%. It was concluded that these ball-disk integrators were accurate within acceptable limits. They performed very well.

The theory of neutron soil moisture probes has been well verified, and factory calibrations are often applied with confidence. However, instances of considerable deviation from standard calibration curves have been reported. To verify the calibration of the probes used for this study, a series of measurements were made in access tubes previously used for a soil water movement study, then the soil moisture was determined gravimetrically using a 3-in. diameter by 3-in. driven core sample. The tubes were located in and adjacent to two small pits about 10-ft in diameter and 2-ft deep which were filled with water for 1 to 2 days, and then allowed to be dry about 3 days before measurements were made. Neutron readings were made at 6-in. intervals below 18 in.; then the soil was excavated and three gravimetric samples taken at each depth and averaged for the calibration. Typical calibration points are shown in figure 18 with the factory rating curve. It was concluded that the neutron probes had been adequately rated and the factory curves were applied.

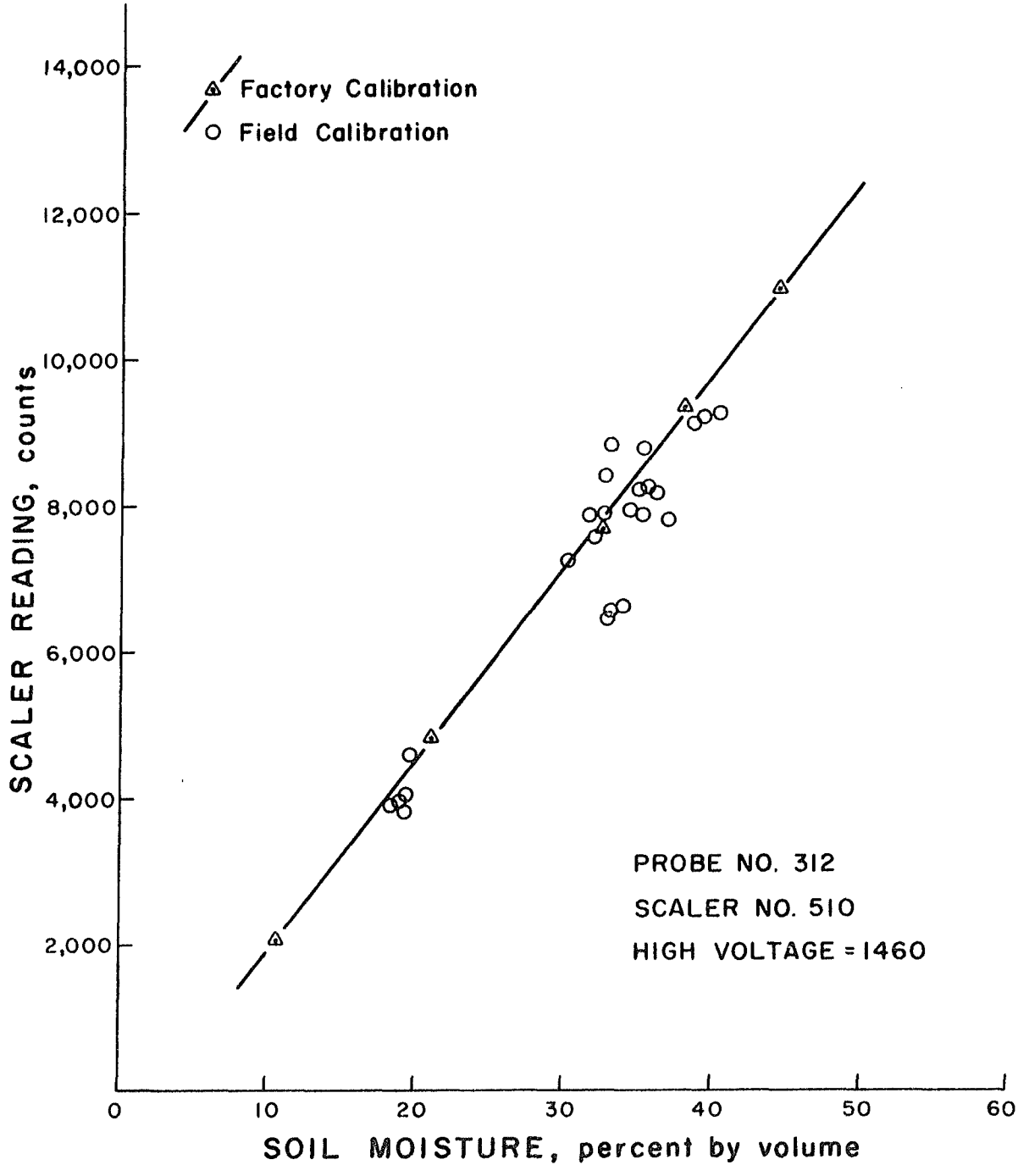

Figure 18. Calibration curve for neutron soil moisture probe

An electrically-ventilated wet and dry bulb psychrometer was used once each one or two weeks to verify the air temperature and dew probe readings (see figure 15). It was usually possible to verify the relative humidity within 5% in the range of 40 to 80% humidity. If less accuracy was obtained, a change of the lithium chloride dew probe bobbins was usually indicated. Although the anemometers could not be independently calibrated, they were frequently inspected and occasionally cleaned to assure free turning and proper operation.

Reduction

All of the data were tabulated from the recorder charts or field records and placed on computer punch cards for processing. This was a straightforward matter, but some decisions were required to insure that the data would match the intended use.

Daily net radiation values were tabulated as three components: (1) midnight-to-sunup negative values, (2) daytime positive values, and (3) sundown-to-midnight negative values. This tabulation allowed flexibility of periods for which the daily values could be summarized. For this

study, the daily values were taken as the daytime amount minus the following sundown-to-sunup nighttime amount. Subtracting this nighttime amount partially compensated for soil heat storage which occurred the previous day.

To obtain a vapor pressure deficit value, it was necessary to first determine the equations for calculating the vapor pressure deficits from recorded values. The two measurements used were ambient air temperature and dew point temperature, with the dew point obtained from the observed dew probe temperature and its calibration curve. The existing vapor pressure and the potential vapor pressure at ambient air temperature are both defined by the saturation line of the psychrometric chart, and the difference between these two vapor pressures is the vapor pressure deficit. Brooker (1967) noted that the Clausius-Clapeyron equation expresses the slope of this saturation line, and he showed that by integrating this equation for conditions above freezing gives:

$$P_s = e^K$$

where:

$$K = 54.6329 - \frac{12301.688}{T} - 5.16923 \ln T$$

P_s = saturated vapor pressure lb in^{-2}

T = ambient air temperature ^oR

and for conditions below freezing

$$K = 23.3924 - \frac{11286.6489}{T} - 0.46057 \ln T \quad .$$

Therefore these two equations were used with the ambient and dew point temperatures to calculate a vapor pressure deficit value.

An average daily vapor pressure deficit value was required for computing a daily potential ET value with the combination equation. The ideal single value would be a true average of the complete daily distribution. Although the continuous records of air and dew probe temperatures would have allowed defining the complete distribution, the volume of tabulations and computations would have been prohibitive. The apparent solution was to select a minimum number of readings that would provide an acceptable average value.

It was concluded from findings of Tanner and Pelton (1960, p. 3400) that day and night values of ET must be treated separately. Because our net radiation values represent the daylight condition, the vapor pressure deficit and wind travel should also be daytime values. Therefore the d_a values should be an average value representing the sunup-to-sundown period.

To arrive at a reduction method, a series of daily vapor pressure distributions was reviewed and several methods of averaging selected values were investigated. Several typical daily vapor pressure distributions are shown in figure 19. Daily distributions were defined for 24 uniformly spaced days during 1968 and 1969 using 2-hour time increments. The objective was to obtain a representative average of the period from 0600 to 1800 hours. After investigating 8 averages from combinations of one to four values, a system was selected which used four readings at 0600, 1000, 1400, and 1800 which were weighted by values of 1,2,2, and 1, respectively, to account for the portion of the day each represented. These 4-value averages were linearly correlated with the 13-value averages obtained by 2-hour increments. Average means for the 24 days were 0.123 and 0.126 for the 4- and 13-value averages, respectively; the correlation equation was $y = -0.001 + 1.025\ x$; the coefficient of determination, R^2, was 0.994. From these results, it was concluded that a weighted 4-value average would give very adequate daily representation, and this system would be manageable for data reduction.

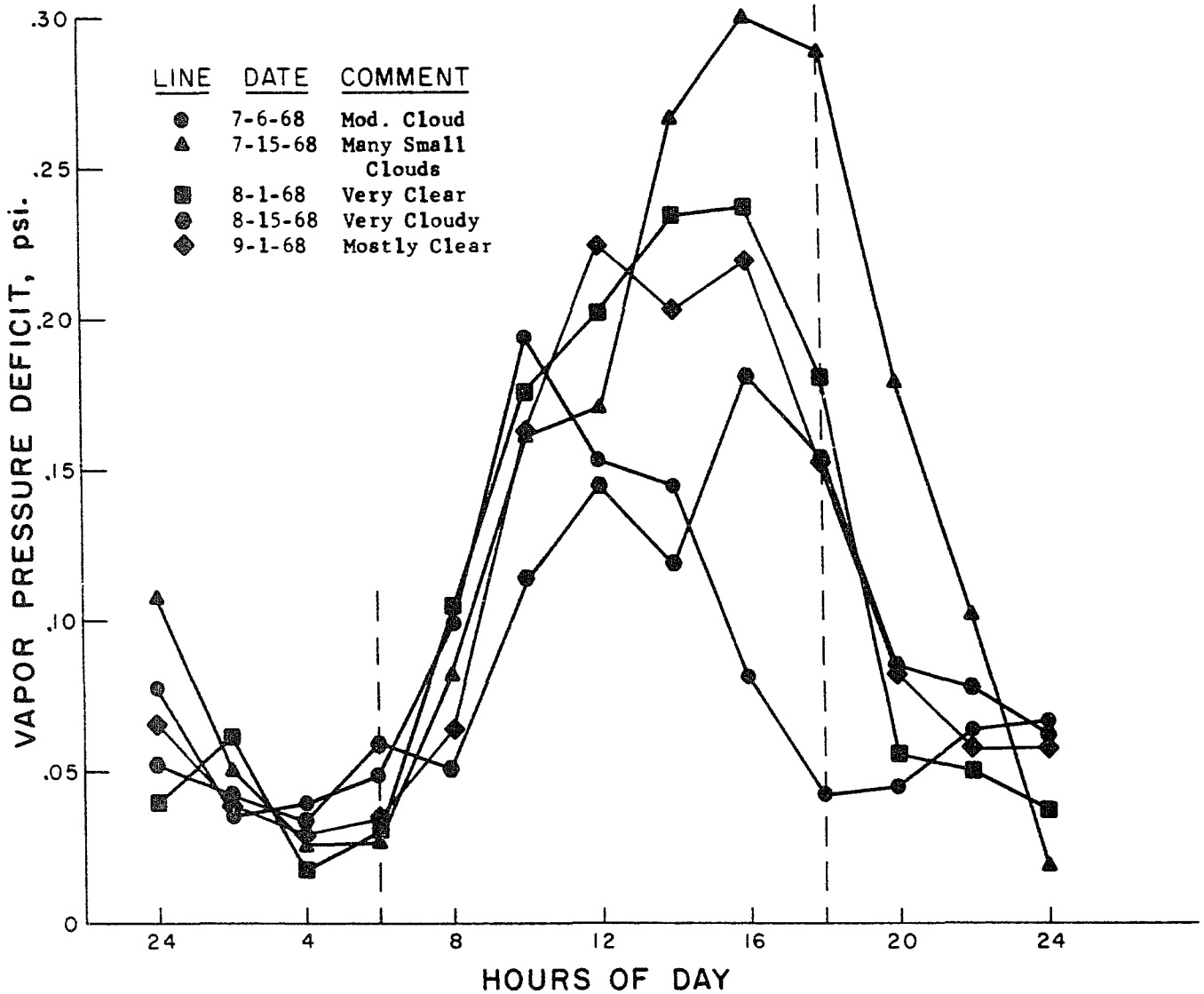

Figure 19. Typical diurnal patterns of vapor pressure deficits

Wind travel was tabulated as the recorded amount for the 12 hours, 0600 to 1800. This period corresponded to that represented by the vapor pressure deficit average, which must be true for proper integration. A more precise method would have been to tabulate the wind travel for each 4-hour period and multiply by its corresponding vapor pressure deficit, but van Bavel (1966) has shown that daily averages can be used with good success. A computational trial which used total daily wind travel, 0000 to 2400, gave values too large for the aerodynamic term, which showed that nighttime values must not be used.

Neutron soil moisture data were reduced by using a computer program to: (1) prorate the field scaler counts by a ratio of recorded shield counts to standard shield counts, (2) determine the moisture percentage represented by each adjusted reading, (3) summarize the amount of moisture in the soil profile, and (4) average the moisture from the several holes to obtain a value representative of the soil moisture status under that crop. This technique had been previously developed by the author and was adapted to this study. The gravimetric soil moisture data which represented the top 2 ft of soil were computed and averaged with a manual calculator. Standard procedures were used to obtain percent-by-weight values; then a standard bulk density

profile was applied which had been previously determined from more than 200 measurements. These bulk density values were 1.33, 1.31, 1.25, 1.22, and 1.21 g/cc for the depths 0-3, 3-9, 9-15, 15-21, and 21-24 in., respectively. Bulk density is quite variable, and applying an average set of values surely introduces some discrepancy and bias. However, this remains as the only practical method of obtaining soil moisture in the surface horizons.

Evaporation pan reductions were simply a mass budget of the pan water. Water added by rain was accounted for by records from the adjacent rain gauge, and an overflow tank was used for periods of large rainfall. Calculated evaporation for days with moderate to heavy rainfall often appeared much larger than expected. The only logical reason was that the pan and rain gauge caught different amounts of rainfall. Values for these days were omitted from further consideration if they were considered unrealistic.

METEOROLOGIC DATA CHARACTERISTICS

It is important to review the data to assure its accuracy and validity before proceeding with computations. Even though instrument calibration precautions were taken, it is possible that error and bias may have been introduced by the data collection and reduction procedures. In addition, there are some interesting features of the variables themselves that are important to understand for this study and for those that will follow.

The data are presented in several ways: (1) plots of annual distributions of daily values, (2) comparisons among the variables, and (3) comparisons of separate measurements of the same variables. Most of the major meteorologic variables will be discussed in the following paragraphs and examples shown of plotted relations.

Net Radiation

Net radiation over a particular surface is primarily a function of the incoming solar radiation and cloud cover. The annual distribution of measured daily net radiation largely reflects these parameters. Data for 1970 corn shown in figure 20 are quite typical. The envelope curve of maximum values is apparent and represents very clear days.

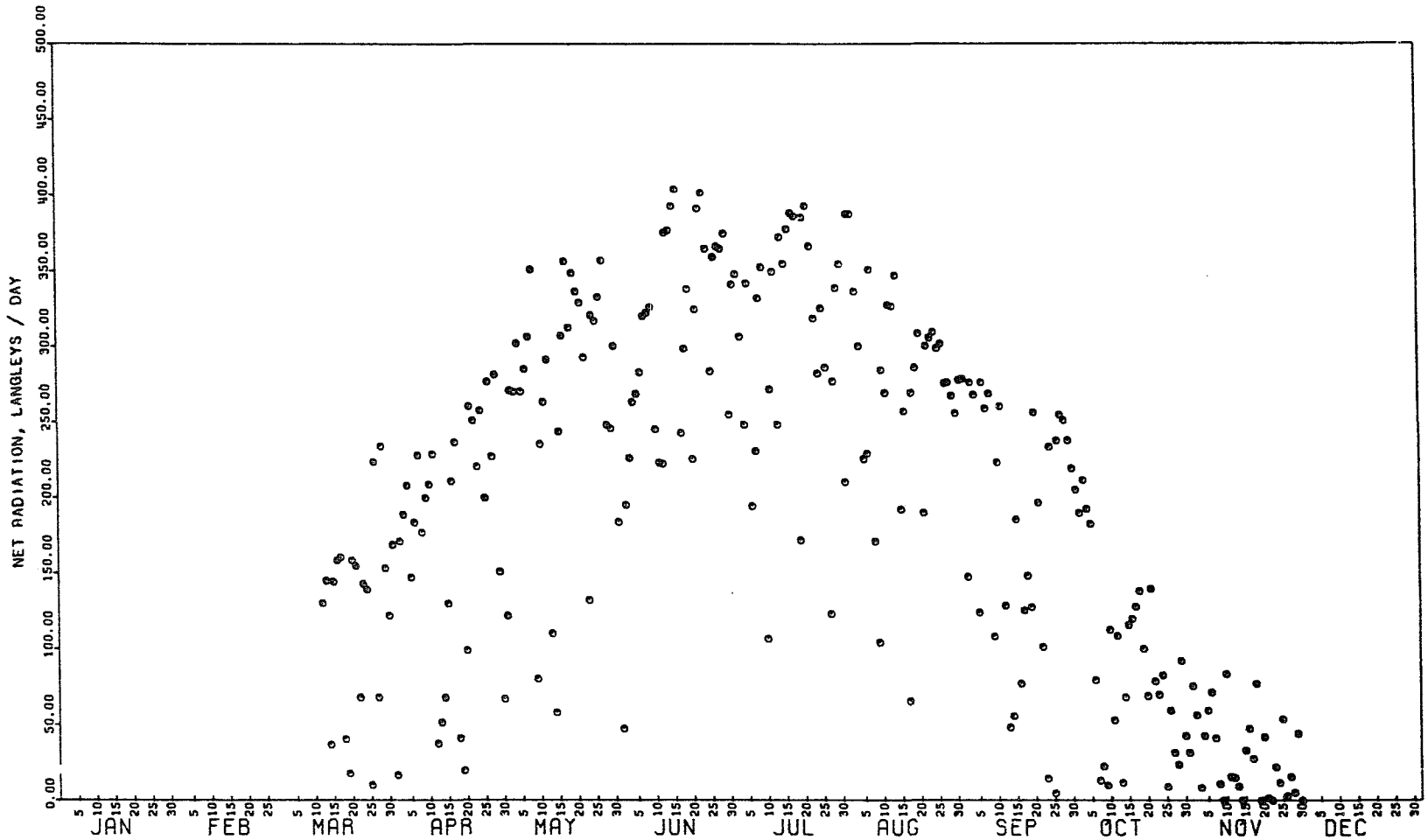

Figure 20. Annual distribution of daily net radiation over grass during 1970

A significant number of days had values below the maximum throughout the year. As we will see later, this net radiation distribution and variability plays an important role in daily potential ET.

The relationship of net radiation to total incoming solar radiation is important because solar radiation is a frequent standard measurement at many meteorologic stations. The measured net radiation was compared with solar radiation measured by the U.S. Weather Bureau at the North Omaha Nebraska airport, located about 25 miles northwest of the instrument sites. They used an Epply pyrheliometer with a millivolt stripchart recorder. The daily traces were manually integrated by using estimated averages for periods of 1 to 2 hours. A typical relation of net versus solar radiation is shown in figure 21 for corn cover from March to December, 1970. The relationship would provide reasonably good predictions, with net radiation averaging about 54% of the solar radiation. However, the ratio of net over solar radiation has a significant annual trend as shown by the example in figure 22. The mean relation, represented by a polynomial equation fit by the least squares technique, shows that the ratio values range from about 0.36 in early March to about 0.56 in July, and return to about 0.36 in late November. This annual variation is

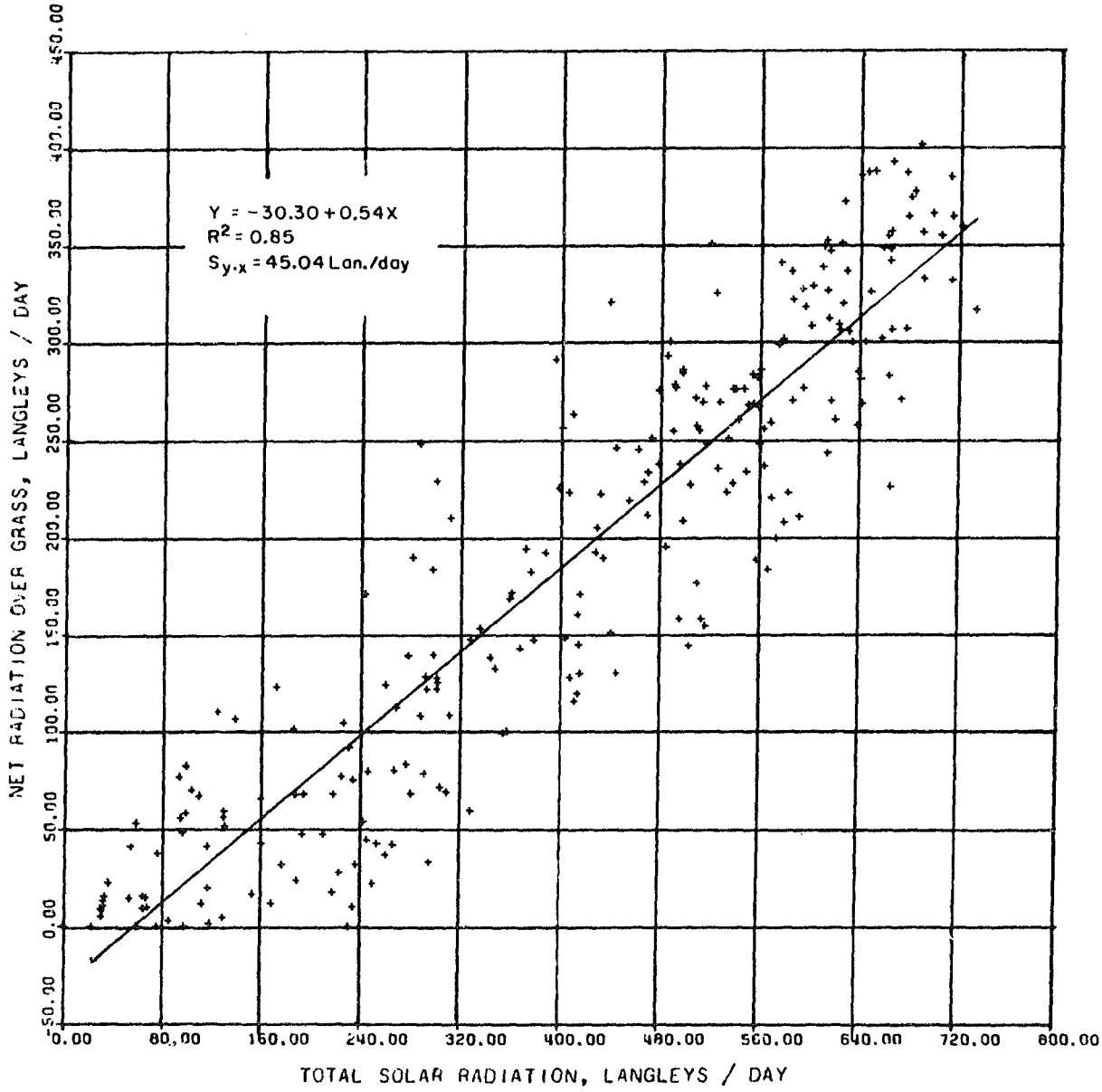

Figure 21. Daily net radiation over grass compared with daily solar radiation at Omaha, Nebraska, March 13 to December 1, 1970

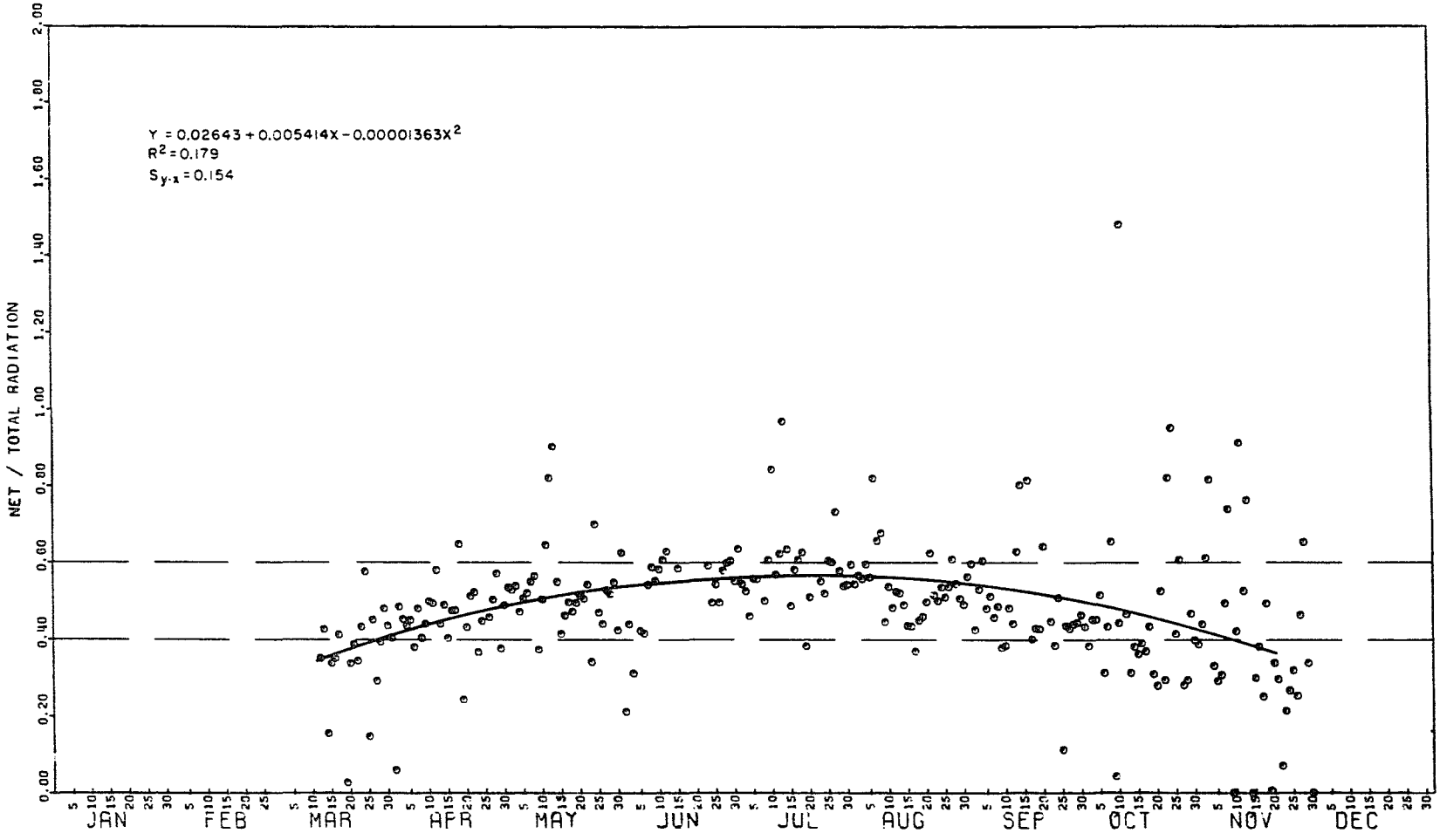

Figure 22. Annual trend of the ratio of net over total radiation during 1970 with corn cover

masked in the scatter comparison of figure 21. Similar relations were obtained for both years over both corn and grass. A summary of the equations is given in table 1. The relatively low values of R^2 are more a result of the generally horizontal least squares line than of predictability, although the values do have considerable scatter, particularly early and late in the year when radiation is small.

The effect of crop cover on net radiation is sometimes subtle and unpredictable because both reflectance and emittance characteristics are involved. The dual net radiation measurements made over corn and grass compared closely as shown by the example in figure 23. Daily ratios of net radiation from grass over that from corn were plotted in an annual distribution, as shown in figure 24. There were some trends, although they were not as apparent as the relation of net over solar radiation. The corn ground had slightly more net radiation until the grass was completely green in early May. Then there were only small differences until about October when the corn matured and was harvested, and the grass began to brown. There appear to be some small, consistent trends within these generalities which are probably real and caused by observable

Table 1. Polynomial equation representing the annual trend of the ratio daily net radiation over daily solar radiation

Year[a]	Crop	Equation Coefficients[b]				
		A	B	C	R^2	Sy.x
1969	Grass	-0.00630	0.006956	-0.00001940	0.445	0.140
1970	Grass	- .22167	.008323	- .00002183	.493	.123
1969	Corn	.19792	.004918	- .00001420	.314	.149
1970	Corn	.02643	.005414	- .00001363	.179	.154
1969-1970	Grass	.11142	.007616	.00002056	.671	.135
1969-1970	Corn	.11388	.005152	.00001389	.468	.155

[a]Inclusive dates of data are March 9 to December 1, 1969 and March 13 to December 1, 1970.

[b]Equation Model is

$$Y = A + BX + CX^2$$

where:
Y = daily net radiation/daily solar radiation
X = consecutive day number of the year

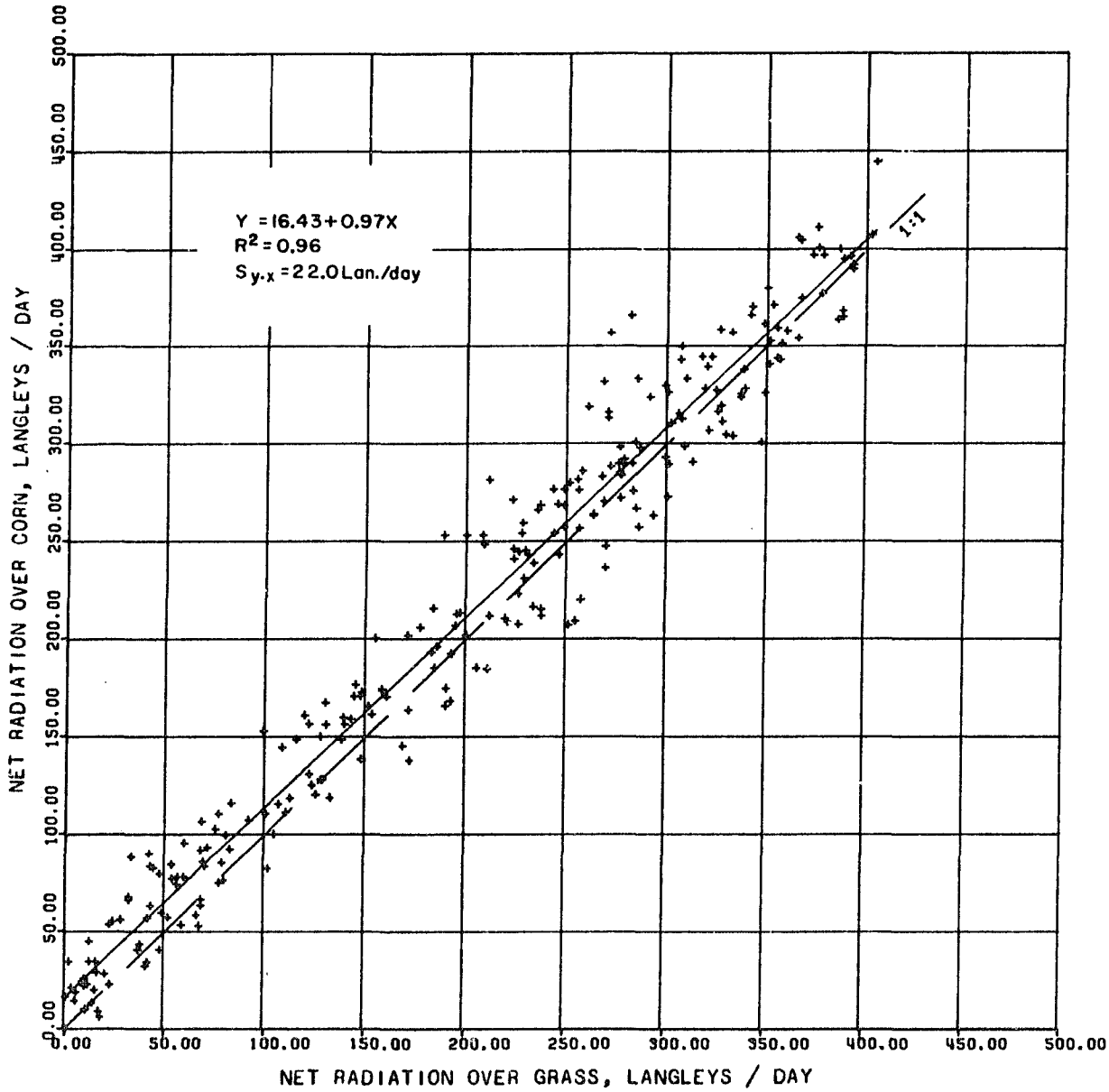

Figure 23. Daily net radiation over grass compared with that over corn, March 13 to December 1, 1970

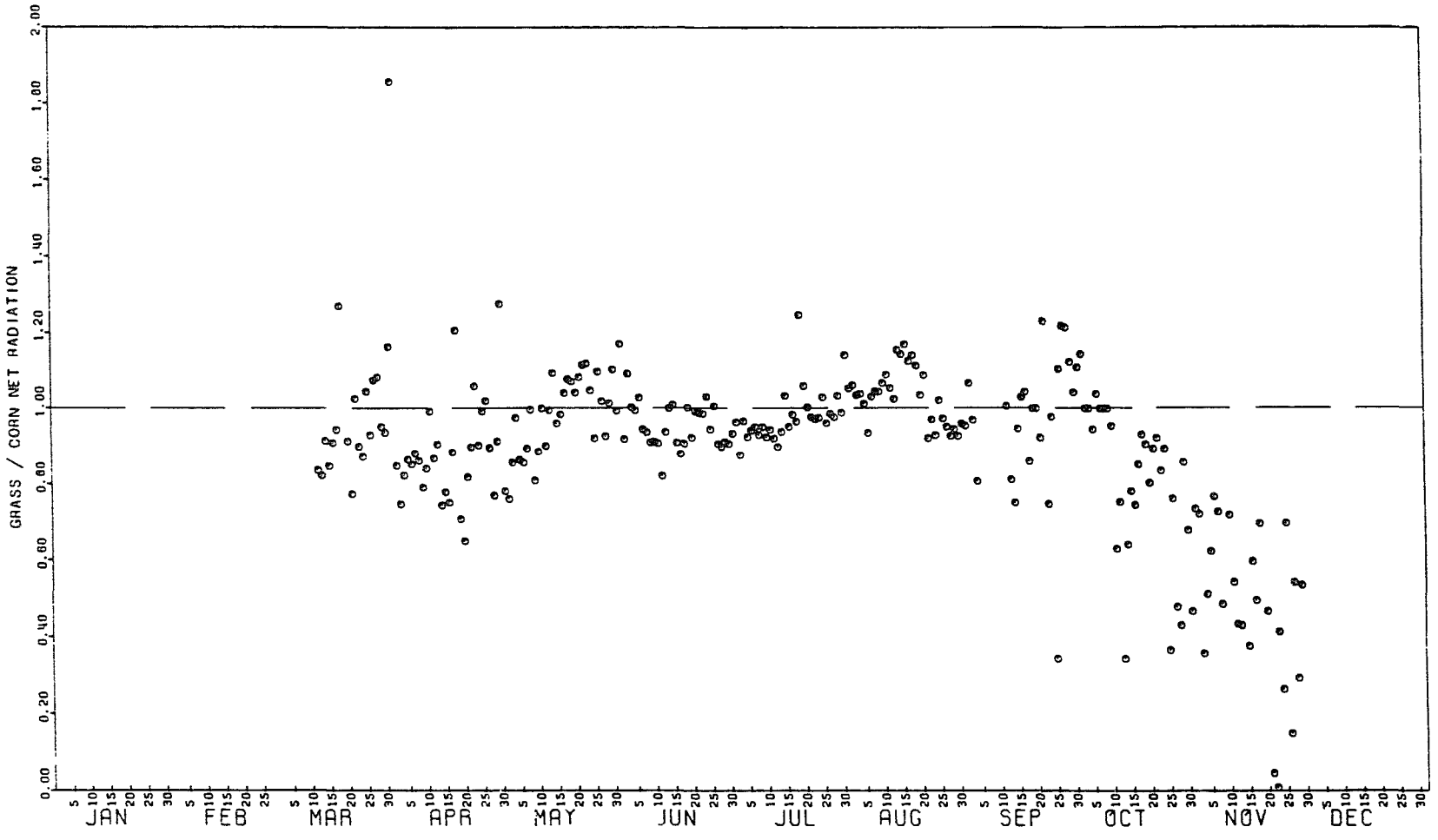

Figure 24. Annual distribution of the ratio of grass over corn daily net radiation during 1970

differences such as soil wetting and farming operations, but these were not investigated. It was concluded that the daily net radiation values were consistent and accurate, and they were applied as measured.

The two single variables most often related to potential ET are net radiation and pan evaporation; thus the relationship between these variables is also significant. A typical relation is shown in figure 25. Net radiation is expressed in units of equivalent water depth, assuming 583 cal/g of water. Pan evaporation is nearly always more than net radiation; the total was nearly double in 1970. This is as expected because the net radiation over the pan would be similar to that over grass (most would evaporate water); in addition the raised evaporation pan is quite exposed to the wind movement which would encourage considerable energy extraction from that source. Later comparisons with calculated potential ET values will confirm that much of the scatter in figure 25 can be explained by the addition of aerodynamic considerations. Annual plots of the ratio of pan evaporation over net radiation such as that shown in figure 26 showed no particular trends.

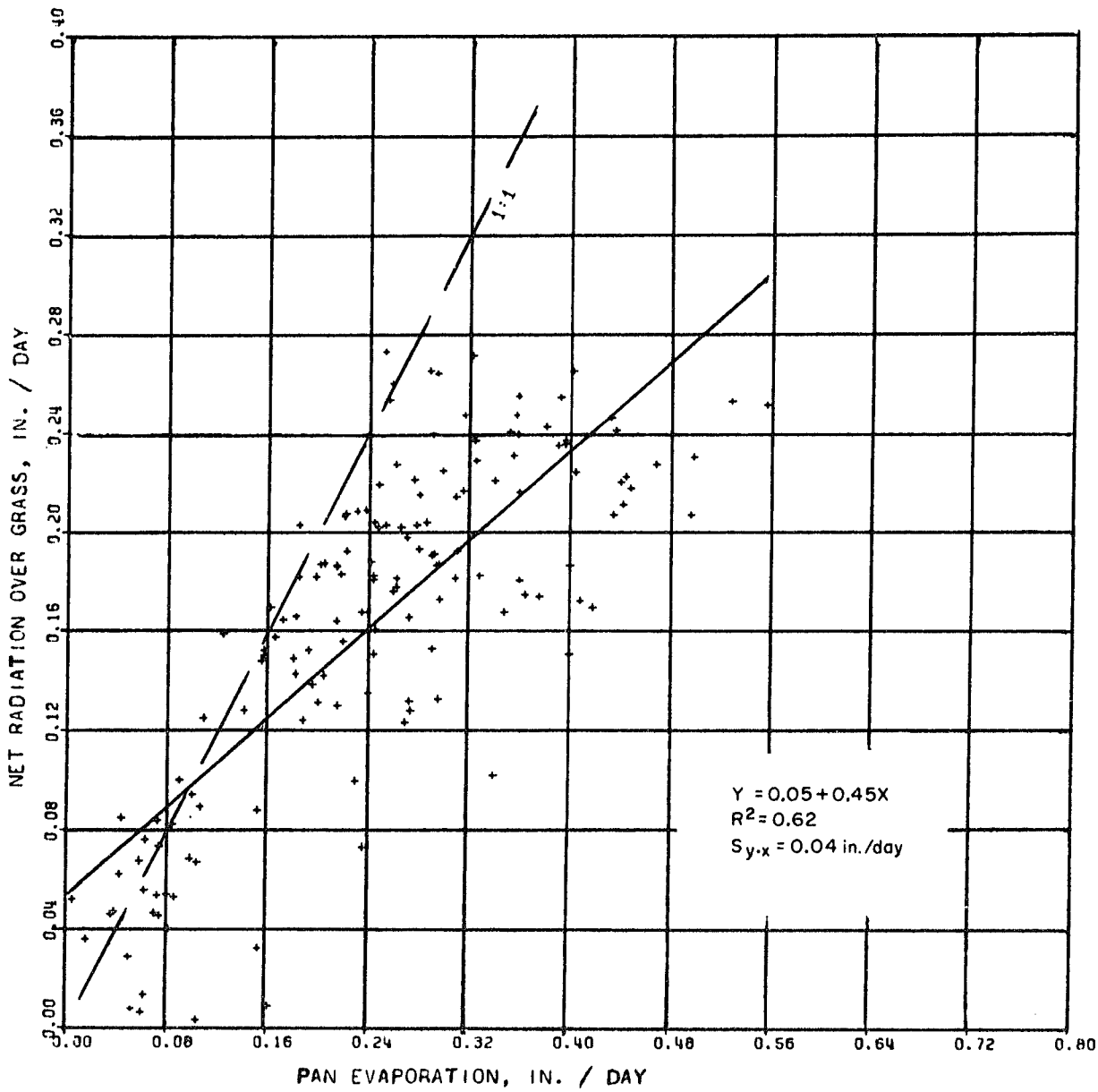

Figure 25. Net radiation over grass compared to class A pan evaporation, March 15 to October 30, 1970

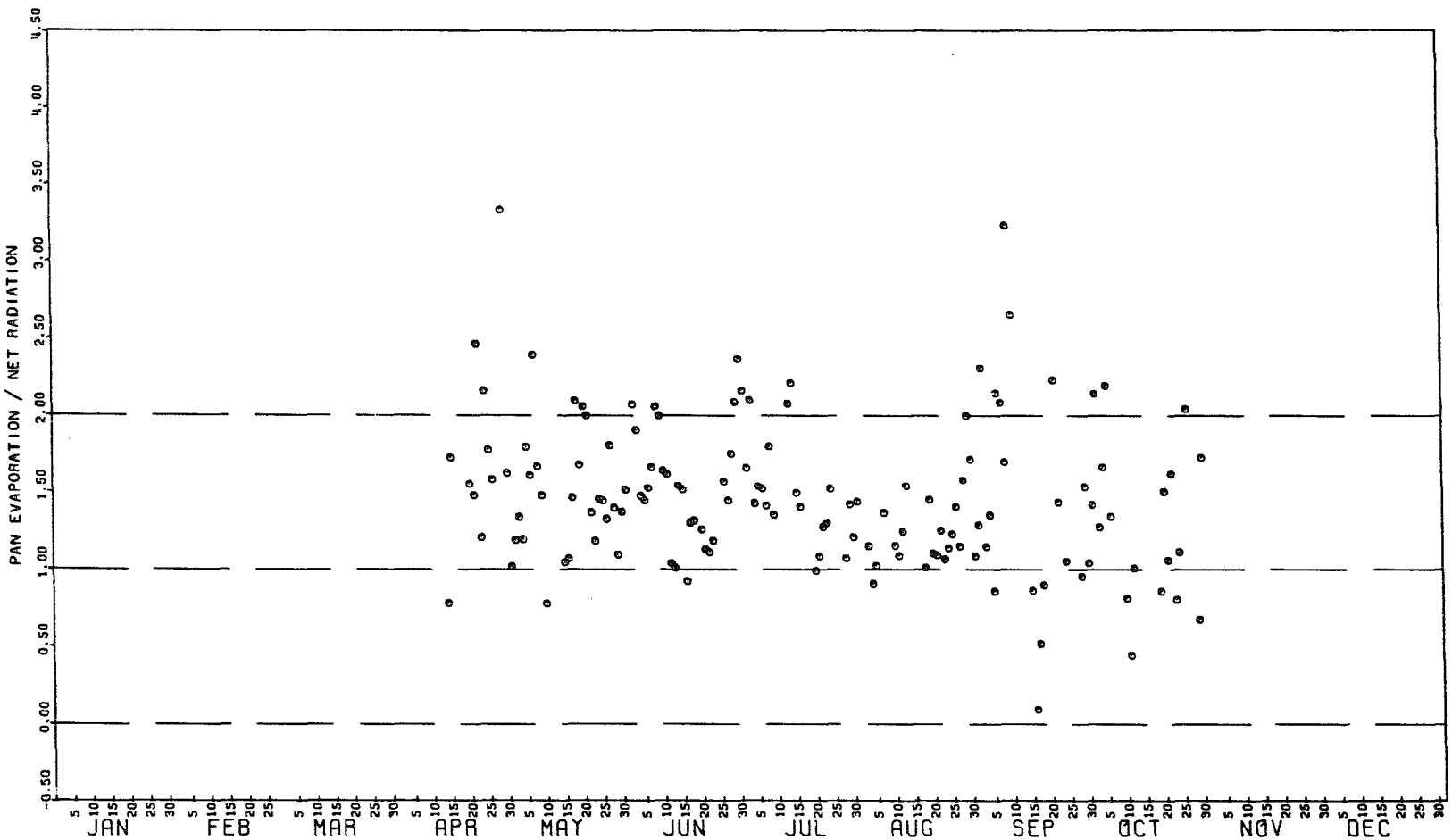

Figure 26. Annual distribution of the ratio of pan evaporation over net radiation over grass during 1970

Other Variables

The slope of the saturation psychrometric line, Δ, is combined with the psychrometric constant, γ, to form the term Δ/γ in the combination equation. The Δ term is a function of air temperature, thus the ratio Δ/γ takes on an annual distribution comparable to air temperature. An example of this distribution is given in figure 27. Air temperatures differed very little over corn and grass and a single value was used for both conditions.

Vapor pressure deficit is a function of both humidity present and air temperature, and these are both quite variable; thus the vapor pressure deficit is expected to vary considerably. An example of daily vapor pressure deficit values for 1 year is shown in figure 28. There is a general envelope of maximum values with a few extreme values; however, considerable scatter occurred most of the year.

The scatter plotting of figure 29 shows that measured vapor pressure deficits over the corn and grass covers were very similar. This is logical because the two sensors were only about 400 feet apart at approximately 1 meter above the crops; thus they were both exposed to the same air mass situation, and the moisture returned to the air by the crops probably did not have a large or differential effect.

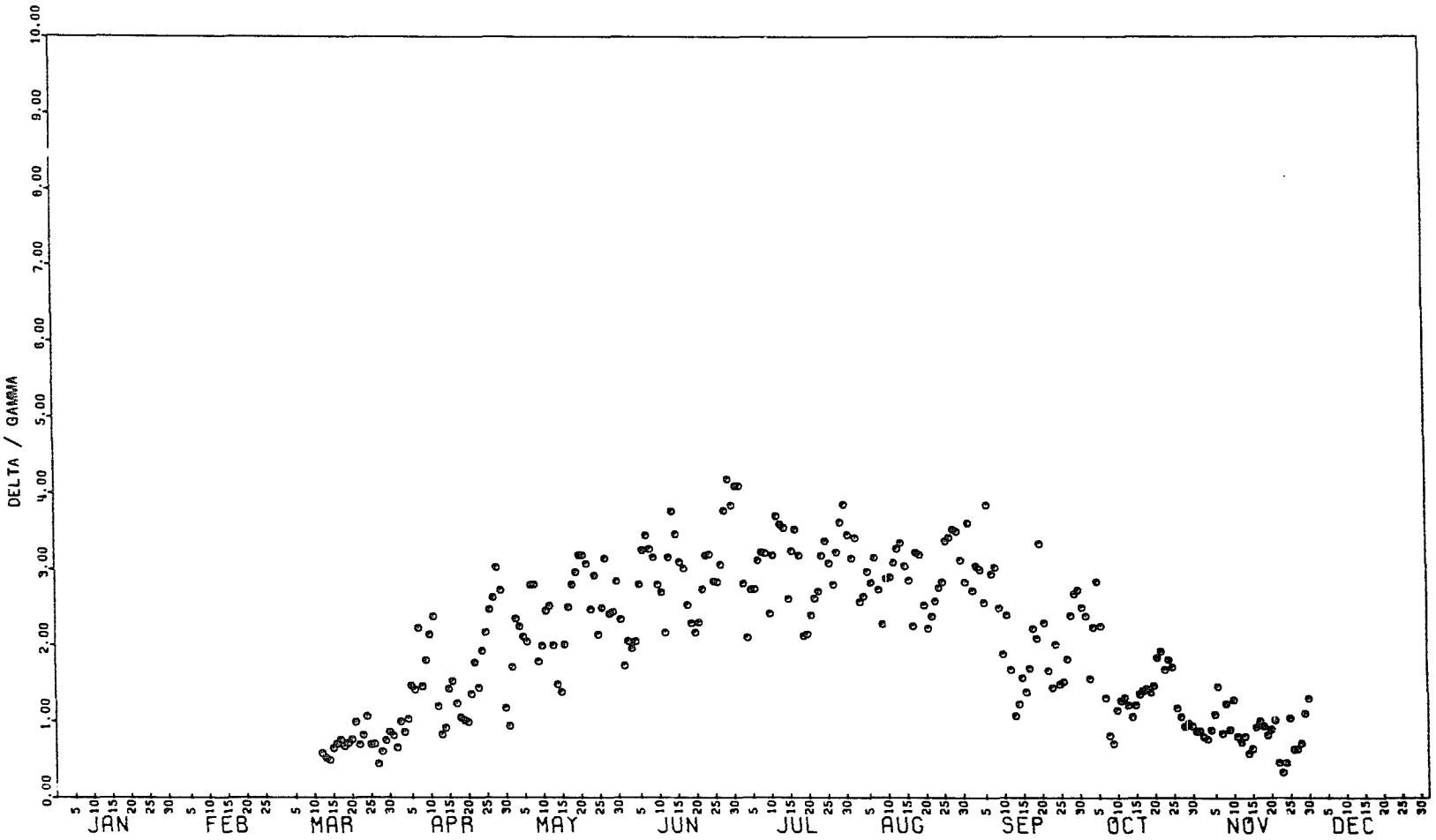

Figure 27. Annual distribution of the ratio delta/gamma during 1970

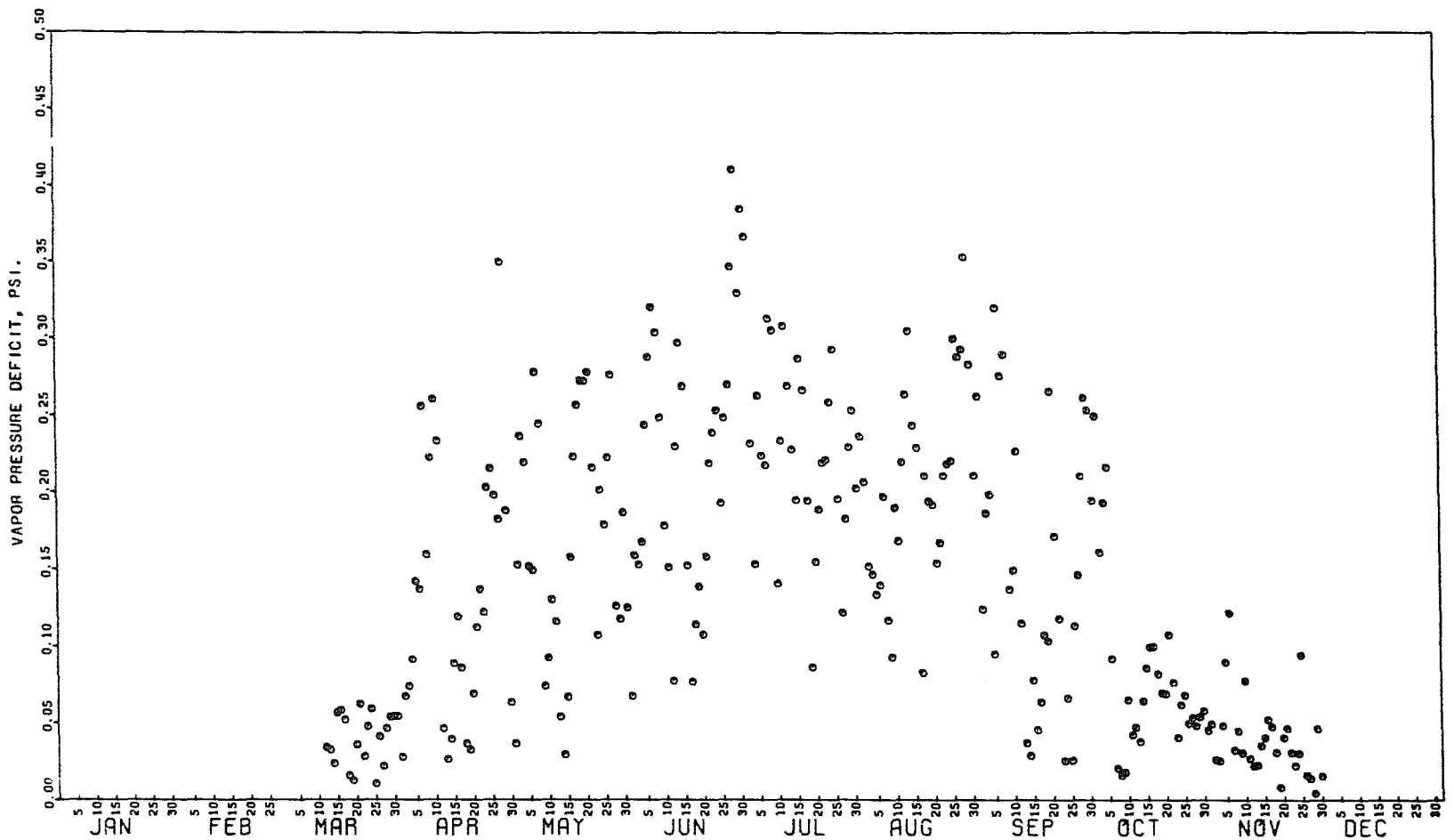

Figure 28. Annual distribution of average daytime vapor pressure deficits during 1970

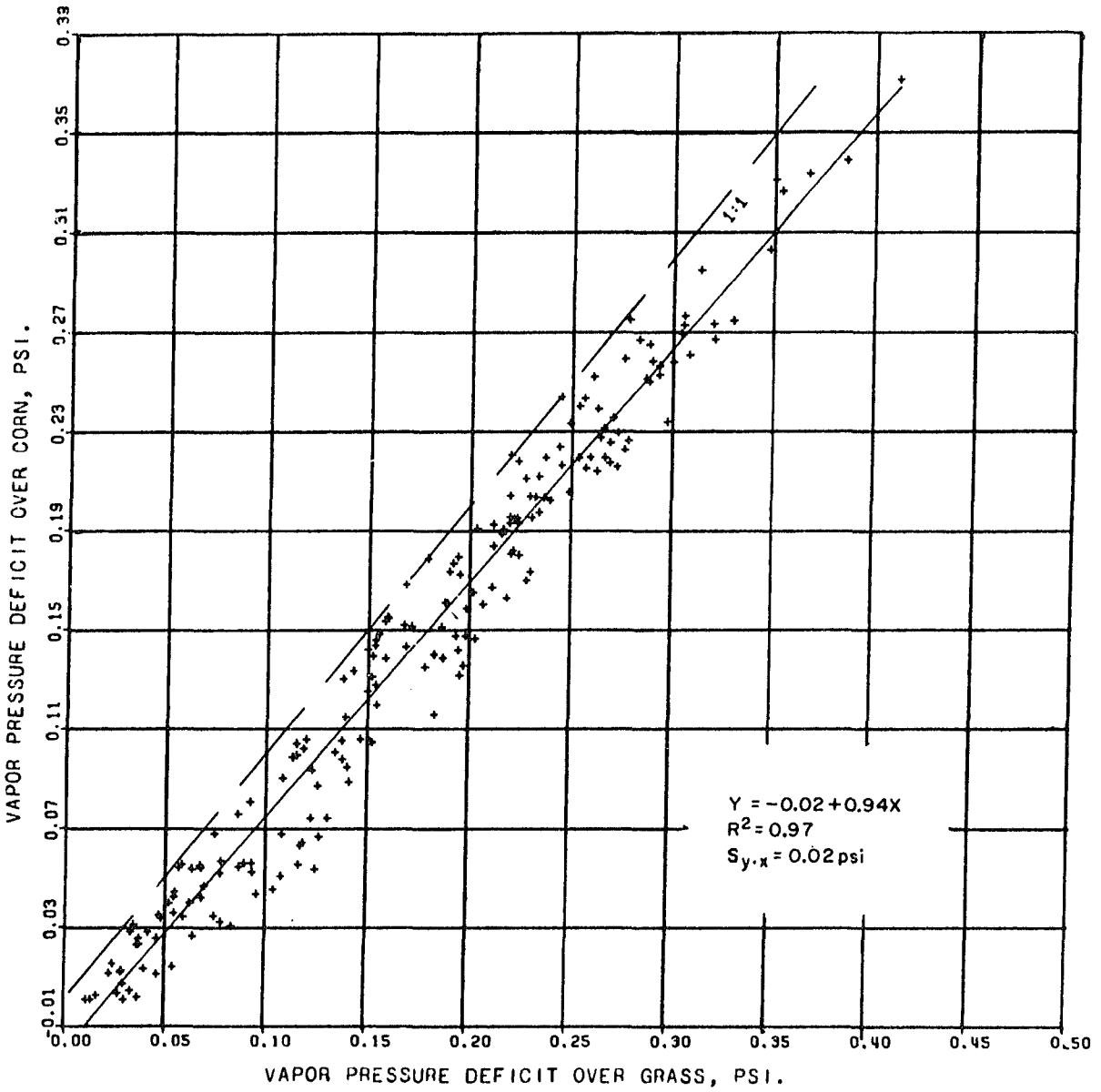

Figure 29. Comparison of average daytime vapor pressure deficits over grass and corn, March 12 to September 22, 1970

There was an apparent bias of about 0.02 psi in the 1970 data shown in figure 29 and a similar relationship in the 1969 data. The reason is not apparent. It could have been an actual difference, instrument bias, or the effect of sensor height. The air intake for corn was about 1.0 to 1.2 meters above the crop surface, whereas the grass air intake was about 0.5 to 0.8 meter. If the 0.02 psi was actually an error, the daily average error would be about 10% over the year. An error analysis, to be discussed later, shows that generally 20% to 40% of any vapor pressure deficit error would be transmitted to the calculated potential ET value; thus the 10% error would result in only a 2% to 4% potential ET error.

Typical daylight wind travel is shown for 1970 in figure 30. The most striking feature is the large day-to-day variation. This variation, coupled with that of the vapor pressure deficit, can be expected to cause large variation in the daily aerodynamic influence on potential ET.

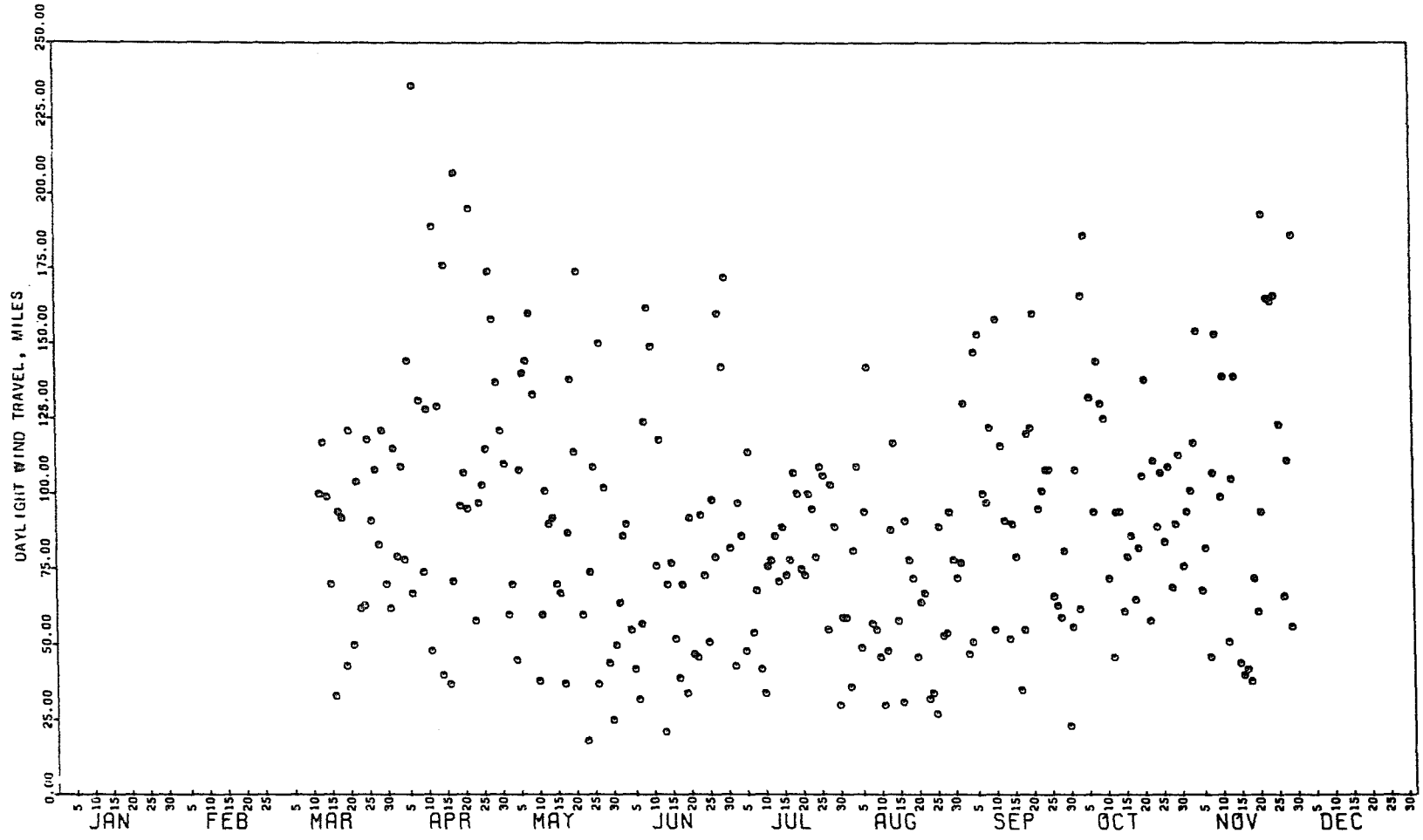

Figure 30. Annual distribution of measured daytime wind travel 0.6 to 0.8 meter above grass surface during 1970

POTENTIAL ET CALCULATIONS

Computing daily potential ET values by use of the combination equation was a straightforward process once all input variables were at hand. The first values calculated showed that the procedures of Appendix B for estimating wind parameters were not applicable, and another approach was required. The calculated potential ET values were very realistic and had good daily response. An error analysis showed the sensitivity of the calculated values to each contributing variable. These items will be discussed in detail in the next paragraphs.

Initial Calculations

A set of potential ET values was first computed using: (1) the observed values of net radiation (R_n), vapor pressure deficit (d_a), and wind travel (u_a); (2) the wind parameter estimating methods outlined in Appendix B; and (3) observed data such as crop height and canopy. Results were quite disappointing. Independent measurements of potential ET values were not available for comparison with the calculated values, but an evaluation was made by plotting the annual distribution of the ratios of net radiation/ potential ET and pan evaporation/ potential ET (figures 39 and 43).

For these first computed values, the net radiation and pan evaporation ratios for grass were about 0.75, with a slight trend of higher to lower values throughout the year. For corn, the ratios had a strong annual trend running from about 1.5 in the spring to 0.5 in the fall. These results indicated that the calculated grass ET values were slightly higher than expected, but the corn values were too small in the spring and too large in the fall.

An annual plot of the estimated wind parameters Z_o and d indicated the Z_o values were probably in error. Grass Z_o values averaged about 2 cm during the growing season, but the wind effects (defined by figure B-2) resulted in daily variations of $\pm$ 0.5 cm. For corn, Z_o values were near 0 in May, 0-2 cm in June, 2-6 cm in July, and 6-16 cm from August to October. The wide range at any particular time was again primarily the result of the wind function.

It was rationalized that Z_o should not vary this much in response to changing wind speeds, and the values themselves seemed high in most cases. Several subsequent sets of calculations were made which used reduced wind effects on Z_o and d, and then with no wind effects;

however, the large Z_o values and unexpected ratio values and trends persisted. After reviewing all other input data for accuracy, it was concluded that the estimating procedures of Appendix B were not applicable. The d values appeared rational, but the Z_o values were too large and varied too much with crop growth and wind travel.

Estimating Wind Parameters

It was apparent that the wind parameters would require estimation by another scheme and that the calculated potential ET values would be subject to these estimations. Two lines of investigation were used to establish criteria. First, it was recognized that the wind parameters were basically used as a modifying term to the wind travel measurements. The wind term was sensitive to: (1) the height of the wind measurement in the wind profile, and (2) the descriptors of the wind profile, d and Z_o. An approach was taken in which values for the complete wind term were estimated and expressed as W,

where:

$$W = \left[\ln\left(\frac{Z_a - d}{Z_o}\right)\right]^2 \quad . \qquad (4)$$

These values were estimated as smooth relations throughout the year and sensitive to those changes that would rationally alter Z_a, d, or Z_o. No effects of wind speed were considered.

The second consideration was to establish criteria for judging the correctness of the calculated potential ET values. This involved a more detailed explanation of the relations of potential ET with pan evaporation and net radiation. Usually potential ET will equal 0.8 to 0.9 of the net radiation when water is not limiting and little advection occurs (Tanner 1957). If moisture is limiting, the air temperature and thus vapor pressure deficit will rise and higher potential ET values will result. And if advection occurs, the potential ET will exceed net radiation (van Bavel 1966). The relative amount represented by these two effects has not been quantified. Thus it was assumed that, on the average, calculated potential ET values should about equal net radiation.

Pan evaporation approximately represents the measurement of a potential for ET, but its open and isolated exposure allows it to abstract more heat from the atmosphere than would a broad expanse of well-watered soil and plants; thus pan evaporation is nearly always more than that

measured in other more typical situations. Veihmeyer (1964, p. 11-7) reports that usual pan-to-pond coefficients are about 0.7, with a range of 0.6 to 0.8. These values suggest that our calculated potential ET values should be about 0.7 of the observed pan evaporation; that is, a pan evaporation / potential ET ratio of about 1.4.

It must be remembered that these comparisons with net radiation and pan evaporation are verification guides and not independent checks. The net radiation and calculated potential ET are quite interdependent because net radiation is used in the ET calculations. Pan evaporation is an independent check and is better than net radiation because it responds to both the vertical radiant energy balance and the aerodynamic terms which are also included in the combination equation.

Several trial curves representing wind parameter values, W, were sketched to arrive at a representative relation. The procedure was to first review the anemometer heights and soil and crop conditions, and then to sketch an annual curve of values which varied as measured Z_a values and estimated d and Z_o values would suggest. The magnitude of the W values was only approximately known; thus the second step was to review the ratios of the calculated potential ET values with net radiation and pan evaporation, and then to reestimate the W curves based on these findings.

This method was first applied to the 1969 data until acceptable results were obtained. It was rationalized that the estimated W values should apply equally well to the 1970 data as an independent check unless the wind measurements or crops differed. For corn, the 1969 W values were applied, unaltered, to the 1970 data. Some adjustment was required for the grass because the grass height was some different below the anemometer, which had a constant height; and the anemometer was raised in midseason.

This estimation scheme introduced an empirical value into an otherwise physically based equation. However, the estimates were rationalized on the basis of the logarithmic wind profile, and the W values represent only one term of the equation. The error analyses of the combination equation discussed in the next section give a good indication of the sensitivity of the equation to these W estimates; that is, what percent of any error in W would be transmitted to the calculated potential ET values.

Potential ET Values

A summary of the calculated potential ET values and their ratios with net radiation and pan evaporation is given graphically in figures 31 to 47. The observed crop

heights and canopies and the final wind profile parameter values, W, are shown in figures 31 to 34. In addition, values of the wind profile displacement, d, and roughness heights, Z_o, are given. These were calculated and plotted to assure that the W values were realistic. The d values were calculated by the relationship

$$d = (0.8)\ (0.9\ \text{Crop Canopy})\ (\text{Crop Height}) \qquad (5)$$

which is a modified version of the relationship presented in Appendix B. Observed crop canopy was reduced 10% to account for the difference in the estimates between radiation and turbulent penetration. After d was calculated from crop characteristics and the estimated W values and anemometer height Z_a were known, Z_o values were directly calculated from the profile equation 4.

The Z_o values appeared rational and contrasted sharply with those first estimated by equations in Appendix B. Values for grass ranged from 0.2 to 0.4 cm compared with first estimates of 1 to 2 cm, which is an 80% change. August corn Z_o values were about 2 cm compared with earlier estimates of 6 to 16 cm. Estimates of d and Z_o are dependent, and this may have contributed somewhat to the

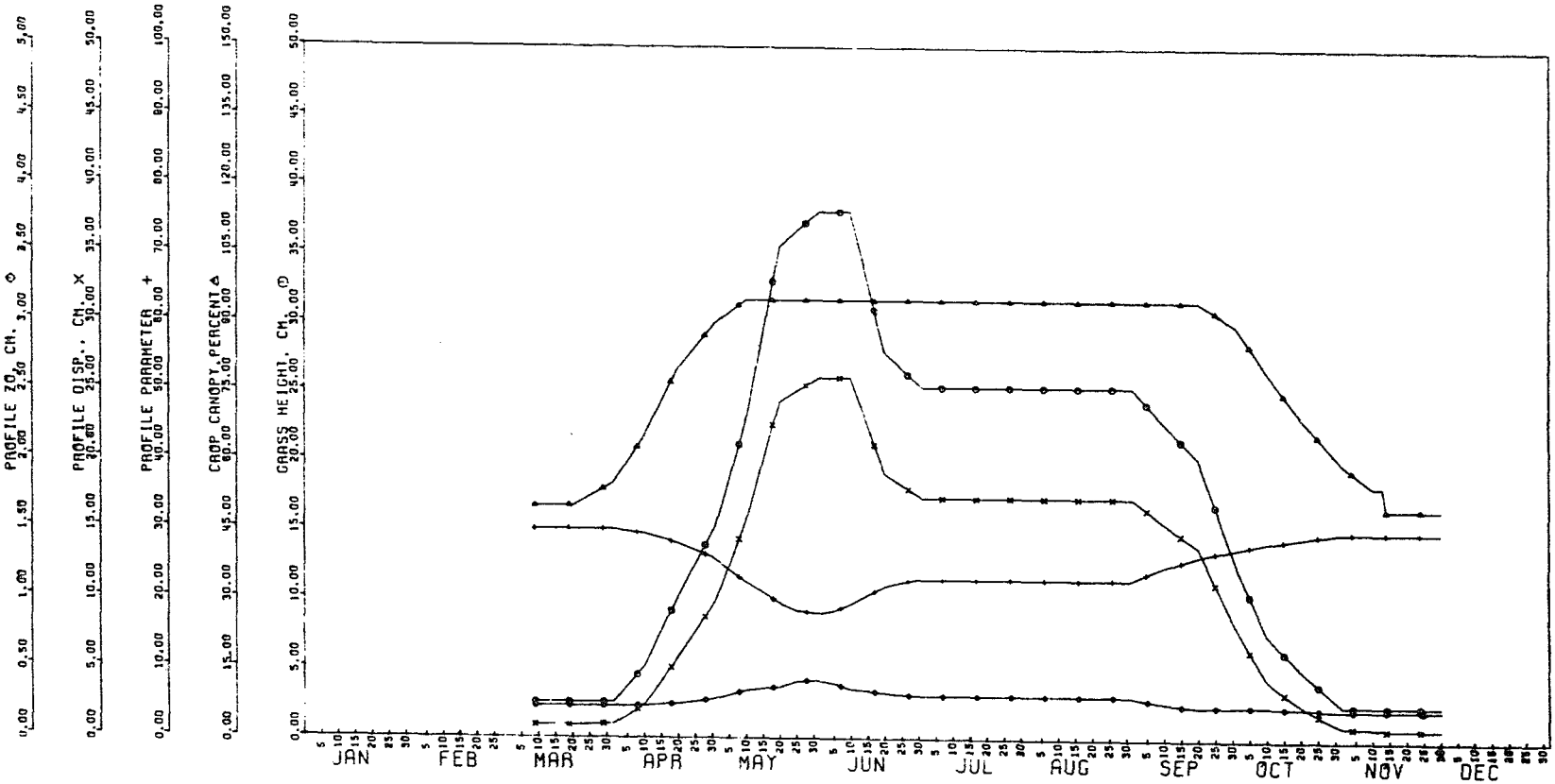

Figure 31. Annual distribution of crop and wind profile parameters for grass during 1969

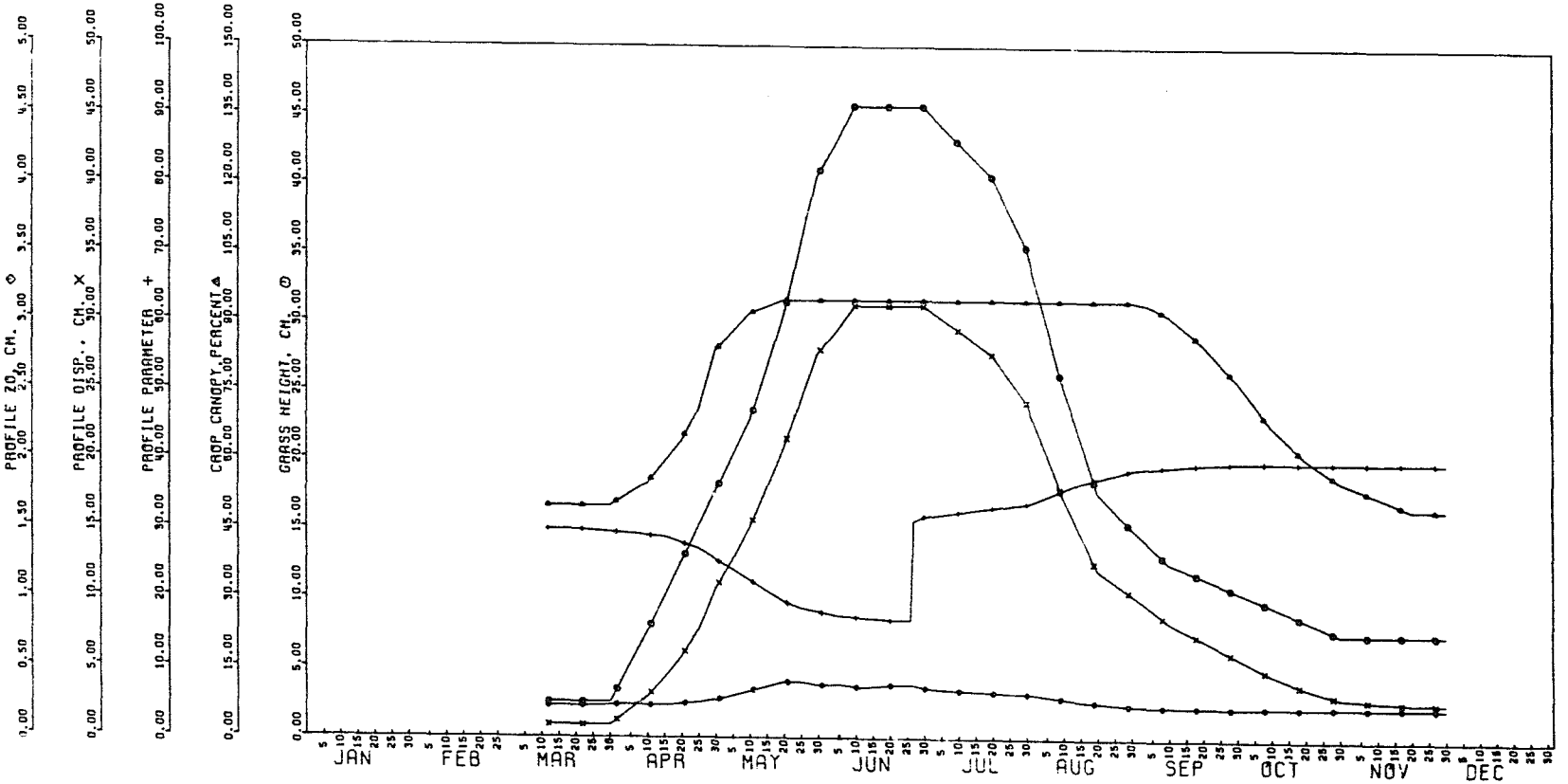

Figure 32. Annual distribution of crop and wind profile parameters for grass during 1970

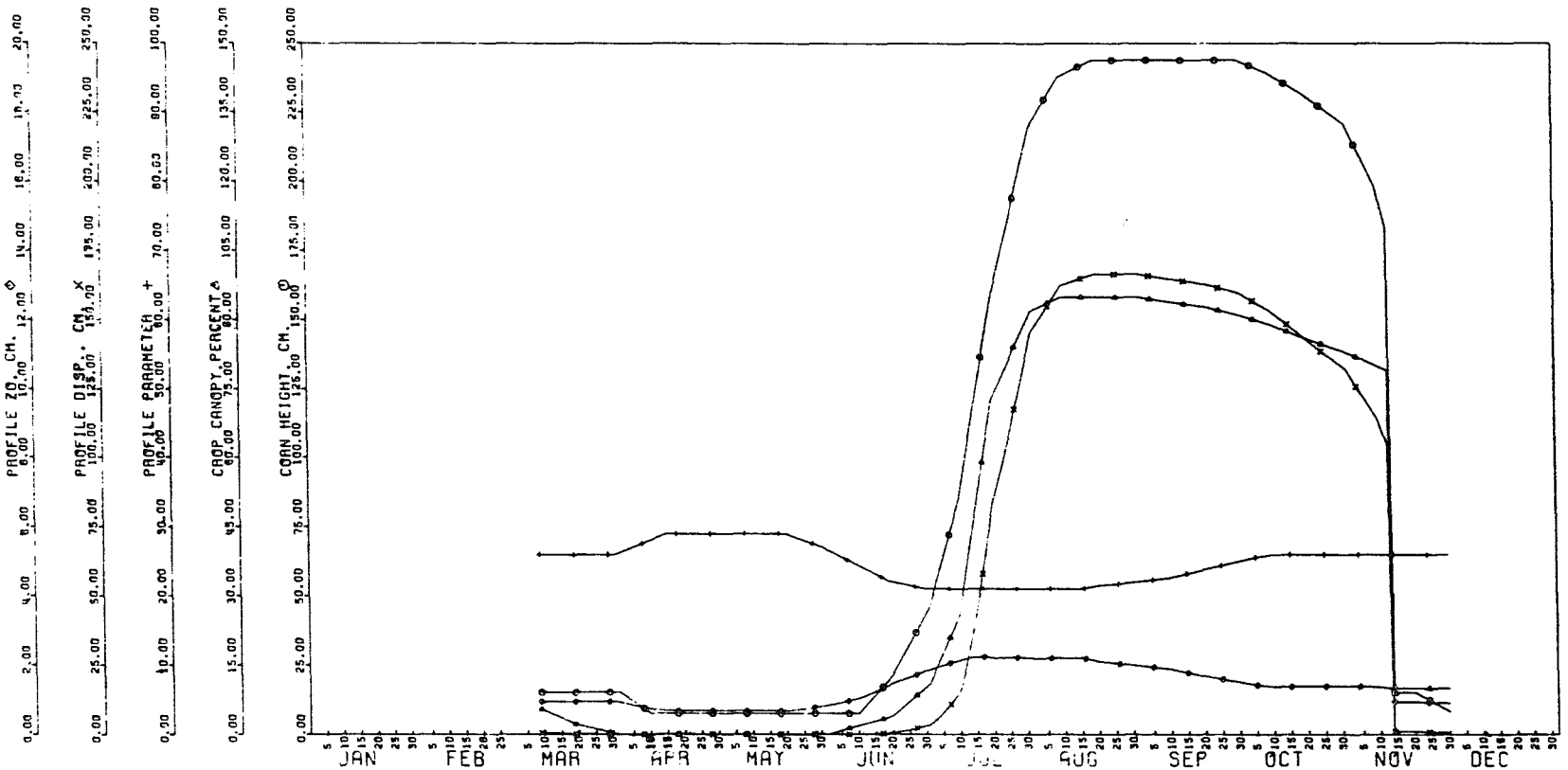

Figure 33. Annual distribution of crop and wind profile parameters for corn during 1969

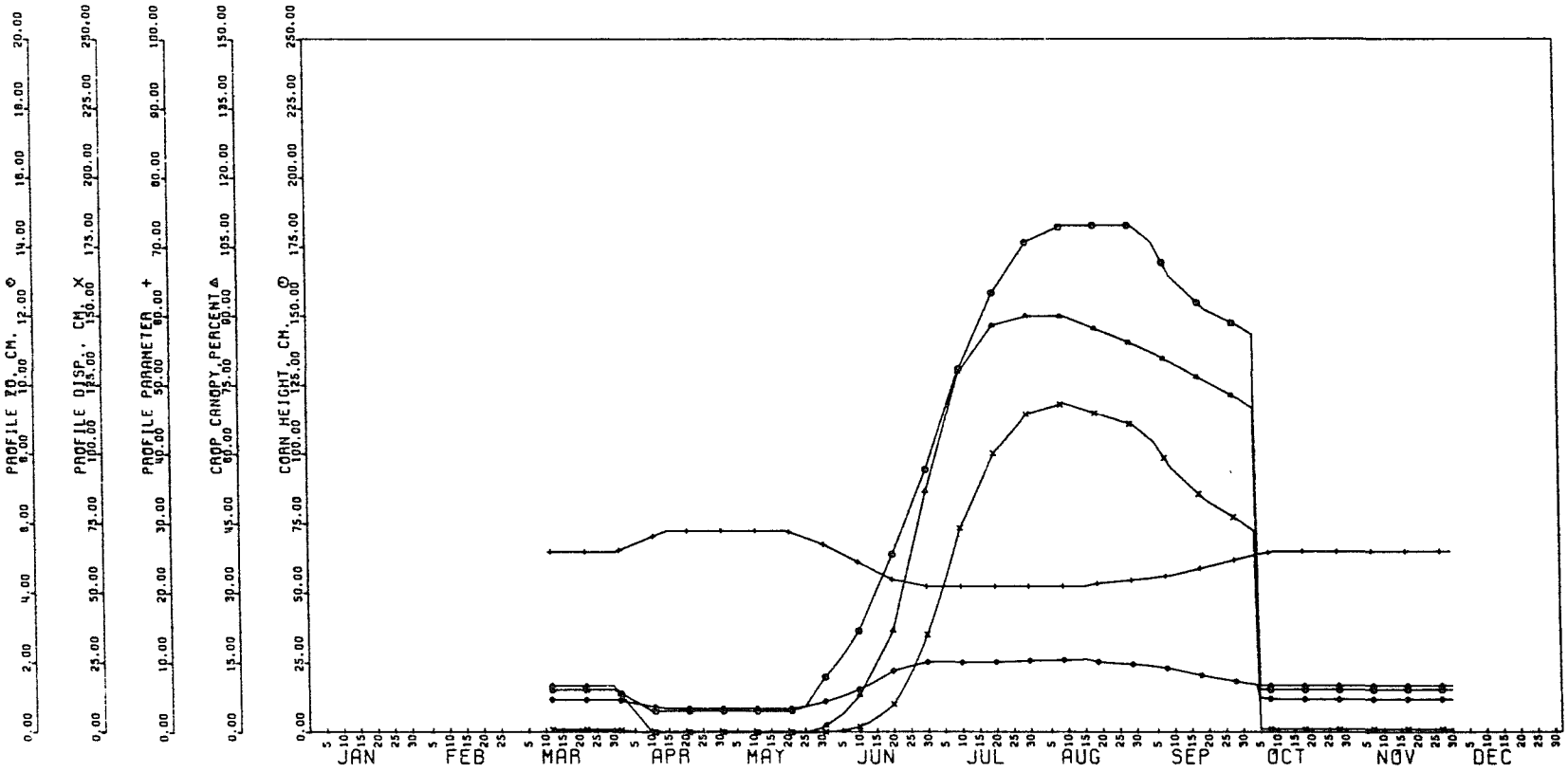

Figure 34. Annual distribution of crop and wind profile parameters for corn during 1970

problem with the earlier estimates. It was not always clear whether d values had been considered for the Z_o prediction equations given in table B-2.

Typical computed potential ET values are shown in figures 35 and 36 for 2 years with grass cover. The seasonal trend is apparent, but there is considerable variation throughout the year. This variation is as expected, however, because of the variation of R_n, d_a, and u_a as shown in figures 20, 28, and 30, respectively.

The computed daily potential ET values were quite similar for the corn and grass crops as shown by the comparison in figure 37 and the ratios in figure 38. This also was expected from comparisons of the variables such as R_n and d_a over the two crops which were shown in figures 23 and 29. The ratio values of figure 38 indicate slightly larger potential ET amounts for the corn before May, but after that they were nearly equal or slightly larger. These values cannot stringently be interpreted because both corn and grass ET values are somewhat dependent on the estimates of the wind parameter values, W.

As previously discussed, the final selection of the W values was partially dependent on comparisons of the calculated potential ET values with net radiation and pan evaporation. Examples of the final comparisons are shown

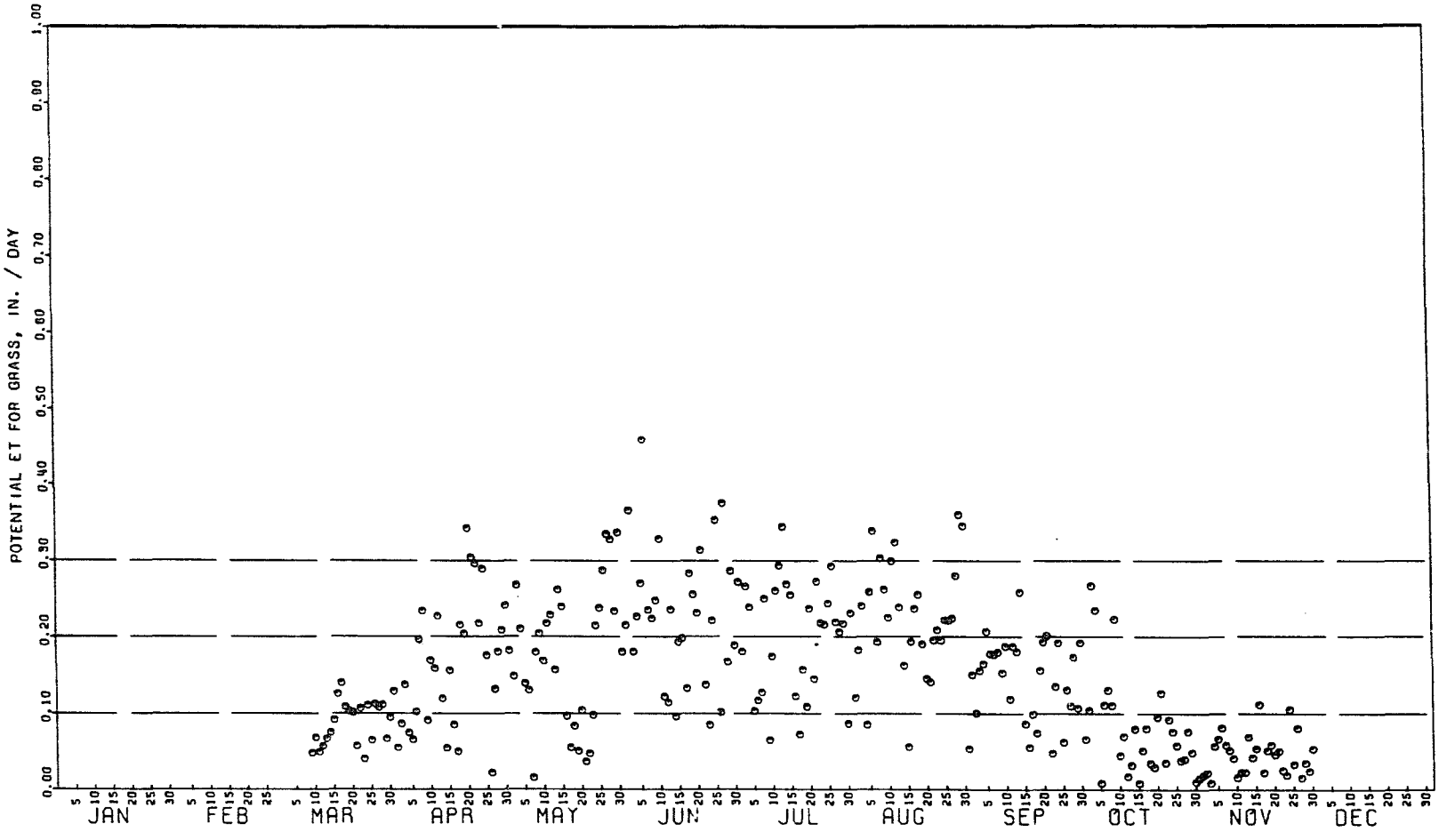

Figure 35. Annual distribution of calculated daily potential ET for grass during 1969

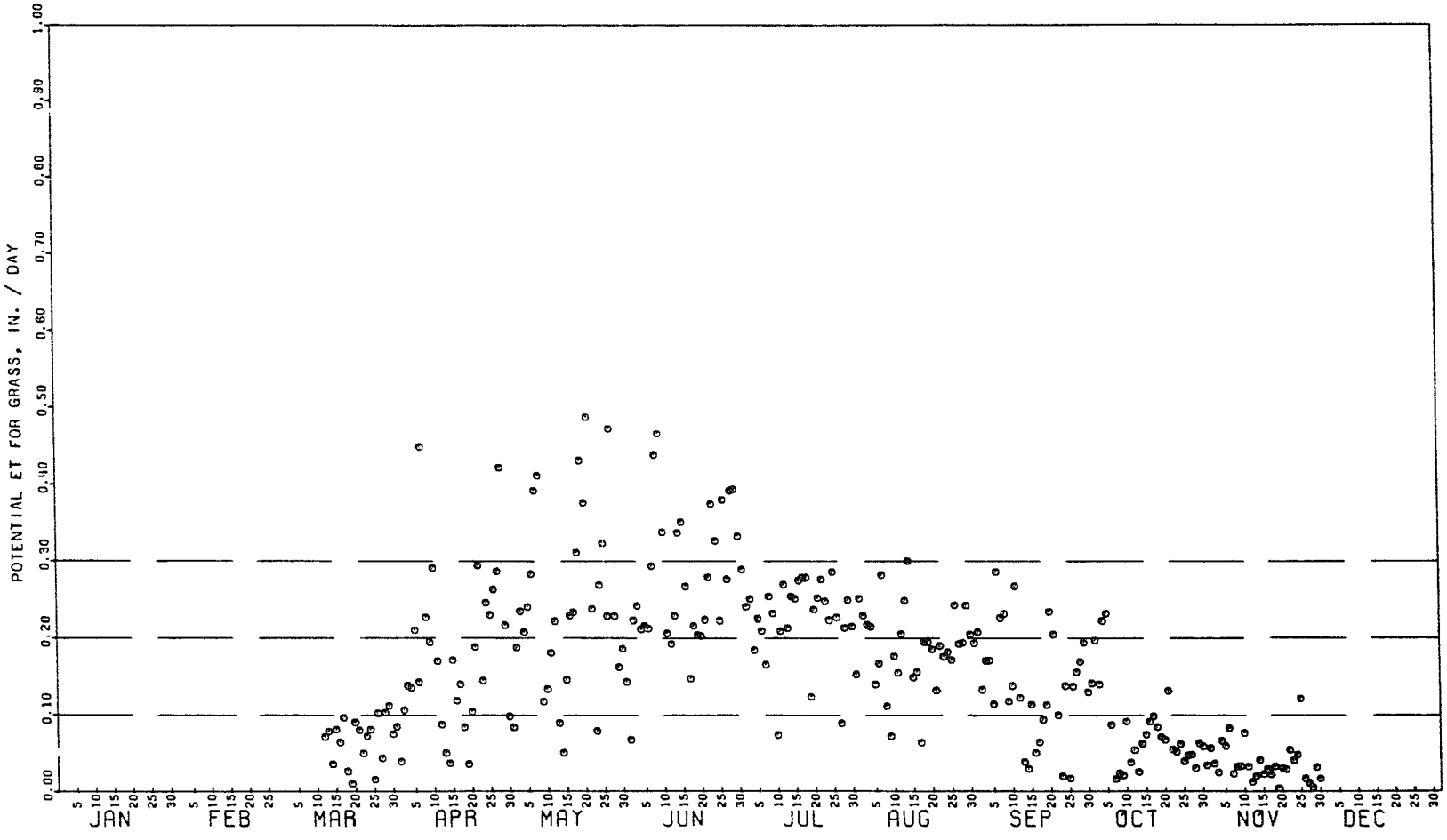

Figure 36. Annual distribution of calculated daily potential ET for grass during 1970

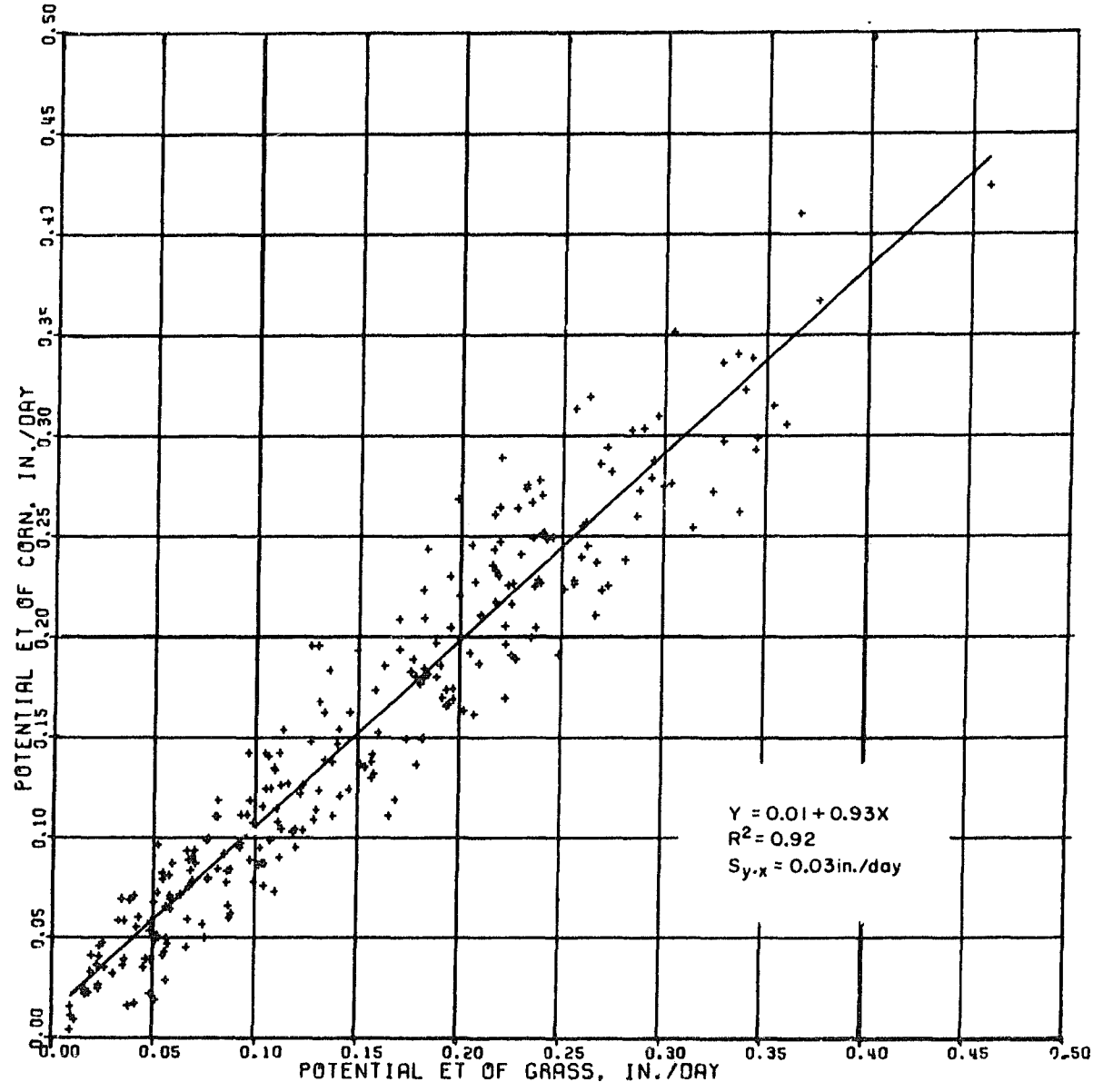

Figure 37. Comparison of computed daily potential ET for grass and corn, March 9 to December 1, 1969

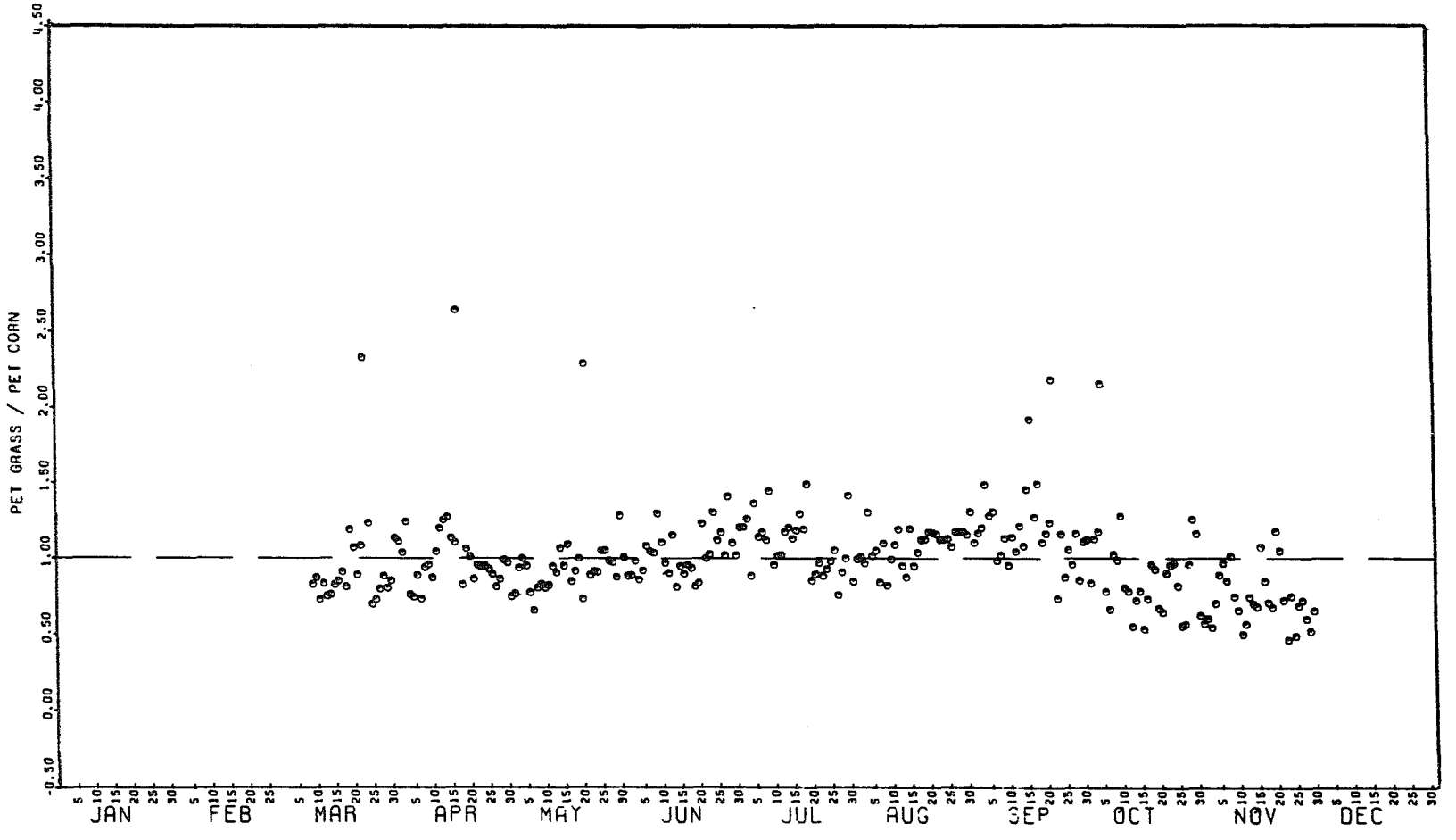

Figure 38. Annual distribution of potential ET of grass over potential ET of corn during 1969

in figures 39 through 43. The ratios with net radiation shown in figures 39 and 40 show that the calculated potential ET (PET) values were about equal to R_n. The March and November points indicate that the PET values were significantly less than R_n in spring and more in the fall. The reason for this is not fully understood but it is probably related to the relative role of the aerodynamic term--which will be discussed later. Another possible cause noted by Tanner and Pelton (1960, p. 3397) was that neglecting soil heat flux caused the largest error in the fall when the soil was rapidly cooling, and in the spring when the latent heat of fusion of snow and ground-frost was required and soil warming occurred.

The correlation of R_n and potential ET of figure 41 shows the effect of the aerodynamic term. Many of the points fall near or slightly below the equal value line, but on a significant number of days potential ET was much more than net radiation. On these days significant advection apparently occurred. This distribution contrasts with the correlation of ET and pan evaporation shown in figure 42. Here, the scatter of points is significantly less--despite the fact that the statistics are no better because of some outliers. This reduction in scatter can be attributed to

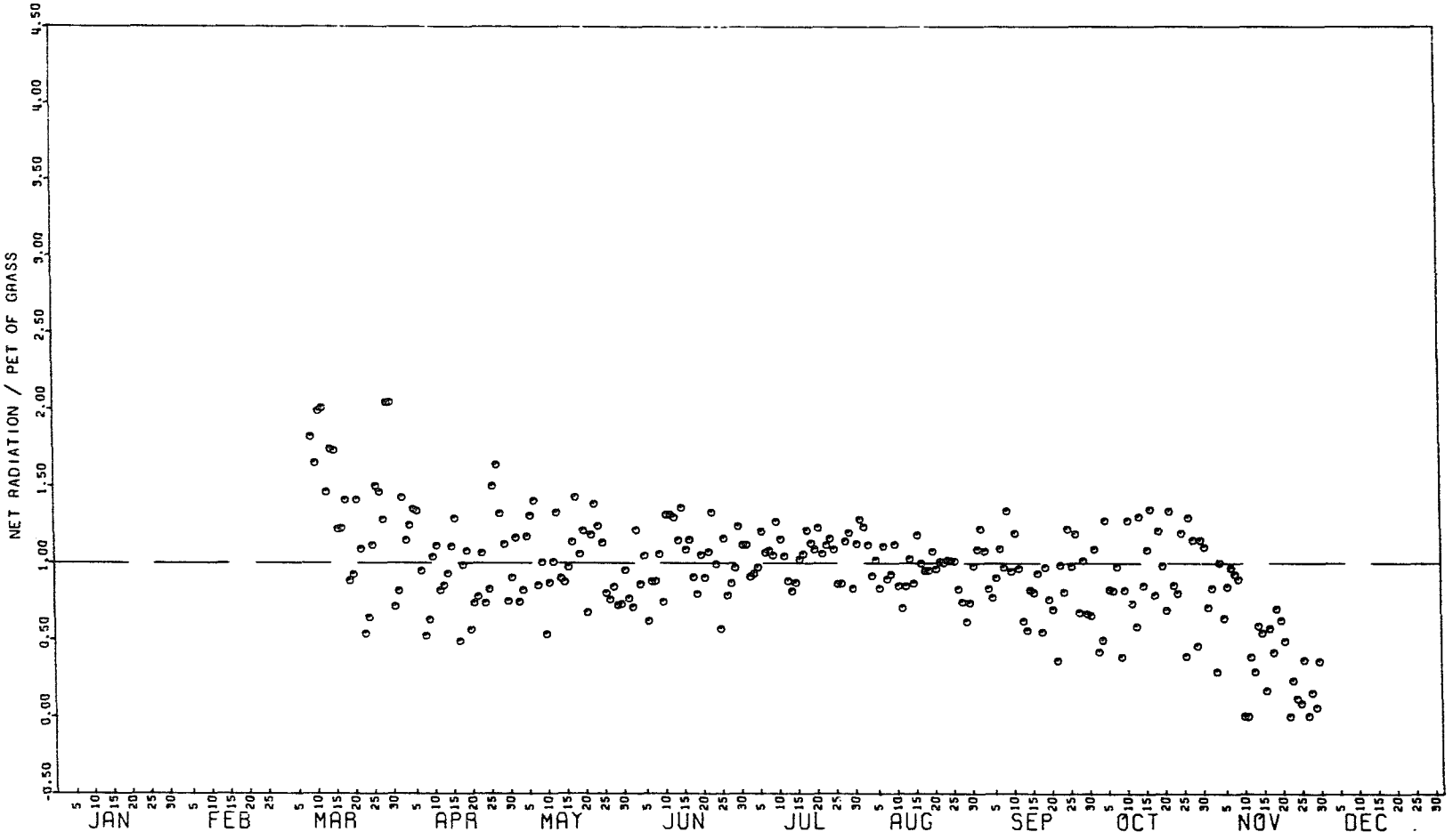

Figure 39. Annual distribution of net radiation over computed potential ET for grass during 1969

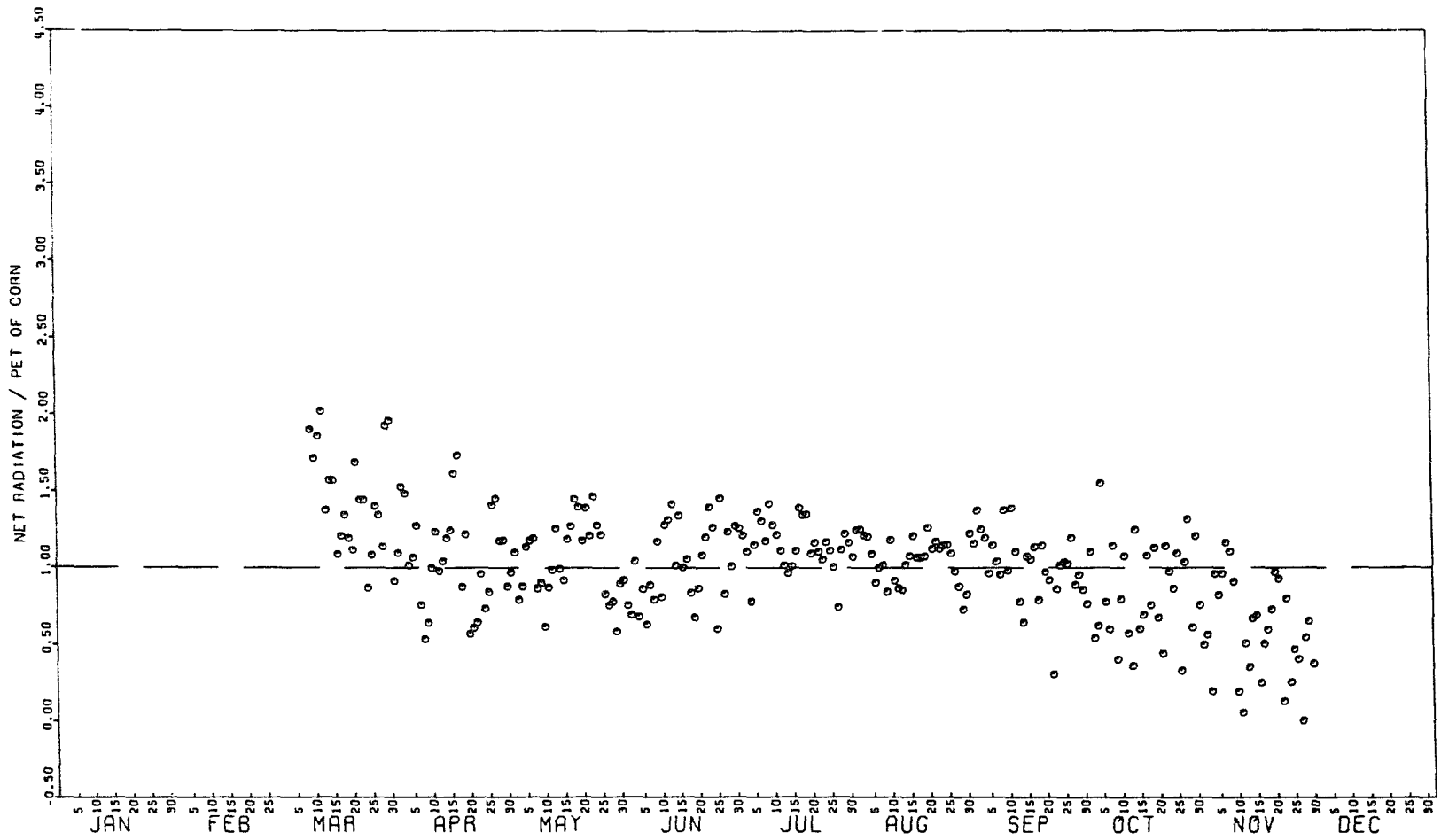

Figure 40. Annual distribution of net radiation over computed potential ET for corn during 1969

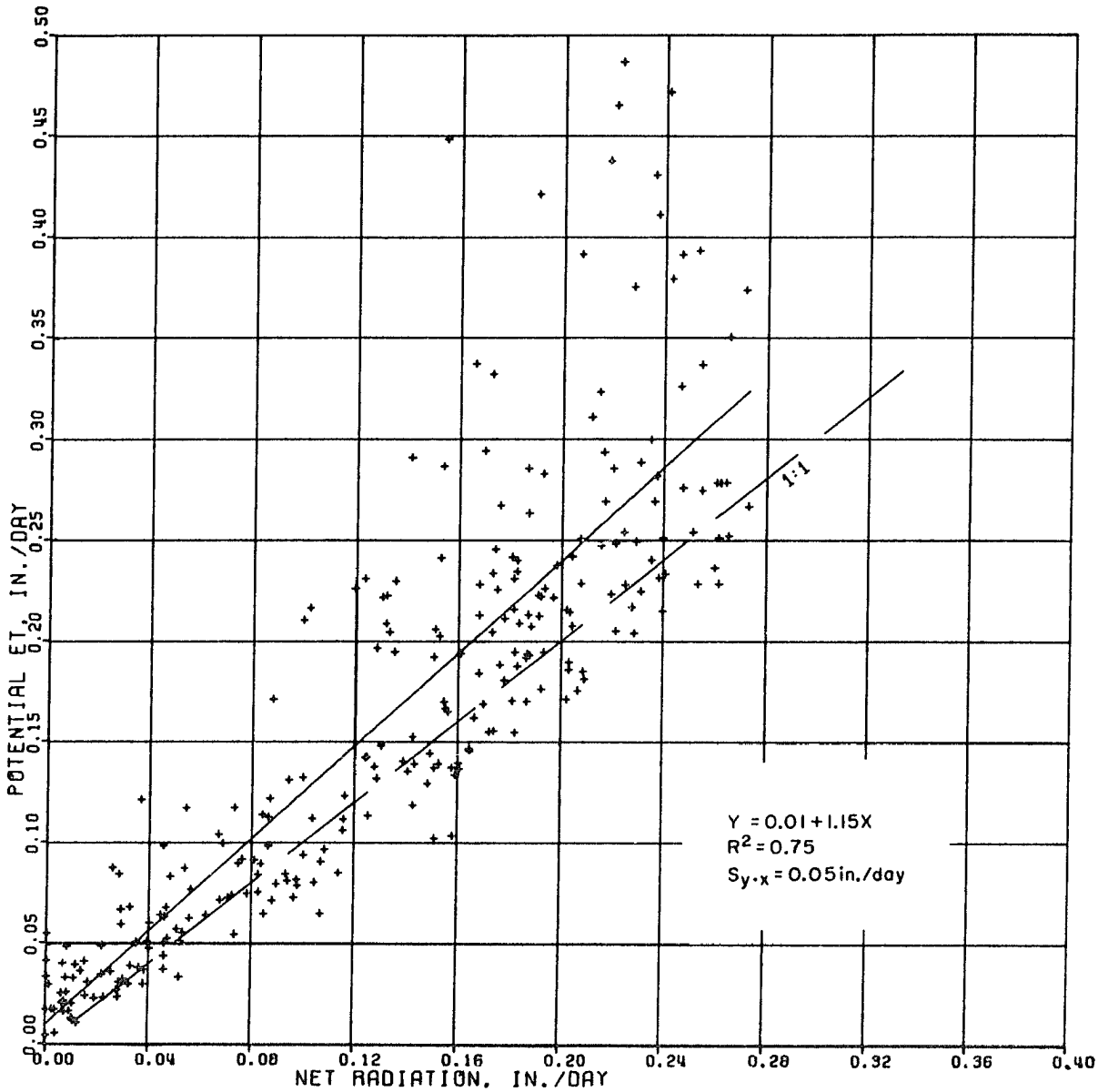

Figure 41. Comparison of computed daily potential ET for grass with net radiation over grass, March 12 to December 1, 1970

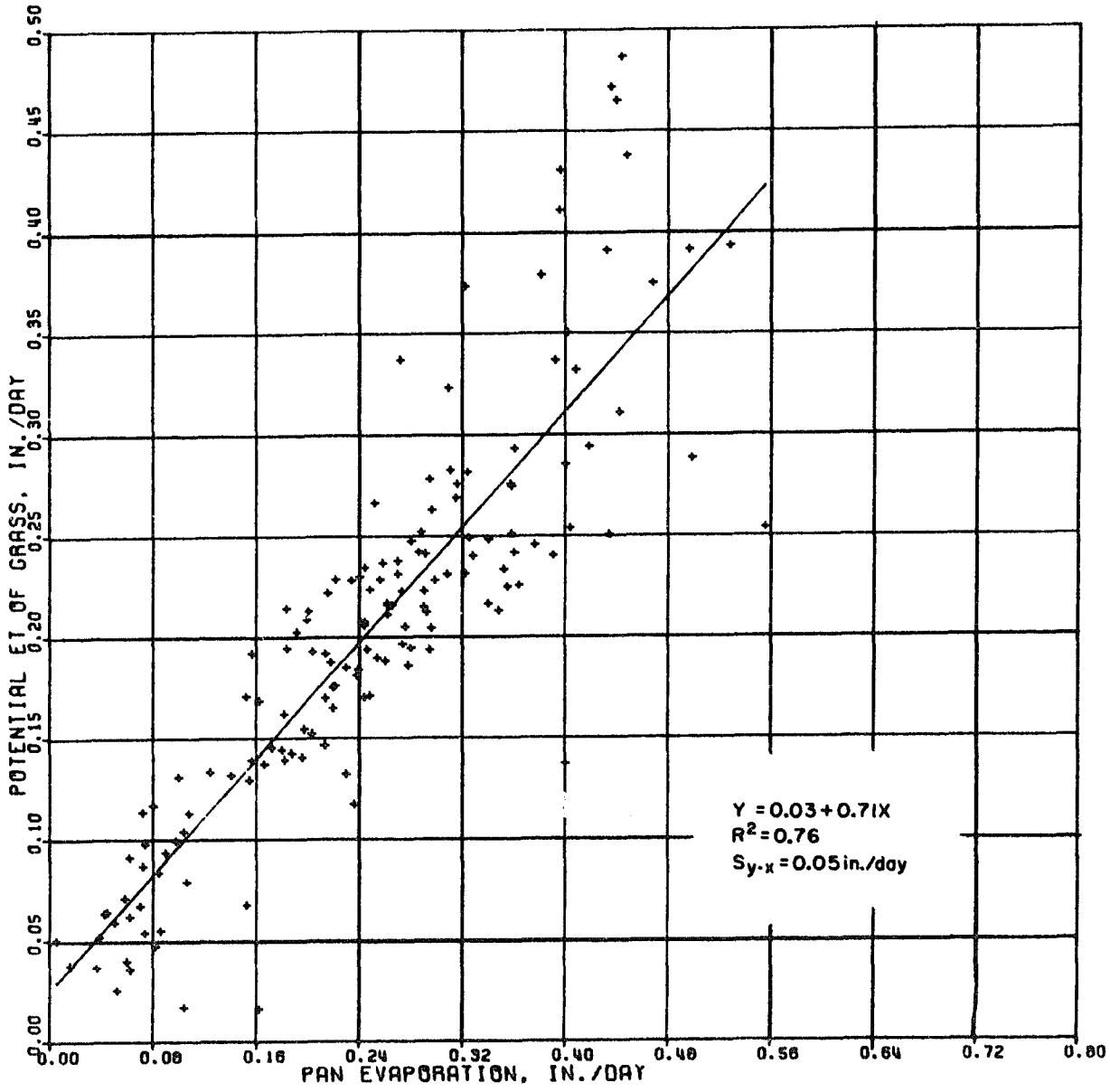

Figure 42. Comparison of computed daily potential ET for grass with pan evaporation, March 15 to October 30, 1970

the fact that both the pan evaporation and ET values respond to the aerodynamic effects. The pan evaporation over ET ratios of figure 43 show a uniform annual relation except for some tendency of increased pan evaporation late in the year. An important aspect of these comparisons is that the computed and observed values have very similar daily sensitivity which makes the computed potential ET values very useful for hydrologic research.

An interesting question about the combination model concerns the relative magnitude of the radiation and aerodynamic terms throughout the year. Ratios of these two terms, $(\Delta/\gamma)\, R_n)/(791\, d_a\, u_a\, W^{-1})$, are shown in figures 44 and 45 for the 2 years of calculations. It is apparent that the aerodynamic term is nearly equal or dominates early and late in the year, but net radiation dominates during the midyear.

The accumulative curves of figures 46 and 47 summarize the net radiation, pan evaporation, and computed potential ET for 1969 and 1970. The 1969 values show that R_n and ET are very similar--as was intended when estimating the wind parameter values. During 1970, however, the ET values were significantly more than R_n. This difference is apparently real because pan evaporation was 49 in. during 1969, and

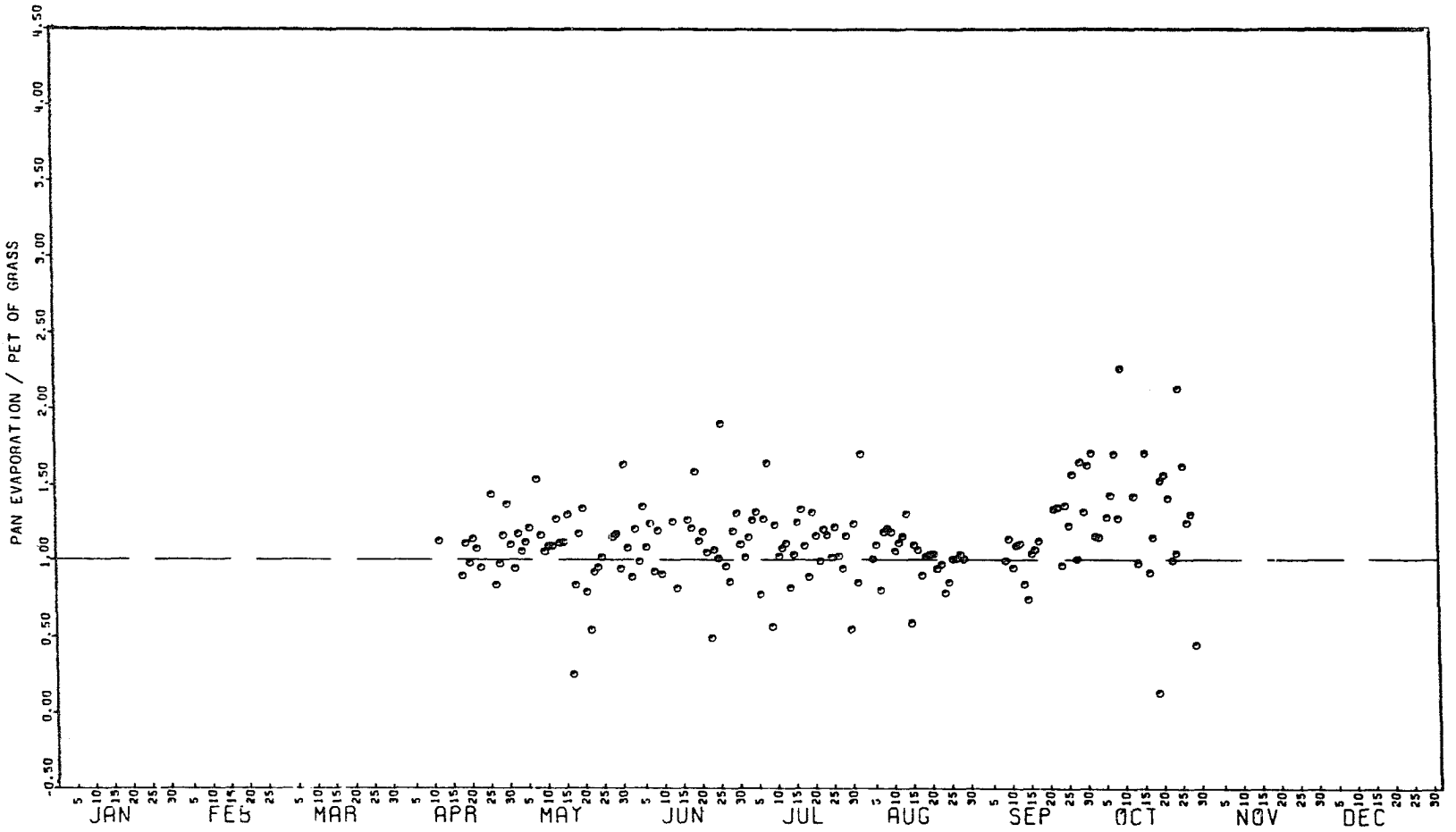

Figure 43. Annual distribution of pan evaporation over computed potential ET for grass during 1969

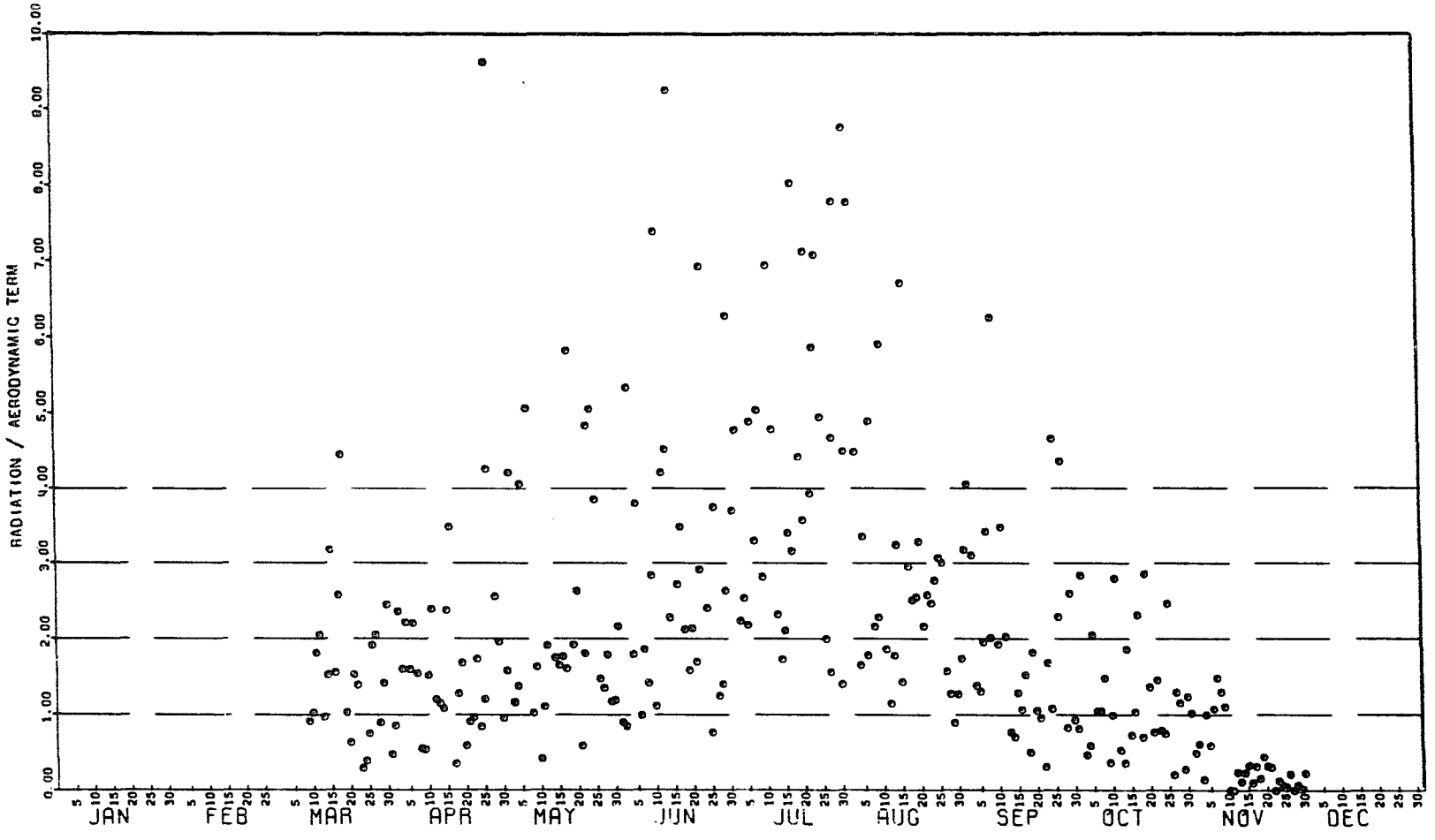

Figure 44. Annual distribution of radiation term over aerodynamic term for grass during 1969

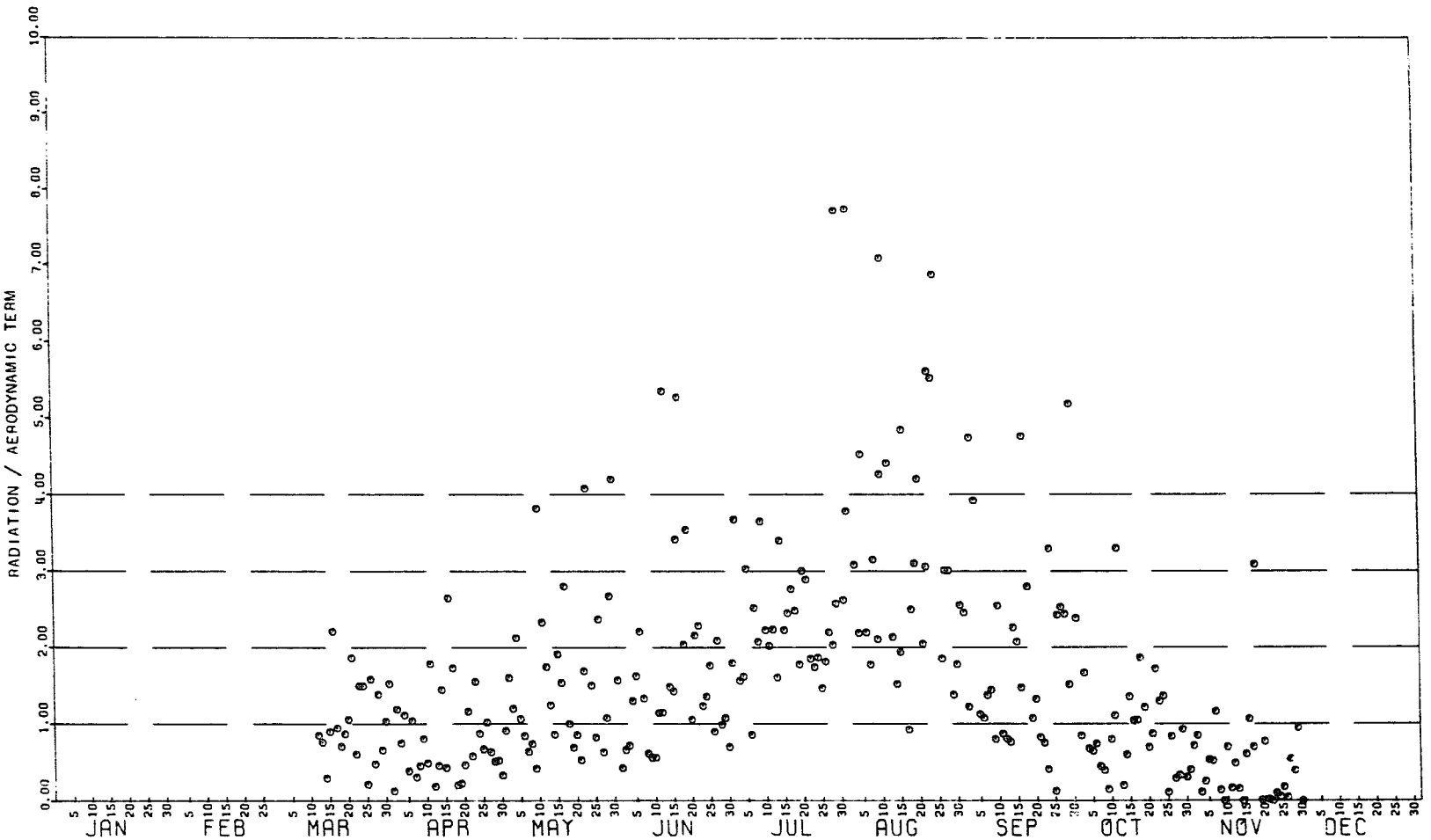

Figure 45. Annual distribution of radiation term over aerodynamic term for grass during 1970

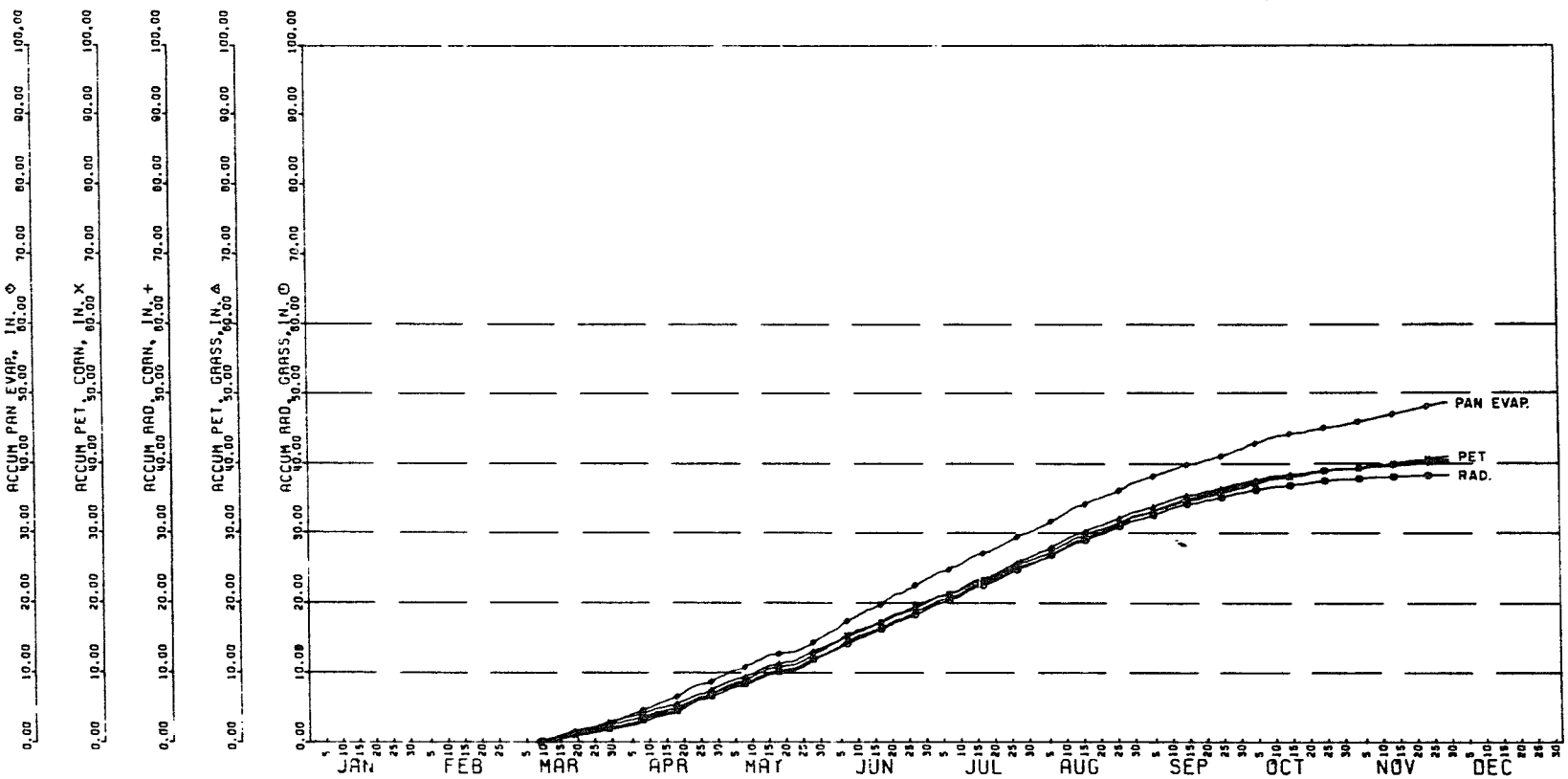

Figure 46. Annual accumulative values of net radiation, calculated potential ET, and pan evaporation for grass and corn during 1969

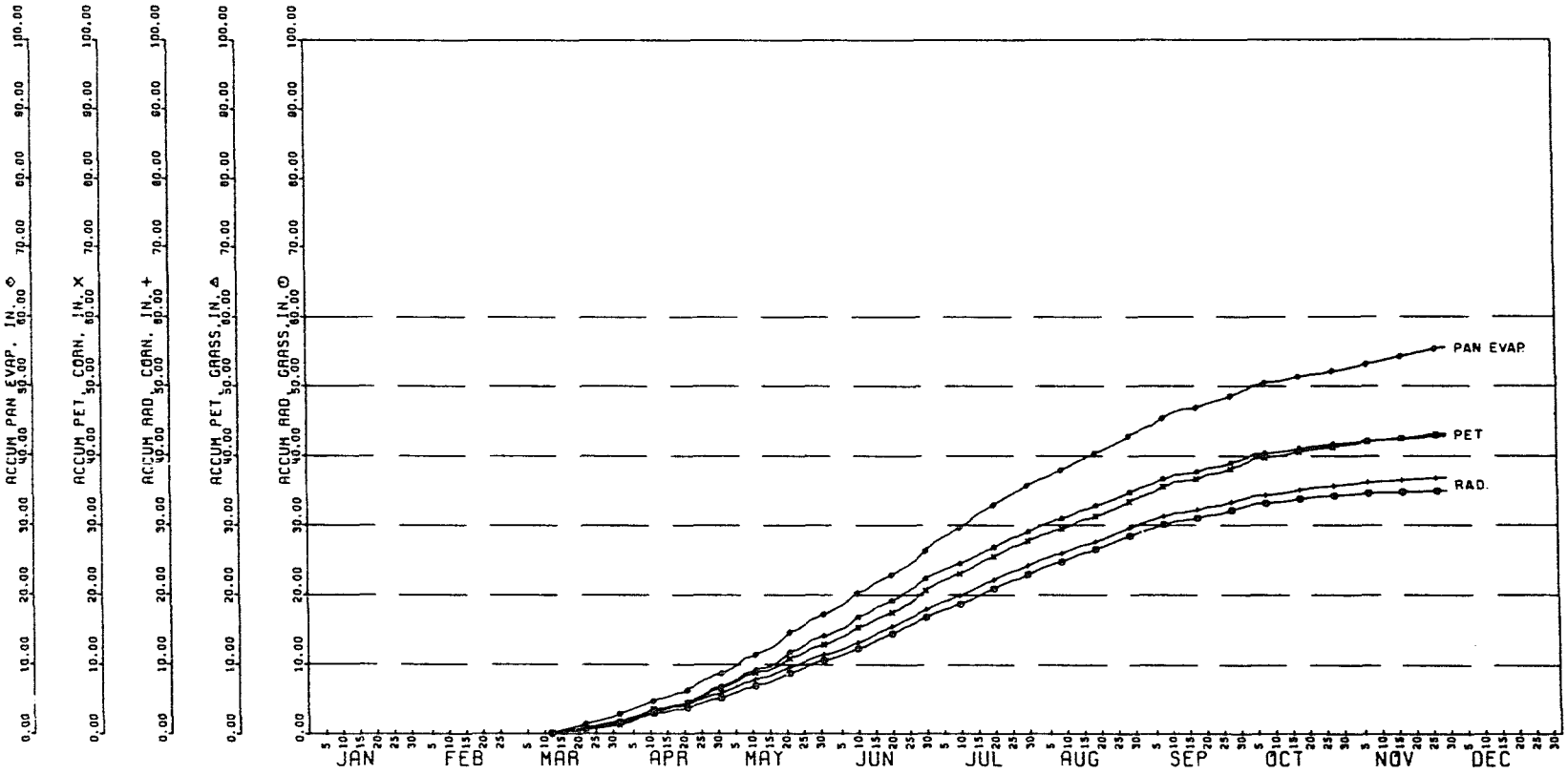

Figure 47. Annual accumulative values of net radiation, calculated potential ET, and pan evaporation for grass and corn during 1970

55 in. for 1970. Potential ET was about 41 and 43 in. for 1969 and 1970, respectively, while equivalent net radiation over corn was 40 and 37 in.; thus the difference between ET and R_n was about 1 and 6 in. for the two years. The summer of 1970 was quite hot and dry compared with 1969 when more uniform rainfall distribution occurred (see figures 58 to 61); thus there probably was more advection in 1970 than 1969.

It is apparent that these accumulative curves are reasonably smooth despite the large daily variation in the values. It is this fact that allows some empirical methods to operate moderately successfully. The potential ET values representing these accumulative curves were used for the actual ET calculations discussed in the next section.

In summary, we have shown that once acceptable wind parameter values were obtained, calculated daily potential ET values compared favorably with net radiation and pan evaporation. Correlations with pan evaporation showed good daily sensitivity, and there was a better correlation between ET and pan evaporation than between ET and net radiation. The apparent reason was the influence of aerodynamic parameters.

Error Analyses

An important aspect of computing ET values by the combination model is the expected error of the computed values. Of course, this error depends on the expected error of the independent variables, but with the working ET model having the form

$$E = \frac{(\Delta/\gamma)\, R_n + 791\, d_a u_a W^{-1}}{(1 + (\Delta/\gamma))\, 1481} \tag{6}$$

where

$$W = \left[\ln\left(\frac{Z_a + d}{Z_o}\right)\right]^2 \tag{7}$$

it is apparent that the error caused by any one variable is quite dependent on the values of the other variables. We can, for example, intuitively see that the percentage of any R_n error transferred to E depends on the relative magnitude of the net radiation and aerodynamic terms.

There are two aspects of error investigations. First, given a probable error of any one variable, we can ask what probable error will be caused in the computed value. This approach is actually a sensitivity analysis; that is, it shows the relative sensitivity of the computed value to each of the independent variables. The second aspect is one of defining expected errors for each of the variables

and defining their combined effect on the dependent variable, E. This aspect is much more complicated.

In this section, we will develop equations to describe the sensitivity of the independent variables and show examples of their results, but only briefly discuss the general error situation.

Scarborough (1958, p. 9) showed that for a function

$$N = f(u_1, u_2, u_3, \cdots) \quad , \tag{8}$$

the relative error of N denoted by the subscript ξ, would be defined as

$$N_\xi = \frac{\Delta N}{N} = \frac{\partial N}{\partial u_1}\frac{\Delta u_1}{N} + \frac{\partial N}{\partial u_2}\frac{\Delta u_2}{N} + \cdots \tag{9}$$

Using this definition of relative error, it is also apparent that

$$u_{1\xi} = \frac{\Delta u_1}{u_1} \quad , \text{ or } \quad \Delta u_1 = u_1 u_{1\xi} \tag{10}$$

Thus, we can write

$$N_\xi = \frac{\partial N}{\partial u_1}\frac{u_1}{N}(u_{1\xi}) + \frac{\partial N}{\partial u_2}\frac{u_2}{N}(u_{2\xi}) + \cdots \tag{11}$$

The relative error is comparable to a decimal percentage. Thus equation 11 can be interpreted as the error percentage of N caused by the percentage errors of u_1, u_2, etc. If the variables are considered singly with the assumption that all other variables have zero error, this equation shows the error percentage of the dependent variable caused by a specified error of the independent variable; that is, the sensitivity of the result to the independent variable. The complete equation 11 would give the total expected error of the dependent variable when the error of each independent variable is specified.

The error solution of equation 11 was applied to the combination equation 6 and wind profile equation 7 for each of their variables individually, and was then applied to the combined variables. For example, the relative error equation representing net radiation, R_n, was developed by first writing

$$E_{\xi} = \frac{\partial E}{\partial R_n} \frac{R_n}{E} \quad R_{n\,\xi} \tag{12}$$

then rearranging the combination model

$$E = \frac{(\Delta/\gamma)\, R_n}{(1+(\Delta/\gamma))\ 1481} + \frac{791\ d_a u_a W^{-1}}{(1+(\Delta/\gamma))1481} \tag{13}$$

and differentiating to give

$$\frac{\partial E}{\partial R_n} = \frac{(\Delta/\gamma)}{(1+(\Delta/\gamma))1481} \quad . \tag{14}$$

Substituting 13 and 14 into 12 gave the result

$$E_\xi = \frac{1}{1 + \left[\frac{791\, d_a u_a W^{-1}}{(\Delta/\gamma)\, R_n}\right]} R_{n_\xi} \quad . \tag{15}$$

Equations representing the other variables are presented in table 2. The three aerodynamic terms are represented by the same equation. The equations for Z_a, d and Z_o for errors of E were developed by substituting equation 7 into 6. Note that the effects of these three variables were also considered separately for both equations 6 and 7. It is apparent from these equations that the effect of any one variable is quite dependent on the magnitude of several others.

Example results are shown in figures 48 to 51 for the 1969 data over grass and corn. In figures 48 and 49, the relative sensitivities of R_n, Δ, d_a, u_a and W are shown; plus the total relative error, which assumed a uniform error of all variables. As expected, E became more sensitive to R_n during midyear when net radiation dominated (figures 44 and 45). The opposite occurred for the aerodynamic

Table 2. Equations defining relative error of the combination model and wind parameter

Variable	Relative Error Equation
	Combination Equation 5
R_n	$E_\xi = \dfrac{1}{\left[\dfrac{791\ d_a\ u_a\ W^{-1}}{(\Delta/\gamma)\ R_n}\right] + 1}\ R_{n\xi}$
Δ	$E_\xi = \dfrac{(R_n - 791\ d_a\ u_a\ W^{-1})}{(\Delta R_n + \gamma\ [791\ d_a\ u_a\ W^{-1}])}\ \dfrac{\gamma\Delta}{\gamma + \Delta}\ \Delta_\xi$
d_a, u_a, W	$E_\xi = \dfrac{1}{\left[\dfrac{(\Delta/\gamma)\ R_n}{791\ d_a\ u_a\ W^{-1}}\right] + 1}\ d_{a\xi}$
Z_a	$E_\xi = \dfrac{2\ W^{-\frac{1}{2}}}{\left[\dfrac{(\Delta/\gamma)\ R_n}{791\ d_a\ u_a\ W^{-1}}\right] + 1}\ \dfrac{1}{(1 - [d/Z_a])}\ Z_{a\xi}$
d	$E_\xi = \dfrac{2\ W^{-\frac{1}{2}}}{\left[\dfrac{(\Delta/\gamma)\ R_n}{791\ d_a\ u_a\ W^{-1}}\right] + 1}\ \dfrac{d}{Z_a - d}\ d_\xi$
Z_o	$E_\xi = \dfrac{2\ W^{-\frac{1}{2}}}{\left[\dfrac{(\Delta/\gamma)\ R_n}{791\ d_a\ u_a\ W^{-1}}\right] + 1}\ Z_{o\xi}$
All	$E_\xi = K_1\ (R_{n\xi}) + K_2\ (\Delta_\xi) + K_3\ (d_{a\xi}) + K_4\ (u_{a\xi}) +$ $K_5\ (Z_{a\xi}) + K_6\ (d_\xi) + K_7\ (Z_{o\xi})$ where K_i to K_7 are as defined above for each variable

Table 2. Continued

Variable	Relative Error Equation
	Wind Parameter Equation 6
Z_a	$W_\xi = 2 \left(\frac{Z_a}{Z_a - d}\right) W^{-\frac{1}{2}} \quad Z_{a\xi}$
d	$W_\xi = 2 \left(\frac{d}{Z_a - d}\right) W^{-\frac{1}{2}} \quad d_\xi$
Z_o	$W_\xi = 2 W^{-\frac{1}{2}} \quad Z_{o\xi}$

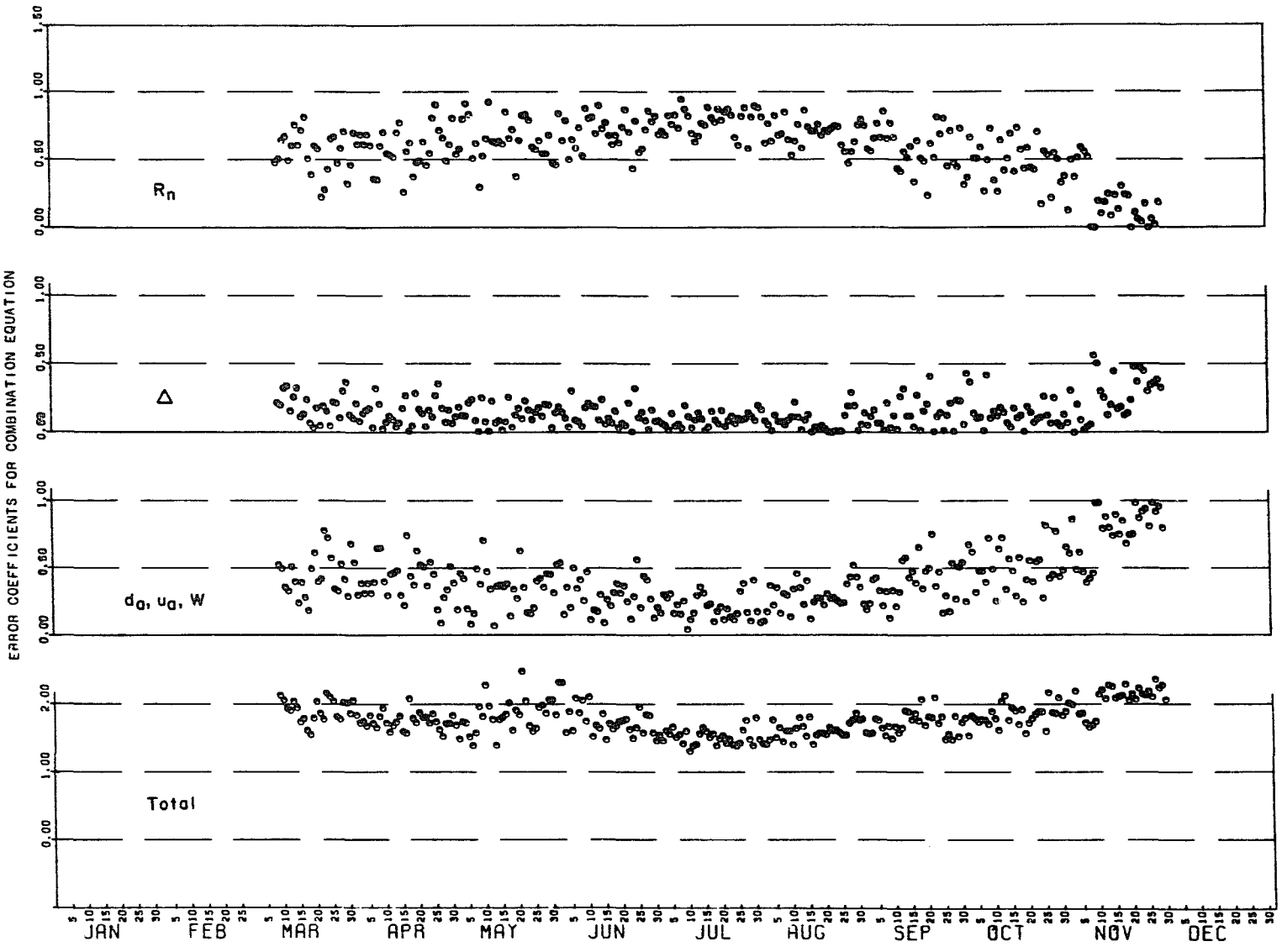

Figure 48. Relative error values for the combination equation for grass during 1969

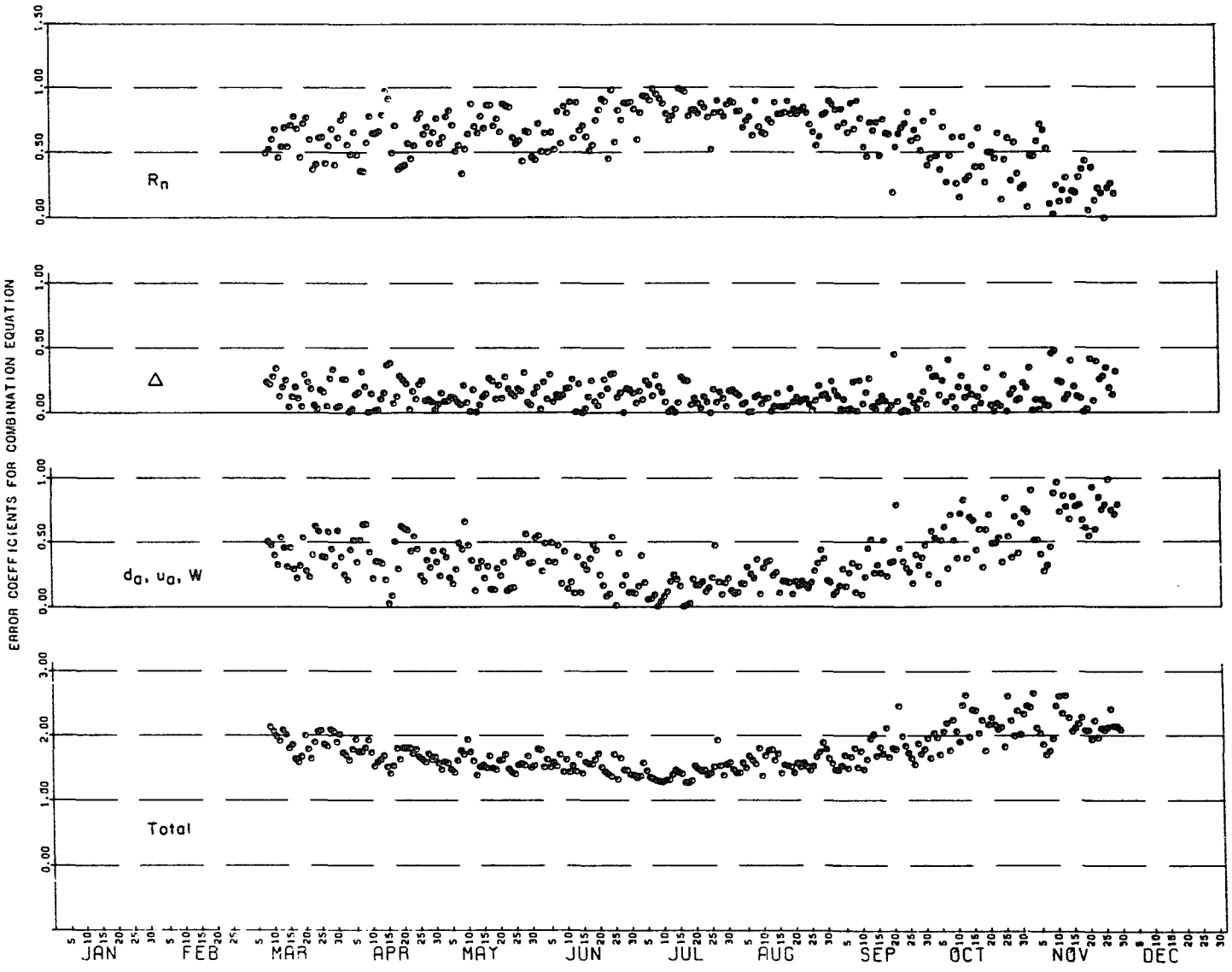

Figure 49. Relative error values for the combination equation for corn during 1969

variables d_a, u_a and W. E was not largely sensitive to Δ. The total error of E was nearly double the error of the independent variables. Thus, if all variables had a +5% error, E would have an error of approximately +10%. A comparison of figures 48 and 49 showed little difference between corn and grass, and very similar magnitudes and distributions were obtained with the 1970 data.

Figures 50 and 51 show the effects of wind profile parameters Z_a, d, and Z_o on both the E values (equation 6) and W values (equation 7). The calculated E values were not too sensitive to Z_a and d values, and of course the relative error of d was 0 until crop height was such that a displacement would be calculated by equation 5. Only 10% to 20% of a Z_o error would be transmitted to calculated E values; however, in this case the magnitude of the expected error became important. We discussed earlier in this chapter the poor results obtained when using estimated Z_o values by the techniques described in Appendix B; when compared with the "acceptable" values, those estimated (Appendix B) were several hundred percent in error. Thus, even though values of figures 50 and 51 suggest that only 10% to 20% of any error of Z_o would appear in E, this amount was significant when the Z_o errors were extreme. Of course, this argument would also apply

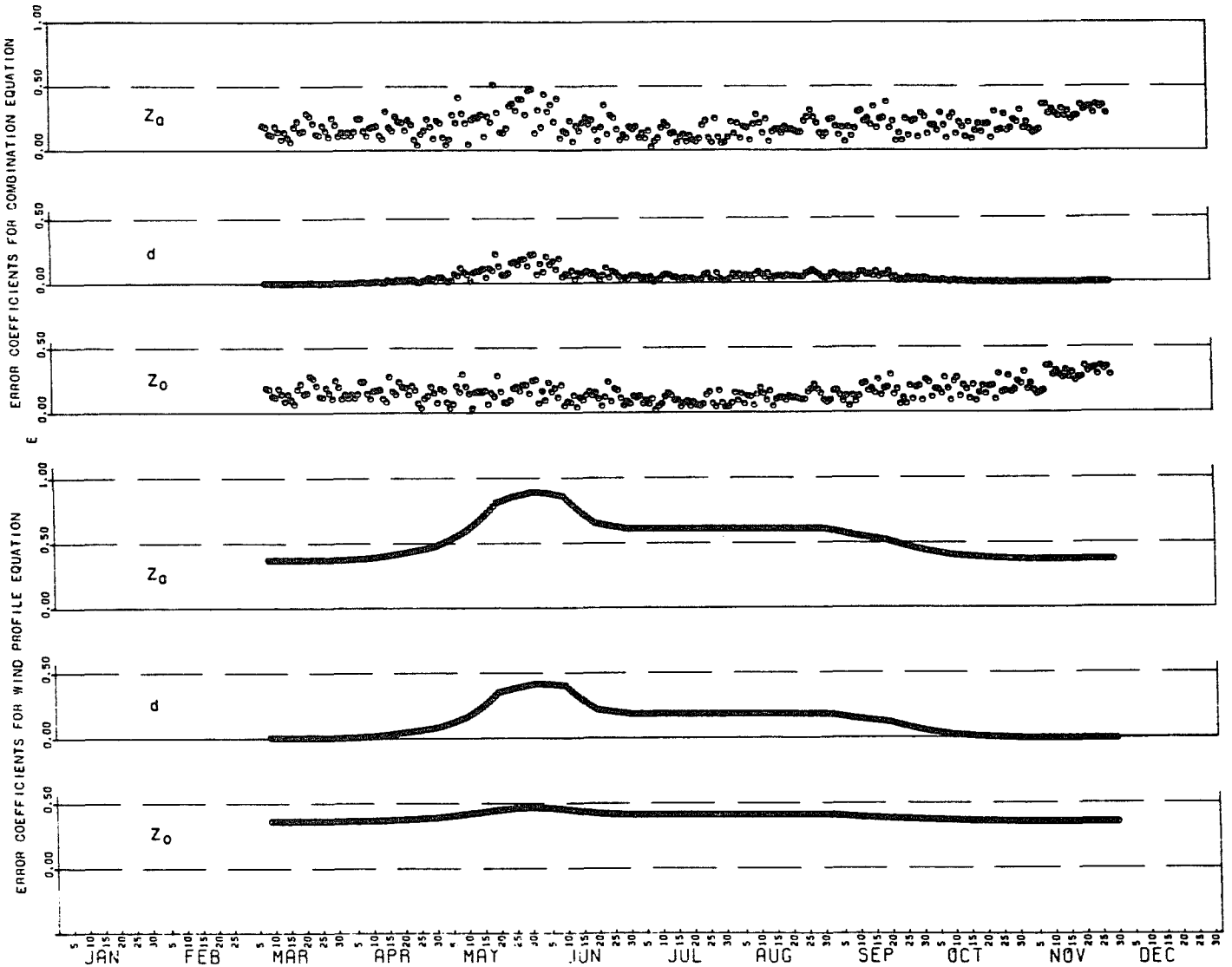

Figure 50. Relative error values for the wind parameters for grass during 1969

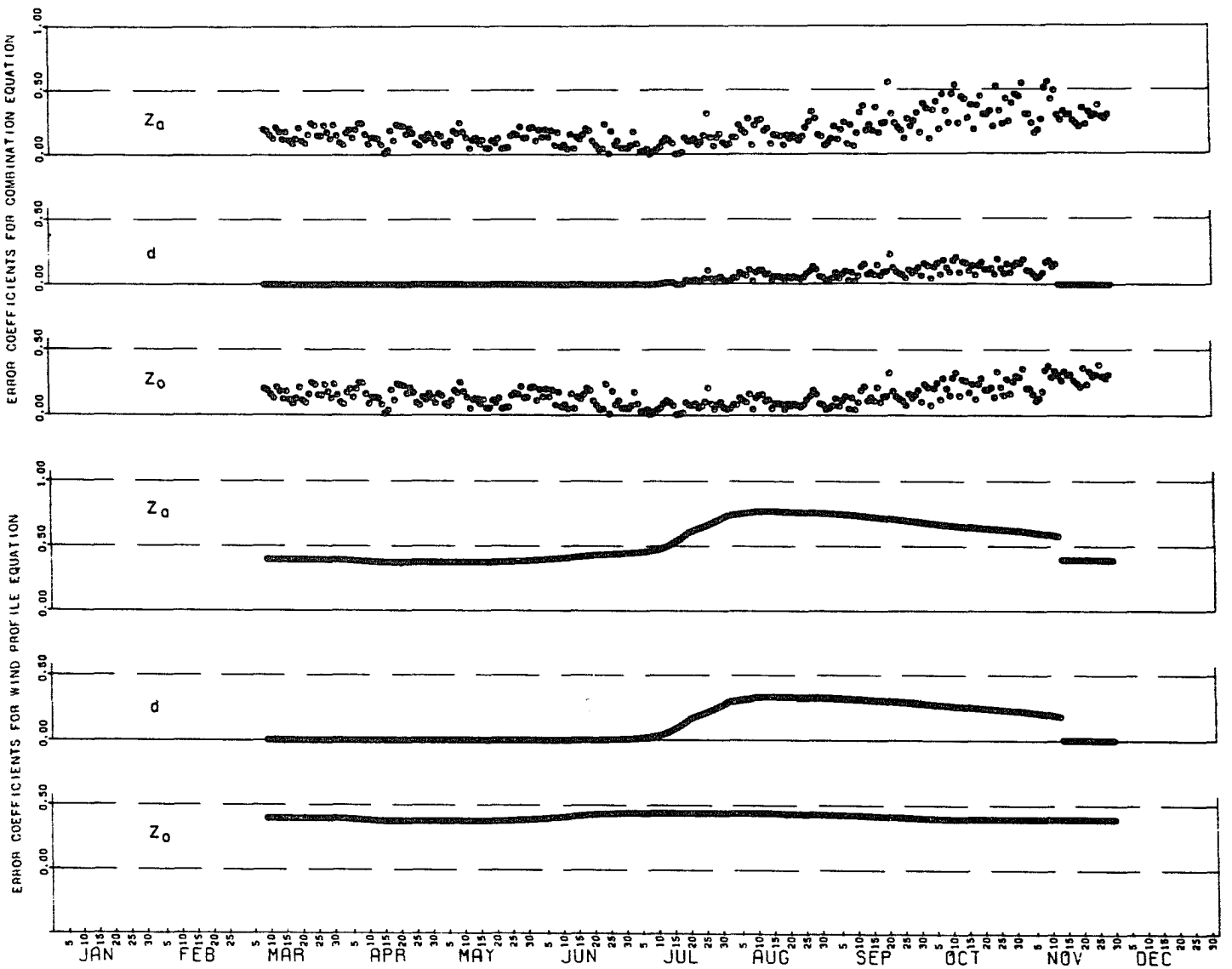

Figure 51. Relative error values for the wind parameters for corn during 1969

to any of the other variables, but their errors are not likely to be this great. The relative errors of Z_o shown in figures 50 and 51 agree reasonably well with those suggested by van Bavel (1966, p. 458), but he did not consider the possible magnitude of the error.

The three bottom graphs of figures 50 and 51 show that the relative errors of W are functionally dependent on the measured Z_a values, estimated W values (figures 31 to 34), and calculated d values (equation 5). The break in the Z_a and d corn curves about mid-November was the effect of corn harvest.

The results of this error study showed the sensitivity of the calculated E values to the independent variables. Because the sensitivity of any single variable is dependent on the magnitude of the others, there is no method of visualizing the potential sensitivity by means other than a day-to-day treatment of the sensitivity equations. The error analyses showed that E values were not exceptionally sensitive to any variable. Net radiation became quite important during midyear and, similarly, the aerodynamic terms became important early and late in the year.

Tanner and Pelton (1960, p. 3396) gave a general error discussion of the equation as applied to their situation, and arrived at similar conclusions. They carried their considerations farther into the expected errors of the several variables and their probable effect. This is the second necessary aspect mentioned earlier, but this amount of detail was beyond the scope of this study.

ACTUAL ET CALCULATIONS

To arrive at a day-to-day soil moisture status, we must know the daily values of the soil-plant-air model shown in figure 1. As discussed in the section on procedures, precipitation and actual ET are the main processes of water movement in this model. Precipitation is most often measured, which leaves actual ET next in importance for consideration. To this point in the study, we have calculated daily potential ET values; however, because of plant and soil characteristics and soil moisture status, actual ET is often less than potential. In this section, we will present the details of a rational model to obtain actual ET from potential ET and will evaluate the results by comparing measured and calculated soil moisture profiles.

In the section on procedures, we discussed the considerations necessary for calculating actual ET and the flow chart shown in figure 2. The reader may wish to review this discussion before proceeding with the details that follow.

Rational ET Model Description

Following the same format as shown in figure 2, a more detailed flow chart of the soil-plant-air model (figure 1) is shown in figure 52. The graphs and curves sketched in figure 52 are examples of those used. These relations will be shown in detail as each process is considered approximately in the sequence shown in figure 52.

In the soil-plant-air model we are primarily interested in water movement, but the energy for this movement comes mostly from the sources which cause ET. Therefore, our first task in developing the model was to consider how the available ET energy is partitioned and what water is moved by this energy; then to consider this water movement and the resulting affect on the soil moisture profile. Thus, all of the processes in figure 52 from potential ET to actual ET consider energy division; and those near the bottom of the figure, connected by crosshatched lines, involve actual water movement.

We begin with a known daily potential ET. In this study we used the potential ET calculated by the combination model. In future applications, this potential may be defined by reduced pan evaporation or other means.

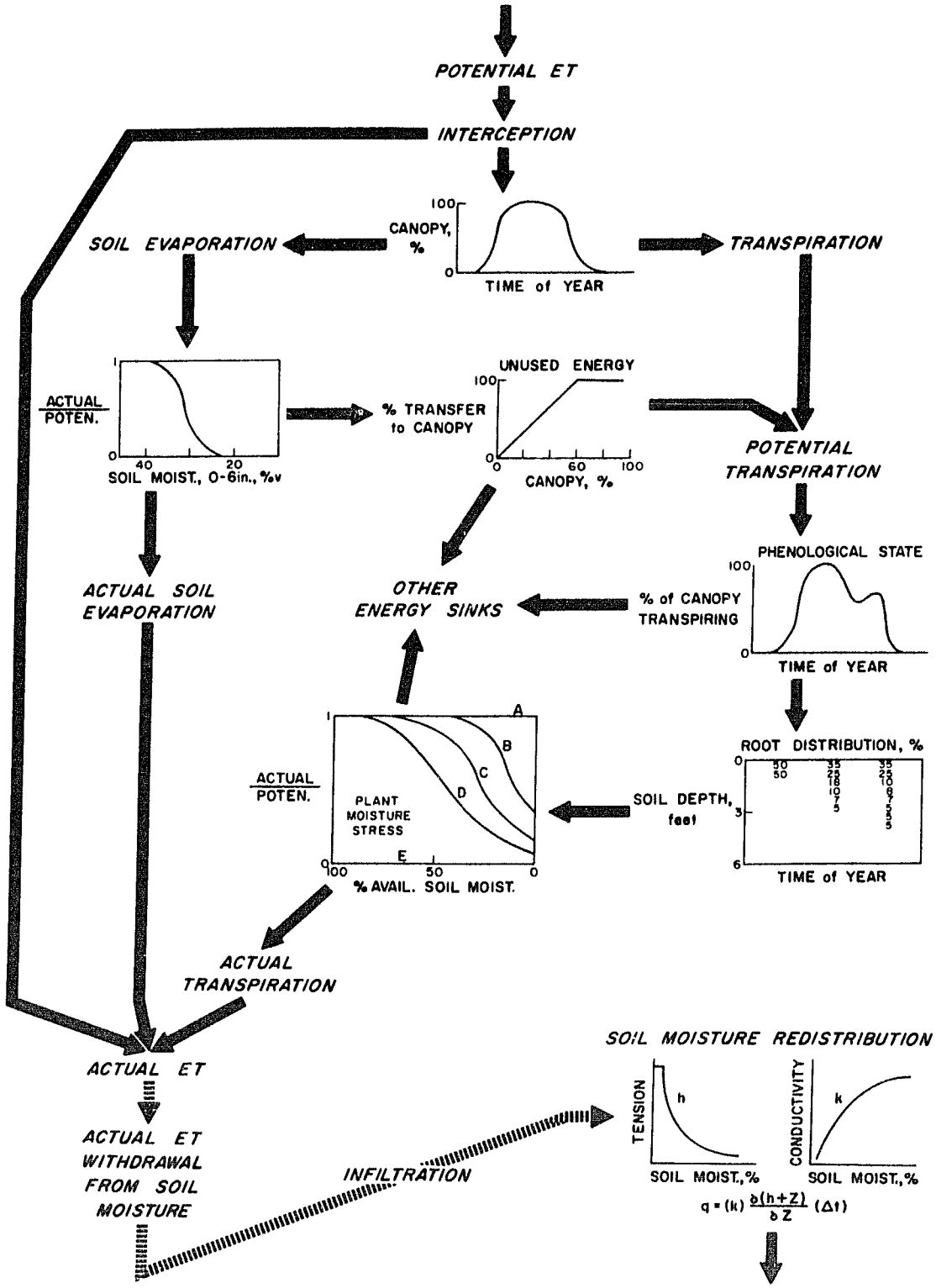

Figure 52. Schematic of the rational model for computing actual evapotranspiration and soil moisture status

Intercepted water lying on the plant leaf surfaces or surface soil particles has the first opportunity to utilize the ET energy. This water would readily evaporate with little restriction. Of course, intercepted water would be present only after rainfall. The quantity of interception is quite variable and is not well documented. For this study, a maximum value of 0.10 inch was assumed, regardless of canopy. In cases of little canopy, this partially allowed for soil evaporation when the soil surface was quite wet. Thus, the model operated by storing 0.10 in. of any daily rainfall as interception, and this was considered to have evaporated at the first opportunity. This interception evaporation became the first component of actual ET.

The remaining energy was next divided between that available for soil evaporation and that for plant transpiration. This division was based on field estimates of canopy shown in figures 31 to 34; thus the split was based mostly on radiation. Some recent studies show detailed measurements of radiation and energy penetration into the plant canopy, which might be used to improve the simplified approach taken here (Hanks et al. 1971).

Gardner and Hillel (1962) showed that soil evaporation proceeds at near the potential rate for an initially wet soil; but soon after the surface dries, the rate is dependent on the soil transmission of water to its surface. This water movement then would depend on the moisture tension and unsaturated conductivity, which both in turn depend on soil moisture content. For the model, a relation of actual/potential soil evaporation versus average soil moisture content of the top 6 in. was estimated which reflected these considerations. This empirical relation, shown in figure 53, allowed for soil evaporation at the potential rate above 40% soil moisture and no evaporation below 25%. A similar curve between 35% and 15% was first used, but this reflected too much soil evaporation when comparisons of calculated and observed soil moisture were made. Having considered some soil evaporation as intercepted water may have influenced this relation. In summary, the model procedures multiplied the actual/potential ratio times the potential for soil evaporation to calculate an amount of energy used for actual soil evaporation.

The potential energy striking the soil surface but not used in evaporation is available for heating the soil and air and other minor energy sinks. This additional heating sets up convective turbulence within the plant canopy

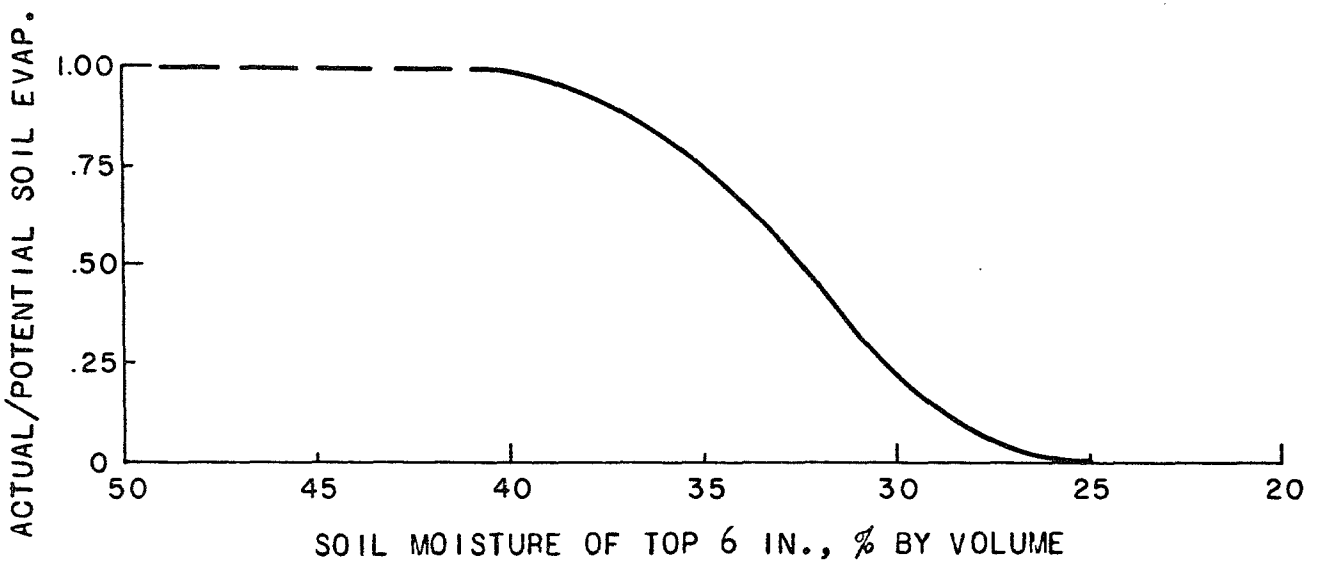

Figure 53. Estimated relationship for converting potential to actual soil evaporation

and increases soil radiation; thus, some of this unused energy becomes available to the plant for transpiration. Tanner (1957) described this procedure, and Hanks et al. (1971) presented data for 2 days which somewhat quantified this within-canopy advection.

The relation shown in figure 54 was used to estimate this soil-to-plant transfer. It was assumed that the transfer would increase linearly to 100% when the canopy reached 60%, and would then continue to be 100% for all denser canopies. It is improbable that the canopy would utilize all unused soil evaporation energy, but the values used appeared to be satisfactory as a first estimate.

The potential for plant transpiration, shown on the right side of figure 52, was the sum of the direct potential energy for transpiration plus an amount of the unused soil evaporation energy. The first aspect in utilizing this potential transpiration was to consider the phenological status of the plant with respect to its ability to transpire. For example, was the canopy a lush green crop actively growing, or a maturing crop with many inactive stems and leaves.

Relationships shown in figure 55 were used to estimate this phenological condition. These were based on field observations. The same curve was used for both years of

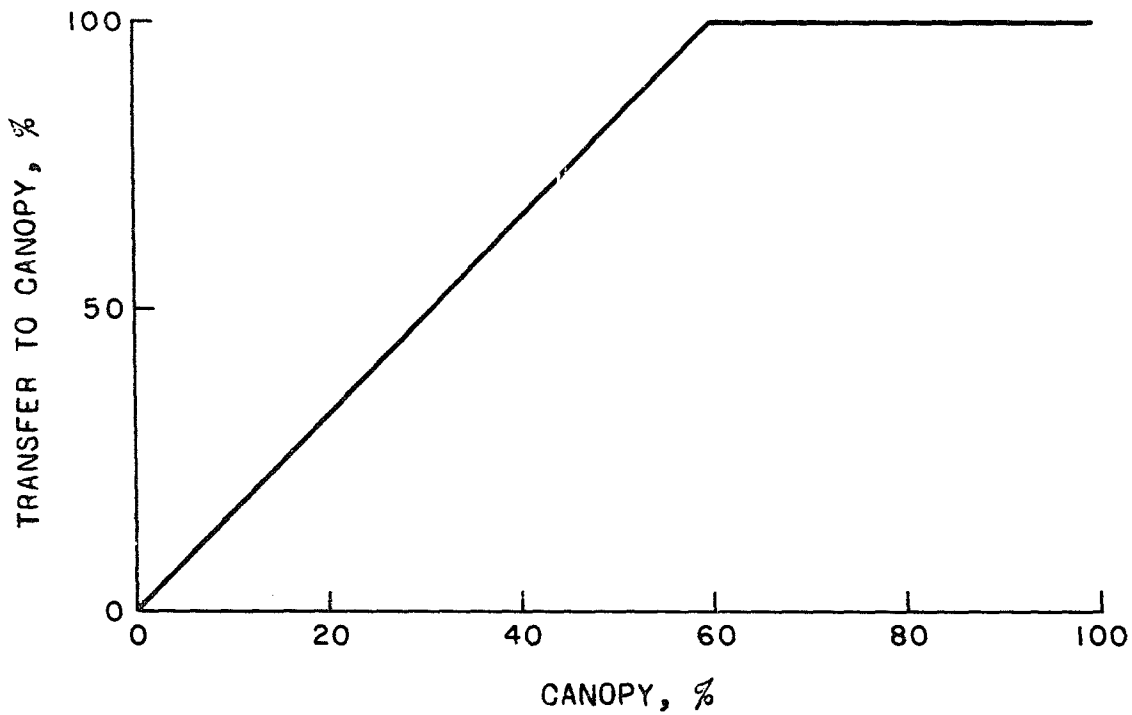

Figure 54. Estimated relationship for soil-to-plant transfer

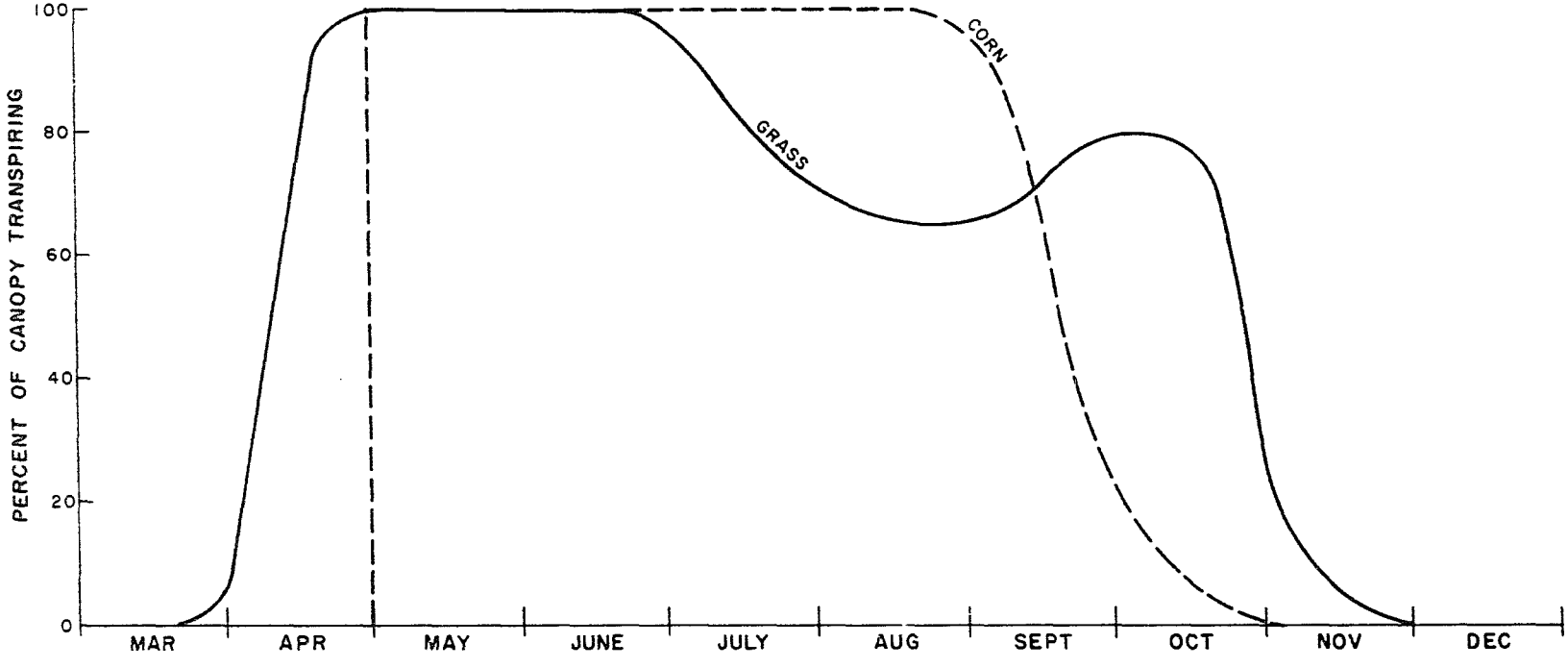

Figure 55. Relationships representing plant transpirability during the year depending upon the phenological plant status

calculations for each crop. For grass, a dead canopy existed during the winter which was gradually replaced as the new growth began in the spring. The cool season grasses at our location become partially dormant during late July and August because of heat and grazing, but they have some regrowth in early fall until frost and grazing again cause dormancy.

Corn was immediately a fully transpiring canopy from emergence until it began maturing in late August. Of course there was little canopy present early in the year, but this was considered in the soil-plant division. Frost and harvest caused a rather abrupt decline in the fall, and only dead residue remained for winter and spring canopy.

Soil moisture availability is one of the primary factors that determines transpiration, but because the soil moisture may vary considerably with depth, it was necessary to know where the plant was attempting to obtain its water. This, of course, primarily depends on root distribution, but additional effort (tension) is also required for a plant to lift deeper water; and if the soil texture varies the tension for extraction will also vary.

For a first approximation in the relatively uniform loess being considered, an extraction pattern was estimated which was based primarily on root distributions of the two

crops as described by others (Linscott, Fox, and Lipps, 1962; Weaver, 1926; Shaw, 1963 and 1964). These sources were compared and summarized, and the results are presented in table 3. Each value in the table represents the percentage of the potential transpiration, reduced by the phenological condition, that would come from that soil zone if adequate water was present. The corn distribution assumed a planting date of about May 1 and growth patterns as shown in figures 33 and 34. The grass was an established stand; thus the same extraction pattern was used for the entire year.

It is well recognized that plants growing with limited available water will transpire at less than the potential rate due to stomatal closure, increased soil tensions, and other physiological responses. This is the last consideration before arriving at an actual transpiration value in the rational model as shown near the center of figure 52.

Denmead and Shaw (1962) have shown that the percentage of potential transpiration that actually occurs under conditions of limited available water is a function of both available soil water and the atmospheric demand (potential transpiration). They represented this effect by a relation like that in figure 52. The ratio values of actual/potential transpiration are plotted versus available soil moisture.

Table 3. Distribution of water extraction by transpiration, percent

Depth of Soil Zone in.	Corn									Grass
	Beginning Date of Period									
	May 10	June 7	June 14	June 27	July 4	July 11	July 18	July 25	Aug 1	All
0-6	100	50	40	35	35	35	35	35	30	35
6-12		50	27	25	25	25	25	25	25	30
12-18			20	20	18	15	10	8	8	20
18-24			13	10	10	8	8	7	7	10
24-30				10	7	7	7	5	5	3
30-36					5	5	5	5	5	2
36-42						5	5	5	5	
42-48							5	5	5	
48-54								5	5	
54-60									5	

The three curves B, C, and D represent three levels of atmospheric demand. Shaw (1963 and 1964) gave details of these curves and defined the demand rates as pan evaporation rates of less than 0.20 in./day (curve B), 0.20 to 0.30 in./day (curve C), and more than 0.30 in./day (curve D). He successfully applied these relationships to both meadow and corn.

These same relationships were applied in this rational model, but the curves B, C, and D were defined in terms of the potential for transpiration as established prior to reductions for phenological status. The transpiration value associated with each curve was estimated by considering Shaw's pan values and trial computations. Pan evaporation would usually be more than the potential for transpiration; thus the transpiration value associated with each curve was usually less than the pan evaporation value. These relationships represent the crop's ability for continued transpiration under moisture stress; thus the same curve values probably would not apply to two different crops. Final assigned values for curves B, C, and D, respectively, were 0.10, 0.20, and 0.30 in. for corn and 0.10, 0.15, and 0.20 in. for grass. Rather than assign a range of values to each curve as did Shaw (1963, 1964), interpolations were made between curves. To allow

full graph interpolation, lines A and E were assigned values of 0.05 and 0.70 in., respectively, for both crops. The plant moisture stress relation was applied independently to each 6-in. soil zone in the 6-ft soil profile. The soil moisture status of each zone and the daily potential transpiration for curve interpolation were used for each calculation.

The difference between the demand values of each curve for corn and grass suggests that grass reduces its transpiration more than corn under equal moisture stress. There was no means within this study to verify this effect. It is possible that the values were required to be different to account for some unknown factors. This is an item that should be considered in more detail.

Thus, to summarize the calculation of actual transpiration from each 6-in soil zone, the daily potential transpiration was first reduced to account for the plants phenological state; then a percentage of this reduced potential was assigned to each soil zone, primarily based on the plants' root pattern; and finally an actual/potential ratio was applied which was derived by considering soil moisture status and the total potential transpiration

(atmospheric demand). This procedure gave a computed actual transpiration to be abstracted from each 6-in. soil zone, and their sum was the calculated daily transpiration.

The total daily actual ET was the sum of the interception evaporation, soil evaporation, and plant transpiration as shown in the lower left portion of figure 52. This daily value represented the energy actually used for ET. In addition, the calculation procedures defined which water was acted upon by this energy. The next steps in the rational model then considered the actual ET soil water abstractions and soil moisture readjustments due to infiltration and moisture tensions.

First, the amount of soil moisture evaporation was abstracted from the top 6-in. soil zone. Transpired amounts were abstracted from the 6-in. soil zones depending on their calculated amount and distribution. Next, infiltration was considered as the average watershed precipitation minus measured runoff and interception (0.10 in.). No time distribution was given to this infiltration, and it was assumed to be stored uniformly within the top 6-in. soil zone until that soil reached 0.9 of saturation; then additional amounts were cascaded to the lower soil zones with the same restrictions.

The last process considered in the rational model was the redistribution of soil moisture by the tension-conductivity concept, as shown in the lower right of figure 52. Changing water contents due to actual ET and infiltration cause non-equilibrium moisture gradients within the soil profile which result in moisture movement. Thus a soil moisture model would be incomplete unless this soil moisture redistribution was considered. The basic Darcy equation of soil moisture movement can be written

$$q = k \frac{\partial (H + Z)}{\partial Z} (\Delta T) \qquad (16)$$

where:

q	=	vertical water movement,	$cm^3\ cm^{-2}$
k	=	conductivity	$cm\ min^{-1}$
H	=	soil moisture tension head	cm
Z	=	elevation head	cm
ΔT	=	element of time	min

In the case of unsaturated soil, both K and H are functions of the soil moisture present, and these relations must be known or determined. For the loess soils of western Iowa, work by Melvin (1970) provided relationships that were applied. The moisture-tension relationships shown in figure 56 were used as the average of the wetting and drying curves shown by Melvin (1970, p. 130). The

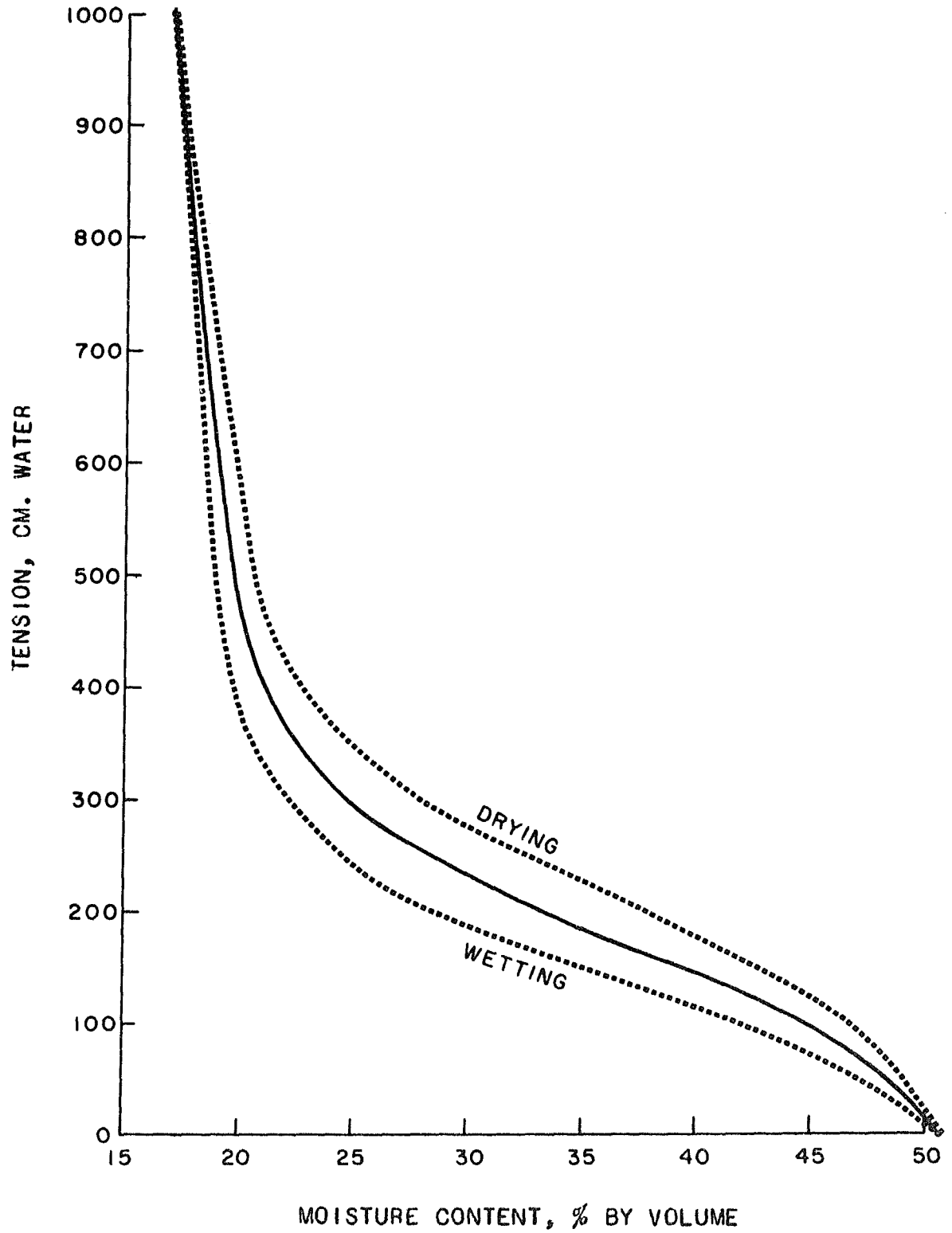

Figure 56. Tension-moisture content relationship for Monona silt loam - 60 in. depth (Melvin 1970, p. 130)

moisture-conductivity relation, shown in figure 57, was used as the lower curve presented by Melvin (1970, p. 169). A curve of higher conductivity values based on tension characteristics was first applied, but excessive moisture movement was computed. These relationships were applied to the complete soil profile because of the relative uniformity of these loess soils. A separate relationship for each 6-in. soil zone could have been applied if necessary and known.

The moisture movement was computed between successive 6-in. soil zones by applying equation 16 over 4-hour time periods; that is, the moisture contents were assumed constant for a 4-hour period; thus tensions, conductivities, and flow rates were held constant. Moisture contents were readjusted after each 4-hour period, new tensions and conductivities determined, and the next 4-hour period considered. Thus, soil moisture was redistributed in six steps per day. Earlier computations using one hour time periods showed almost identical results. In most cases, it would probably be possible to use periods longer than 4 hours with little error.

The complete 6-ft soil profile was considered by 6-in. increments for each 4-hour period and moisture allowed to flow either up or down, depending on the tension and

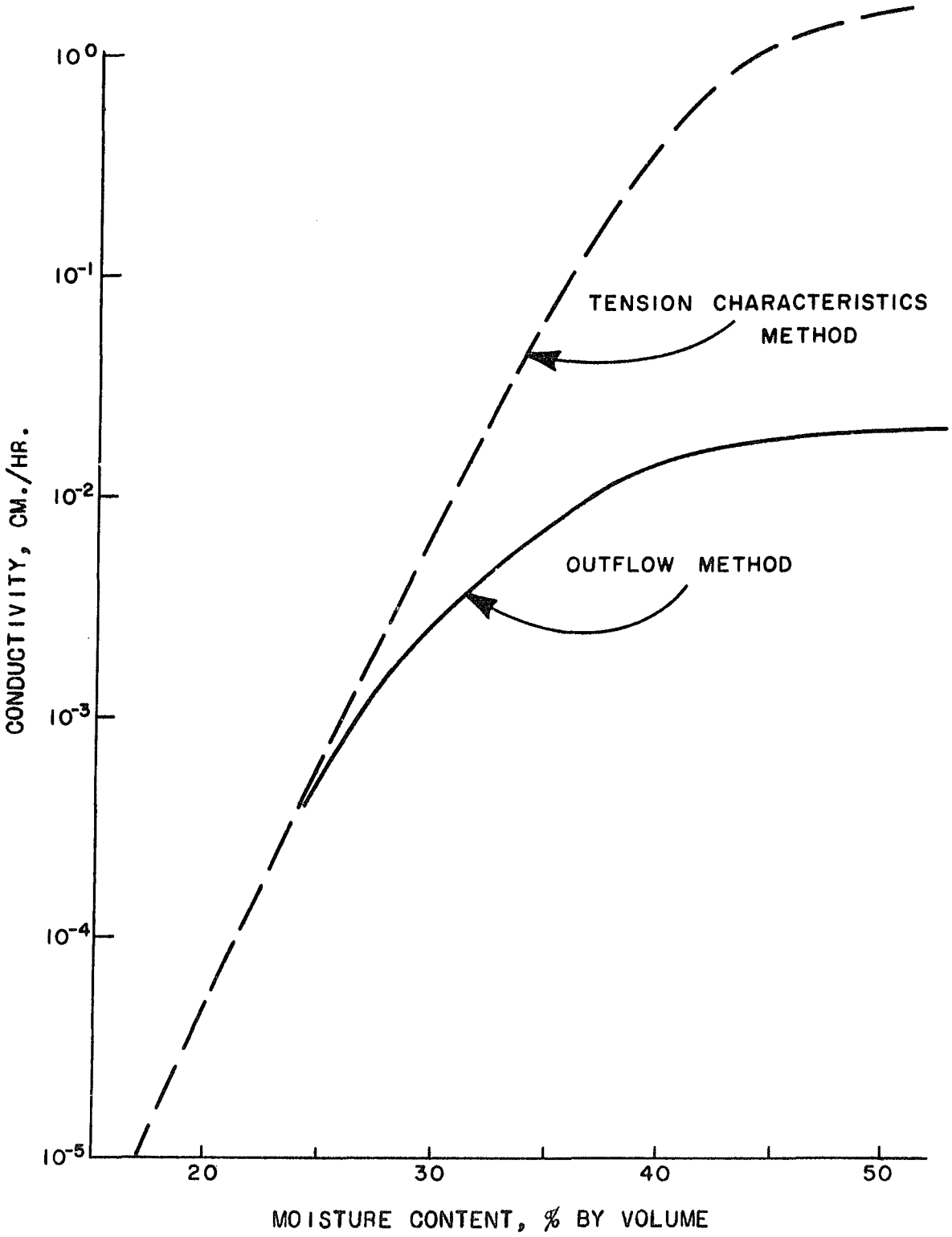

Figure 57. Conductivity estimates for Monona silt loam - 60 in. depth (Melvin 1970, p. 169)

gravity gradients. The 6-in. zone directly below the 6-ft soil profile was held at a constant moisture content of 0.9 field capacity (one-third bar tension). This procedure considered percolation into or out of the 6-ft root zone.

Several processes within the rational model required values of the soil moisture constants of saturation, field capacity, and wilting point. These values were determined by considering those published by Shaw et al. (1959), unpublished data of the Soil Conservation Service Soil Survey Laboratory at Lincoln, Nebraska, and observed soil moisture data on the Treynor, Iowa experimental watersheds. The values used were 11, 30, and 44% by volume for wilting point, field capacity, and saturation, respectively. Recent field data indicate that the wilting point and field capacity values should probably be 2% to 3% more.

In summary, the soil moisture in the 6-ft root zone was adjusted daily by withdrawing actual ET, considering infiltration into the surface horizons, and redistributing soil moisture by the tension-conductivity concept. These three steps allowed computing soil water quantities and the soil moisture profile in 6-in. increments. The sequence of considering the processes was somewhat arbitrary; they actually proceed simultaneously but the results indicate this method of application did not cause significant error.

The computed soil moisture values were important from two aspects: (1) the actual ET was quite dependent on the soil moisture status, and (2) the primary method of evaluation, to be discussed later, was based on a comparison of measured and computed soil moistures.

The complete rational model was programmed on an I.B.M. 360-65 computer, and a complete set of calculations was made for the same periods considered for computing potential ET values. The soil moisture values calculated for each day were used as input to the calculations of the following day. Initial soil moisture values were estimated as 0.8 of field capacity, but calculated values were set equal to observed values on the day of the first sampling of the season. The calculated values from that time forward were then dependent only on the model's operation.

Results and Evaluation

The rational model was operated by the use of: (1) the relations described in the previous section, (2) precipitation and runoff values, and (3) the first set of observed soil moisture values early in the year. The results of these calculations will be summarized in this section. These are only a few of the results that can be obtained from a model which encompasses the many facets of the system

represented. By necessity, most of the results will be presented as graphical summaries. This masks and omits many interesting details such as withdrawal patterns of transpiration from soil moisture, changing soil moisture tension patterns, and water movement between the soil zones; but these data are too numerous and are only obliquely related to the immediate objectives of this study.

The actual ET values were arrived at by several trials with the rational model. We have mentioned most of the changes which were made during these trials as we discussed the details of the relations in the preceding section. After the initial run, the adjustments can be summarized as: (1) changing the soil evaporation actual/potential relation, (2) accounting for the phenological decline of the grass during late summer, (3) slightly adjusting the assigned transpiration values of the moisture stress curves B, C, and D, and (4) selecting the curve with lower soil moisture conductivities as presented by Melvin (1970). Only two or three trial runs were used to make these adjustments and arrive at the results presented. Data from both years were usually used for each trial.

Accumulative volumes of the principal variables that were considered for the calculations of both potential and actual ET are presented in figures 58 through 61. Some of the variables related to potential ET were presented earlier, but they are repeated here for direct comparison with the actual ET variables. The uppermost line in each graph presents a comparison of calculated and observed total soil water in the top 6 ft of soil. Note that the calculated values were made equal to those observed on the first sampling date. Although total profile soil water provides one good comparison, the moisture of soil depth zones shown later (figures 66-73) provides much more detail; thus the discussion of soil moisture will be delayed until this presentation.

Actual ET was, of course, significantly less than the potential values. The reasons are as complex as the rational model and vary from day to day as the relations in the model require. The amounts of the actual ET components--interception evaporation, soil evaporation, and transpiration--are shown in figures 62 through 65. Although no direct methods are available for evaluating these amounts, they appear rational. The actual ET

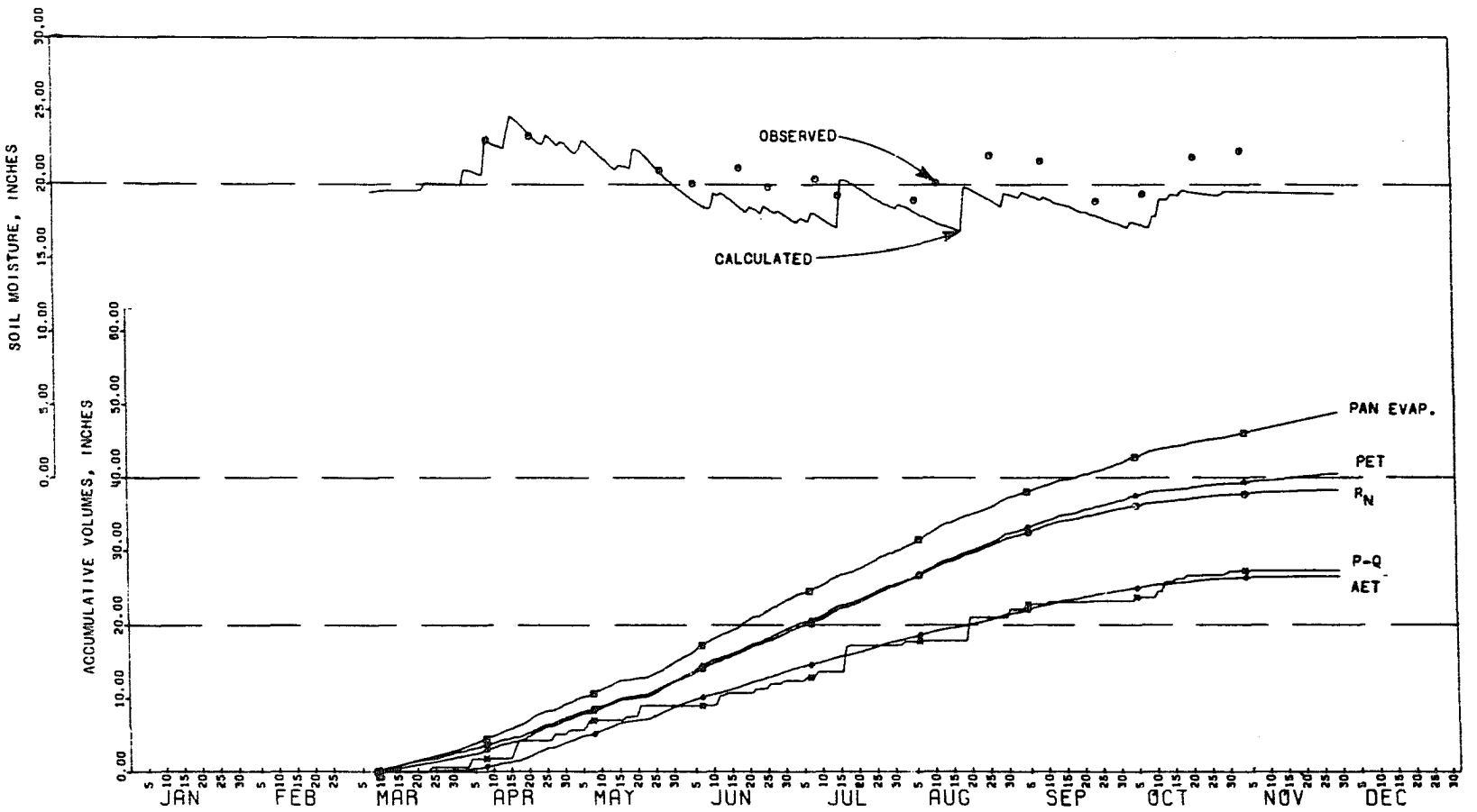

Figure 58. Accumulative volumes related to potential and actual ET and soil moisture in the top 6 feet, for grass during 1969

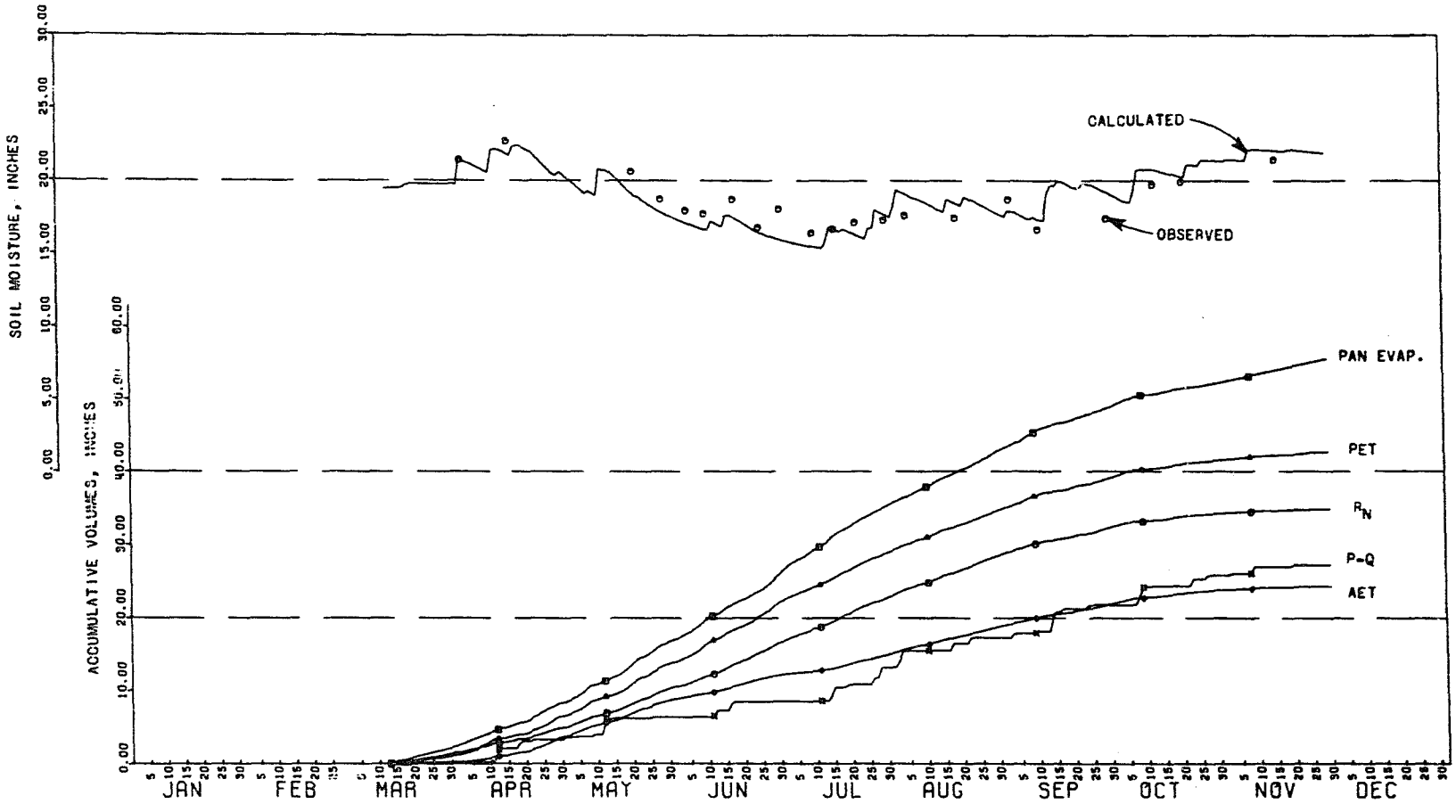

Figure 59. Accumulative volumes related to potential and actual ET and soil moisture in the top 6 feet, for grass during 1970

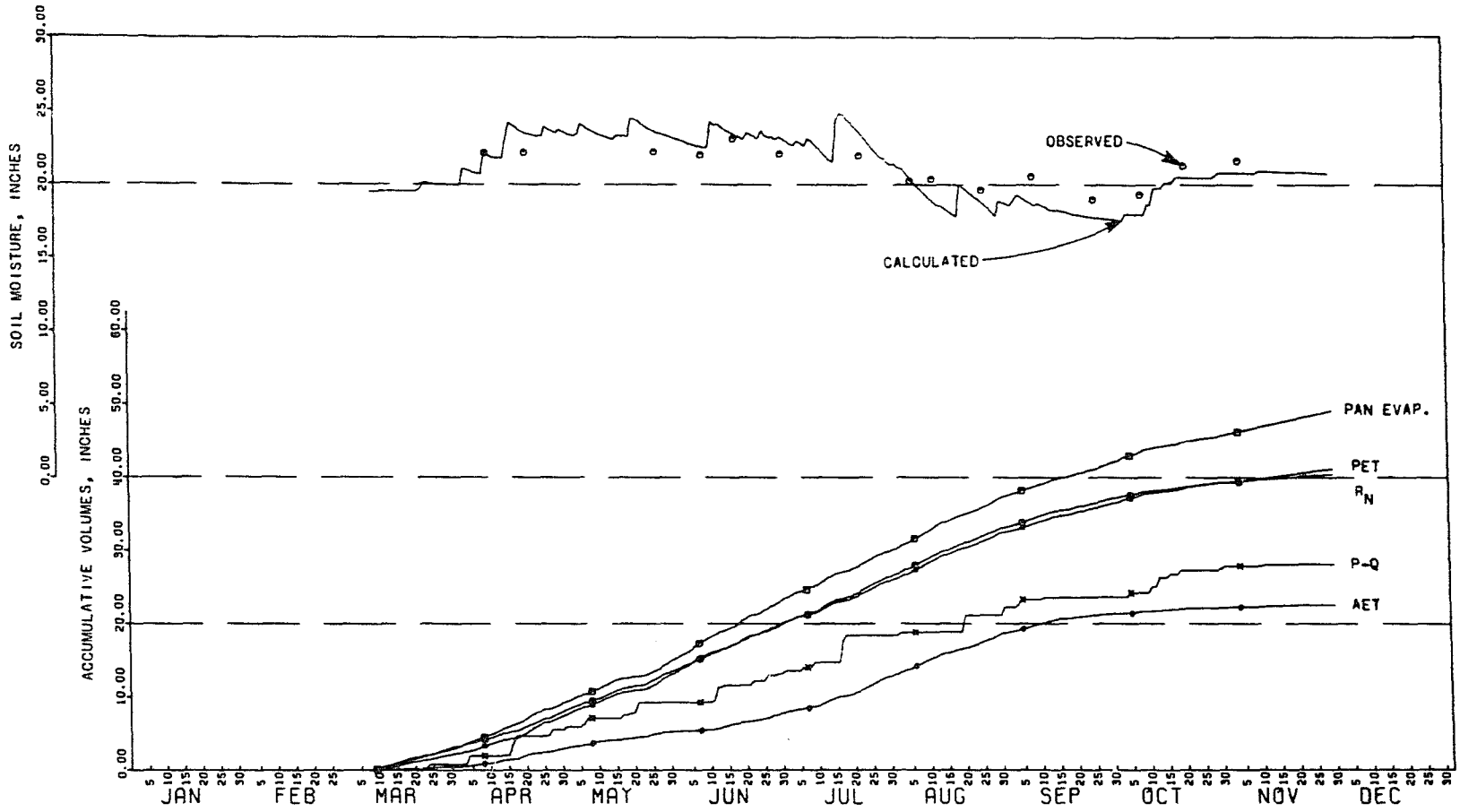

Figure 60. Accumulative volumes related to potential and actual ET and soil moisture in the top 6 feet, for corn during 1969

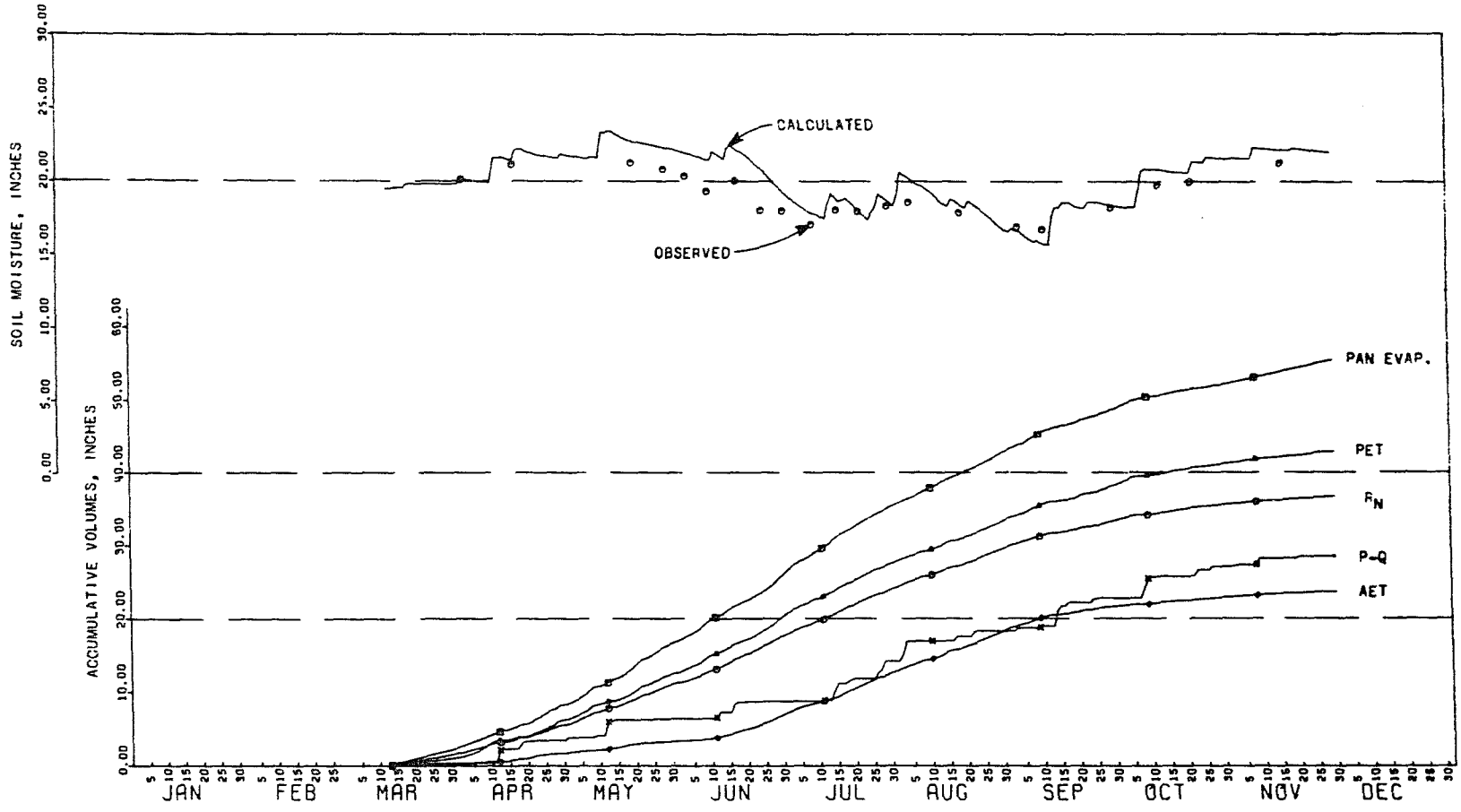

Figure 61. Accumulative volumes related to potential and actual ET and soil moisture in the top 6 feet, for corn during 1970

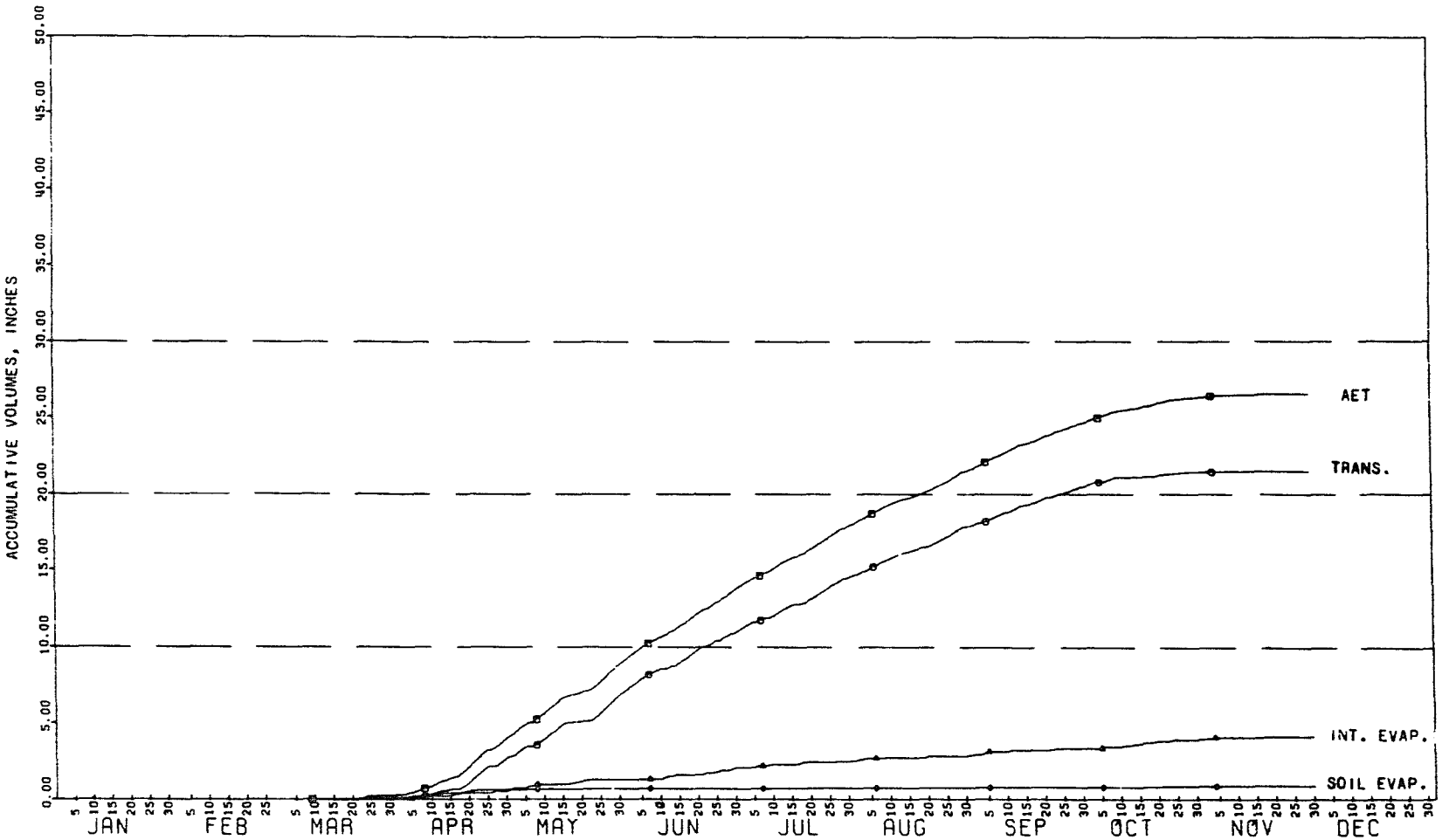

Figure 62. Accumulative actual ET and its components of transpiration, soil evaporation, and interception evaporation for grass during 1969

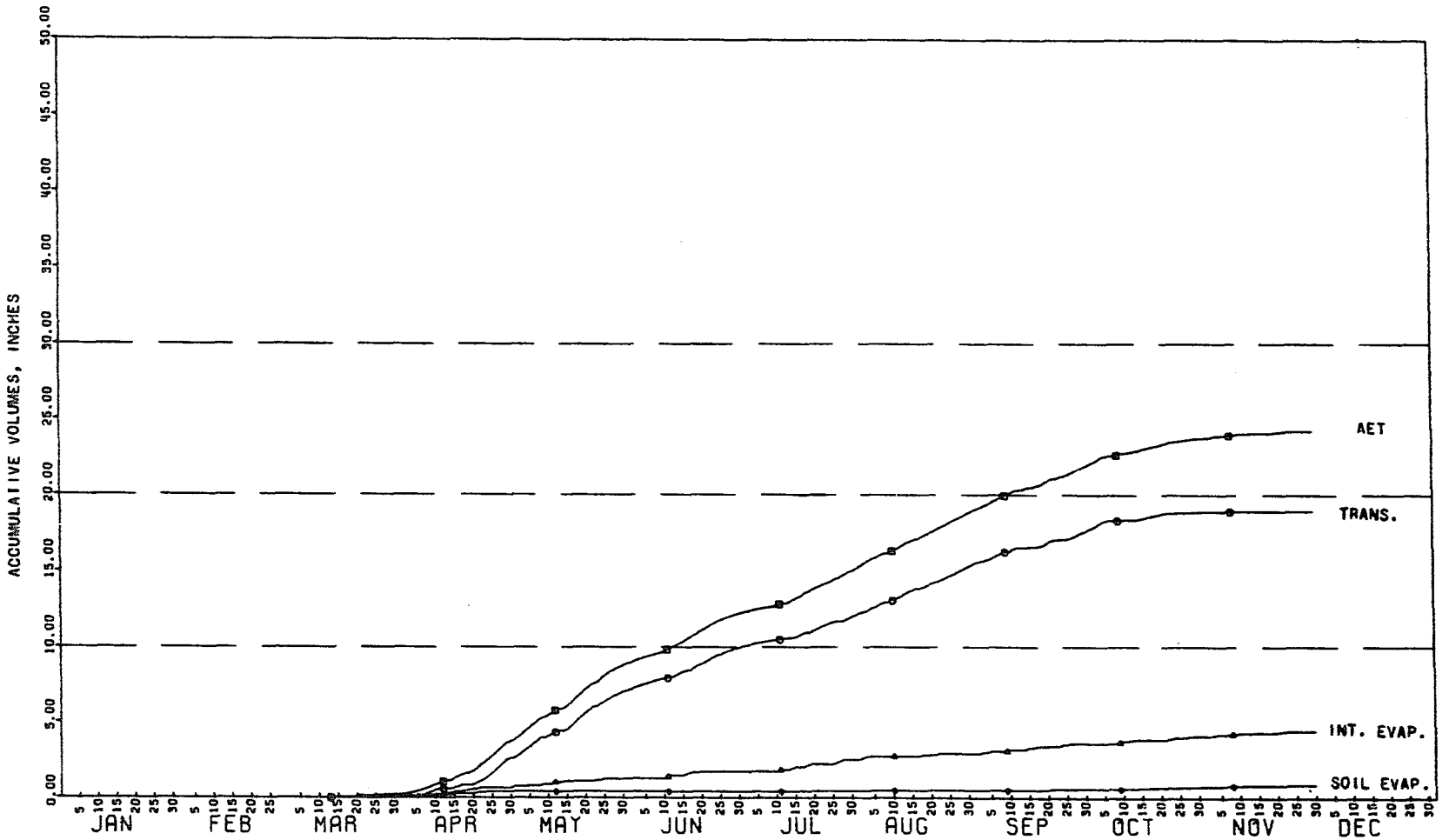

Figure 63. Accumulative actual ET and its components of transpiration, soil evaporation, and interception evaporation for grass during 1970

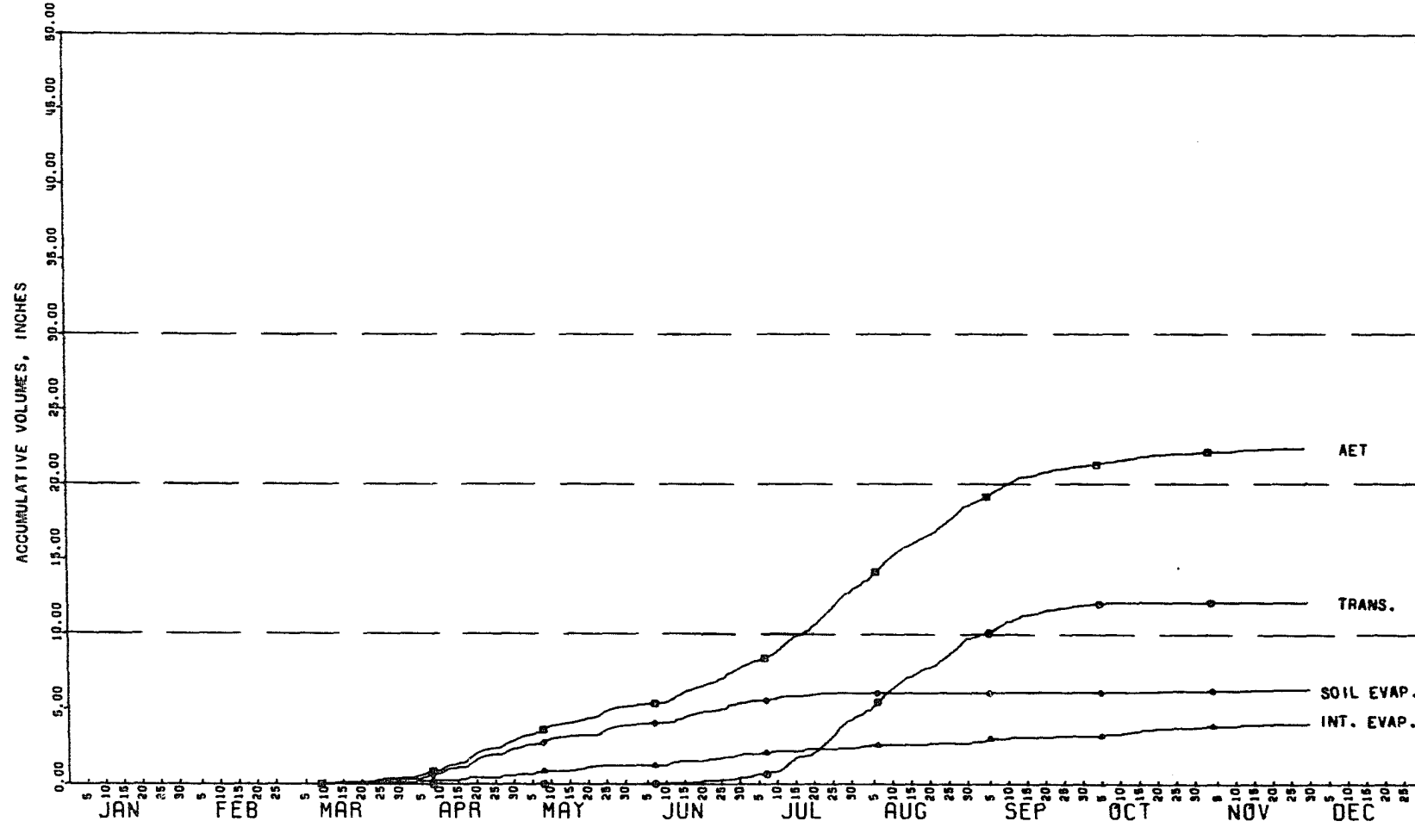

Figure 64. Accumulative actual ET and its components of transpiration, soil evaporation, and interception evaporation for corn during 1969

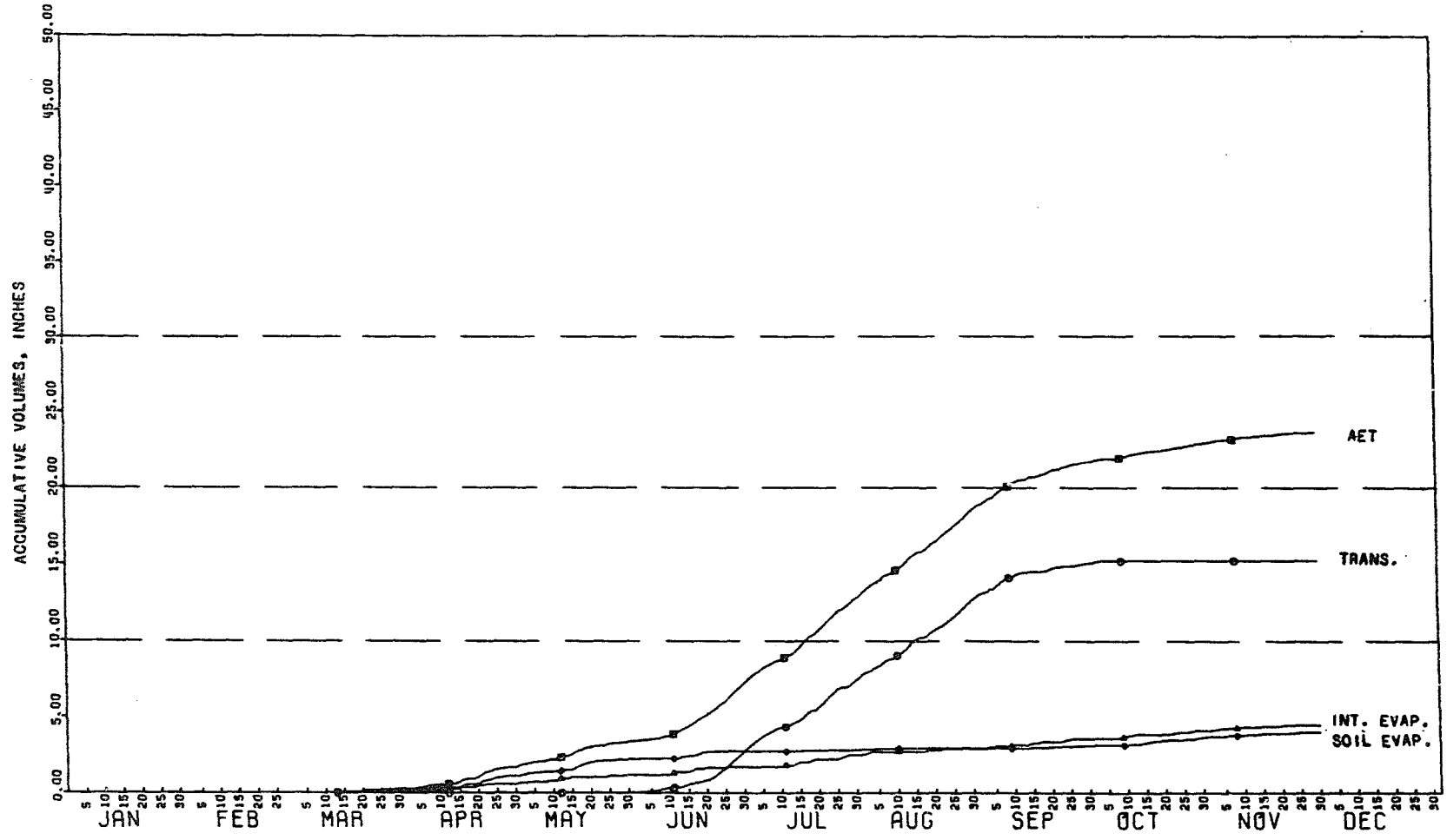

Figure 65. Accumulative actual ET and its components of transpiration, soil evaporation, and interception evaporation for corn during 1970

components are subject to the relations defined in the model, but total actual ET is constrained by actual observations of precipitation and soil moisture so it must be reasonably accurate.

Monthly and total values of the curves shown in figures 58 through 65 are summarized in tables 4 and 5. The results for the 2 years are quite similar. In both years, the grass had slightly more actual ET than corn. An interesting difference between corn and grass soil evaporation and transpiration was caused by their canopy differences. Of course interception evaporation was nearly identical because canopy was not considered in this calculation and only minor precipitation differences occurred between the two watersheds, 1 and 3.

The principal method of evaluating the results of the rational model and the computed actual ET was by comparison of measured and observed soil moisture. In figures 66 through 73 are shown the soil moisture values of 7 soil zones below both grass and corn for the two study years.

A visual comparison shows good general agreement between the calculated and observed values. Small biases are yet present, such as in the deeper zones under grass during 1969. Some adjustments may still be warranted,

Table 4. Monthly summary of calculated ET, components, and related variables for 1969

	Crop	Pan Evap.[a]	Net Rad.	Pot. ET	Actual ET	Inter. Evap.	Soil Evap.	Trans.	P-Q[b]	Perc.[c]
		in.	in.	in.	in.	in.	in.	in.	in.	in.
March[d]	Grass	2.99	2.73	2.07	0.30	0.14	0.13	0.03	0.69	-0.21
	Corn		3.18	2.27	.41	.12	.29	.00	.76	- .21
April	"	6.20	4.61	4.93	3.71	.44	.53	2.74	4.49	.50
	"		4.77	5.10	2.49	.43	2.06	.00	4.78	.12
May	"	5.94	5.16	5.50	4.99	.75	.05	4.19	3.90	1.36
	"		5.63	5.87	2.30	.72	1.58	.00	3.71	1.60
June	"	7.99	6.43	6.86	4.71	.78	.01	3.91	3.43	.75
	"		6.30	6.75	2.51	.66	1.45	.41	3.93	1.62

[a]Class A pan at meteorologic station near boundary of corn and grass watersheds.

[b]Average watershed precipitation minus runoff and interception.

[c]Calculated amount moving across the bottom of the 6-ft soil profile, positive downward.

[d]Beginning March 9.

Table 4. Continued

	Crop	Pan Evap.[a]	Net Rad.	Pot. ET	Actual ET	Inter. Evap.	Soil Evap.	Trans.	P-Q[b]	Perc.[c]
		in.	in.	in.	in.	in.	in.	in.	in.	in.
July	Grass	6.98	6.55	6.28	4.22	0.47	0.04	3.72	4.86	0.34
	Corn		6.66	6.05	5.30	.52	.69	4.07	5.20	1.46
Aug.	"	7.22	6.31	6.77	3.61	.35	.03	3.23	4.77	.16
	"		6.48	6.39	5.60	.36	.02	5.24	3.85	.80
Sept.	"	4.60	3.93	4.43	3.09	.45	.03	2.62	1.12	.09
	"		3.98	3.94	2.62	.44	.02	2.15	1.35	.07
Oct.	"	3.78	1.94	2.44	1.70	.60	.07	1.02	4.09	.07
	"		2.15	2.83	.85	.57	.09	.19	4.15	- .02
Nov.	"	3.30	.66	1.37	.26	.17	.03	.06	.09	.06
	"		1.09	1.85	.35	.23	.12	.00	.27	.06
Totals	"	49.00	38.32	40.65	26.59	4.15	.92	21.52	27.44	3.12
	"		40.24	41.05	22.43	4.05	6.32	12.06	28.00	5.48

Table 5. Monthly summary of calculated ET, components, and related variables for 1970

	Crop	Pan Evap.[a]	Net Rad.	Pot. ET	Actual ET	Inter. Evap.	Soil Evap.	Trans.	P-Q[b]	Perc.[c]
		in.	in.	in.	in.	in.	in.	in.	in.	in.
March[d]	Grass	2.47	1.59	1.30	0.23	0.14	0.07	0.02	0.36	-0.21
	Corn		1.69	1.18	.26	.14	.12	.00	.39	- .21
April	"	5.96	3.41	5.33	3.52	.55	.36	2.61	3.07	.63
	"		3.93	5.21	1.42	.44	.98	.00	3.14	.11
May	"	8.55	5.53	7.37	5.16	.63	.02	4.51	3.08	.68
	"		5.68	6.32	1.71	.61	1.09	.02	3.03	.68
June	"	9.16	6.13	8.26	3.32	.47	.00	2.85	2.12	.37
	"		6.45	7.78	3.80	.53	.54	2.72	2.35	1.14

[a]Class A pan at meteorologic station near boundary of corn and grass watersheds.

[b]Average watershed precipitation minus runoff and interception.

[c]Calculated amount moving across the bottom of the 6-ft soil profile, positive downward.

[d]Beginning March 13.

Table 5. Continued

	Crop	Pan Evap.[a]	Net Rad.	Pot. ET	Actual ET	Inter. Evap.	Soil Evap.	Trans.	P-Q[b]	Perc.[c]
		in.	in.	in.	in.	in.	in.	in.	in.	in.
July	Grass	9.56	6.34	6.94	2.92	0.77	0.03	2.12	4.72	0.17
	Corn		6.52	7.30	5.71	.79	.10	4.82	5.39	.76
Aug.	"	7.38	5.74	5.80	3.78	.40	.06	3.32	3.95	.06
	"		5.60	5.91	5.76	.40	.11	5.25	4.11	.09
Sept.	"	5.77	3.64	4.17	2.95	.68	.10	2.17	4.51	.00
	"		3.64	4.63	3.09	.68	.16	2.25	4.50	- .20
Oct.	"	3.42	1.89	2.45	1.90	.48	.13	1.29	4.08	.01
	"		2.20	2.99	1.24	.51	.55	.18	4.33	- .21
Nov.	"	3.30	.60	1.11	.49	.33	.11	.05	1.38	.30
	"		1.05	1.61	.71	.38	.33	.00	1.37	.23
Totals	"	55.57	34.87	42.73	24.27	4.45	.88	18.94	27.27	2.01
	"		36.76	42.98	23.70	4.48	3.90	15.24	28.61	2.39

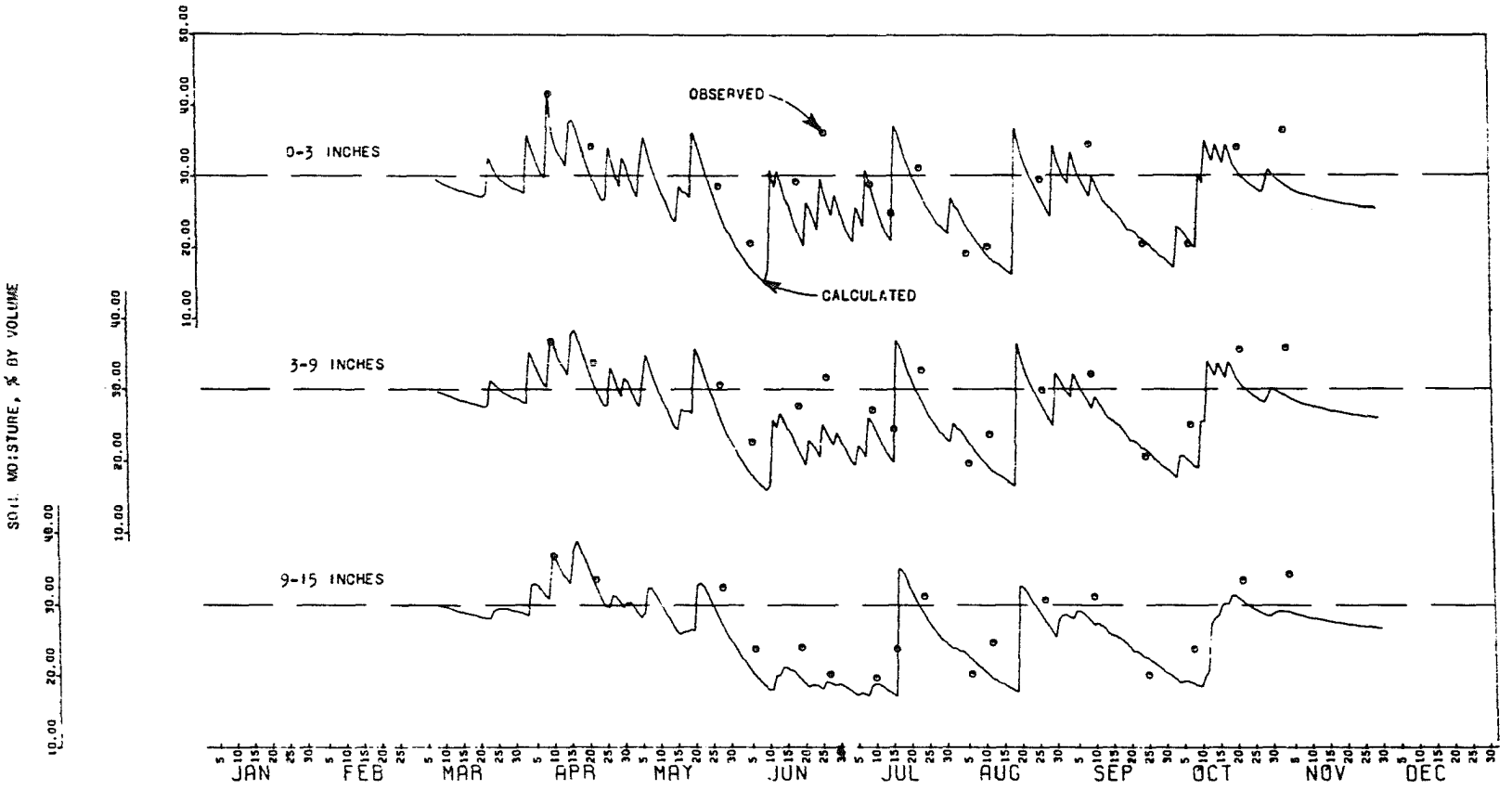

Figure 66. Soil moisture volumes calculated by the rational ET model compared to observed values for grass during 1969

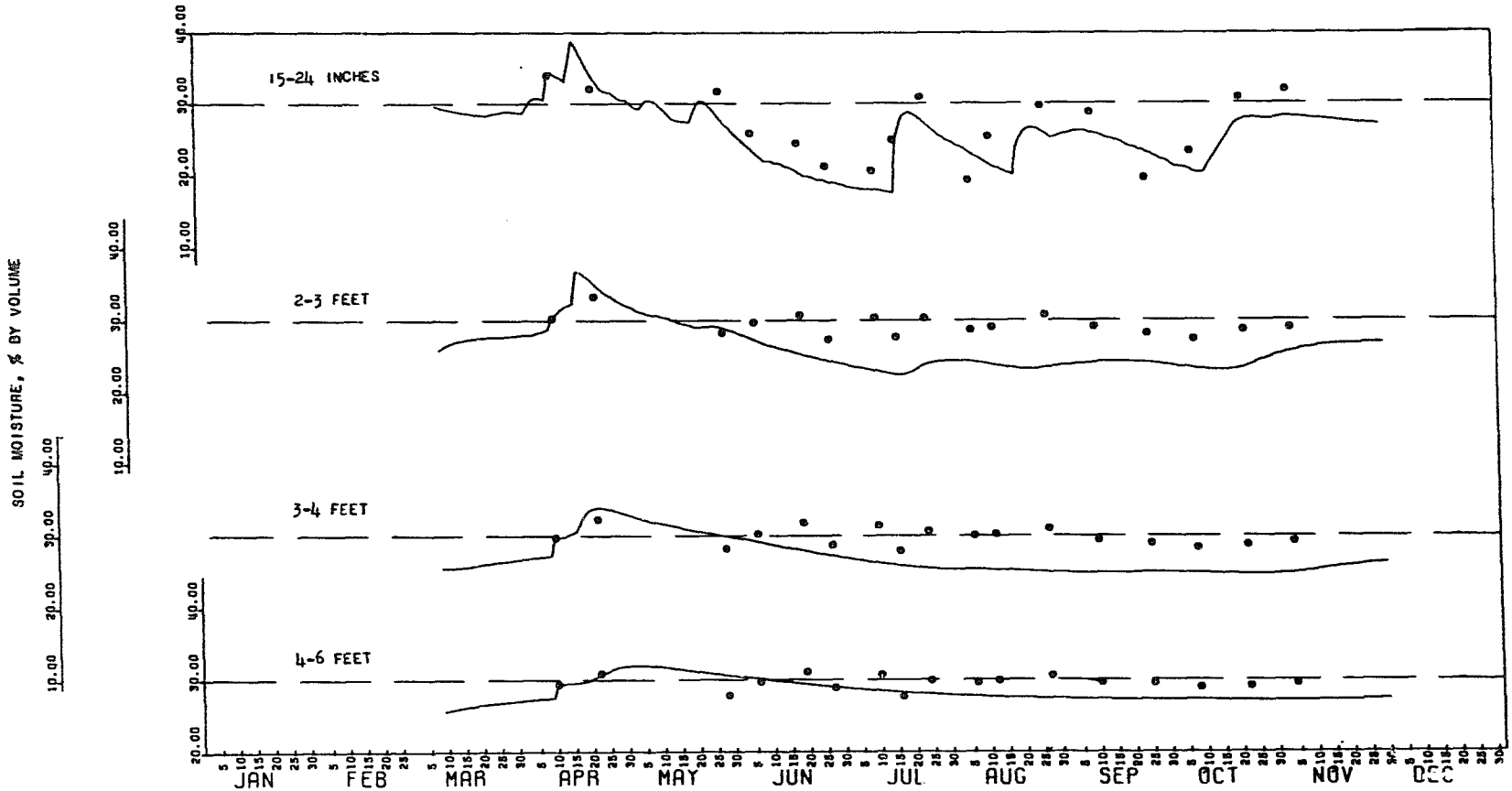

Figure 67. Soil moisture volumes calculated by the rational ET model compared to observed values for grass during 1969

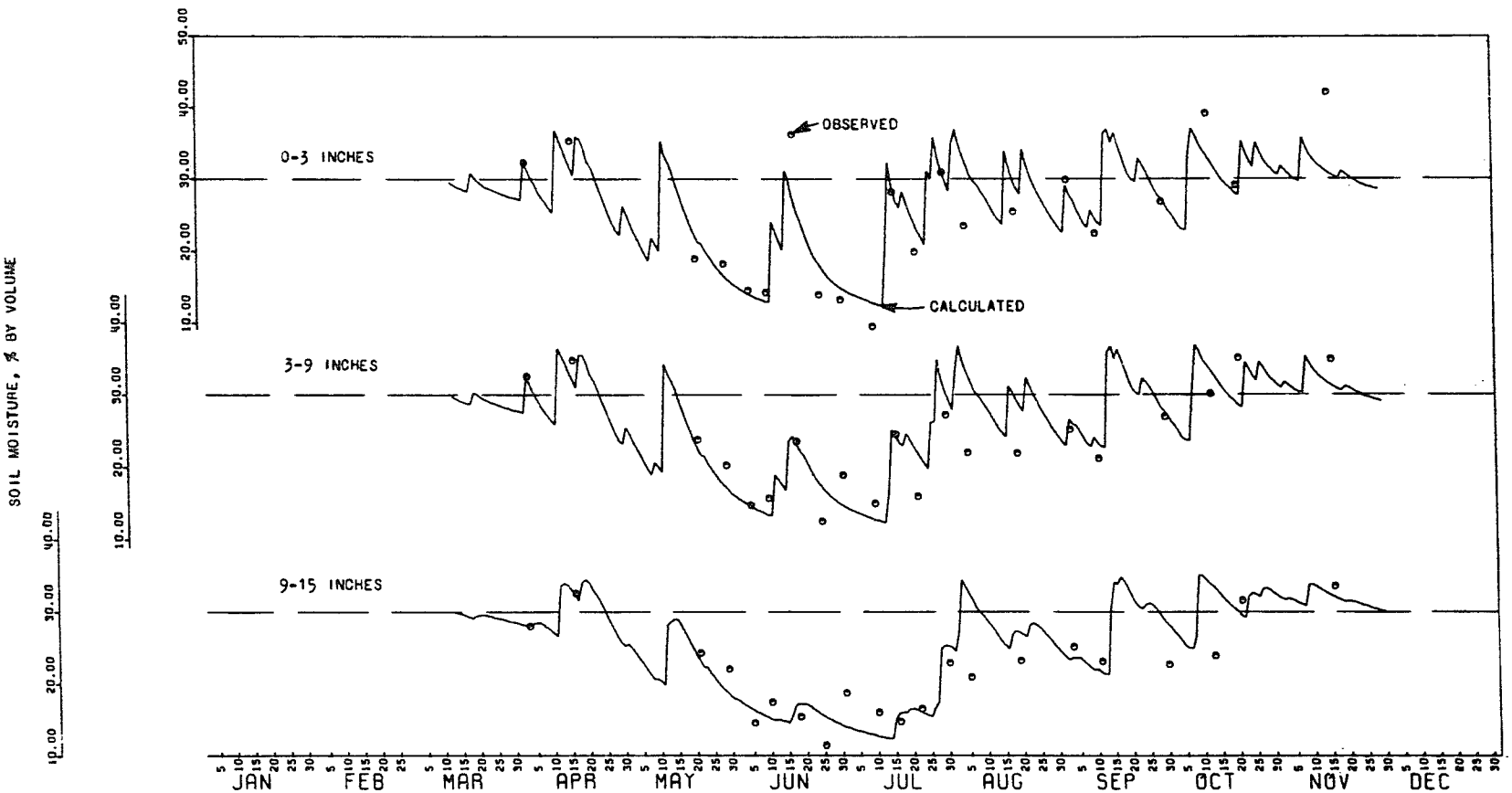

Figure 68. Soil moisture volumes calculated by the rational ET model compared to observed values for grass during 1970

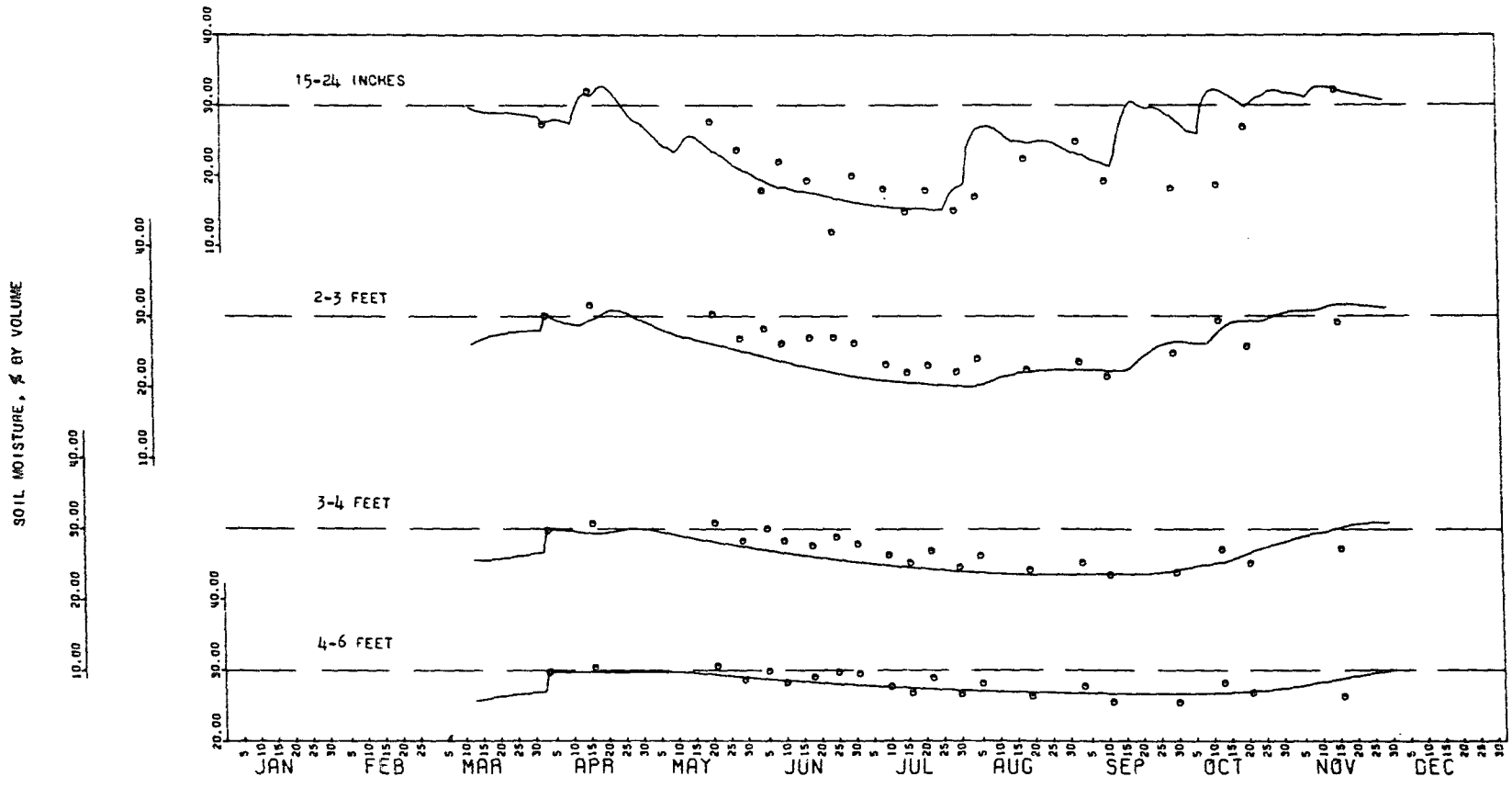

Figure 69. Soil moisture volumes calculated by the rational ET model compared to observed values for grass during 1970

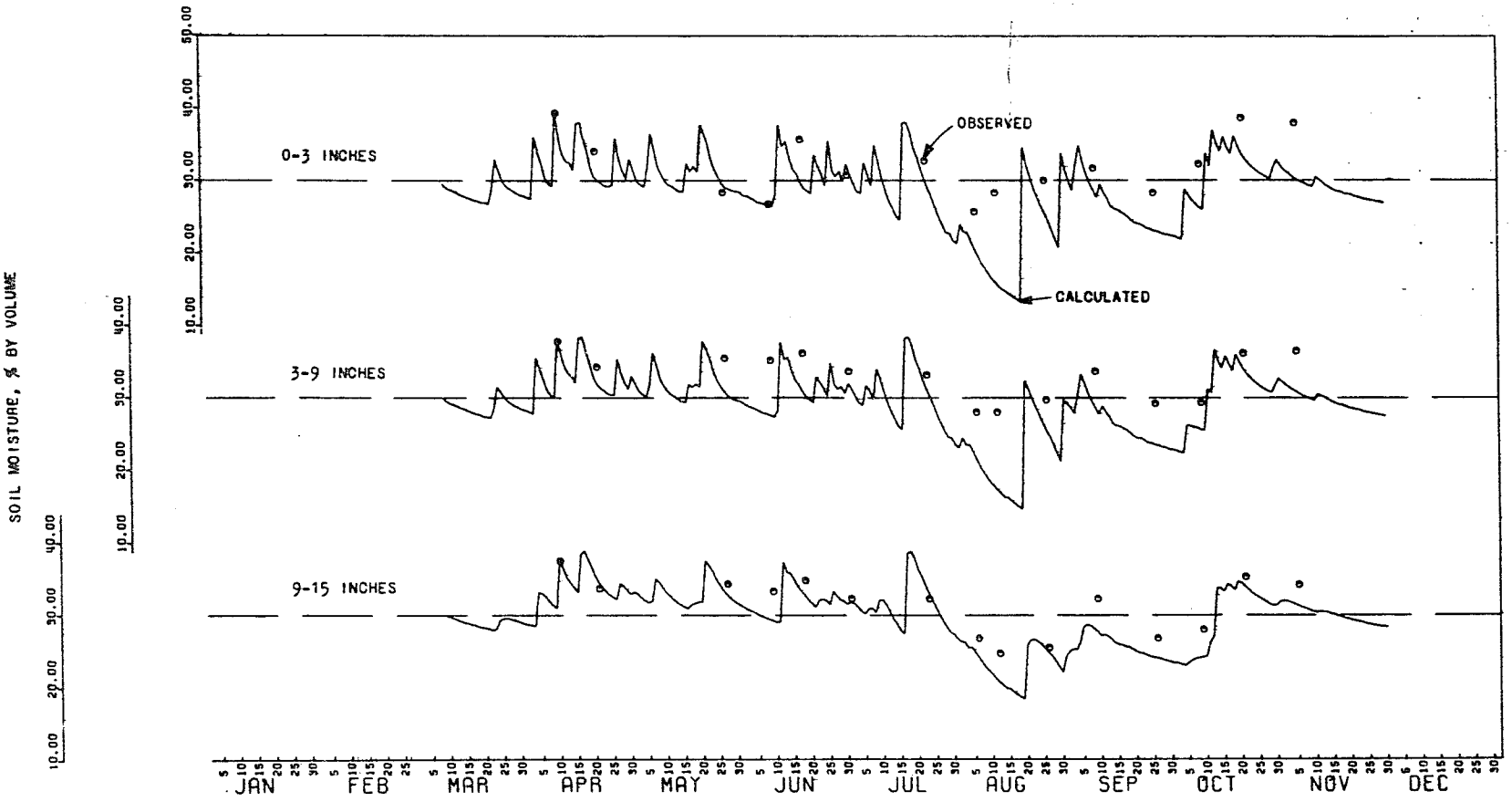

Figure 70. Soil moisture volumes calculated by the rational ET model compared to observed values for corn during 1969

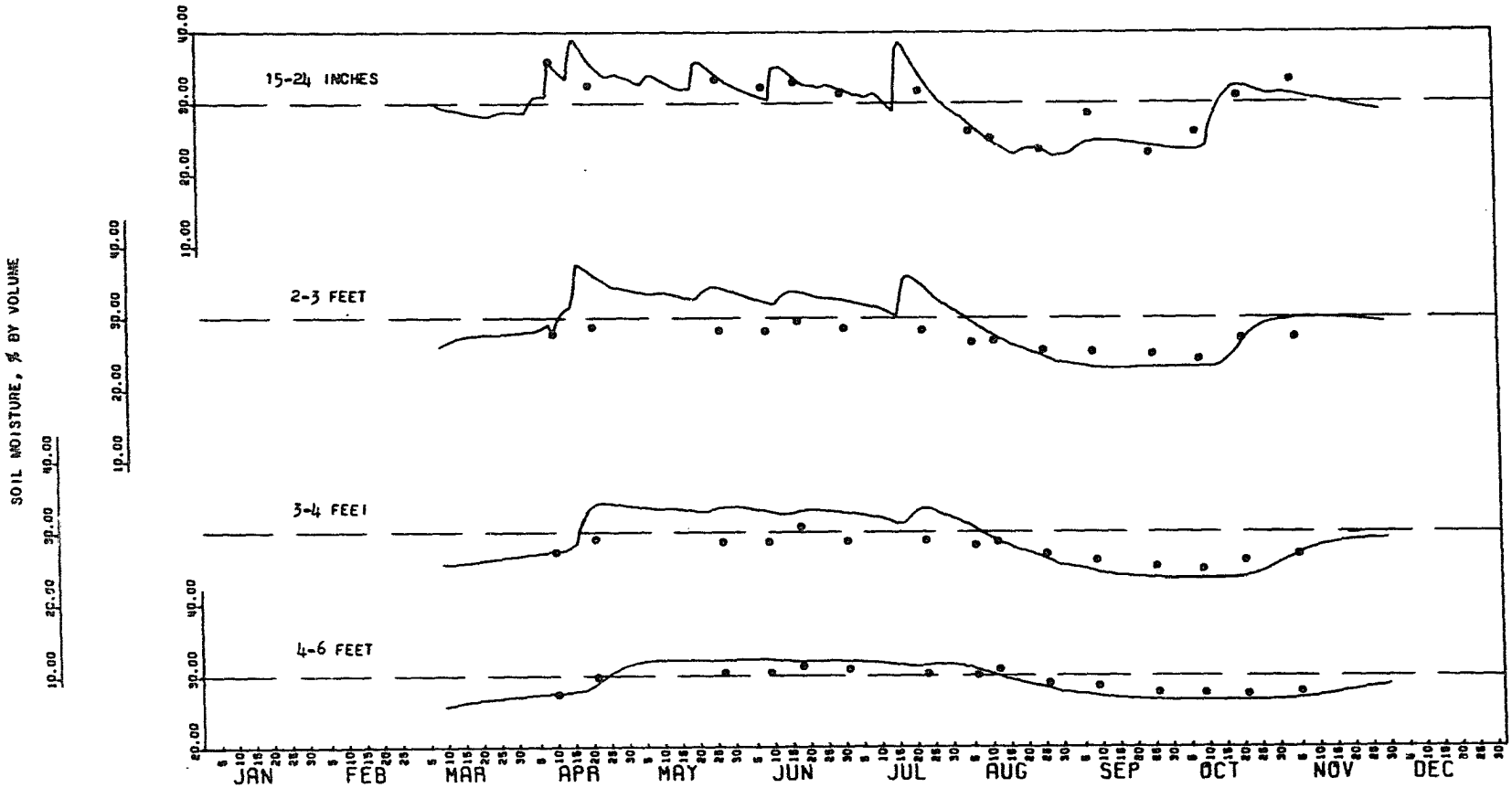

Figure 71. Soil moisture volumes calculated by the rational ET model compared to observed values for corn during 1969

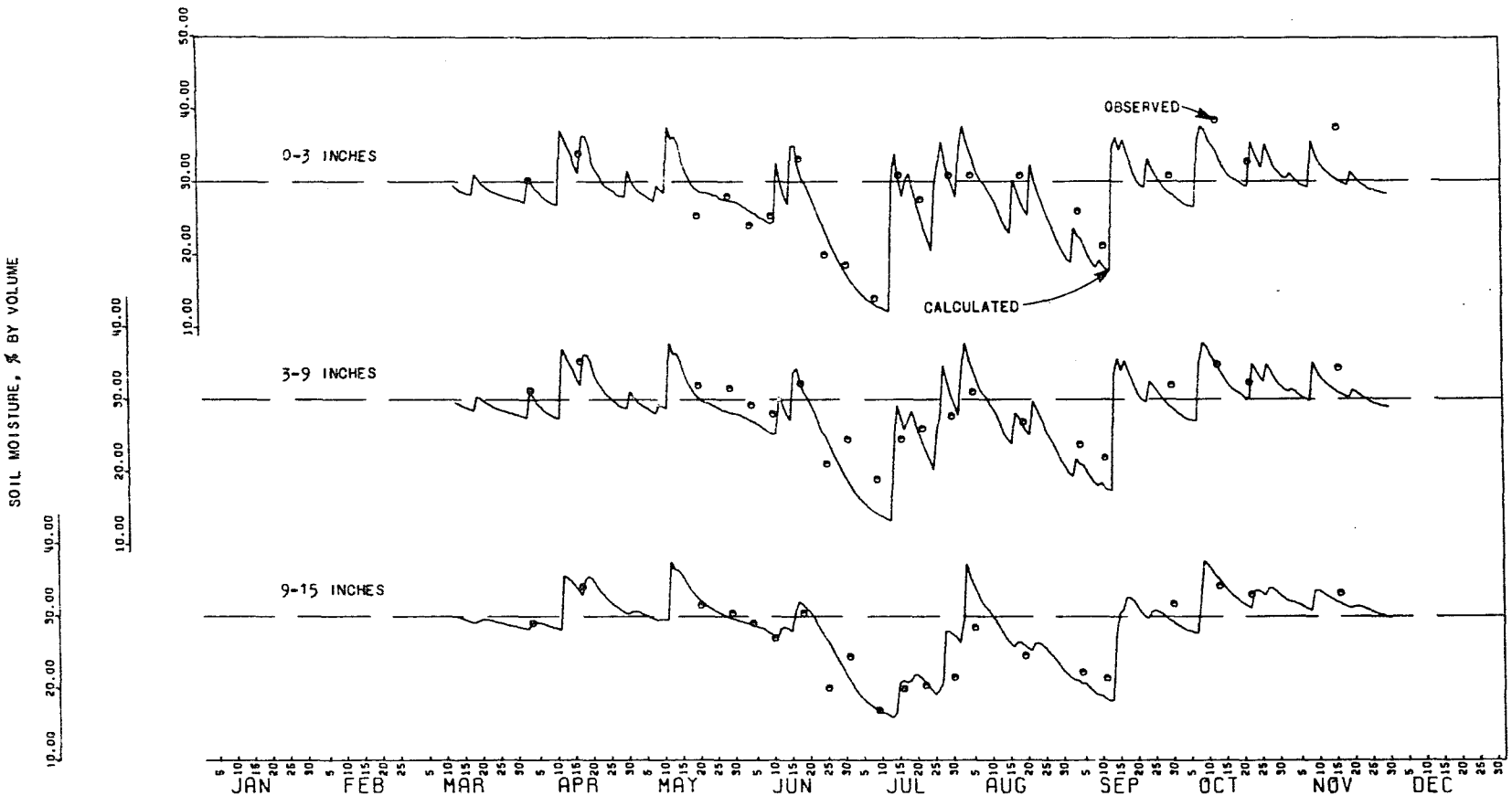

Figure 72. Soil moisture volumes calculated by the rational ET model compared to observed values for corn during 1970

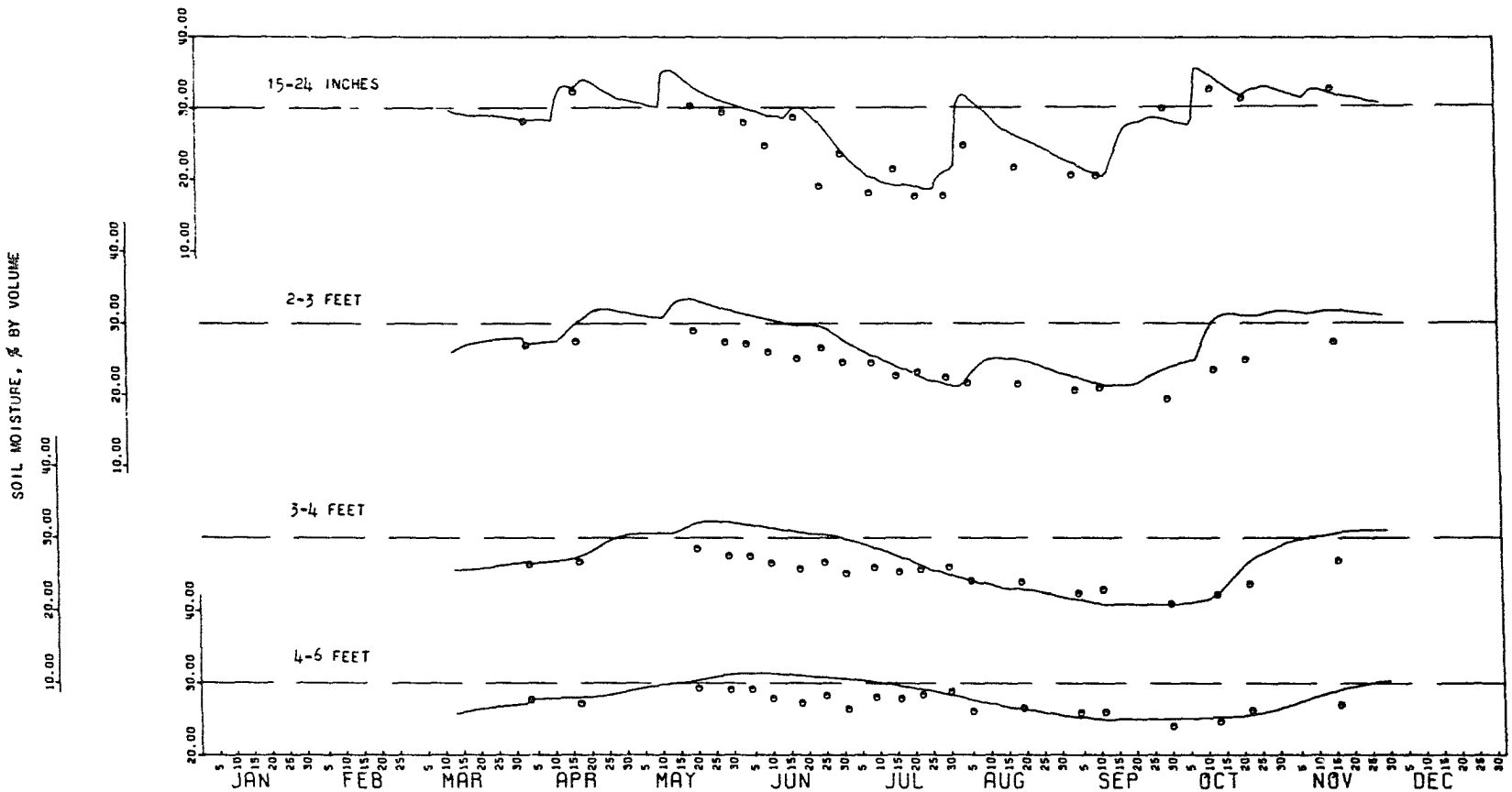

Figure 73. Soil moisture volumes calculated by the rational ET model compared to observed values for corn during 1970

particularly if more effort is given toward defining the process relations of the rational model, such as the crop moisture stress curves. By observing the profile zones, errors in specific relations, such as soil evaporation or root distribution, soon became apparent and adjustments were made accordingly. Some error compensation was also inherent in the model; that is, too little computed soil evaporation would have allowed some overestimation of transpiration in the upper zone.

The summary given in table 6 is another example of details available from the rational model. The total water movement into and out of the 6-in. soil zones because of infiltration, percolation, and actual ET is shown. This summary also shows the amount of water calculated to have percolated out of the 6-ft profile. A watershed budget of the ground water elevations and base flow measurements was made, and the computed percolation amounts were quite similar. This point strengthens the soil moisture verification.

Table 6. Summary of soil moisture movement, for grass during 1969

Soil Zone	Infiltration		Percolation		Net	Net	Actual
	in	out	in	out	in	out	ET
ft	in.	in.	in.	in.	in.	in.	in.
0.0-0.5	23.02	7.19	0.0	8.26	23.02	15.45	8.59
0.5-1.0	7.19	2.42	8.26	7.00	15.45	9.42	6.35
1.0-1.5	2.42	.82	7.00	5.32	9.42	6.14	4.13
1.5-2.0	.82	.52	5.32	3.59	6.14	4.11	2.22
2.0-2.5	.52	.14	3.59	3.24	4.11	3.38	.69
2.5-3.0	.14	.00	3.24	2.95	3.38	2.95	.47
3.0-3.5	.00	.00	2.95	3.02	2.95	3.02	.00
3.5-4.0	.00	.00	3.02	3.14	3.02	3.14	.00
4.0-4.5	.00	.00	3.14	3.24	3.14	3.24	.00
4.5-5.0	.00	.00	3.24	3.30	3.24	3.30	.00
5.0-5.5	.00	.00	3.30	3.27	3.30	3.27	.00
5.5-6.0	.00	.00	3.27	3.12	3.27	3.12	.00

SUMMARY AND CONCLUSIONS

Many procedures are available for estimating evapotranspiration (ET), but two stand out as being particularly applicable to watershed hydrologic research. Lysimeters are a rather direct method but they are expensive and difficult to maintain. A combination model which includes the vertical energy balance and aerodynamic effects allows calculating only a potential for ET, but this method is practical and offers the best opportunity for routine use. This procedure was tested for a 2-yr period on research watersheds in western Iowa. A rational model of crop and soil characteristics was used to convert the potential ET values to actual ET.

The research data consisted of measurements from two sets of meteorologic instruments, one over corn and the other over grass; and crop and soil moisture observations were made. Measurements were made from March through November during 1969 and 1970. The meteorologic instruments measured net radiation, humidity, temperature, and wind travel; and they were operated continuously. Crop observations were made each 2 or 3 days and soil moisture was measured each 1 or 2 weeks.

Daily potential ET was calculated by the combination model which was presented by Penman (1948), and modified and verified by Tanner and Pelton (1960) and van Bavel (1966). The observed meteorologic values were applied in conjunction with estimated wind profile parameters. Standard methods for estimating wind profile parameters could not be applied; thus another method was developed. Calculated potential ET values were quite similar for the two crops, exhibited a strongannual trend, and had considerable day-to-day variation throughout the year. The daily potential ET values compared better with pan evaporation than net radiation, apparently because the evaporation pan and the combination model both respond to aerodynamic effects. Accumulative potential ET was nearly equal to accumulative net radiation for 1969, but ET was about 6 in. more in 1970. Total calculated potential ET amounts were about 0.84 and 0.77 of pan evaporation for the two years, and had very similar annual distributions.

The potential ET values calculated by the combination model were used as input values to a rational model for calculating actual ET (see figure 52). Plant and soil moisture effects were considered by a sequence of empirical relations which represented the major factors in the

soil-plant-air system. The calculated actual ET values were the sum of estimated amounts of interception evaporation, soil evaporation, and transpiration. The ET withdrawal profile from the soil was calculated; infiltration was considered as measured precipitation minus measured watershed runoff and interception; and soil moisture redistribution was calculated by applying tension and conductivity relationships in the Darcy equation for unsaturated flow.

The total calculated actual ET was 26.6 in. and 24.3 in. for grass during 1969 and 1970, respectively, and 22.4 in. and 23.7 in. for corn. These are about 55% to 65% of the total calculated potential ET, but their annual distributions are somewhat different. The calculated amounts of the actual ET components--interception evaporation, soil evaporation, and transpiration--differed considerably between corn and grass; and although they were quite indicative, there was no verification of their correctness.

The calculated actual ET amounts were verified by graphical comparisons of calculated and observed soil moisture. Good agreement was achieved throughout the year which assured that the calculated ET amounts were reasonably accurate. This verification was strengthened by a favorable comparison of calculated total percolation from the 6-ft

soil profile with estimates from ground water budgets of the loessial watersheds.

The combination energy budget-aerodynamic method provided good estimates of daily potential ET. However, the correct representation of the wind profile parameters was difficult to assess for watershed conditions. Usual estimation methods could not be used. Good agreement was obtained between calculated potential ET values and pan evaporation, which suggests that adjusted pan evaporation values may provide an adequate estimate of watershed potential ET. This possibility needs further verification.

The rational model of the soil-plant-air system provided satisfactory values of actual ET. Although several relationships and coefficients were estimated by trial, this approach holds considerable promise for representing the major processes and interrelations that occur in this system. The estimated relationships can be improved as we add to our knowledge. Many factors are considered in this model which will be useful to the agronomist or hydrologist, such as crop moisture stress, soil moisture profiles, and infiltration potentials.

LITERATURE CITED

Amer. Soc. Agr. Eng. 1962. Water requirements of crops. Amer. Soc. Agr. Eng. Special Publication SP-SW-0162.

Amer. Soc. Agr. Eng. 1966. Evapotranspiration and its role in water resources management. Amer. Soc. Agr. Eng. Conference Proc. Chicago, Ill., Dec. 5-6. 65 pp.

Amer. Soc. Civil Eng. 1966. Methods for estimating evapotranspiration. Irrigation and Drainage Speciality Conference Proceedings, Las Vegas, Nev., Nov. 2-4.

Baier, W. 1969. Concepts of soil moisture availability and their effect on soil moisture estimates from a meteorologic budget. Agr. Meteor. 6:165-178.

Biswas, A. K. 1970. History of hydrology. North-Holland Pub. Co., New York, N.Y.

Blaney, H. F. and W. D. Criddle. 1950. Determining water requirements in irrigated areas from climatological and irrigation data. U.S. Dept. Agr. Soil Cons. Service TP-96. 48 pp.

Bond, J. J. and W. O. Willis. 1970. Soil water evaporation: First stage drying as influenced by surface residue and evaporation potential. Soil Sci. Soc. Amer. Proc. 34(5):924-928.

Bowen, I. S. 1926. The ratio of heat losses by conduction and by evaporation from any water surface. Phys. Rev. 27:779-787. Original not available; cited in: Tanner, C. B. 1960. Energy balance approach to evapotranspiration from crops. Soil Sci. Soc. Amer. Proc. 24(1):1-9.

Bresler, E. and W. D. Kemper. 1970. Soil water evaporation as affected by wetting methods and crust formation. Soil Sci. Soc. Amer. Proc. 34(1):3-8.

Brooker, D. B. 1967. Mathematical model of the psychrometric chart. Trans. Amer. Soc. Agr. Eng. 10(4):558-560, 563.

Businger, J. A. 1956. Some remarks on Penman's equation for the evapotranspiration. Neth. J. Agr. Sci. 4:77-80.

Businger, J. A. 1959. A generalization of the mixing-length concept. J. Meteor. 16:516-523.

Byers, H. R. 1959. General Meteorology. Third ed. McGraw-Hill Book Co. Inc., New York, N.Y.

Chow, Ven Te. (ed.) 1964. Handbook of Applied Hydrology. McGraw-Hill Book Co., New York, N.Y.

Cooley, K. R. 1969. Energy balance considerations in the design of floating covers for evaporation suppression. Ph.D. thesis. Univ. of Ariz. 108 pp. (Mic. 69-19,247, Univ. Microfilms Inc., Ann Arbor, Mich.)

Dale, R. F. 1966. Evapotranspiration and weather forecasts for agriculture. pp. 10-11. In: Evapotranspiration and its role in water resources management. Amer. Soc. Agr. Eng. Conference Proc., Chicago, Ill., Dec. 5-6.

Dalton, J. 1802. Experimental essays on the constitution of mixed gases; on the force of steam and vapour from water and other liquids in different temperature, both in a torricellian vacuum and in air, on evaporation, and on the expansion of gases by heat. Memoirs, Literary, and Philosophical Society of Manchester 5(2):536-602. Original not available; cited in: Biswas, A. K. 1970. History of Hydrology. North-Holland Pub. Co., New York, N.Y.

Denmead, O. T. and R. H. Shaw. 1962. Availability of soil water to plants as affected by soil moisture content and meteorologic conditions. Agron. J. 45:385-390.

Dreibelbis, F. R. and C. R. Amerman. 1964. Land use, soil type, and practice effects on the water budget. J. Geophys. Res. 69(16):3387-3393.

Eagleson, P. S. 1970. Dynamic hydrology. McGraw-Hill Book Co., New York, N.Y.

Ekern, P. C., Jr., J. S. Robins and W. J. Staple. 1967. Soil and cultural factors affecting evapotranspiration. Chapter 28, pp. 522-533. In: Hagan, R. M., H. R. Haise and T. W. Edminister (ed.) Irrigation of Agricultural Lands. Amer. Soc. Agron., Madison, Wisc.

Fleagle, R. G. and J. A. Businger. 1963. An introduction to atmospheric physics. Academic Press, New York, N.Y.

Fritschen, L. J. 1963a. Construction and evaluation of a miniature net radiometer. J. Appl. Meteor. 2(1):165-172.

Fritschen, L. J. 1963b. Condensation on shielded net radiometers. J. Appl. Meteor. 2(2):308-310.

Fritschen, L. J. 1965a. Miniature net radiometer improvements. J. Appl. Meteor. 4(4):528-532.

Fritschen, L. J. 1965b. Accuracy of evaporation determinations by the Bowen ratio method. Bul. Intern. Assoc. Sci. Hydrol. 2:38-48.

Fuchs, M., C. B. Tanner, G. W. Thurtell and T. A. Black. 1969. Evaporation from drying surfaces by the combination method. Agron. J. 61:22-26.

Gardner, W. R. and C. F. Ehlig. 1963. The influence of soil water on transpiration by plants. J. Geophys. Res. 68(20):5719-5724.

Gardner, W. R. and D. I. Hillel. 1962. The relation of external evaporative conditions to the drying of soils. J. Geophys. Res. 67(11):4319-4325.

Gates, D. M. and R. J. Hanks. 1967. Plant factors affecting evapotranspiration. Chapter 27, pp. 506-521. In: Hagan, R. M., H. R. Haise and T. W. Edminister (ed.) Irrigation of Agricultural Lands. Amer. Soc. Agron. Madison, Wisc.

Goodell, B. C. 1966. Watershed treatment effects on evapotranspiration. pp. 477-482. In: National Science Foundation. International Symposium on Forest Hydrology Proceedings. Penn. State Univ., Aug. 29-Sept. 10, 1965. Pergamon Press, New York, N.Y.

Great Plains Agricultural Council. 1970. Evapotranspiration on the great plains. Seminar Proceedings, Bushland, Texas, March 23-25. Printed by Kansas State Univ., Manhattan, Kan. 401 pp.

Hanks, R. J., L. H. Allen and H. R. Gardner. 1971. Advection and evapotranspiration of wide-row sorghum in the central great plains. Agron. J. 62:520-527.

Harrold, L. L. 1966. Measuring evapotranspiration by lysimetry. pp. 28-33. In: Evapotranspiration and its role in water resources management. Amer. Soc. Agr. Eng. Conference Proceedings, Chicago, Ill., Dec. 5-6.

Hellickson, M. A. 1969. Evaporation as a function of meteorological conditions and soil water. Ph.D. thesis. West Virginia Univ. 73 pp. (Mic. 69-20,707, Univ. Microfilms Inc., Ann Arbor, Mich.)

Hershfield, D. M. 1966. Meteorology in watershed hydrology research. Hydata, Amer. Water Resources Assoc. 2(9):1

Hillel, D. I. 1971. Soil and water--physical principals and processes. Academic Press, New York, N.Y.

Holmes, R. M. and G. W. Robertson. 1963. Application of the relation between actual and potential evapotranspiration in dry land agriculture. Trans. Amer. Soc. Agr. Eng. 6(1):65-67.

Holtan, H. N., N. E. Minshall and L. L. Harrold. 1962. Field manual for research in agricultural hydrology. U.S. Dept. Agr. Handbook No. 224. 215 pp.

Idso, S. B. 1970. The relative sensitivities of polyethylene shielded net radiometers for short and long wave radiation. The Review of Scientific Instruments. 41(7):939-943.

Jensen, M. E. and R. H. Haise. 1963. Estimating evapotranspiration from solar radiation. Proc. Amer. Soc. Civil Eng. J. of Irrig. and Drainage Div. 89(IR4):15-41.

Klute, A. 1969. The movement of water in unsaturated soils. pp. 821-888. In: National Science Foundation. The Progress of Hydrology. Proceedings, First International Seminar for Hydrology Professors, Univ. Ill., July 13-25.

Knisel, W. G., Jr. and R. W. Baird. 1969. Runoff volume prediction from daily climatic data. Water Resources Res. 5(1):84-94.

Kozlowski, T. T. (ed.) 1968. Water deficits and plant growth, Vol. I and II. Academic Press, New York, N.Y.

Kung, E. 1961. Derivation of roughness parameters from wind profile data above tall vegetation. pp. 27-35. In: Lettau, H. H. Annual Report, Studies of the Three-Dimensional Structure of the Planetary Boundary Layer. Univ. of Wisc., Dept. of Meteor., Madison, Wisc.

Lemon, E. R. 1963. The energy budget at the earths surface, part II. U.S. Dept. Agr., Agr. Res. Ser. Production Res. Report No. 72.

Linacre, E. T. 1967. Climate and the evaporation from crops. Proc. Amer. Soc. of Civil Eng. J. Irrig. and Drainage Div. 93(IR4):61-79.

Linscott, D. L., R. L. Fox and R. C. Lipps. 1962. Corn root distribution and moisture extraction in relation to nitrogen fertilization and soil properties. Agron. J. 54:185-189.

McGuinness, J. L. and L. L. Harrold. 1962. Seasonal and areal effects on small-watershed stream flow. J. of Geophys. Res. 67(11):4327-4334.

Marsh, G. P. 1864. Man and nature; or, physical geography as modified by human action. 560 pp. Charles Scribner, New York, N.Y. Original not available; cited in: Thorthwaite, C. W. and B. Holzman. 1942. Measurement of evaporation from land and water surfaces. U.S. Dept. Agr. Tech. Bul. No. 817. 143 pp.

Melvin, S. W. 1970. Determination of deep percolation losses in loessial soils. Unpublished Ph.D. thesis. Iowa State University Library, Ames, Iowa.

Mustonen, S. E. and J. L. McGuinness. 1968. Estimating evapotranspiration in a humid region. U.S. Dept. Agr. Tech. Bul. 1389. 123 pp.

National Research Council of Canada. 1961. Evaporation. Hydrology Symposium No. 2, Proceedings, Toronto, Canada, March 1-2. 263 pp.

O'Brien, J. J. 1965. An investigation of the diabatic wind profile of the atmospheric boundary layer. J. of Geophys. Res. 70(10):2277-2290.

Penman, H. L. 1948. Natural evaporation from open water, bare soil, and grass. Proc. Royal Soc. Series A, No. 1032, 193:120-145.

Penman, H. L. 1956. Estimating evaporation. Amer. Geophys. Union 4(1):9-29.

Reifsnyder, W. E. and H. W. Lull. 1965. Radiant energy in relation to forests. U.S. Dept. Agr. Tech. Bul. 1344.

Rider, N. E. 1954. Evaporation from an oat field. Quar. J. Royal Meteor. Soc. 80(344):198-211.

Robinson, S. A. 1962. Computing wind profile parameters. J. Atm. Sci. 19:189-190.

Robinson, T. W. and A. I. Johnson. 1961. Selected bibliography on evaporation and transpiration. U.S. Geological Survey Water-Supply Paper 1539-R.

Rose, C. W. 1966. Agricultural Physics. Pergamon Press Inc., New York, N.Y.

Rosenberg, N. J., H. E. Hart and K. W. Brown. 1968. Evapotranspiration review of research. Nebr. College of Agr. and Home Econ. MP20. 78 pp.

Saxton, K. E. and A. T. Lenz. 1967. Antecedent retention indexes predict soil moisture. Proc. of Amer. Soc. of Civil Eng. J. Hydr. Div. 93(HY4):223-241.

Saxton, K. E., R. G. Spomer and L. A. Kramer. 1971. Hydrology and erosion of loessial watersheds. Proc. of the Amer. Soc. of Civil Eng. J. Hydr. Div. 97(HY11):1835-1851.

Scarborough, J. B. 1958. Numerical mathematical analysis. The Johns Hopkins Press, Baltimore, Md.

Sellers, W. D. 1965. Physical climatology. Univ of Chicago Press, Chicago, Ill. 272 pp.

Shaw, R. H. 1963. Estimation of soil moisture under corn. Iowa Agr. and Home Econ. Exp. Sta. Res. Bul 520.

Shaw, R. H. 1964. Prediction of soil moisture under meadow. Agron. J. 56(3):320-324.

Shaw, R. H., D. R. Nielsen and J. R. Runkles. 1959. Evaluation of some soil moisture characteristics of Iowa soils. Iowa Agr. and Home Econ. Exp. Sta. Res. Bul. 465.

Skidmore, E. L., H. S. Jacobs and W. L. Powers. 1969. Potential evapotranspiration as influenced by wind. Agron. J. 61(4):543-546.

Sutton, O. G. 1953. Micrometeorology. McGraw-Hill Book Co., New York, N.Y.

Szeicz, G., G. Endrödi and S. Tajchman. 1969. Aerodynamic and surface factors in evaporation. Water Resources Res. 5(2):380-394.

Tanner, C. B. 1957. Factors affecting evaporation from plants and soils. J. Soil and Water Cons. 12:221-227.

Tanner, C. B. 1960. Energy balance approach to evapotranspiration from crops. Soil Soc. Amer. Proc. 24(1):1-9.

Tanner, C. B. 1967. Measurement of evapotranspiration. Chapter 29. pp. 534-574. In: Hagan, R. M., H. R. Haise and T. W. Edminister (ed.) Irrigation of Agricultural Lands. Amer. Soc. of Agron., Madison, Wisc.

Tanner, C. B. and M. Fuchs. 1968. Evaporation from unsaturated surfaces: a generalized combination method. J. Geophys. Res. 73(4):1299-1304.

Tanner, C. B. and W. L. Pelton. 1960. Potential Evapotranspiration estimates by the approximate energy balance method of Penman. J. Geophys. Res. 63(10):3391-3413.

Thornthwaite, C. W. and B. Holzman. 1942. Measurement of evaporation from land and water surfaces. U.S. Dept. Agr. Tech. Bul. No. 817. 143 pp.

Udagawa, T. 1966. Variation of aerodynamical characteristics of a barley field with growth. J. Agr. Meteor. 22(1):7-14.

U.S. Dept. of Agr. 1967. Irrigation water requirements. U.S. Dept. Agr. Soil Conservation Service Technical Release No. 21. 88 pp.

van Bavel, C. H. M. 1966. Potential evaporation; the combination concept and its experimental verification. Water Resources Res. 2(3):455-467.

Veihmeyer, F. J. 1964. Evapotranspiration. Chapter 11. In: Chow, V. T. (ed.) Handbook of Applied Hydrology. McGraw-Hill Book Co., New York, N.Y.

Weaver, J. E. 1926. Root development of field crops. McGraw-Hill Book Co., New York, N.Y.

Webb, E. K. 1965. Aerial microclimate. Chapter 2. Agricultural Meteorology. Meteor. Monographs 6(28).

Webb, E. K. 1970. Profile relationships: the log-linear range, and extension to strong stability. Quar. J. Royal Meteor. Soc. 96(407):67-90.

Wright, J. L. and E. R. Lemon. 1966. Photosynthesis under field conditions. VIII. Analysis of windspeed fluctuation data to evaluate turbulent exchange within a corn crop. Agron. J. 58:255-261.

ACKNOWLEDGEMENTS

I wish to sincerely acknowledge the cooperative effort of the USDA Agricultural Research Service who supplied the entire support for this project. I give particular thanks to the staff of the USDA ARS North Central Watershed Research Center at Columbia, Missouri and Council Bluffs, Iowa; especially to "Bill" Heinemann, Ralph Spomer, Larry Kramer, and Bob Poggensee.

To the staff of Iowa State University I extend a sincere thought of gratitude. I particularly thank Dr. Howard Johnson for his friendship, encouragement, and gracious gift of his time while shepherding me through my studies and research. Thanks also to Dr. Shaw for his council during the course of this research project. And to the other members of my committee, Drs. Bockhop, Sendlein, and Beer, I extend a note of thanks for their concern and interest.

Lastly, I am most deeply indepted to my family for their encouragement, support, and tolerance. Especially to my children, Debora and Kelvin, who so often shared their time with these goals. And to my wife, Mary Lou, goes my deepest sense of gratitude for her sustenance throughout these years of study; exemplified by her typing of this manuscript.

APPENDIX A

DERIVATION OF THE COMBINATION EQUATION

The combination energy budget-aerodynamic equation for calculating potential ET which is derived in the following pages is often called the "Penman Method." Although it contains the basic phenomena proposed by Penman (1948)[1], it has been further refined by using measured net radiation and a wind profile function consistent with the modern representation of turbulent wind movement over rough surfaces. The derivation that follows is not original work of the author but an attempt to systematically present the theory and assumptions underlying the combination equation. The steps in the derivation are:

1. A representation of the vertical energy budget of the soil or plant surface,
2. Apply the Dalton-type transport function to define Bowen's ratio,
3. Apply Penman's psychrometric simplification to eliminate the need of a surface temperature,
4. Apply the vertical transport equation obtained from turbulent transport theory.

---

1. References are included in Literature Cited of main text.

Although the combination equation is physical[illegible] it contains a number of assumptions which must be c[illegible]ed. An example is the Penman psychrometric adjustment [illegible] as-sumes a saturated vapor pressure at the surface; thus, the equation cannot strictly be applied to dryer conditions. The turbulent transport theory contains several assumptions, among them that the eddy diffusivities for momentum and water vapor are equal, which has been shown to be only approximately true. Usually the error associated with these assumptions is insignificant in the final result.

Step I: Vertical Energy Balance

The vertical energy budget shown in figure A-1 (at the end of this section) may be expressed as

$$R_n = LE + A + S + X \qquad (1)$$

where:

R_n =	Net radiation	$Cal\ cm^{-2}\ min^{-1}$
A =	Sensible heat of air	$Cal\ cm^{-2}\ min^{-1}$
LE =	Latent heat of water vapor	$Cal\ cm^{-2}\ min^{-1}$
L =	Heat of vaporization	$Cal\ cm^{-3}$
E =	Depth of evaporated water	$Cm^3\ cm^{-2}\ min^{-1}$
S =	Soil heat	$Cal\ cm^{-2} min^{-1}$
X =	Miscellaneous heat sinks such as photosynthesis, plant and air heat storage.	$Cal\ cm^{-2}\ min^{-1}$

These terms are of energy flux density, expressed as energy per unit area per unit time. Practical units are often expressed as water depth per unit time by assuming the energy per unit volume needed for liquid-to-vapor phase conversion of water. The units cal cm^{-2} are often defined as Langleys, Ln.

In evapotranspiration work, the heat stored in the soil and plants and the miscellaneous heat sinks (Tanner 1960) are usually negligible quantities over a day's time when compared with other quantities in the budget. This is not true for shorter periods because of heat storage during the day and its release at night. With these assumptions,

$$R_n = LE + A \quad . \tag{2}$$

It is possible to measure R_n, but it is quite difficult to separate the two righthand terms to allow the desired solution for LE and thus E. As a first step, Bowen (1926) proposed using the ratio

$$\beta = \frac{A}{LE} \tag{3}$$

because this ratio could be estimated with better accuracy than either of the terms individually. Using equation 3 in equation 2 gives

$$LE = \frac{R_n}{1+\beta} \tag{4}$$

Step II: Applying Dalton Transport Function

Bowen's ratio gave little advancement until values of β could be determined. A solution was suggested by the earlier work of Dalton (1802). He proposed that the amount of transfer from the surface was a function of the horizontal wind speed and the vertical gradient of the property. Expressions for heat and moisture would be

$$A = \gamma f_o(u) (T_o - T_1) \quad (5)$$

$$LE = f_o(u) (e_o - e_1) \quad (6)$$

where:

γ	= psychrometric constant of air = $(C_p P)/(\xi L) = 0.667$	mb $^oC^{-1}$
C_p	= sp. heat of air = 0.242	cal g^{-1} $^oC^{-1}$
P	= barometric pressure = 1,000	mb
ξ	= ratio of mole weights of water over air = 0.622	-
L	= latent heat of vaporization of water = 583	cal g^{-1}
$f_o(u)$	= a horizontal wind function	cm sec^{-1}
T_o	= air temperature at lower height	^oC
T_1	= air temperature at upper height	^oC
e_o	= vapor pressure at lower height	mb
e_1	= vapor pressure at upper height	mb

Substitution of equations 5 and 6 into 3 gives

$$\beta = \gamma \frac{T_o - T_1}{e_o - e_1} \tag{7}$$

Thus, if the Dalton relations hold, the Bowen ratio can be estimated by measuring the temperature and humidity gradients above the evaporating surface. With the advent of sensitive instruments in the past 10 years, this technique has been used with good success. Fritschen (1965b) gave a good account of this approach. The principal difficulty lies in the sensitivity of instrumentation required. If the lower height is taken at ground level, the very difficult measurement of surface temperature is required.

Step III: Penman's Psychrometric Assumption

By a further assumption, Penman (1948) was able to eliminate the need of a surface temperature and reduce the measurements to only temperature and vapor pressure deficit at a single height above the evaporating surface. He began by considering the air in contact with a wetted surface which would be essentially saturated with water vapor; and the air at some height, Z_1, which would be less than saturated. These conditions can be noted on a psychrometric chart as sketched in figure A-2. Point 1 represents the air near the wetted surface, and point 2

the air conditions at some height above the surface. By the relations of this sketch, the slope, Δ , of the saturation line at T_1 may be approximated by

$$\Delta = \frac{e_o - e_1^*}{T_o - T_1} \qquad (8)$$

The saturation line is a known relation of T and e and thus Δ can be found by the derivative de/dT. Tabled values of Δ/γ are available (van Bavel 1966). A better estimate of Δ could be obtained at the temperature $(T_o + T_1)/2$, but this would require an iterative solution with only slightly improved values.

Penman (1948) combined equations 7 and 8 as follows:

$$\beta = \gamma \frac{(T_o - T_1)}{(e_o - e_1)} \cdot \frac{\Delta}{\Delta}$$

$$= \gamma \frac{(T_o - T_1)}{(e_o - e_1)} \cdot \frac{\left[\frac{e_o - e_1^*}{T_o - T_1}\right]}{\Delta}$$

$$= \frac{\gamma}{\Delta} \frac{e_o - e_1^*}{e_o - e_1}$$

By adding and subtracting e_1 in the numerator

$$\beta = \frac{\gamma}{\Delta} \frac{(e_o - e_1) - (e_1^* - e_1)}{(e_o - e_1)}$$

and by multiplying and dividing by $f_o(u)$

$$\beta = \frac{\gamma}{\Delta} \frac{f_o(u)}{f_o(u)} \frac{(e_o-e_1) - (e_1^*-e_1)}{e_o-e_1} \qquad (9)$$

The Dalton relation of equation 6 was

$$LE = f_o(u)\ (e_o-e_1)$$

which when substituted into both numerator and denominator of 9 gives

$$\beta = \frac{\gamma}{\Delta} \frac{LE - f_o(u)\ (e_1^*-e_1)}{LE} \qquad (10)$$

The term $(e_1^* - e_1)$ is commonly called the vapor pressure deficit, d_a, because it represents the difference between actual and saturation vapor pressures of the air at the upper-level temperature as shown in figure A-2. Equation 10 can be combined into equation 4 to give

$$LE = \frac{R_n}{1 + (\gamma/\Delta) \frac{LE - f_o(u)d_a}{LE}}$$

$$= \frac{LE \cdot R_n}{LE + (\gamma/\Delta)(LE - f_o(u)d_a)}$$

$$R_n = LE + \frac{\gamma}{\Delta} LE - \frac{\gamma}{\Delta} f_o(u)d_a$$

$$LE\ (1 + \frac{\gamma}{\Delta}) = R_n + \frac{\gamma}{\Delta} f_o(u)d_a$$

$$LE = \frac{R_n + (\gamma/\Delta)\, f_o(u) d_a}{1 + (\gamma/\Delta)}$$

$$LE = \frac{(\Delta/\gamma)\, R_n + f_o(u) d_a}{(1 + (\Delta/\gamma))} \qquad (11)$$

Equation 11 is the Penman equation, or also commonly called the combination equation because it combines both the vertical energy budget and an aerodynamic transport function. A solution of 11 is possible by measuring

1. Air temperature at height Z_1
2. Dew point or humidity at height Z_1
3. Net radiation
4. Horizontal wind movement.

The air temperature and dew point measurements allow calculating the Δ and d_a terms, and R_n is applied directly. However, the form of the wind function, $f_o(u)$, now needs to be considered.

Step IV: Turbulent Transport Theory

The form of $f_o(u)$ must represent the vertical wind profile because, as will be seen later, it is through this function that the vertical moisture transport is related to horizontal air movement. Penman first applied an empirical wind relation that represented the mean conditions over oceans (Penman 1948). He also showed that this

relation needed to be modified for application over evaporation pans and vegetated surfaces. This transport portion of the combination equation was reevaluated by Businger (1956) and others who showed that vertical transport in the atmosphere at these low levels is mostly the result of turbulent diffusion and they applied these theories. A brief outline of these considerations follow.

For the usual representation of turbulent transport phenomena (Fleagle and Businger 1963, p. 182), we can write

$$F_s = \overline{\rho w s} \qquad (12)$$

where

F_s = Vertical transport of some property, s. $\quad g\ cm^{-2}\ sec^{-1}$

s = Concentration of property, such as water mass. $\quad g\ g^{-1}$

ρ = Air density $\quad g\ cm^{-3}$

w = Vertical air velocity $\quad cm\ sec^{-1}$

For horizontal laminar air flow, w = 0; thus there would be no vertical transport except molecular diffusion. For turbulent air flow, we need to consider the instantaneous velocity fluctuations. If we were to measure w with a fast response instrument, we would get a representation as shown in figure A-3. Thus we can represent the instantaneous

velocity as the mean value $\bar{w}$, plus some deviation from the mean, w', such that

$$w = \bar{w} + w' \tag{13}$$

Similarly, we could expect the property s to fluctuate about some mean value and thus be represented by

$$s = \bar{s} + s' \tag{14}$$

Now, using these representations in equation 12 gives

$$F_s = \overline{[\bar{\rho}\bar{w} + (\rho w)'] (\bar{s} + s')} \tag{15}$$

where the bar indicates a time average. It can be shown that a time average of a single primed or barred value would be 0, thus equation 15 reduces to

$$F_s = \overline{(\rho w)' s'} \tag{16}$$

which is the defining equation for turbulent transport, but it is not practical to apply because w' and s' are very difficult to measure.

To arrive at a more useful concept but not one which increases our understanding, a physical model of how turbulent transport might occur was created (Fleagle and Businger 1963, p. 185). Air was considered as discrete moving partials which possess the property of their surrounding air. They maintain that property when moved vertically to some other level where they dispense their property and assume the condition of the air at that level. This concept is known as the mixing length model and may be

visualized as shown in figure A-4. Just as the velocity fluctuated about some mean, these partials of air move away from their mean elevation in varying distances. The mean of these distances represents the average vertical movements and is called the mixing length, l.

How this random air movement accomplishes transport can be visualized by noting a typical vertical distribution of some property, s, as sketched in figure A-4. Those partials moving upward find themselves in a region of lower concentration and add to their environment; downward-moving partials find themselves in a region of higher concentration and absorb from their environment. These movements result in a net upward transport.

Based on this mixing length model,

$$s' = l \frac{\partial \bar{s}}{\partial Z} \tag{17}$$

Combining this into equation 16 gives

$$F_s = \overline{(\rho w)' l} \frac{\partial \bar{s}}{\partial Z}$$

and if air density, ρ , is considered a constant

$$F_s = \rho \overline{w' l} \frac{\partial \bar{s}}{\partial Z}$$

An eddy diffusivity factor (turbulent transfer coefficient) may be defined as

$$K = \overline{w' l}$$

thus:

$$F_s = \rho K \frac{\partial \bar{s}}{\partial Z} \qquad (18)$$

Equation 18 represents the vertical transport of a property s and can be applied if the density, eddy diffusivity, and property gradient are known. Common forms of this equation are written for:

Heat $F_h = -\rho C_p K_h \left[\frac{\partial \bar{T}}{\partial Z} - \lambda \right]$ cal cm^{-2} sec^{-1} (19)

Water Vapor $F_E = -\rho L K_E \frac{\partial \bar{q}}{\partial Z}$ g cm^{-2} sec^{-1} (20)

Momentum $F_m = -\rho K_m \frac{\partial \bar{u}}{\partial Z}$ g cm^2 sec^{-1} (21)

where:

K_h, K_E, K_m = respective eddy diffusivity values

λ = adiabatic cooling rate $^oC\ cm^{-1}$

q = water vapor concentration g gm^{-1}

u = horizontal wind movement, m sec^{-1}

Again, these equations are not useful without some basis for estimating eddy diffusivity values. For the case of momentum transport, the phenomenon can be defined by the use of Newton's laws of motion to arrive at values for K_m. By assuming that $K_m \approx K_E$, the turbulent transport of water vapor can also be obtained. The equation of motion for a turbulent, non-viscous fluid is the Navier-Stokes

equation (Sutton 1953, p. 16)

$$\rho \frac{d\bar{w}}{dt} = - \frac{\partial P}{\partial x} + \frac{\partial (- \rho \overline{u'w'})}{\partial Z} \qquad (22)$$

which can be intrepted as:

(Mass) (acceleration) = pressure force + Eddy shear stress force

The last term contains the eddy shear stress

$$\tau' = - \rho \overline{u'w'} \qquad (23)$$

Equation 23 is equal to the transport equation 16 when $s' = u'$. Thus τ' represents the vertical transport of momentum, F_m. Again considering the mixing length model, equation 17 shows that

$$S' = l \frac{\partial \bar{s}}{\partial Z}$$

Thus, we similarly can write

$$u' = l \frac{\partial \bar{u}}{\partial Z} \qquad (24)$$

It has been found that

$$u' \approx w'$$

thus combining 24 with 23 for both u' and w' gives

$$\tau' = - \rho l^2 \left[\frac{\partial \bar{u}}{\partial Z}\right]^2 \qquad (25)$$

It has also been shown that the mixing length, l, is a function of distance above the surface, such that

$$l = k\,Z \tag{26}$$

where k is a proportionality factor (usually a constant) of about 0.4 and known as von Karman's constant (Fleagle and Businger 1963, p. 188). Combining equation 26 with 25 gives

$$\tau' = -\rho k^2 Z^2 \left(\frac{\partial \bar{u}}{\partial Z}\right) \left|\frac{\partial \bar{u}}{\partial Z}\right| \tag{27}$$

The second gradient term is included in absolute brackets to that the negative sign will cancel. Within the few lower meters of the atmosphere, τ' can be regarded as a constant without introducing a significant error. This assumesonly mechanical turbulence, but a correction for thermal turbul.nce is sometimes added. Equation 27 is often rewritten (by dropping the negative)

$$\sqrt{\left(\frac{\tau'}{\rho}\right)} = \sqrt{\left[k^2 Z^2 \left(\frac{\partial \bar{u}}{\partial Z}\right)^2\right]} = kZ \frac{\partial \bar{u}}{\partial Z} \tag{28}$$

The left-hand term has units of velocity, and is usually defined

$$u^* = \sqrt{\frac{\tau'}{\rho}} \tag{29}$$

where u^* is called the friction velocity and is considered a constant. Thus,

$$u^* = kZ \frac{\partial \bar{u}}{\partial Z}$$

or

$$\partial \bar{u} = \frac{u^*}{kZ} \partial Z \tag{30}$$

If equation 29 is integrated between two levels, u_o at Z_o and u_1 at Z_1, then

$$u_1 - u_o = \frac{u^*}{k} \ln \left(\frac{Z_1}{Z_o}\right)$$

or

$$u^* = k \frac{u_1 - u_o}{\ln(Z_1/Z_o)} \tag{31}$$

This form allows evaluating u^* by measuring $\bar{u}$ at two levels. Combining 31 with 30 gives

$$\frac{\partial \bar{u}}{\partial Z} = \frac{1}{Z} \frac{(u_1 - u_o)}{\ln(Z_1/Z_o)} \tag{32}$$

which is an equation of the mean horizontal wind velocity profile based upon the turbulent theory just outlined.

To continue the task of defining τ' and a relation describing K_m, substituting 32 into 27 yields

$$\tau' = -\rho\, k^2 z^2 \left\{ \frac{1}{z^2} \frac{(u_1 - u_o)^2}{\left[\ln\left(\frac{z_1}{z_o}\right) \right]^2} \right\}$$

or

$$\tau' = \frac{-\rho\, k^2 (u_1 - u_o)^2}{\left[\ln(z_1/z_o) \right]^2} \qquad (33)$$

Just after equation 23 we noted that

$$\tau' = F_m$$

that is, equations 23 and 21 are comparable. Thus we can also set the right-hand sides of 21 and 33 as being equal; which gives

$$-\rho\, K_m \frac{\partial \bar{u}}{\partial z} = \frac{-\rho k^2 (u_1 - u_o)^2}{\left[\ln\left(\frac{z_1}{z_o}\right) \right]^2}$$

Substituting 32 into the left side,

$$K_m \frac{1}{z} \frac{(u_1 - u_o)}{\ln (z_1/z_o)} = \frac{k^2 (u_1 - u_o)^2}{\left[\ln (z_1/z_o) \right]^2}$$

and solving for K_m gives

$$K_m = \frac{k^2 z (u_1 - u_o)}{\ln (z_1/z_o)} \qquad (34)$$

This now provides a means of evaluating the eddy diffusivity for momentum transfer by measuring the horizontal travel at two elevations although the Z term associated with the mixing length remains ambigous. We have arrived at equation 34 by applying laws of mechanics which describe mass movement, and the mixing length model.

For the transfer of heat or water vapor we have no such laws to bring to bear, but it has been found that the assumption

$$K_m \approx K_E \approx K_h$$

can be applied in most cases without large errors (Fleagle and Businger 1963, p. 193; Tanner 1967, p. 546). This seems logical because each property moves with the turbulent air. Thus, if we consider K_E as the right hand side of equation 34 and assume a log profile of specific water vapor content, q, expressed similar to that for wind velocity given by equation 32 except with reversed order due to higher concentrations nearer the ground, then

$$\frac{\partial q}{\partial Z} = \frac{1}{Z} \frac{q_o - q_1}{\ln (Z_1/Z_o)} \qquad (35)$$

Putting equations 34 and 35 into the transport equation 20 gives the vertical transport of water vapor as:

$$F_E = -\rho L \frac{k^2 Z (u_1 - u_o)}{\ln(Z_1/Z_o)} \cdot \frac{1}{Z} \frac{q_o - q_1}{\ln (Z_1/Z_o)}$$

$$= \frac{-\rho L k^2 (u_1 - u_o) (q_o - q_1)}{[\ln (Z_1/Z_o)]^2} \qquad (36)$$

To relate specific humidity, q, (grams of water vapor per gram of dry air) to vapor pressure, the following relation is applied

$$q = \frac{\text{mass water}}{\text{mass dry air}} \cdot \frac{e}{P} \qquad (37)$$

where e is the water vapor pressure and P is total atmospheric pressure. The mass ratios may be reduced to molecular weight ratios, thus 37 becomes

$$q = 0.622 \frac{e}{P}$$

or

$$q = \xi \frac{e}{P} \qquad (38)$$

Thus, the vertical transport of water vapor can be represented by turbulent transport theory by substituting 38

into 36 which gives:

$$F_E = \left[\frac{-\rho L k^2 \xi (u_1 - u_o)}{P \quad [\ln(Z_1/Z_o)]^2}\right](e_o - e_1) \qquad (39)$$

which expresses the vertical transport of water vapor in terms of turbulent flow and vapor pressures. Because we set out to define the $f_o(u)$ in the Dalton transport equation, it will be useful to rewrite equation 6.

$$LE = f_o(u)\ (e_o - e_1) \qquad (6)$$

Both LE and F_E represent water vapor transport, thus the right sides of equation 6 and 39 must also be equal. By inspection we note that the bracketed terms on the right side of 39 must equal $f_o(u)$ such that

$$f_o(u) = \frac{-\rho L k^2 \xi}{P} \quad \frac{(u_1 - u_o)}{[\ln(Z_1/Z_o)]^2} \qquad (40)$$

This then provides the $f_o(u)$ function for equation 11 which is consistent with the current representation of turbulent transport over rough surfaces.

In deriving equation 11, we reduced our measurements to one height by considering Z_o near the ground surface, or at least near the evaporating surface such that the air could be considered saturated. We similarly can take Z_o in equation 40 as that elevation where u_o equals zero.

This represents a logarithmic wind profile whose zero velocity would be slightly above the existing boundary. It is common to substitute $Z_a - d$ for Z_a, where d is a wind profile displacement height caused by crops taller than clipped grass (Sellers 1965, p. 150).

The two equations 11 and 40 combine to form:

$$LE = \frac{(\Delta/\gamma)\, R_n + (K\, L\, d_a\, u_a) / [\ln(\frac{Z_a - d}{Z_o})]^2}{1 + (\Delta/\gamma)} \qquad (41)$$

where

$$K = \frac{-\rho k^2 \xi}{P} \qquad (42)$$

This is the Penman combination model. All terms in K and the value of L are treated as constants in most applications. Care must be exercised to maintain consistency in the units.

The symbols, definitions, and representative units are:

E	=	potential evapotranspiration rate	cm day^{-1}
Δ	=	slope of psychrometric saturation line	mb $^{\circ}C^{-1}$
γ	=	psychrometric constant	mb $^{\circ}C^{-1}$
R_n	=	net radiation flux	cal cm^{-2} day^{-1}
L	=	latent heat of vaporization	cal g^{-1}
d_a	=	saturation vapor pressure deficit of air ($e_o - e_1$)	mb
u_a	=	windspeed at elevation Z_a	m day^{-1}
Z_a	=	anemometer height above soil	cm
d	=	wind profile displacement height	cm
Z_o	=	wind profile roughness height	cm
ρ	=	air density	g cm^{-3}
k	=	von Karman coefficient (0.41)	-
ξ	=	water/air molecular ratio (0.622)	-
P	=	ambient air pressure	mb

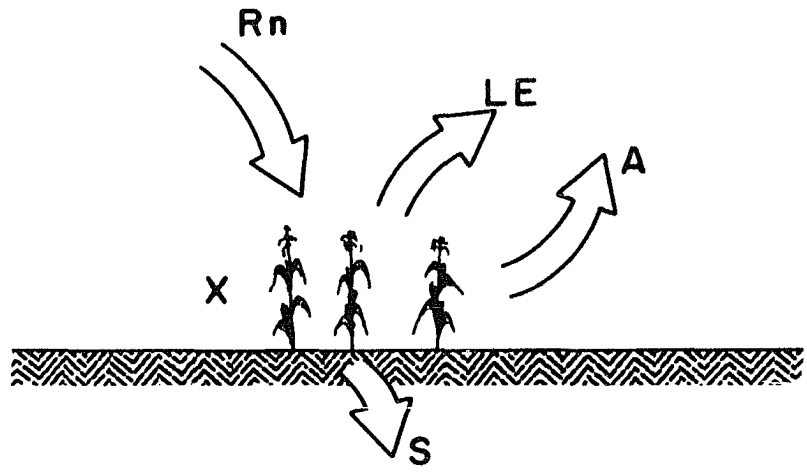

Figure A-1. Major vertical energy components during daylight conditions for an agricultural field

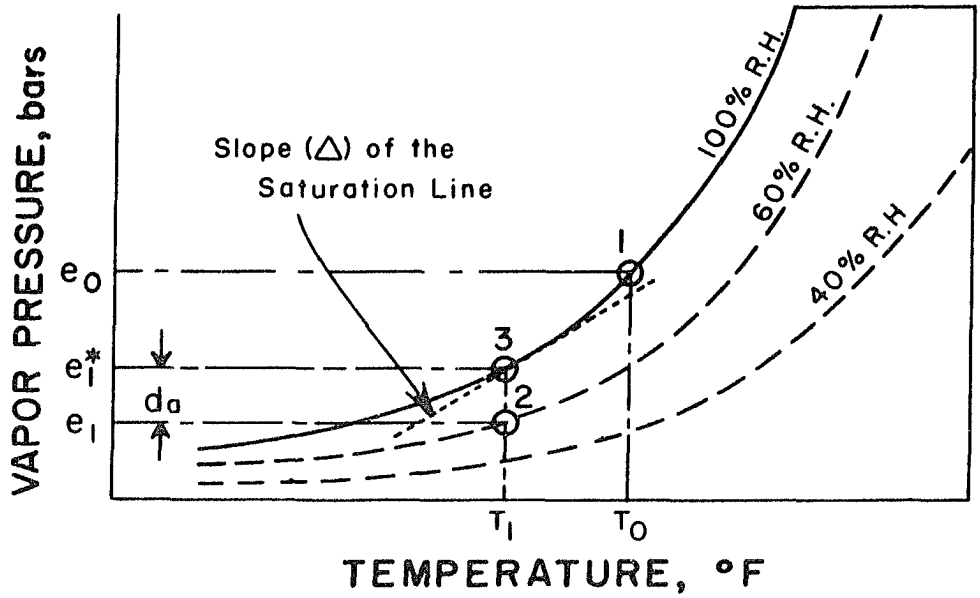

Figure A-2. Schematic of psychrometric chart for demonstrating Penman's assumptions

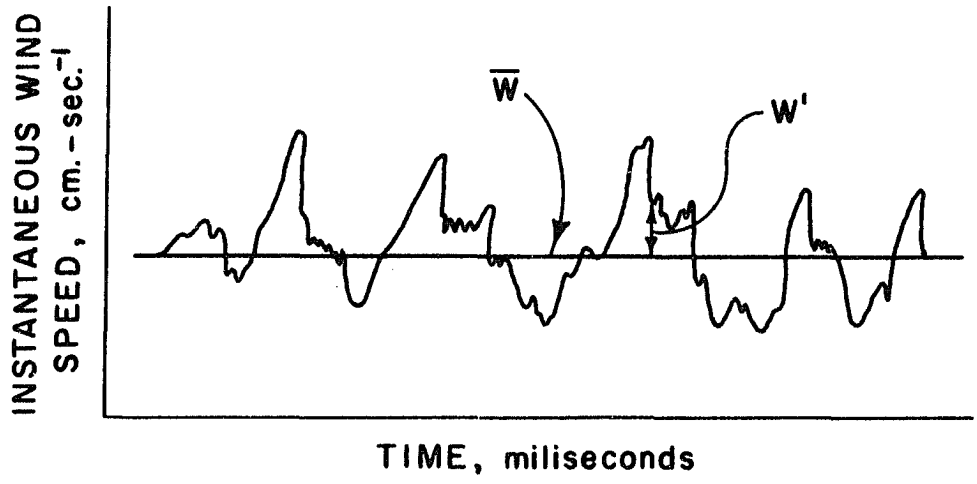

Figure A-3. Schematic of instantaneous vertical wind velocities

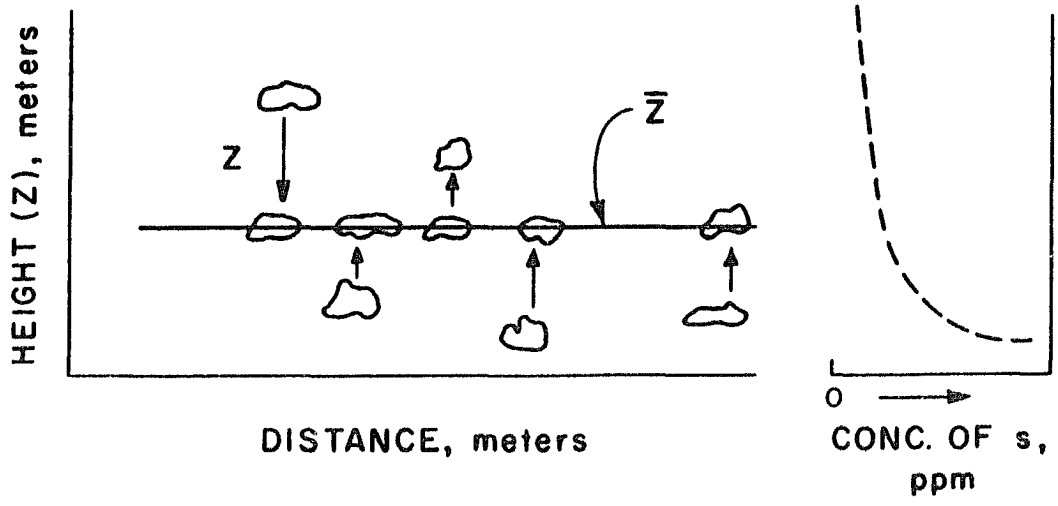

Figure A-4. Definition sketch of mixing length concept

APPENDIX B

REVIEW OF WIND PROFILE PARAMETERS

Introduction of the aerodynamic features into the combination ET model can be followed in detail in the complete derivation given in Appendix A. Briefly, it involved the use of the turbulent diffusion theory and the logarithmic wind profile, whose parameters Z, Z_o, and d appear in the aerodynamic transport term of the combination equation.

van Bavel (1966, p. 458) acknowledged that to obtain accurate working values for these wind parameters was difficult, but he showed that a 10% error in the wind profile terms would cause only ½% to 1% error in the calculated PET values. However, Skidmore, Jacobs, and Powers (1969), Rosenberg et al. (1968), and the author have all found that calculated PET values are often more sensitive to these wind parameter values than suggested by van Bavel. Therefore, for successful application of the combination model, considerable attention must be given to the accurate representation of these aerodynamic terms.

It has been quite well established during recent years that the logarithmic wind profile can give realistic representation to the wind profile under conditions of bare soil, open water, or short grass--all under near adiabatic

conditions and adequate fetch (Webb 1970, O'Brien 1965, Wright and Lemon 1966). As conditions deviate from these, different wind profiles develop which require different descriptive parameters. Thus, in addition to the wind speed variation throughout the day, the wind profile parameters also vary during the day depending on such factors as lapse rates, wind speed, and soil and crop conditions. And variations also occur over longer time periods as crops grow, mature, and are harvested, soil moisture conditions change, and average daily wind speeds vary. Thus, to measure the wind profile at any instant or an average profile over a short time interval gives only <u>that</u> profile and does not represent the profiles that exist at other times within that day or the days to follow.

The logarithmic wind profile is most commonly written:

$$u = \frac{u^*}{k} \ln \left(\frac{Z-d}{Z_o}\right) .$$

In the solutions of this relation with wind profile measurements, u^* and k are treated as constants, Z is the height of measurement, and d and Z_o are parameters for which values are usually determined by graphical or least square treatment of wind data taken at several levels (Robinson 1962). Many profiles have been measured and

characterized using this model, but it is yet quite difficult to predict useable values of the parameters d and Z_o because of the many factors which affect the wind profile development.

Roughness length, Z_o, is the most difficult to assess. Its solution from profile data is quite sensitive to anemometer placement and errors, and its relation to soil and crop conditions somewhat ambiguous. As the height where the mean wind velocity is 0, Z_o must exist somewhere below the top of a crop; but the distance of penetration depends on crop density and form. On a 1.6-cm lawn, Z_o becomes a very small value such as 0.16 cm, and it ranges up to 300.0 cm for a 2700-cm pine forest (Szeicz et al. 1969). Over tall crops, the effect of increased wind speeds bending the crop and thus reducing the value of Z_o has been shown several times; for example this effect was shown by Rider (1954) over oats, Udagawa (1966) over barley, and Szeicz et al. (1969) over pine forest, potatoes, and lucerne. In most cases, Z_o was shown to decrease exponentially as wind speed increased.

The zero plane displacement, d, is dependent on both crop height and crop density. By definition, d equals 0 for bare soil or open water conditions. Only when crops become sufficiently tall and dense so that the wind profile essentially develops above this new surface does it become

necessary to correct for this upward displacement. In practice, d is usually calculated from profile measurements by trial and error until a best fit of the data to the logarithmic profile is obtained; which also then defines a Z_o value. Many have shown that d does not vary with wind velocities or deviations from adiabatic conditions (Szeicz et al. 1969), although others show such relations (Rider 1954, Udagawa 1966). A single value is often used to represent a cropped surface for one to several days (Szeicz et al. 1969, Lemon 1963).

To apply the combination potential ET model, it is necessary to arrive at useful and realistic daily values for the wind parameters d and Z_o. To define daily potential ET values throughout a growing season, these parameters must be an average of any daily variation, but be varied on a day-to-day basis as aerodynamic and surface conditions change. To predict these daily values, it then becomes necessary to select observed values from the literature, sort out those effects that cause significant day-to-day variation and those that can be averaged, and then relate these effects to field observations such as crop height, crop canopy, and average daily wind velocity.

The effects of large topographic land features are not often discussed in connection with boundary layer wind profiles. Nearly all verification efforts of the logarithmic

profile have been made over large, level fields or bodies of water. Yet in applications, effects of slopes, ridges, valleys, and orientation with respect to wind direction become a factor. The magnitude of these effects is quite variable and their overall affect unassessed. On a watershed basis, the orientation of the entire watershed may become important if winds are predominantly from one direction. As the relief becomes steeper, these topographic effects become more pronounced. There seems to be little current methodology available to account for this topographic-aerodynamic effect. However, under mild relief such as that found in the Midwest plains, it may not be highly significant.

Wind profile characteristics from several references are summarized in table B-1. Although there is obviously great diversity, there are also some common strains. First, with respect to displacement height, d, these data tend to indicate that this parameter is closely related to crop height; in fact most researchers show it as a ratio with crop height (Webb 1965, Rider 1954). However, this ratio logically varies with crop canopy density, because an open, sparse crop would certainly not displace the profile upward the same amount as a very dense crop of similar height. The effect on d of a varying wind velocity seems yet unresolved. Some researchers, such as Rider (1954), Lemon

(1963), and Udagawa (1966), show definite wind effects; while others such as Szeicz et al. (1969) show d to remain nearly constant for crops of potatoes and lucerne. There are at least two reasons that d should vary. First, if the crop bends because of the wind to the extent that its profile is less, the effective displacement may be reduced. Secondly, with increased wind velocity, the turbulence will increase and penetrate farther into the crop canopy, which will have the effect of decreasing the wind profile displacement.

From these data and rationale, it seems logical to develop a working relation in which d is a function of: (1) crop height, H, (2) crop canopy, and (3) wind speed. The relationship

$$d = (0.80) \quad (\% \text{ Canopy}) \quad \frac{d}{d_2} \quad (H) \qquad \text{(B-1)}$$

was empirically developed to define these effects. The ratio d/d_2 represents the relative d values compared with those at a wind speed of 2 m sec^{-1}, and suggested values versus wind speed are shown in figure B-1. These were estimated with guidance from data of Lemon (1963). The percentage of canopy is subject to interpretation but should be estimated according to ease of turbulent penetration. Equation B-1 will yield d = 0.96 H for very light winds and a solid canopy; but even under dense grass,

the maximum canopy density is probably never greater than 85%, in which case d = 0.82 H. Under moderate wind conditions of 6 m sec^{-1}, d = 0.60 H for this same canopy. For a more sparse canopy of 40%, d = 0.23 H at moderate wind. The canopy percentages estimated in the field work of this study were based on the possible penetration of direct radiation; thus, these percentage estimates should be lowered, perhaps by 20%, when used for turbulent penetration.

By combining the results of several studies, it is generally agreed that Z_o values vary mostly with crop height and wind velocity. There is not a good concensus to show how these should be related. Many other factors such as crop form and stiffness apparently have enough effect that they cloud the issue.

Several have shown that Z_o can be related to crop height quite well by use of a logarithmic relation as summarized in table B-2. The several relations seem to be quite similar, but some of the same data are used in several cases. Szeicz et al. (1969) made one of the latest and most complete summaries; thus, their relationships will be applied. Note that a relationship is given for maize and sugar cane and another for other crops; with the justification that tall, stiff crops bend and streamline differently.

Nearly all serious aerodynamic studies have shown that Z_o is a function of wind velocity and usually decreases exponentially with increased wind. However, useable working relations are rarely given. Lemon (1963, p. 39) gave a set of "idealized" Z_o values as a function of wind velocities for alfalfa, corn, and wheat. These were estimated from data collected at several sites. Data showing the variation of Z_o with wind, as compiled by other investigators, are summarized in table B-1. From these several sources, a working relation was estimated for crops of corn and grass and is shown in figure B-2. The brome grass curve was derived mostly from alfalfa data from Lemon (1963), and the corn curve is a modified version of a corn curve from the same reference. The original curve showed the corn Z_o increasing fivefold from 2 to 8 m sec^{-1}. This seemed somewhat unrealistic, so I reduced this ratio to 2.5 times over this same wind range. Note that the corn Z_o continues to increase until quite strong winds prevail, whereas the grass Z_o increases only up to about 2 m sec^{-1} and then declines. This point of change is generally attributed to the plant structure and its flexibility. Grass bends and streamlines much sooner than the corn-stalk and its leaves. Corn is also a much more "open" crop and thus allows deeper turbulent penetration as the turbulence increases with increased wind speed.

Note that the wind speed 2 m sec^{-1} (4.5 mi hr^{-1}) at a height of (d + 2) meters was chosen as the point with unity ratio in both figures B-1 and B-2. This was suggested by Szeicz et al. (1969) as a mild-to-moderate wind speed which approximates the conditions under which many of the aerodynamic studies were made.

The use of these working relations for calculating d and Z_o values is demonstrated in table B-3 where a set of typical values is shown. The effects of crop height, canopy, and wind can be seen. The corn values are particularly interesting due to the large change in crop height and canopy conditions. The last two data sets show the effects of leaf drop and canopy reduction in the late fall with no height reduction. The reader is cautioned, however, that Z_o and d values predicted by these relations did not provide reliable solutions when applied in the combination ET equation. A more thorough discussion is given in the chapters on data reduction and calculations.

Table B-1. Summary of wind profile parameter values from various references

Reference	Crop	H cm	d cm	Zo cm		Notes
				wind		
				weak	strong	
Szeicz et al. (1969)	Potatoes	60	20	9	4	Zo=f(u)
	Lucerne	60	28	8	3	"
Udagawa (1966)	Barley	d/H≈0.8 ≈0.5				u < 2 m sec^{-1} u > 4 m sec^{-1}
Lemon (1963)						
	Alfalfa	75	≈ 50	10-30-10		Zo=f(u), bell shaped
	Wheat	100	100-30	4 - 12		d and Zo = f(u) weak to strong wind
	Idealized Summary					
	Alfalfa			5-20-1		
	Corn			4-15-25		no streamlining
	Wheat			3-13-3		bends harder than alfalfa
Kung (1961)	Corn Field	70-90	88	6.4		
	Brush field	130	125	15.7		
Webb (1965)	General crops		d≈h/2			

Table B-1. Continued

Reference	Crop	H cm	d cm	Zo cm	Notes
Rider (1954)	Oats	80	d/h ≈0.5		$u > 4$ m sec^{-1}
			≈0.2		$u < 1$ m sec^{-1}
	Oats	30	d/h ≈0.5		$u = 1$ to 4 m sec^{-1}
Sutton (1953)	Lawn	<1		0.1	Zo decreases with increasing U.
	Thin grass	<10		.7	
	Thick grass	<10		2.3	
	Thin grass	<50		5.0	
	Thick grass	<50		9.0	
	Short grass	1-3	0	0.5	for $u = 5$ m sec^{-1} at 2 meters height
	Long grass	60-70	30	3.0	
Deacon (1953, as summarized by Kung 1961)	Smooth mud			.001	
	Smooth snow on short grass			.005	
	Sea			.02	

Table B-1. Continued

Reference	Crop	H cm	d cm	Zo cm	Notes
Deacon (1953, as summarized by Kung 1961) continued					
	Desert			.03	
	Snow			.10	
	Mown grass	1.5		0.2	
		3.0		0.7	
		45.		2.4	V_2 = 2 m sec^{-1}
		"		1.7	V_2 = 6 to 8 m sec^{-1}
	Long grass			9.0	V_2 = 1.5 m sec^{-1}
				6.1	V_2 = 3.5 m sec^{-1}
				3.7	V_2 = 6.2 m sec^{-1}

Table B-2. Summary of prediction equations for roughness parameter, Zo

Reference	Equation[a]	Notes
Szeicz et al. (1969)[b]	$\log_{10} Zo = -0.98 + \log_{10} H$	All crops except maize and sugar cane.
	$\log_{10} Zo = -1.6 + 1.1 \log_{10} H$	Corn and sugar cane
Kung (1961)	$\log Zo = -1.24 + 1.19 \log H$	
Tanner and Pelton (1960)	$\log Zo = -0.883 + 0.997 \log H$	r = 0.97

[a] Zo = roughness parameter, cm.

H = crop height, cm.

[b] Summarizes the work of six other sources.

Table B-3. Example values of calculated wind profile parameters Z_o and d

H cm	C[a] %	U m sec^{-1}	Z_{o-2} cm	d_2 cm	Z_o cm	d cm
			GRASS			
2	50	1	.21	0.64	0.147	0.704
		2			.210	.640
		4			.126	.550
		8			.073	.384
20	95	1	2.09	12.2	1.46	13.4
		2			2.09	12.2
		4			1.25	10.5
		8			.73	7.3
			CORN			
1	0[b]	1	.0252	0.0	0.0138	0.0
		2			.0252	.0
		4			.0428	.0
		8			.0630	.0
20	5	1	.676	.64	0.372	.70
		2			.676	.64
		4			1.15	.55
		8			1.69	.38

[a] These canopy values were based on radiation penetration and were reduced 20% for profile displacement calculations.

[b] Before planting.

Table B-3. Continued

H cm	C[a] %	U m sec^{-1}	Z_{o-2} cm	d_2 cm	Z_o cm	d cm
182 (6')	80	1	7.58	93.2	4.17	102.5
		2			7.58	93.2
		4			12.91	80.2
		8			18.98	55.8
243 (8')	90[c]	1	10.48	140.	5.76	154.
		2			10.48	140.
		4			17.82	120.
		8			26.20	84.
243 (8')	60[d]	1	10.48	93.3	5.76	102.5
		2			10.48	93.3
		4			17.82	80.2
		8			26.20	55.8

[c]Mid-August.

[d]Late September.

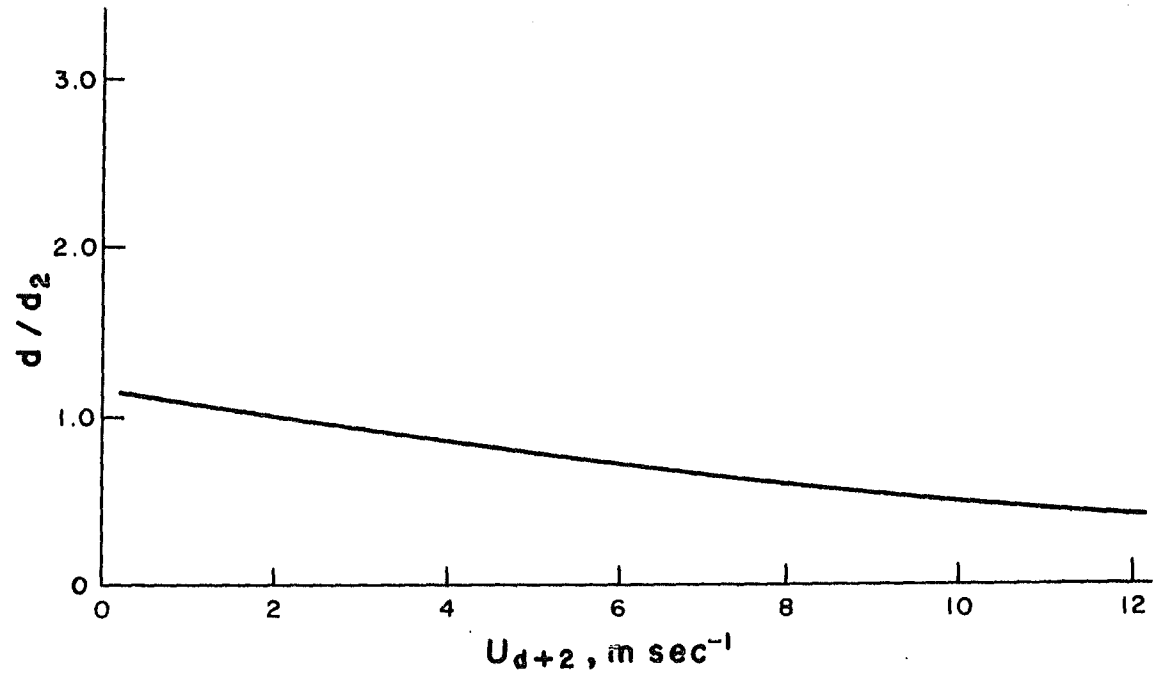

Figure B-1. Wind effects on d for corn and grass

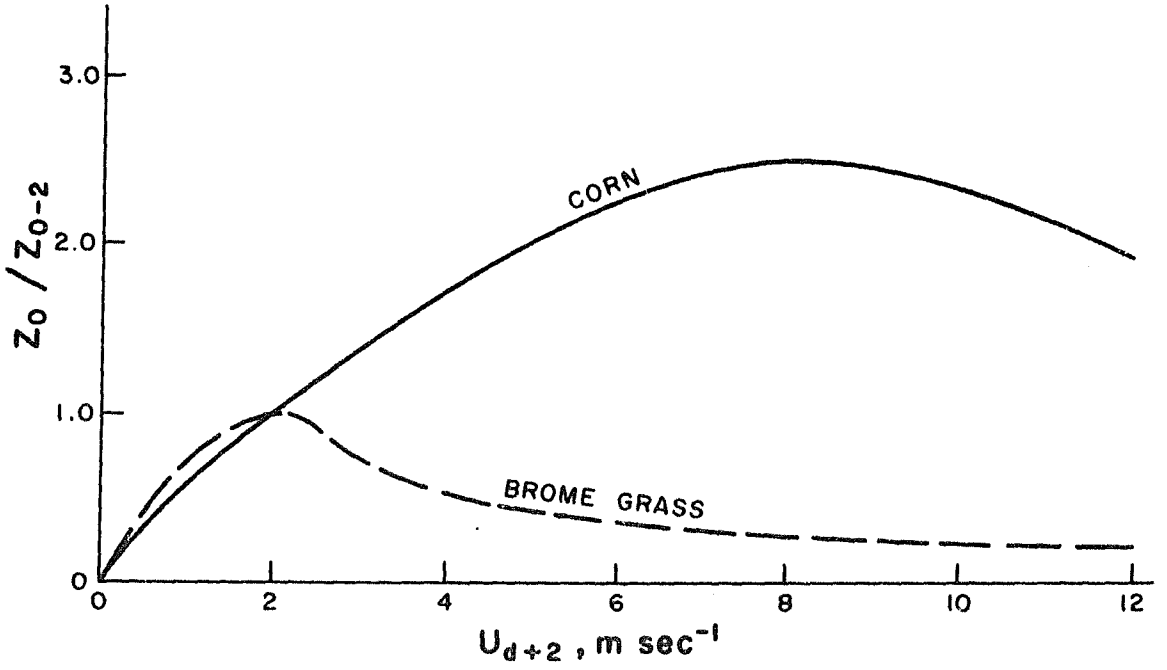

Figure B-2. Wind effects on Z_o